ЖУРНАЛ
ПРИКЛАДНОЙ ХИМИИ

JOURNAL OF
APPLIED CHEMISTRY
OF THE USSR

(ZHURNAL PRIKLADNOI KHIMY)

IN ENGLISH TRANSLATION

VOL. 30 NO. 8

CONSULTANTS BUREAU, INC.

227 WEST 17TH STREET, NEW YORK 11, N. Y.

an agency for the interpretation of international knowledge

JOURNAL OF APPLIED CHEMISTRY OF THE USSR

(ZHURNAL PRIKLADNOI KHIMII)

Volume 30, No. 8

August, 1957

(A Publication of the Academy of Sciences of the USSR)

IN ENGLISH TRANSLATION

CONSULTANTS BUREAU, INC.
227 West 17th Street
New York 11, N.Y.

Printed in the United States

	Domestic	Foreign
Annual Subscription	$60.00	$65.00
Annual Subscription for libraries of non-profit academic institutions	20.00	25.00
Single Issue	7.50	

SIGNIFICANCE OF ABBREVIATIONS MOST FREQUENTLY ENCOUNTERED IN SOVIET PERIODICALS

FIAN	Phys. Inst. Acad. Sci. USSR.
GDI	Water Power Inst.
GITI	State Sci.-Tech. Press
GITTL	State Tech. and Theor. Lit. Press
GONTI	State United Sci.-Tech. Press
Gosenergoizdat	State Power Press
Goskhimizdat	State Chem. Press
GOST	All-Union State Standard
GTTI	State Tech. and Theor. Lit. Press
IL	Foreign Lit. Press
ISN (Izd. Sov. Nauk)	Soviet Science Press
Izd. AN SSSR	Acad. Sci. USSR Press
Izd. MGU	Moscow State Univ. Press
LEIIZhT	Leningrad Power Inst. of Railroad Engineering
LET	Leningrad Elec. Engr. School
LETI	Leningrad Electrotechnical Inst.
LETIIZhT	Leningrad Electrical Engineering Research Inst. of Railroad Engr.
Mashgiz	State Sci.-Tech. Press for Machine Construction Lit.
MEP	Ministry of Electrical Industry
MES	Ministry of Electrical Power Plants
MESEP	Ministry of Electrical Power Plants and the Electrical Industry
MGU	Moscow State Univ.
MKhTI	Moscow Inst. Chem. Tech.
MOPI	Moscow Regional Pedagogical Inst.
MSP	Ministry of Industrial Construction
NII ZVUKSZAPIOI	Scientific Research Inst. of Sound Recording
NIKFI	Sci. Inst. of Modern Motion Picture Photography
ONTI	United Sci.-Tech. Press
OTI	Division of Technical Information
OTN	Div. Tech. Sci.
Stroiizdat	Construction Press
TOE	Association of Power Engineers
TsKTI	Central Research Inst. for Boilers and Turbines
TsNIEL	Central Scientific Research Elec. Engr. Lab.
TsNIEL-MES	Central Scientific Research Elec. Engr. Lab.–Ministry of Electric Power Plants
TsVTI	Central Office of Economic Information
UF	Ural Branch
VIESKh	All-Union Inst. of Rural Elec. Power Stations
VNIIM	All-Union Scientific Research Inst. of Meteorology
VNIIZhDT	All-Union Scientific Research Inst. of Railroad Engineering
VTI	All-Union Thermotech. Inst.
VZEI	All-Union Power Correspondence Inst.

Note: Abbreviations not on this list and not explained in the translation have been transliterated, no further information about their significance being available to us. – Publisher.

WEIGHT RATIO OF THE SOLID AND LIQUID PHASES IN DOUBLE SUPERPHOSPHATE AND THE OPTIMUM CONCENTRATION OF THE ORIGINAL PHOSPHORIC ACID

K. S. Krasnov
The Ivanovo Institute of Chemical Technology

In our previous communication [1] we used data on the kinetics of the conversion of apatite in saturated solutions of the ternary system $CaO-P_2O_5-H_2O$ and solubility data for calculation of the optimum conditions for the production of double superphosphate.

Calculations show that the optimum concentration of phosphoric acid is equivalent to 54-55% P_2O_5. It was emphasized in this communication that the results obtained by interpretation of the kinetic data on the solubility diagram cannot in themselves provide a complete solution to the problem of the optimum conditions of double superphosphate production, which involves a complex topochemical reaction. The influence of many factors must be taken into account for a complete solution.

One such factor, which is of great significance in the decomposition of apatite during its conversion into double superphosphate, is the weight ratio of the solid and liquid phases in the reacting system, which we denote by S/L.

The system consists of monocalcium phosphate, $Ca(H_2PO_4)_2 \cdot H_2O$ (the reaction product), residues of unreacted apatite, phosphoric acid, and water. The solid phases are apatite and monocalcium phosphate, and the liquid phase is a solution of monocalcium phosphate in phosphoric acid.

The S/L ratio varies as decomposition of the apatite proceeds. If S/L < 1, "nonsetting" pulps are formed. Conversely, if at the end of the den stage process the S/L ratio is high, subsequent decompositionof the apatite is hindered, as the contact between the acid liquid phase and the unreacted apatite is diminished considerably. The optimum S/L ratio, at which further conversion during the cure of the superphosphate is not hindered, is about 1.5-2.

Since we found that the optimum H_3PO_4 concentration is equivalent to 54-55% P_2O_5, it was of interest to determine whether the use of such acid also gives the optimum ratio S/L ≈ 1.5-2 at the end of the den stage, when the conversion coefficient K reaches 60%.

In this paper we present calculations of the S/L ratio as a function of the original phosphoric acid concentration and of the temperature; it is shown that with acid containing 54-55% P_2O_5 the S/L ratio is close to the optimum value; the influence of temperature on the curing of superphosphate is also considered.

Calculation of the S/L Ratio

The value of S/L depends on several variables, namely: the temperature, the concentration of the original phosphoric acid, and the percentage conversion K attained at a given instant.

This relationship is expressed by the equation derived by Chepelevetskii [2]

$$\frac{S}{L} = \frac{\frac{100}{100-w}(98.3+126.2D)\frac{\alpha}{1-\alpha}+(100-K)}{\frac{100}{100-w}(98.3+126.2D)-(100-K)}, \quad (1)$$

where D is the stoichiometric ratio for the conversion of apatite, w is the water content of the product (in %), and α is the fraction of monocalcium phosphate crystals, the decomposed part of the phase complex. The phase complex is taken to mean the principal components of the system less the unreacted apatite and HF, i.e., water, acid, and monocalcium phosphate [1].

When D is unity, Equation (1) is simplified:

$$\frac{S}{L} = \frac{\frac{22450}{100-w} \cdot \frac{\alpha}{1-\alpha} + (100-K)}{\frac{22450}{100-w} - (100-K)}. \quad (2)$$

Equation (2) is used in our calculations.

Equation (2) does not contain either the original H_3PO_4 concentration or the temperature. However, both these quantities enter the equation in implicit form, as for a given value of K the value of α is uniquely determined by the concentration of the original acid and the temperature.

The value of α is found graphically from the solubility diagram for the ternary system $CaO-P_2O_5-H_2O$. The details of the method are given in the previous paper [1]. The ratio $\alpha/(1-\alpha)$ increases with increasing concentration of the original phosphoric acid.

The moisture content w of the superphosphate can be calculated by means of Chepelevetskii's formula:

$$w = \frac{72.4 - [P_2O_5]}{0.724 + 0.0078\,[P_2O_5]}, \quad (3)$$

where $[P_2O_5]$ is the P_2O_5 content of the original acid (in %).

In Equation (3) moisture loss by evaporation is not taken into account, and the values found for w are too high; but since w enters both the numerator and the denominator of Equation (2) this does not have any significant effect on the value of S/L, especially at high values of K. For example, if an acid containing 54% P_2O_5 is used for for the conversion at K = 75%, w calculated from Equation (3) is 16%, while the experimental value of w = 10%. Substitution of the calculated value of w into Equation (2) at K = 50% gives S/L = 1.34; substitution of the experimental value of w gives S/L = 1.38; at K = 75% the values of S/L are 2.24 and 2.26 respectively.

Analysis of Equation (2) shows that the S/L ratio for superphosphate increases with increasing concentration of the original phosphoric acid with increasing conversion coefficient, and with decreasing temperature of the superphosphate.

Table 1 gives the values of the S/L ratio in double superphosphate at t = 75°, for different concentrations of the original phosphoric acid, and at different conversion stages. The values of S/L were calculated from Equation (2).

TABLE 1

Values of the S/L Ratio in Double Superphosphate at 75°

Concentration of the original acid (in % P_2O_5)	S/L ratio at different values of the conversion coefficient K				
	50	60	75	80	85
45	0.835	0.863	1.02	0.996	0.975
50	1.05	1.29	1.60	1.83	1.73
54	1.34	1.58	2.24	2.52	2.86
56.5	1.53	1.83	2.67	3.17	3.56
60	1.83	2.34	3.79	4.44	5.35

It follows from the data in Table 1 that with acid containing 45% P_2O_5 it is impossible to obtain an S/L ratio higher than unity. Although the superphosphate pulp "sets" at this ratio, the S/L value is quite inadequate, and the physical properties of the superphosphate are poor owing to the high amount of liquid phase.

If acid of considerably higher concentration is used, for example, with 54-56% P_2O_5, a "setting" pulp with a good S/L ratio is obtained even when K is only 50%. A further increase of a few per cent in the acid concentration, say to 60% P_2O_5, gives a high value of the S/L ratio even at low coefficients of conversion. Moderate values of S/L (1.5-2) attained at the end of the den stage of the conversion process favor setting of the superphosphate and

more complete crystallization of $Ca(H_2PO_4)_2 \cdot H_2O$. The liquid phase loses the crystallizing salt and becomes more active in the process. On the other hand, very high values of S/L attained at the end of the den stage (K = 60%) hinder further conversion of the superphosphate during the cure, as the liquid phase is separated from particles of undecomposed apatite by large masses of solid phase.

The data of Table 1 were used to plot S/L against the conversion coefficient attained (Fig. 1). Isothermal isoconcentration lines for acids containing 45, 50, 54, 56.4 and 60% P_2O_5 at 75° are plotted in the diagram.

The ratio S/L = 1.75 may be regarded as the most favorable for further conversion of the superphosphate after discharge from the den (1.75 is chosen as the average value of 1.5 and 2). In Fig. 1 a straight line is drawn parallel to the abscissa axis, with the ordinate S/L = 1.75. This line cuts the isoconcentration curves. The abscissas of the intersections give the values of K at which S/L = 1.75. For acid with 50% P_2O_5 K = 77.5, with 54% P_2O_5 K = 64.8 , for 56.5% acid K = 57.5, and for 60% acid K = 48%. These values are used to plot values of K at which S/L = 1.75 is attained, against the initial acid concentration (Fig. 2) at 75°.

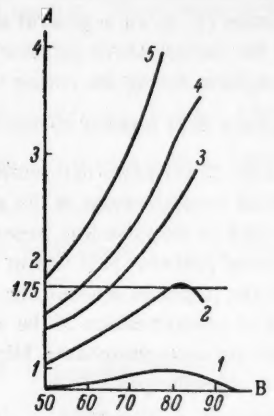

Fig. 1. Variations of S/L ratio in double superphosphate with the conversion coefficient K reached, and with the concentration of the original phosphoric acid at 75°.
A) S/L ratio, B) conversion coefficient K (%).
Concentration of original phosphoric acid (as % P_2O_5): 1) 45, 2) 50, 3) 54, 4) 56.5, 5) 60.

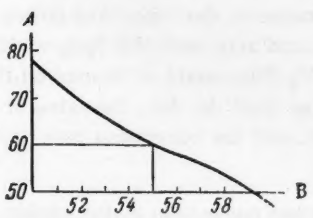

Fig. 2. Values of the conversion coefficient K at which S/L = 1.75 is reached, at different concentrations of the original acid at 75°.
A) Conversion coefficient K (%), B) acid concentration (% P_2O_5).

TABLE 2

Effect of Cooling on the S/L Ratio in Double Superphosphate Made with Phosphoric Acid Containing 54% P_2O_5

Temperature (°C)	S/L ratio at different values of the conversion coefficient K				
	50	60	75	80	85
75	1.34	1.58	2.24	2.52	2.86
25	1.55	1.82	2.47	2.90	3.22

TABLE 3

Values of the Limiting Coefficient of Conversion Reached in the Process, up to Formation of Impermeable $CaHPO_4$ Films on the Apatite Grains

P_2O_5 in the original acid (%)	Value of "limiting" coefficient of conversion at temperatures (°C)		
	100	75	40
30	—	—	62
35	—	40	71.5
40	—	57	78.5
45	47	69	84.5
50	65	76	90
55	77.5	86	98

This graph can be used to find the acid concentration which gives S/L = 1.75 at the end of the den process, i.e., when K = 60%.

A straight line parallel to the abscissa axis is drawn on the graph, with ordinate K = 60. The abscissa of its intersection with the curve gives the acid concentration. This is equal to 55% P_2O_5.

This is the answer to our problem. In the previous communication we calculated the optimum concentration of the original acid for double superphosphate production at which the liquid phase at the end of the den stage is most active with respect to the unconverted apatite. The optimum concentration of the original acid was found to be equivalent to 54-55% P_2O_5.

We have now shown that this is also the optimum acid concentration for themost favorable solid–liquid ratio at the end of the den stage, which facilitates the cure of the superphosphate.

The effect of cooling of the superphosphate after discharge from the den on the S/L ratio is illustrated by the data in Table 2, for an original acid containing 54% P_2O_5.

It follows from the data in Table 2 that the S/L ratio of the discharged superphosphate (K = 60%) increases within permissible limits, namely, from 1.58 to 1.82, so that difficulties in the cure cannot arise. Thus, from this aspect the concentration of 54-55% P_2O_5 in the original acid is also the most favorable.

Study of the S/L ratio and of its influence in the cure of double superphosphate provides one illustration of the fact that although studies of the kinetics of the dissolution of apatite in saturated solutions in the system $CaO-P_2O_5-H_2O$ provide a basis for the selection of various optimum parameters [1, 3, 4], a general solution of the problem of the optimum process conditions requires consideration of all the factors which influence the course of the complex topochemical reaction in the solid product – superphosphate during the curing stage.

The question of the effect of cooling during the cure of the superphosphate is of interest in this connection.

The increase of the S/L ratio during cooling of the superphosphate (Table 2) indicates that additional crystallization of $Ca(H_2PO_4)_2 \cdot H_2O$ takes place, with a decrease in the degree of neutralization of the acid in the liquid phase; this can be easily demonstrated by the graphical method described in thepreceding paper [1]. A decrease in the degree of neutralization of the acid should accelerate the curing process. It is known that at a high degree of neutralization of the first H^+ ion in phosphoric acid (30-50%) the reaction between the acid and apatite dies down almost completely[5]. Therefore a decrease of the degree of neutralization of the acid on cooling should favor the cure. This was demonstrated by Brutskus [6] for ordinary superphosphate. Here we shall consider another aspect of the question, concerned with the cooling of double superphosphate.

At a high degree of neutralization of H_3PO_4, when $CaHPO_4$ begins to crystallize out of the liquid phase, the reaction between the acid and apatite, which is already dying down, stops completely owing to the formation of impermeable $CaHPO_4$ films on the surface of the apatite [3].

The above-mentioned graphical method [1] can be used to calculate the "limiting" coefficient of conversion which may be reached at a given temperature and acid concentration up to the formation of impermeable $CaHPO_4$ films on the apatite grains. (As has already been stated, this limit is not reached in practice during mixing, as the reaction is greatly retarded owing to the decreased concentration of the free hydrogen ions of the acid).

An example of such a calculation for the reaction between apatite and an acid containing 30% P_2O_5 is given in the preceding paper [1]. Results calculated for different concentrations of the original acid are given in Table 3.

The data in Table 3 show that the limiting coefficient of conversion reached in a reaction with an acid of a given concentration increases with decrease of temperature. This may account for the fact, reported by Bridger, that the conversion coefficient increases with decrease of temperature in the mixer and during curing [7]. If the temperature of the superphosphate remained at 100° all the time, and acid with 55% P_2O_5 could not give a conversion coefficient greater then 77%, as an impermeable $CaHPO_4$ film would be formed on the apatite grains. Because of the natural cooling of the superphosphate after discharge from the den, the value of the limiting coefficient of conversion, as Table 3 shows, reaches almost 100%, and the conversion may proceed further as far as the hydrogen ion concentration of the acid allows.

It may be assumed that natural cooling of double superphosphate favors conversion during curing, as is the case for ordinary superphosphate.

Artificial cooling of the product after discharge, by means of aeration, shoveling, etc., may also be considered. However, the whole question is, to what temperature should theproduct be cooled?

The superphosphate is mainly a solid mass during the curing stage. Movement of the liquid phase in its capillaries and diffusion of hydrogen ions to the apatite grain surfaces become more difficult with decrease of temperature. The decomposition occurs as the result of interaction between the H^+ ions of the liquid phase and the apatite.

Therefore there must be a certain temperature, below which cooling would have an unfavorable effect on the conversion of apatite during the cure; i.e., there is a certain optimum curing temperature. This temperature is below the temperature of the process in the den stage. It may be found by direct experiment, as all the necessary data for its calculation are not yet available.

SUMMARY

1. It is shown that in the conversion of apatite into double superphosphate the optimum ratio of the solid and liquid phases required for the curing process is obtained with the use of acid containing 54-55% P_2O_5.

2. It is shown that cooling of the double superphosphate after discharge from the den assists conversion of the residual apatite. There must be a certain optimum curing temperature below which curing is retarded.

LITERATURE CITED

[1] K. S. Krasnov, J. Appl. Chem. 30, 1, 25 (1957).*

[2] M. L. Chepelevetskii, Dissertation (Moscow, 1947).

[3] K. S. Krasnov, J. Appl. Chem. 26, 1114 (1953).*

[4] K. S. Krasnov, J. Appl. Chem. 28, 1275 (1955).*

[5] M. L. Chepelevetskii, Trans. Sci. Res. Inst. Fertilizers and Insectofungicides 137 (Chem. Theoret. Press, 1937).

[6] E. B. Brutskus, Dissertation (Moscow, 1945).

[7] G. L. Bridger, R. B. Burt and W. W. Cerf, Ind. Eng. Chem. 37, 9, 829 (1945).

Received March 5, 1956

* Original Russian pagination. See C. B. Translation.

EVALUATION OF THE STRUCTURE OF SOME OPOKAS* OF THE VOLGA REGION BY THE SORPTION OF WATER AND BENZENE VAPORS

F. A. Slisarenko, E. M. Timofeeva, S. I. Sorokin and V. A. Zabelin

The Saratov State Pedagogic Institute

Increasing attention is now being paid to natural sorbents which may become cheap substitutes for costly, artificially prepared materials.

As has been noted by Dubinin, Bykov, and Kiselev, investigation of natural sorbents is a difficult problem in view of the diversities of the internal structure and the different chemical and mineralogical nature of these substances.

It is therefore rational to study natural sorbents by a multiplicity of methods, including investigations of the sorptional properties and the chemical and mineralogical composition of these substances. The results of such multiple investigations of opokas of the Volga region indicate that they can be successfully used as bleaching earths in various branches of the national economy. Papers by the present authors and other investigators report that opokas may be used for refining vegetable oils [1], for regeneration of used mineral oils, for purification of gasolines, and for drying vapors, air, and gases [2]. Therefore further studies of opokas of the Volga region are of direct interest in relation to our national economy.

In view of the very scanty literature data on the opokas, in our opinion it is desirable to carry out deeper studies of the sorptional and structural properties of opokas of the Volga region by the adsorptional–structural method. This provides an objective evaluation of the quality of sorbents in relation to their uses in various branches of industry [3].

EXPERIMENTAL

The experimental method used in our investigation was similar to that used by Bykov for studying the sorptional properties of natural sorbents of the Far East [4].

For studying the sorption of vapors by Volga opokas, a vacuum installation with a quartz balance was assembled, similar to the apparatus developed by Chmutov [5], with certain modifications. The apparatus is shown diagrammatically in Fig. 1. The balance consisted of the quartz springs 1 at constant tensions of 2.97 mg/mm and 1.63 mg/mm. The quartz spring with the pan 2 was suspended from the hook of a glass stopper fitted by a ground joint with a mercury seal into a glass tube connected with a vacuum installation. Changes in the length of the spring relative to a stationary scale were read off by means of a cathetometer with a micrometer eyepiece. The sensitivity of the balance in our determinations was therefore 0.028 and 0.015 mg per division of the micrometer eyepiece.

The calibration of the balance was regularly checked during the work. The apparatus was evacuated by means of a high-vacuum three-stage Langmuir mercury vapor pump with a RVN-20 preliminary exhaust pump. The system could be evacuated down to $1 \cdot 10^{-5}$ mm Hg. The pressure in the apparatus was measured by means of of a McLeod gage 3 and an ordinary mercury manometer 4, which was read with the aid of a cathetometer to an accuracy of 0.05 mm. The vapors were admitted into the system from a flask 5 containing degassed water, with the aid of an electromagnetic mercury feed device 6. The whole apparatus was contained in a case with Plexiglas doors.

Samples of opokas weighing 50-100 mg in the form of powders or grains with average diameter 2 mm were taken for the experiments.

* Opokas are diatomaceous earths – Publisher's note.

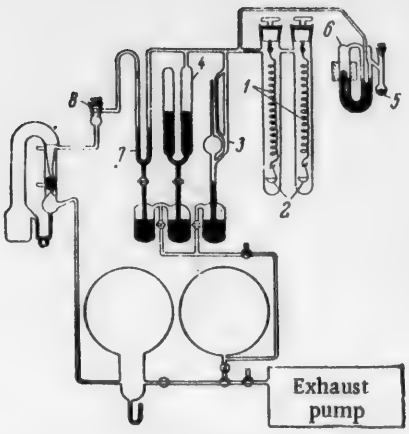

Fig. 1. The vacuum installation. Explanations in text.

Most of the specimens were first studied in granular form; the grains were then ground and the powders investigated.

For completeness, several samples of opokas from each site were taken. The weighed sample was placed in the balance pan, and the system was then evacuated while the ends of the tubes were heated to 200° in an electric furnace to remove adsorbed vapors and gases from the sample. The heating and evacuation were continued for 2-3 hours. The apparatus was then disconnected from the evacuation system by means of the mercury seal 7 and stopcock 8, the lengths of the spirals were measured, and the weight of the dry adsorbent free from gases found. All the calculations were based on 1 g of dry sorbent.

For determination of the vapor sorption isotherms, the ends of the tubes with the balance were placed in a water thermostat at 20°. When a vapor pressure close to the saturation pressure had been reached in the system, the case containing the apparatus was maintained at a temperature somewhat above 20° to prevent premature condensation of the vapor on the walls of the apparatus.

The isotherms for the sorption and desorption of the vapors were determined 2-3 times, from a high vacuum to the saturated vapor pressure and back. The equilibrium in sorption and desorption was established in 2-5 hours, and the saturated vapor pressure equilibrium in 10-12 hours.

RESULTS AND DISCUSSION

The sorption of water vapor by samples of opokas from five different sites in the Volga region was studied. The results of the determinations were used to plot sorption isotherms (Fig. 2). They all have the characteristic S shape typical for sorption accompanied by capillary condensation. The existence of capillary condensation in opokas is also confirmed by the extensive regions of sorptional hysteresis in all the isotherms.

The hysteresis is irreversible at low relative pressures. In the sorption–desorption cycle, even with prolonged exhaustion of the system to a high vacuum, the balance pointers do not return to the original positions. This indicates that the sample retains a certain volume of sorbed moisture bound more firmly with the surface of the sorbent than the rest of the moisture adsorbed and condensed in the pores. Irreversible hysteresis in the sorption of water vapor has been observed by some investigators on other silicate materials; for example, Zhdanov [6] described this effect in the sorption of water vapor by porous glasses; it has also been observed for silica gels [7]. In our opinion, the irreversible sorptional hysteresis in opokas may be explained by the existence of pores with diameters not much greater than the diameter of the water molecule in the opokas. A water molecule, which has a large dipole moment, becomes bound so firmly with the surface on entering such a pore that desorption from this pore requires much more energy than that required for desorption ofother adsorbed molecules. Such molecules, fixed in pores of molecular dimension, are desorbed only when the sample is heated. Brunauer [8] gives a similar explanation for the irreversibility of sorptional hysteresis.

Attention must be drawn to the isotherms of water vapor sorption on Zolotoe No. 84 opoka (Fig. 2,a). This opoka has a greater reversibility of the sorptional hysteresis anda larger micropore volume than any of the others studied. A distinguishing feature of its isotherms is that the sorption curve of the 1st sorption–desorption cycle does not coincide with the corresponding curves in subsequent cycles. The sorption curve for the 1st cycle lies below those of the subsequent cycles. In the 2nd cycle this curve occupies a higher position than in the 1st, and its position then remains unchanged. A similar effect was observed in the sorption of water vapor by montmorillonite clays [9], which have a number of common features with the opokas studied, both in mineralogical structure and in chemical composition. A possible explanation for the displacement of the sorption curve is that the water molecules on entering pores of molecular dimensions push the walls of these pores apart to some extent, thus forming an additional area for sorption. If this is the case, the deformation of the opoka framework must be regarded as elastic, as this effect is reproduced after calcination of the opoka.

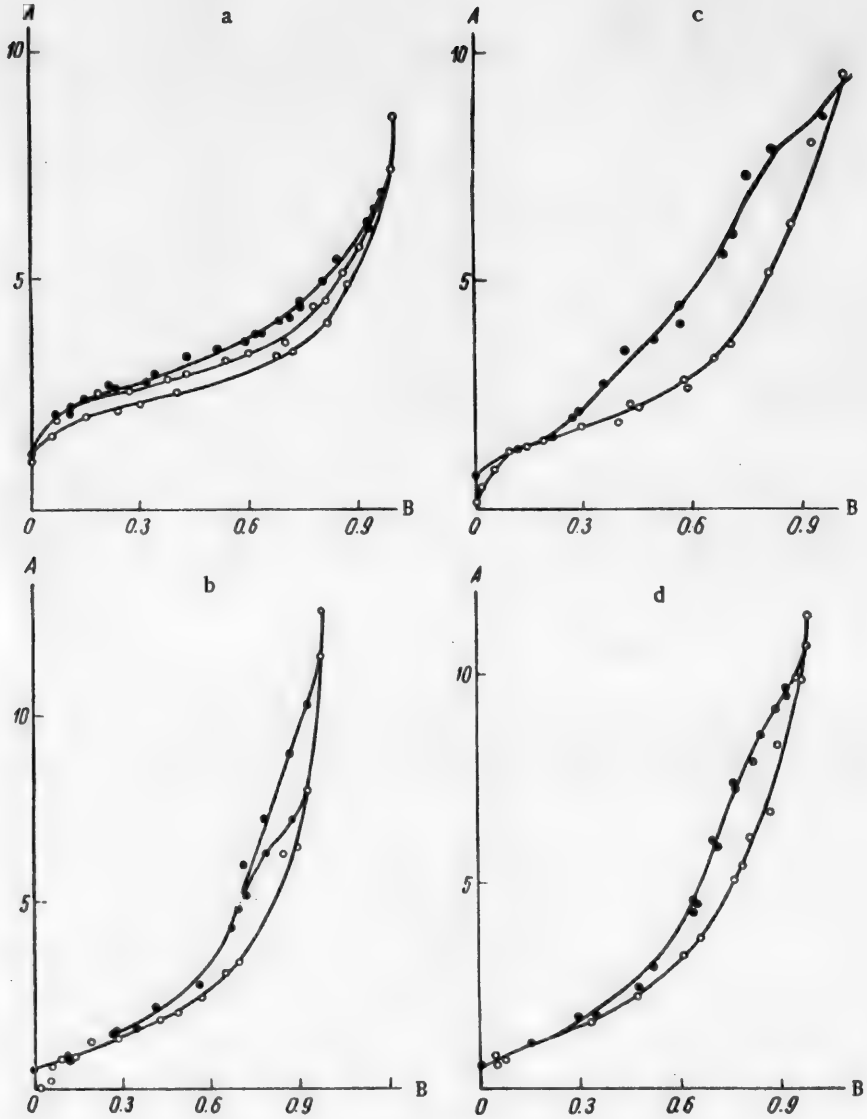

Fig. 2. Isotherms of the sorptionand desorption of water vapor by opakas. A) Amount of vapor adsorbed by the opaka (millimoles/liter), b) relative vapor pressure. Opokas: a) Zolotoe No. 84; b) Privol'sk No. 11; c) Lysaia Gora No. 1; d) Saratov No. 108.

The isotherms for the sorption of water vapor were used for evaluation of the pore structure of the opokas and estimation of their specific surface.

The pore volume distribution curves (Fig. 3) indicate that most of the opokas studied belong to the homogeneously porous sorbents of the 2nd structural type, by Kiselev's classification [10], and only the Lysaia Gora No. 1 opoka can be classified as a sorbent of mixed porosity, of the 4th structural type (Table 1).

TABLE 1

Sorption of Water Vapor by Opokas of the Volga Region

Site of origin	Sample No.	Dispersity of samples	P/P_s at start of sorptional hysteresis	Volume of sorbed liquid water (cc/g)					
				at start of sorptional hysteresis	$P/P_s = 0.25$	$P/P_s = 0.5$	$P/P_s = 0.95$	$P/P_s = 1.0$	Residual $P/P_s = 0$
Zolotoe	84	Grains	0.2	0.045	0.047	0.062	0.119	0.155	0.021
		Powder	0.2	0.043	0.06	0.06	0.124	0.166	0.021
Saratov	108	Grains	0.25	0.025	0.025	0.043	0.178	0.206	0.011
		Grains	0.24	0.025	0.025	0.046	0.8	0.209	0.01
		Powder	0.25	0.025	0.025	0.046	0.198	0.226	0.01
		Powder	0.25	0.025	0.025	0.042	0.198	0.228	0.01
Privol'sk	11	Grains	0.27	0.026	0.024	0.042	0.18	0.234	0.01
		Powder	0.29	0.025	0.024	0.043	0.202	0.251	0.01
Kamennyi Iar	121	Grains	0.31	0.03	0.027	0.051	0.292	0.346	0.011
Lysaia Gora	1	Grains	0.23	0.031	0.034	0.07	0.156	0.173	0.014

TABLE 2

Porosity of Volga Opokas. Specific Surfaces of the Opokas

Site of origin	Sample No.	Dispersity of samples	Most probable effective pore radius (in A)	Pore volume (cc/g)			Specific surface (m^2/g)	
				micropores* $r \leqslant 15$ A	intermediate* $15 \leqslant r \leqslant 200$ A	at saturation	BET method	Kiselev's method
Zolotoe	84	Grains	29	0.056	0.062	0.155	115	160
		Powder	29	0.054	0.068	0.166	120	155
Saratov	108	Grains	27	0.038	0.139	0.206	70	90
		Powder	27	0.036	0.156	0.226	70	90
Privol'sk	11	Grains	26	0.034	0.154	0.234	70	90
		Powder	26	0.034	0.167	0.251	70	90
Kamennyi Iar	121	Grains	40	0.040	0.250	0.346	80	110
Lysaia Gora	1	Grains	—	0.057	0.099	0.173	85	110

TABLE 3

Sorption of Benzene Vapor by Opokas of the Volga Region

Site of origin	Sample No.	P/P_s at start of hysteresis	Volume of sorbed liquid benzene (cc/g)				
			at start of hysteresis	$P/P_s = 0.25$	$P/P_s = 0.5$	$P/P_s = 0.95$	$P/P_s = 1.0$
Zolotoe	84	0.24	0.11	0.012	0.024	0.039	0.11
Saratov	108	0.24	0.035	0.040	0.085	0.170	0.204
Privol'sk	11	0.26	0.03	0.028	0.072	0.18	0.230
Kamennyi Iar	121	0.37	0.040	0.035	0.069	0.302	0.336
Lysaia Gora	1	0.24	0.025	0.027	0.076	0.114	0.116

* The pore radii were calculated from the Thomson equation with a correction of 3 A for the thickness of the adsorbed film.

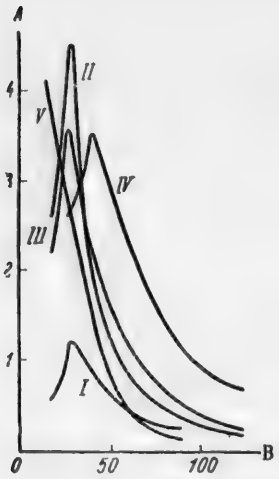

Fig. 3. Curves for the distribution of opoka pore volumes by radius. A) Ratio of volume difference of sorbed vapors to the pore radius difference $\frac{\Delta w}{\Delta r}$, B) pore radii of opokas (in A). Opokas: I) Zolotoe No. 84, II) Saratov No. 108, III) Privol'sk No. 11, IV) Kamennyi Iar No. 121, V) Lysaia Gora No. 1.

The micropore volume of the opokas is relatively small, considerably less than the volume of the intermediate pores; the two volumes are roughly equal only in Zolotoe No. 84 opoka (Table 2). The high content of intermediate pores evidently accounts for the high sorptive activity of opokas when they are used as bleaching earths.

The specific surface of the opokas was determined by the Brunauer, Emmett, and Teller method [3]; the area per 1 mole of water in a continuous monomolecular layer was taken as 10.8 A. Despite the fact that the equation of Brunauer, Emmett, and Teller (BET) is satisfactorily obeyed by the sorption of water vapor by opokas over a fairly wide range of pressures, in most cases the specific surface of the opoka skeleton determined by the BET method is smaller than the specific surface of the adsorption film determined by Kiselev's method [11]. Evidently the sorption of water vapor by opokas does not conform to the theory of multilayer adsorption.

On the basis of the results obtained by studies of isotherms for the sorption of vapors by powders and large grains of the same opoka samples certain comments may be made on methods for studying porous bodies. Studies of opokas show that the specific surfaces of the sorbent skeleton andof the adsorbed film do not depend on whether the sample was taken in granular or powdered form. This shows that these opokas of the Volga region do not contain closed pores. However, at high relative pressures and at saturated vapor pressure the volume of sorbed water is greater in samples taken in powder form than in granular samples. In our opinion, this difference is caused not by differences in the internal structure of the opokas, but by the pores formed between the particles of the powder, owing to capillary condensation of the vapor in these pores. In consequence investigations of powdered sorbents give high values for the intermediate pore volume and thetotal porosity. We consider that investigations of porous sorbents in granular form give a more correct picture of the pore volume and total porosity; this is especially important for natural sorbents, as in a number of cases the volume of the intermediate pores determines their sorptional properties.

In addition to the studies of the sorption of water vapor, the structure of opokas was studied by the sorption of benzene vapor by the same samples of opokas of the Volga region. It is known that benzene molecules are larger than water molecules and have no dipole moment, and therefore the sorption of benzene vapor should differ somewhat from that of water vapor. For example, sorption of water vapor may restore dehydrated surface hydroxyl groups; this does not occur in the sorption of benzene vapor. Further, because of their larger diameter, benzene molecules will not penetrate into some pores which are accessible to water molecules. By studies of the sorption of vapors of substances with progressively larger molecules it is possible to elucidate the micropore structure of the sorbent and to estimate the specific surface accessible to different molecules.

The results of the determinations are given in Table 3 and Fig. 4.

All the isotherms are characteristically S-shaped with large hysteresis loops. Irreversible hysteresis or displacement of the adsorption curve were not observed. The pore structures of the opokas were estimated from the desorption curves of the isotherms for benzene vapor (Table 4). A significant feature is the considerable decrease in the micropore volume accessible to sorption; in our opinion, this is entirely the consequence of an ultraporosity effect. This confirms our hypothesis that highly disperse opokas contain some pores 2-4 A in diameter. Estimation of the volume of intermediate pores ($15 \leq r \leq 200$ A) from the sorption of benzene vapor gives approximately the same results as those found from the sorption of water vapor. The pore volume distribution curves determined from the sorption of benzene vapor are shifted somewhat in the direction of smaller radii relative to the distribution curves determined from the isotherms for the sorption of water vapor (Fig. 5).

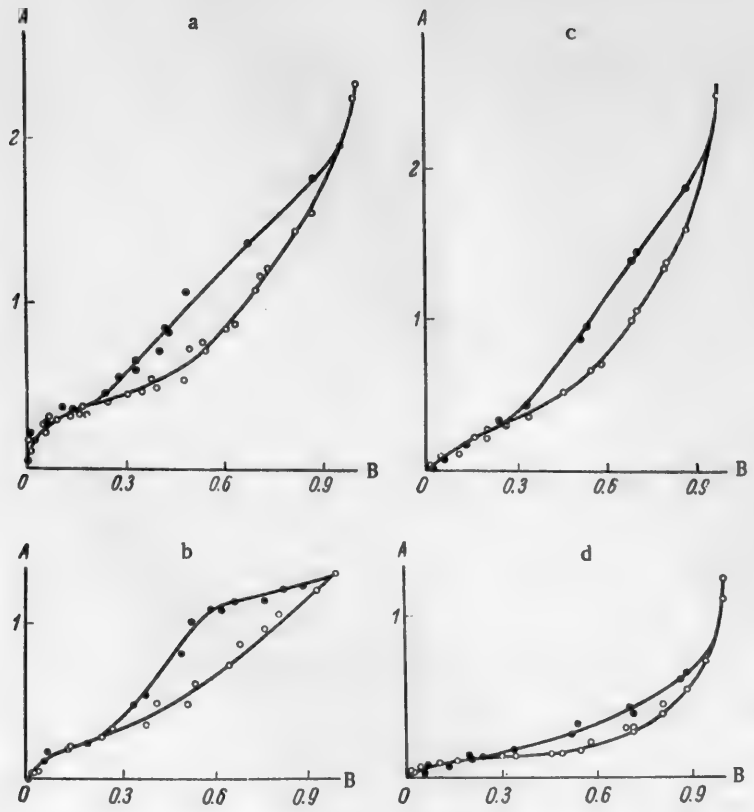

Fig. 4. Sorption and desorption isotherms for benzene vapor on opokas. A) Amount of vapor adsorbed (millimoles/g), B) relative vapor pressure. Opokas: a) Saratov No. 108, b) Lysaia Gora No. 1, c) Privol'sk No. 11, d) Zolotoe No. 84.

TABLE 4

Estimation of the Porosity and Specific Surface (S) of Opokas from Isotherms for the Sorption of Benzene Vapor*

Site of origin	Sample No.	Most probable effective pore radius (in A)	Volume of micropores (cc/g) $r \leqslant 15$ A	Volume of intermediate pores (cc/g) $15 \leqslant r \leqslant 200$ A	Total pore volume (cc/g)	S (m^2/g) by BET method	S (m^2/g) by Kiselev's method	S (m^2/g) by start of hysteresis
Zolotoe	84	25	0.009	0.055	0.11	15	20	20
Saratov	108	24	0.028	0.13	0.204	60	70	70
Privol'sk	11	23	0.02	0.15	0.230	55	65	65
Kamennyi Iar	121	32	0.025	0.25	0.336	60	80	80
Lysaia Gora	1	—	0.018	0.093	0.116	50	55	55

* The pore radii were calculated from Thomson's equationwith a correction of 3 A for the thickness of the adsorbed film.

This displacement can be attributed to the low accuracy of the determination of the thickness of the adsorbed film. As with the sorption of water vapor, the values found for the volume of intermediate pores and for the total porosity were higher for the samples taken in powder form than for granular samples. This increase of the

sorptional volume is evidently caused by the pores formed between the powder particles.

The specific surfaces of the opokas were estimated from these sorption isotherms. The specific surface of the opoka skeleton was initially determined by the method of Brunauer, Emmett, and Teller [12]; the area occupied by a benzene molecule in a continuous monolayer was taken as $\omega = 30.3$ A. The specific surface of the opoka skeleton estimated by the BET method was again found to be less than the specific surface of the adsorbed benzene film determined by Kiselev's method [13]. Estimation of the specific surface by Dubinin's method [14], from the displacement of the structural curves determined from the sorption of water and benzene vapors, gave results close to the values of the specific surface of the adsorbed water film calculated by Kiselev's method.

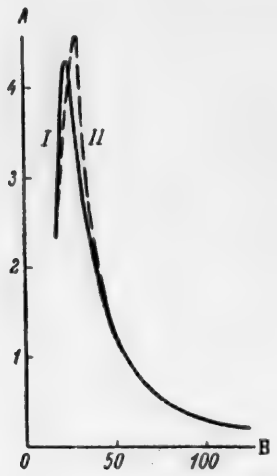

Fig. 5. Curves for the pore volume distribution by radius in Saratov opoka. A) $\frac{\Delta w}{\Delta r}$, B) pore radii (in A). Calculated from sorption isotherms for I) benzene vapor, II) water vapor.

Determinations of the thickness of the adsorbed film by Dubinin's method showed that a surface monomolecular layer is formed in most samples only at the start of capillary condensation.

In our opinion this accounts for the low values of the specific surface of the skeleton as found by the BET method. This fact also provided yet another method for estimating the specific surface of opokas. On the assumption that the start of sorptional hysteresis corresponds to the start of capillary condensation, we took the volume of the monomolecular layer to be the volume of the sorbed substance at the start of hysteresis. The specific surface was then calculated from the known formula:

$$S = X_m \cdot N\omega_0,$$

where X_m is the "capacity" of the monomolecular layer; N is the Avogadro number, X_m being expressed in moles per gram; ω_0 is the area occupied by one molecule in a continuous monolecular layer.

Estimations of the specific surface of opoka skeletons by this method gave results close to the specific surfaces determined by Kiselev's method [15]. In addition, the specific surfaces of skeletons of natural sorbents from the Far East were estimated from the isotherms for the sorption of benzene vapor determined by Bykov [16].

Good results were obtained in all cases.

SUMMARY

1. Opokas of the Volga region have been studied by the adsorptional–structural method, the nature of their porosity was evaluated and their specific surfaces estimated.

2. Comparison of the sorption of vapors by powder and grains of the same adsorbent shows that it is preferable to study the sorption of vapors on porous adsorbents taken in granular form.

3. Owing to the monomolecular nature of the adsorbed layer formed at the start of capillary condensation it is possible to estimate the specific surface of the skeleton from the value of the sorption at the start of sorptional hysteresis.

4. It was confirmed that good sorptional properties of a natural sorbent are determined by similarity of the values of the specific surface of the skeleton of the sorbent and the adsorbed film.

LITERATURE CITED

[1] F. A. Slisarenko and E. M. Timofeeva, Summaries of Papers at the Scientific Conference Reviewing the Results of Scientific Research in 1954.

[2] S. I. Sorokin and V. A. Zabelin, Sci. Mem. Saratov State Univ., Saratov State Pedagogic Inst. (1955).

[3] A. V. Kiselev, Bull. Moscow State Univ. 11, 111 (1949).

[4] B. N. Bykov, Bull. Acad. Sci. USSR, Div. Chem. Sci. 4, 585 (1952).*

[5] M. Dubinin and K. Chmutov, Physicochemical Principles of Antigas Defense (VKhA Press, Moscow, 1939).**

[6] S. P. Zhdanov, Proc. Acad. Sci. USSR, 61, 853 (1948).

[7] N. N. Avgul', O. M. Dzhigit, A. V. Kiselev, and K. D. Shcherbakova, J. Phys. Chem. 26, 977 (1952).

[8] S. Brunauer, The Adsorption of Gases and Vapors (Russian Translation), 1 (IL, Moscow, 1948).

[9] V. P. Bering, V. P. Dreving, A. V. Kiselev, V. V. Serpinskii, M. D. Suvorova, and K. D. Shcherbakova, Colloid J. 14, No. 6, 398 (1952).*

[10] A. V. Kiselev, J. Phys. Chem. 23, 466 (1948).

[11] A. V. Kiselev, Progr. Chem. 14, 367 (1945).

[12] S. Brunauer, The Adsorption of Gases and Vapors (Russian Translation), 1948.

[13] A. V. Kiselev, Progr. Chem. 14, 367 (1945).

[14] M. M. Dubinin, Physicochemical Principles of Sorption Technology, 2nd edn. (ONTI, 1935).**

[15] N. N. Avgul', O. M. Dzhigit, A. V. Kiselev, and K. D. Shcherbakova, J. Phys. Chem. 26, 982 (1952).

[16] V. T. Bykov, Bull. Acad. Sci. USSR, Div. Chem. Sci. 4, 587 (1952).*

Received May 17, 1955

* Original Russian pagination. See C. B. Translation.

** In Russian.

PECULIAR FORM OF CRYSTALLINE CARBON CONCRETIONS

A. P. Sizov

Theoretical and experimental investigations relating to the production of artificial highly carbonaceous materials of definite physicochemical properties are of great practical importance at the present time.

Moreover, the conditions for the formation of solid carbon deposits on certain surfaces, especially incandescent, of gas retorts and other equipment are understood very little, although it is known that these undesirable solid growths arise and grow spontaneously on the retort walls as the result of pyrolysis of gases containing carbon.

The properties of these lustrous retort carbons have been studied by many workers [1, 2]; it has been reported that they are very hard, the hardness reaching up to 9 units on the Mohs scale. Their density is over 2. These deposits have high chemical purity, low sorptive capacity, low specific resistance, about 0.004 ohm/cm·cm^2, and a number of other properties of practical value.

We have carried out experiments to study, under laboratory conditions, the pyrolysis of ordinary coal gas from the Moscow gas supply.

The experiments were carried out in a temperature range up to 2000°, the conditions being so chosen that the products were not contaminated with extraneous impurities. High-frequency induction heating was used, and a special reactor with walls of quartz glass was designed for the purpose.

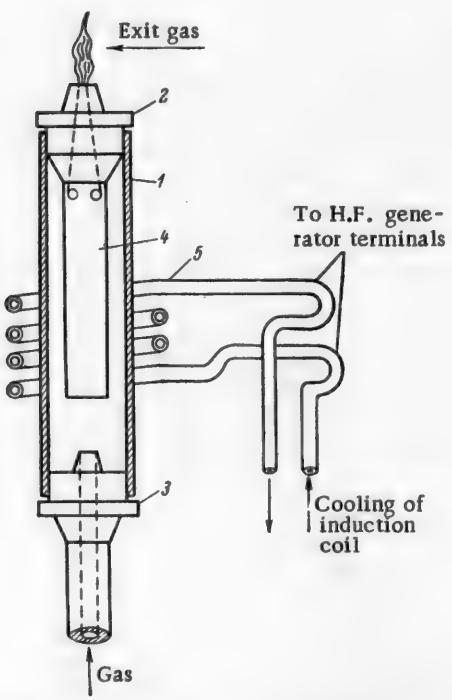

Fig. 1. Schematic diagram of reactor. Explanations in text.

A simple conventional diagram of the reactor used for these experiments is given in Fig. 1. The cylinder 1 is a section of quartz glass tube. The quartz tube is closed at each end with closely fitted graphite bungs with fireclay supports. A graphite core 4 is fixed in the top bung. In order to remove any impurities present in this core, it was heated thoroughly in the induction furnace before each experiment to above 2500°.

The induction coil 5 was made from copper tubing and was cooled with water. It loosely surrounded the quartz cylinder with a 4-6 mm gap on each side between the glass and the coil. Gas from the ordinary supply was fed in through a nozzle in the lower bung 3; its supply was controlled by a special screw valve not shown in the diagram. The chemical composition of the gas was that of ordinary Moscow town gas, which consists mainly of methane and carbon monoxide with an admixture of various higher hydrocarbons. The exit gases escaped from the reactor through openings and a channel in the upper part of the core 4, and were burned on reaching the air.

The supply of fresh gas into the reactor from the mains can be regulated by observation of the height and color of the flame of the burning exit gas. A simple portable spectroscope was used to observe visually the qualitative composition of the exit gas for more accurate regulation of the gas supply. The high-frequency current source for

Fig. 2. Appearance of the core after the experiment.

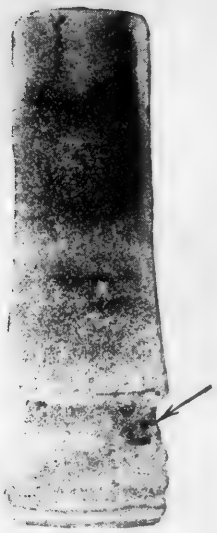

Fig. 3. Portion of the core from which a sample of concretions was removed for investigation (place indicated by arrow).

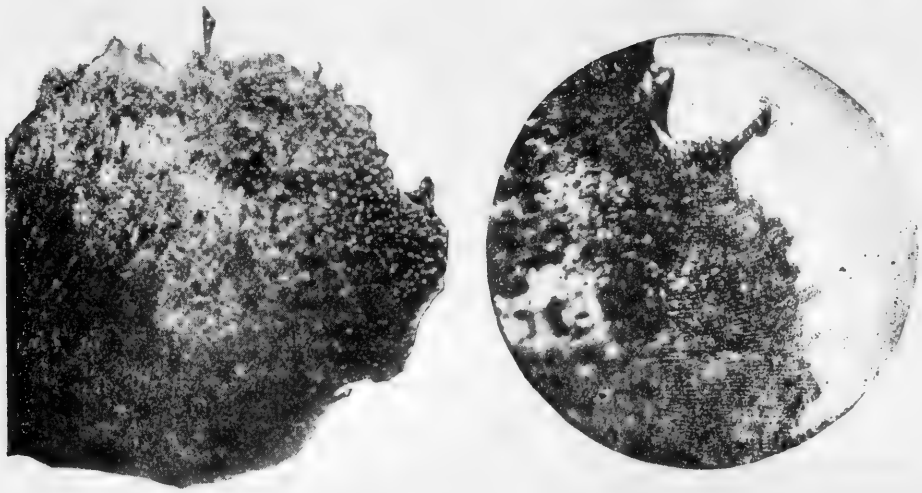

Fig. 4. Sample of concretions.
Left, front view; right, side view.

induction heating of the core was a standard 2-tube generator type AZ-46 with an operating frequency range of $5\text{-}6 \cdot 10^4$ cycles/second.

The duration of each individual experiment was 80-90 minutes, or about 1.5 hours on the average. Each experiment was repeated many times, approximately the same results being obtained each time. The appearance of the cooled core after extraction from the cylinder of the reactor is shown in the photograph (Fig. 2).

Fig. 5. Individual concretion of typical form.

Fig. 6. Concretions characteristically oriented relative to the vertical axis of the core.

The surface of the core is clearly seen to consist of three bands of different colors, namely: almost black below, pale gray above, and a very pale narrow band between them. These three bands correspond to three different maximum zone temperatures reached on the core surface during the experiment. The lower dark band corresponds to 1250-1300 ± 50°. The middle pale band corresponds to 1500-1550 ± 50°. The upper gray band corresponds to 1600-1650 ± 50°. The temperatures were measured by means of an optical pyrometer when a steady thermal state had been reached.

The pale gray band formed in the 1600-1650° zone differs sharply from the other two both in color and in the nature of the deposits. It has a gray color with a metallic luster (roughly the color of freshly cast zinc). Examination of the core under a binocular microscope with 50-fold magnification clearly shows that this band consists of numerous concretions of an unusual wormlike shape, oriented in the direction of the gas stream, i.e., upward.

Figure 3 shows a secretion of the core with two adjacent bands obtained under the action of equal temperatures, 1600 ± 50°. The arrow indicates the point of extraction of the sample, a "concretion brush," shown in Fig. 4 on the left.

Figure 4, on the right, is a micrograph of the same aggregate of concretions, but from a different angle. Individual wormlike concretions (of the appearance of annulated worms) and their relative positions in the whole mass on the carbon core can be clearly distinguished in these micrographs. The bands of deposits in regions of different cores where the temperature was about 1600° consist entirely of many hundreds of such concretions, which appear to grow from the body of the carbon core and are arranged in continuous rows around the core (one row above the next, etc.).

The concretions could not have been formed from substances liberated from the core, as the cores were thoroughly heated at high temperatures before the experiments; in some cases (as a check) the temperature was taken to over 3000°.

In the 70-90 minutes of each experiment large numbers of such growths were formed; each individual wormlike concretion has the following actual dimensions: length 0.75-0.80 mm, diameter at the base 0.03-0.04 mm, diameter at the head 0.08-0.09 mm. Each such concretion has 6-7 turns per 0.1 mm of its length, in the form of a close conical diverging spiral, with the external appearance of a tightly coiled spiral spring (see Fig. 5). All such concretions, without exception, are oriented in the direction of the gas stream, i.e., upward, and are at an angle of about 35-40° to the vertical axis of the core. The great majority of the concretions are slightly curved along a certain radius, almost the same for all of them, away from the core surface, as is seen in the photograph in Fig. 6.

These concretions are gray in color, of various shades including black, with a strong oily luster. The true hardness of the isolated concretions has not yet been determined, as the ordinary methods of microhardness determination, such as the Khrushchev and Berkovich methods, are inapplicable owing to the very small size of the individual concretions and the absence of any, even small, flat regions for application of the diamond indenter.

Fig. 7. Specimens of distorted concretions.

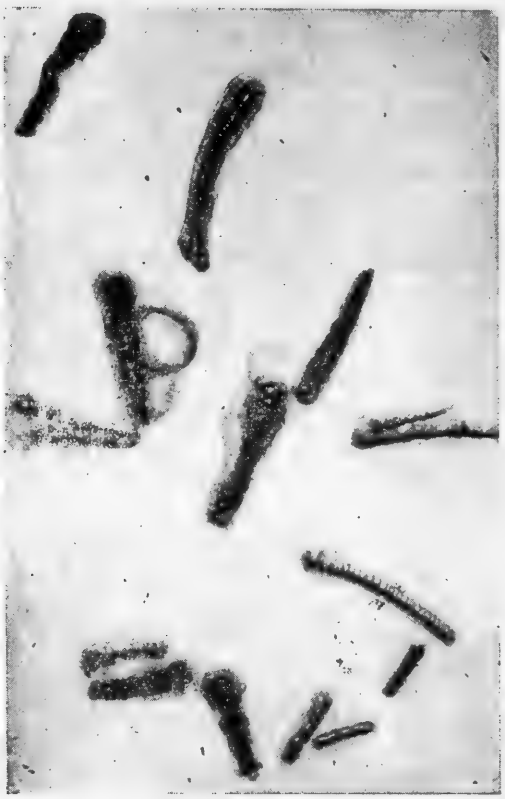

Fig. 9. Prepared specimens of concretions. Longitudinal sections.

Fig. 8. Specimens of peculiar distorted form, but with the spiral structure retained.

However, it may be provisionally estimated that the strength of these crystalline concretions is probably considerable. For example, they are difficult to break by pressure between glass slides; they break with a sharp crack and give large numbers of very small fragments. The glasses between which the samples are crushed are marked with fine scratches which are clearly visible through the microscope. Among the great majority of regularly formed concretions there are a few individual variations with various distortions of the basic shape. Some of these distorted growths are shown in the micrograph (Fig. 7). For comparison, a "normal" concretion of characteristic form is indicated by an arrow; the others represent various distortions.

The photograph in Fig. 8 also shows concretions with various distortions of the basic shape, formed at low gas speeds. A striking feature is that all these concretions have an external spiral structure, up to a typical corkscrew shape, as shown in the specimen indicated by an arrow in Fig. 8.

Figure 9 is a photograph of several concretions cut longitudinally through the middle. For comparison, some are shown intact in the right-hand bottom corner of the picture. It is clearly seen that all these concretions have a solid internal structure.

X-ray photographs of specimens oriented in the camera reveal a structure along the 002 line, as shown by nonuniform blackening of the ring.

It follows that during growth of the concretions the carbon networks are situated with their planes parallel to theprincipal axis of the growing concretion. All this, in turn, is highly characteristic of the needlelike structure of lustrous carbons.

Preliminary spectroscopic investigations showed that the principal constituent of these growths is carbon, with small amounts of impurities such as Mg, Al, Ca, Si, Fe, etc., the contents of which vary from .01% to several thousandths of one per cent.

The specific gravity of the concretions was determined by immersion in a heavy liquid (bromoform solution) for a few specimens; the value was 2.20-2.35. More accurate determination of specific gravity is still very difficult because, even in any one experiment, the concretions formed at different regions of the core may have similar form and size, but differ greatly in their wettability and immersibility in the liquid.

Examination of the concretions in a stereoscopic microscope under high magnification, or of photographs of typical concretions, suggests a resemblance between the shape of the concretions and a solidified sand whirl, i.e., a figure formed as the result of complex turbulent eddy motion of elementary particles.

As is known, when a conducting core, such as carbon, is subjected to induction heating by a high-frequency electromagnetic field, induced currents are produced. These currents, known as Foucault currents, are essentially eddy currents, forming electromagnetic fields in the form of closed eddy rings.

It is therefore quite natural that as the result of high-frequency induction heating, the solid formations formed, which consist of carbon particles with definite magnetic properties liberated from the gaseous medium, have the shape of eddy figures, apparently frozen in their complex motion.

An examination of the concretion of this type, such as that shown in Fig. 5, clearly reveals spiral rings, with a kind of double screw thread. The origin of these rings is in all probability associated with periodic temperature fluctuations in the reactor while the heat was switched on and off during the experiment, which was done at 1-1.5 minute intervals throughout. This was necessary in order to control the temperature of the core and to keep it at the necessary optimum level of about 1550 ± 50°.

For comparison, experiments were performed with the same reactor, the same gas, and in the same temperature ranges of about 1550 ± 50°, but the reactor was heated by being connected in a direct-current circuit in one case, and in an alternating-current circuit of the normal frequency of 50 cycles in another. The solid deposits formed on the core in these experiments did not contain any of the characteristic concretions of the kind formed by induction heating in a high-frequency field. This leads to the tentative conclusion that the cause of the formation of peculiar concretions of almost pure carbon of the type described was the use of induction heating (at a frequency of 600,000 cycles/second in our case). We suggest the name "carbolites" (uglerolity) (by analogy with the existing terminology) for these experimentally prepared carbon concretions. It is seen that their form is unusual for known types of carbon deposits; it is not found either among fossil coals and graphites, or among known natural or artificial carbonaceous materials [3]. In conclusion, the following preliminary deductions may be drawn. The method of high-frequency electromagnetic heating used in these experiments on gas pyrolysis has a definite influence on the formation of the carbon particles liberated from the gaseous medium, which aggregate into concretions of definite form. These peculiar carbolites, which are deposited in dense masses under appropriate conditions, are capable of forming large anisotropic carbon formations, since the individual carbolites in such a formation are strictly oriented in the same direction.

These growths are almost pure carbon in chemical composition, while in their physical properties they are similar to the so-called lustrous and retort carbons. By control of high-frequency electromagnetic fields and their individual parameters, it is also possible to influence in a definite way the processes of high-temperature crystallization of certain other substances liberated from the gas phase as the result of pyrolysis or dissociation of various compounds under the action of induction heating.

LITERATURE CITED

[1] V. S. Veselovskii, Carbon (Diamond, Graphite, Coal, and Methods of Their Investigation) (ONTI, 1936).*

[2] Pirani, Electrothermics (Russian Translation), edited by D. L. Orshanskii et al. (GONTI, 1939).

[3] A. E. Fersman, The Minerals of the USSR (Izd. AN SSSR, 1939).*

Received January 17, 1956

* In Russian.

DETERMINATION OF THE COMPOSITION OF THREE-COMPONENT SYSTEMS BY MEASUREMENT OF A SINGLE PROPERTY

V. B. Kogan and V. M. Fridman

State Institute of Applied Chemistry

Chemical or physicochemical methods of analysis are generally used for determination of the composition of multicomponent mixtures. Chemical methods of analysis are by no means always applicable, even to three-component systems, while if appropriate methods are available their accuracy is often inadequate for research or practical purposes.

Methods for physicochemical determination of the composition of three-component mixtures, based on determinations of two properties – boiling point and refractive index, or density, etc. – are widely known. The error with the use of these methods depends on the accuracy to which the properties are determined, and on the nature of their dependence on the composition; such an error diminishes with increase of the angle of intersection between the lines for constant values of the selected properties in the so-called analytical triangle. However, in a number of cases it proves impossible to select two properties to give the required accuracy.

A method for the analysis of three-component systems based on determinations of a single property is described in this paper.

The proposed method depends on the geometric properties of the Gibbs concentration triangle. The method is based on the following considerations.

It is known that if two solutions are mixed, the composition of the mixture is represented in the Gibbs triangle by a point which lies on a straight line joining the compositions of the original solutions, while the relative amounts of the solutions used for making the mixture are determined by the lever rule. Suppose that the compositions of the mixtures for which the given property has a constant value n are represented in the Gibbs triangle by the line AB (Fig. 1). If to an arbitrary mixture of composition O we add the solution T_1, the composition of the resultant mixture will vary continuously along the line OT_1 from the point O to the point T_1.

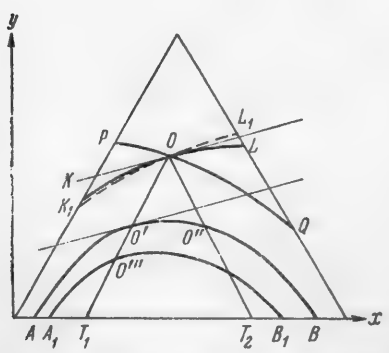

Fig. 1. Gibbs triangle for determination of the composition of systems by the proposed method.

The value of the property will, of course, also vary; it becomes equal to the chosen value n at the point O'. If the relative amounts of the mixtures O and T_1, used to give the composition O', are known, it is possible to construct the curve KL such that a line drawn to this curve from the point T_1 is divided by the curve AB into parts in the same ratio as the ratio of the amounts of the mixtures O and T_1. Therefore, the required composition of the mixture O will be given by a point lying on the curve KL. By repeating this procedure for mixtures of O and T_2, we obtain a curve PQ, the distance of which from the point T_2 will be divided by the curve AB into parts in the ratio $OO''/O''T_2$. The required composition of the mixture O is given by the point of intersection of the curves KL and PQ. Thus, determination of the composition reduces to determination of the amounts of the mixtures T_1 and T_2 required to change the property to the chosen value. As in chemical

analysis, in which the solution is titrated with a particular reagent up to a certain point known as the end point, in the present instance the solution of unknown composition O is "titrated" with mixtures of its components until the selected value of the property is reached. The accuracy to which the composition of the mixture is determined increases with increasing accuracy of determination of the consumption of the mixtures T_1 and T_2 and with increasing angle of intersection of curves KL and PQ. It is easily seen that the angle of intersection of curves KL and PQ depends on the form of the "base line" AB. An infinitesimal displacement of the point O' along the curve AB will change the coordinates of the points by Δy and Δx, while the slope of the tangent at this point will be given by the ratio $\Delta y_1 / \Delta x_1$. An infinitesimal displacement of the point O' will also displace the point O along the curve PQ and will change the coordinates of this point by Δy_2 and Δx_2. However, the coordinates of the conjugate points lying on the curves PQ ($x_2 y_2$) and AB ($x_1 y_1$) and on the line drawn from the point T_1 are connected by the following expression:

$$y_2 = K_1 y_1 \text{ and } x_2 = x_{T_1} + K_1 x_1, \text{ where } K_1 = OT_1/O'T_1 = \text{const},$$

from which it follows that:

$$dy_2 = K_1 dy_1 \text{ and } dx_2 = K_1 dx_1 \text{ and } \frac{dy_2}{dx_2} = \frac{dy_1}{dx_1}.$$

Thus, the slopes of the tangents to the curves AB, KL, and PQ at the conjugate points O and O', and also at the points O and O", are equal, and therefore the angle of intersection of the curves KL and PQ is equal to the angle formed by the tangents to the base line at its points of intersection with lines OT_1 and OT_2. It is quite obvious that it is not necessary to use the same base line in "titration" from the points T_1 and T_2. For example, "titration" with mixture T_1 can be performed to the base line A_1B_1, and with the mixture T_2 to the base line AB (Fig. 1). In this case the angle of intersection of the curves K_1L_1 and PQ will be equal to the angle between the tangent to the curve A_1B_1 at the point O"' and the tangent to the curve AB at the point O".

It follows from the above that this method can only be used when the chosen property is not additive in the system. If the property varies additively, the lines for constant values of the property are a set of parallel straight lines, the curves KL and PQ merge into one straight line, and determination of the composition of the mixture by the method described becomes impossible.

In real systems all properties usually deviate from additivity to some extent. Therefore, for determination of the compositions of mixtures by this method, any property can in principle be used, such as density, boiling point, viscosity, electrical conductance, refractive index, transition from a homogeneous to a heterogeneous state, etc.

However, some properties of solutions, such as density and refractive index, generally show relatively small deviations from additivity, and the iso-property lines therefore may have only a small degree of curvature. The property should therefore be selected for each particular system on a basis of the nature of its deviations from additivity in the system, and with consideration of the required accuracy of determination.

EXPERIMENTAL

To test and demonstrate this method, the compositions of several mixtures in the following systems were determined: 1) acetone–methanol–water, 2) n-butanol–n-octane–n-nonane, and 3) methanol–water–acetic acid.

The components used for preparation of the mixtures were fairly pure; this was confirmed by satisfactory agreement of their physicochemical constants with literature data.

The property chosen was the boiling point for the first two systems, and electrical conductance for the third. The boiling point was determined with the aid of an ebullioscope 40-50 ml in capacity (Fig. 2) and a thermometer with 0.1° scale divisions, the bulb of which was placed between the projections of the inner tube in the ebullioscope. The upper end of the condenser was connected to a manostat consisting of a series of round-bottomed flasks with a total capacity of about 30 liters. The manostat was used to maintain aconstant pressure of 760 mm in the apparatus.

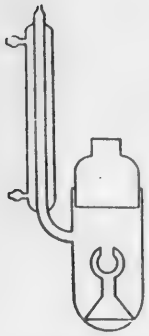

Fig. 2. Apparatus for boiling-point determinations.

TABLE 1

Isotherm for 65° for the System Acetone–Methanol–Water

Point No.	Composition (in wt. %)		
	acetone	methanol	water
1	0	98.8	1.2
2	9.3	83.9	6.8
3	24.2	56.6	19.2
4	34.7	34.7	30.6
5	35.1	23.4	41.5
6	35.0	15.0	50.0
7	34.4	8.6	57.0
8	31.7	3.5	64.8
9	29.0	0	71.0

The mixtures were prepared from calculated amounts of the components weighed on an analytical balance to the nearest 0.0002 g.

The conductance was determined in an electrolytic cell, 50 ml in capacity, with electrodes coated with platinum black, about 1 cm^2 in area. The distance between the electrodes was 3 mm. The cell was placed in a Hoeppler thermostat maintained at 18 ± 0.05°. The resistance was measured by means of an improved instrument of the Wheatstone bridge type, to an accuracy of ± 0.2Ω.

A sensitive galvanometer was used as the null instrument. Since we were not concerned with absolute conductivities, the cell constant was not determined, and the resistance of the solution in the cell was determined directly.

To obtain the data necessary for construction of the base lines, the values of the chosen properties were determined for solutions of various compositions.

The boiling-point data are given in Tables 1 and 2.

TABLE 2

Isotherms for the System n-Butanol–n-Octane–n-Nonane

Temperature (°C)	Composition (in wt. %)			Temperature (°C)	Composition (in wt. %)		
	n-butanol	n-octane	n-nonane		n-butanol	n-octane	n-nonane
113	10.5	89.5	—	117	5.5	94.5	—
	17.6	70.4	12.0		8.1	73.3	18.6
	28.2	45.9	25.9		13.4	53.6	33.0
	38.6	33.6	27.8		19.8	32.4	47.8
	73.6	18.4	8.0		24.0	21.0	55.0
	83.5	16.5	—		36.2	9.1	54.7
115	7.8	92.2	—		42.8	4.8	52.4
	9.1	82.2	8.7		97.3	2.7	—
	15.4	61.4	23.2	122	1.4	98.6	—
	23.7	38.6	37.7		4.0	76.0	20.0
	31.2	27.2	41.6		6.2	56.0	37.8
	52.3	13.0	34.7		9.2	36.8	54.0
	74.9	8.3	16.8		12.7	20.7	66.6
	91.4	8.6	—		13.8	12.1	74.1
					17.0	4.2	78.8
					18.1	2.0	79.9
					27.0	—	73.0

TABLE 3

Results of Experimental Determinations of the Composition of Synthetic Mixtures

System	Point No.	Actual composition (in wt. %)			Composition found (in wt. %)		
		1	2	3	1	2	3
Acetone (1) – methanol (3) – water (3)	I	10	60	30	10.5	59.3	30.2
	II	20	30	50	21.0	27.9	51.1
	III	20	10	70	20.0	9.4	70.6
n-Butanol (1) – n-octane (2) – n-nonane (3)	IV	35	45	20	35.6	44.5	19.9
	V	50	20	30	49.8	20.1	30.1
	VI *	20	10	70	20.4	9.8	69.8
Methanol (1) – water (2) – acetic acid (3)	VII	20	60	20	20.0	59.4	20.6
	VIII	35	35	30	34.9	34.7	30.4
	IX	70	20	10	69.9	19.5	10.6

* Additional "titration" was performed with pure nonane for the 122° base line, with a specific consumption of 0.31 g/g.

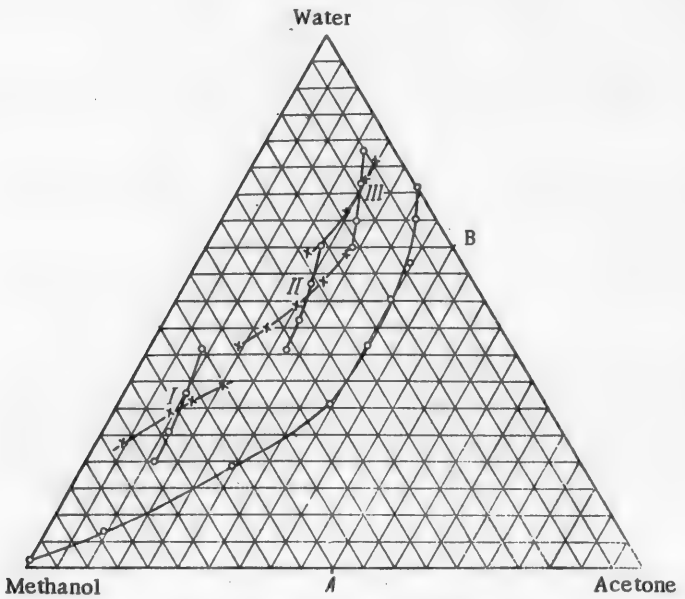

Fig. 3. The system acetone–methanol–water.

The data in these tables were used to plot the isotherm–isobars given in Figs. 3 and 4. Lines for constant resistances of 100, 200, 300, and 500 ohms for the system methanol–water–acetic acid, plotted from the experimental data, are given in Fig. 5.

The results obtained in determinations of the composition of a number of synthetic mixtures are given in Table 3, which also contains the compositions and specific consumptions of the "titrating" mixtures. Each analysis was performed as follows. First the value of the property (boiling point or conductance) of the mixture to be analyzed was determined, and the region in the Gibbs triangle which could contain the point for the required composition was found.

Suitable compositions were then chosen for the "titrating" mixtures, convenient for the subsequent graphical constructions.

TABLE 3 (continued)

Composition of "titrating" mixtures (in wt. %)				Base line used	Specific consumption of titrating mixtures (in g/g)			
A	B	C	D		A	B	C	D
Acetone 50, methanol 50	Acetone 40, water 60	—	—	65°	0.568	4.330	—	—
		—	—	65°	0.772	2.150	—	—
		—	—	65°	1.020	1.456	—	—
Octane 50, nonane 50	Butanol 50, nonane 50	Butanol 30, octane 70	Butanol 70, octane 30	115°	0.743	1.720	—	—
				115°	0.866	0.450	—	—
				115°	—	—	0.836	0.754
Methanol 50, water 50	Methanol 50, acetic acid 50	Water 70, acetic acid 30	—	100 Ω	0.470	0.305	—	—
			—	200 Ω	1.720	0.170	—	—
			—	200 Ω	1.400	0.422	1	—

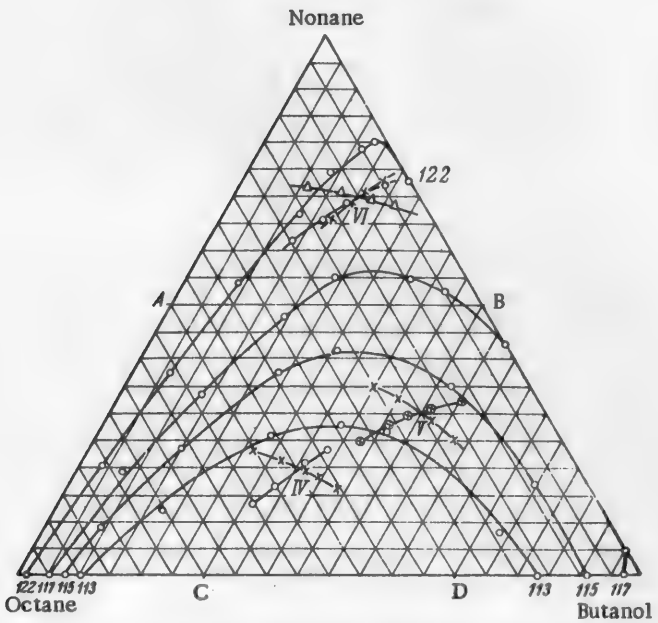

Fig. 4. The system n-butanol–n-octane–n-nonane.

To a weighed amount of the unknown solution, accurately measured amounts of the "titrating" mixture were added, and the boiling point or conductance was measured after each addition. The specific consumption of the "titrating" mixture at which the property reaches a value corresponding to the selected base line was found from the results by interpolation.

The specific consumption of the "titrating" mixtures can be determined much more simply by continuous addition of the mixture from a buret, as in volumetric titration.

A separate column in Table 3 contains the values of the properties chosen for the base lines. These lines, corresponding to constant values of the properties, were used for determinations of the compositions of the solutions

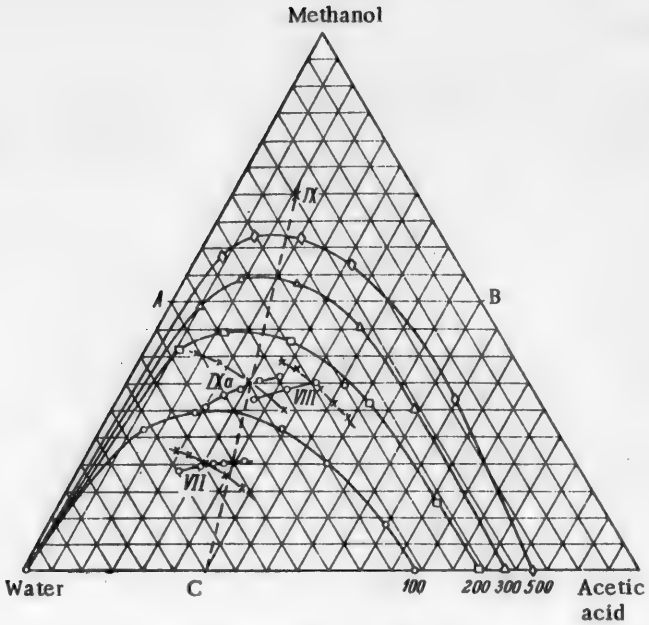

Fig. 5. The system methanol–water–acetic acid.

at each point. The values found for the specific consumptions of the "titrating" mixtures were used to plot auxiliary lines with the aid of the lever rule; the intersection ofthese lines determined the composition of the unknown mixture. To demonstrate that the composition of the "titrating" mixtures can be varied, the mixtures C and D and pure n-nonane were used for titration of mixture VI in the system n-butanol–n-octane–n-nonane. It is seen in Fig. 4 that all three auxiliary lines intersect at one point, satisfactorily near to the true composition of the mixture.

It is sometimes found when the chosen property of the unknown mixture has been determined that the composition of the mixture lies in a concentration region in which it is difficult or impossible to use theexisting base lines. In such a case a definite amount of a mixture of known composition may be added to the unknown mixture, giving a new mixture of a composition which is in a region of the Gibbs triangle favorable for analysis. As an illustration, this procedure was used for analysis of mixture IX in the system methanol–water–acetic acid. To this mixture (which had a resistance of 778 ohms in the cell used) an equal weight of solution C was added. The composition of the new mixture IXa was determined by titration with solutions A and B, and the composition of the original unknown mixture IX was calculated from the result. With the aid of this method it is possible to analyze almost any mixture even if only a limited number of base lines is available.

It is seen in Table 3 that good agreement was obtained between the found and actual compositions in all cases; this confirms the practical applicability of theproposed method.

This method is also applicable in principle to systems of more than three components. However, its practical application in such cases is extremely difficult, as even for a four-component system a space diagram must be used to represent the concentrations, while the base line becomes a surface.

SUMMARY

1. A method for determination of the composition of three-component systems, based on measurement of a single property, is proposed.

2. The method has been tested for 3 three-component systems: acetone–methanol–water, n-butanol–n-octane–n-nonane, and methanol–water–acetic acid, the property determined being the boiling point or the electrical conductance.

The results confirmed the practical applicability of the proposed method.

Received June 6, 1956

ISOTHERMS FOR THE RECIPROCAL AQUEOUS SYSTEM AMMONIUM MONOPHOSPHATE – SODIUM NITRATE – WATER AT LOW TEMPERATURES, −10, −15, and −20°

S. Ia. Shpunt

Scientific Research Institute of Fertilizers and Insectofungicides

As reported in the preceding paper [1], diagrams for ternary systems and diagonal and internal sections [2-5] for the reciprocal aqueous system ammonium monophosphate–sodium nitrate–water were used to derive the isotherms for +30, +20, and 0°. In the present investigation the polythermal method was used to plot isotherms for the same system in a region of lower temperatures: −10, −15, and −20°. One of these, for −10°, was checked by the isothermal method.

The isotherm for −10° (Table 1, Fig. 1) is characterized by five saturation fields: $NaNO_3$, NH_4NO_3, $NH_4H_2PO_4$, $NaH_2PO_4 \cdot 2H_2O$ and ice.

The ice field is bounded by the crystallization curves for ice in the ternary systems $NH_4H_2PO_4-NH_4NO_3-H_2O$ and $NH_4H_2PO_4-NaH_2PO_4-H_2O$ and the curve in the quaternary system separating the monoammonium phosphate and ice fields.

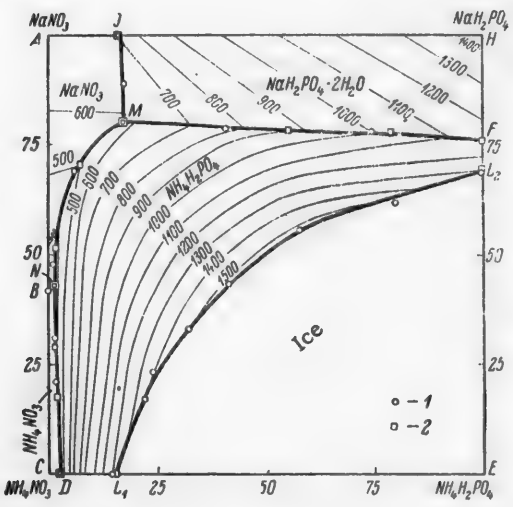

Fig. 1. The isotherm for −10°.
Data: 1) polythermal, 2) isothermal.

The isotherm for −15° (Table 1, Fig. 2) has three univariant points: M, N, and R.

At the point R the solution is in equilibrium with the solid phases $NH_4H_2PO_4 + NaH_2PO_4 \cdot 2H_2O$ + ice. The ice field is bounded by curves for the quaternary systems separating the fields of: a) monosodium phosphate and ice, and b) monoammonium phosphate and ice.

The isotherm for −20° (Table 1, Fig. 3) has three univariant points Q, R, and S in addition to points M and N. At the point Q the solution is in equilibrium with the solid phases $NaNO_3 + NaH_2PO_4 \cdot 2H_2O$ + ice; at the point R, with $NH_4H_2PO_4 + NaH_2PO_4 \cdot 2H_2O$ + ice; and at the point S, with $NH_4H_2PO_4 + NH_4NO_3$ + ice.

The ice field at −20° is bounded by curves for the quaternary systems separating the fields of: a) sodium nitrate and ice; b) monosodium phosphate and ice; c) monoammonium phosphate and ice; and d) ammonium nitrate and ice.

Data on the multiple points in the isotherms for −20, −15, and −10° are given in Table 2.

In order to follow variations in the composition at the univariant points M and N, and to determine graphically the composition and temperature for the invariant points, 3 projections were drawn on the coordinate planes $NaNO_3-O-t°$, $NH_4NO_3-O-t°$ and $NaH_2PO_4-O-t°$, based on the data in Table 3.

TABLE 1

Curves JM, FM, MN, BN, and DN in the Isotherms at −10, −15, and −20°

Point	Contents in solution (in moles per 100 moles of dry salts)					Method
	$NaNO_3$	NH_4NO_3	$NH_4H_2PO_4$	NaH_2PO_4	H_2O	
Isotherm for −10°						
Curve *JM*						
$NaH_2PO_4 \cdot 2H_2O + NaNO_3$						
J	83.5	—	—	16.5	714	Isothermal
	83.7	—	—	16.3	721	Polythermal
	71.0	10.8	18.2	—	681	Polythermal
$NaH_2PO_4 \cdot 2H_2O + NaNO_3 + NH_4H_2PO_4$						
M	80.3	2.3	17.4	—	579	Isothermal
Curve *FM*						
$NH_4H_2PO_4 + NaH_2PO_4 \cdot 2H_2O$						
F	—	—	23.7	76.3	1141	Polythermal
	28.2	—	22.0	56.8	967	Isothermal
	25.1	—	21.6	53.3	997	Polythermal
	44.5	—	21.5	34.0	865	Isothermal
	58.9	—	21.1	20.1	841	Polythermal
$NH_4H_2PO_4 + NaH_2PO_4 \cdot 2H_2O + NaNO_3$						
M	80.3	2.3	17.4	—	579	Isothermal
Curve *MN*						
$NH_4H_2PO_4 + NaH_2PO_4 \cdot 2H_2O + NaNO_3$						
M	80.3	2.3	17.4	—	579	Isothermal
	82.3	—	17.1	—	638	Polythermal
$NaNO_3 + NH_4H_2PO_4$						
	70.5	22.3	7.2	—	500	Isothermal
	69.4	24.6	6.0	—	533	Polythermal
	51.7	46.2	2.1	—	369	Isothermal
	47.9	50.9	1.2	—	348	Polythermal
$NaNO_3 + NH_4H_2PO_4 + NH_4NO_3$						
N	43.0	55.8	1.2	—	325	Isothermal
Curve *BN*						
$NaNO_3 + NH_4NO_3$						
B	41.5	58.5	—	—	323	Polythermal
$NaNO_3 + NH_4H_2PO_4 + NH_4NO_3$						
N	43.0	55.8	1.2	—	325	Isothermal

TABLE 1 (continued)

Point	Contents in solution (in moles per 100 moles of dry salts)					Method
	$NaNO_3$	NH_4NO_3	$NH_4H_2PO_4$	NaH_2PO_4	H_2O	
			Curve *DN*			
			$NH_4H_2PO_4 + NH_4NO_3$			
D	—	97.4	2.6	—	497	Isothermal
	—	97.3	2.7	—	498	Polythermal
	17.6	80.4	2.0	—	426	Isothermal
	21.1	77.3	1.6	—	401	Polythermal
	28.9	69.6	1.5	—	377	Isothermal
	30.8	67.9	1.3	—	373	Polythermal
			$NaNO_3 + NH_4H_2PO_4 + NH_4NO_3$			
N	43.0	55.8	1.2	—	325	Isothermal
			Curve L_1L_2			
			$NH_4H_2PO_4 +$ ice			
L_1	—	84.8	15.2	—	1243	Isothermal
	—	85.1	14.9	—	1246	Polythermal
	16.8	60.8	22.4	—	1386	
	23.7	53.0	23.3	—	1387	
	32.7	34.8	32.5	—	1500	
	42.9	15.3	41.8	—	1550	
	41.8	—	43.9	14.3	1540	
	19.5	—	38.6	41.9	1485	
L_2	—	—	30.8	69.2	1325	Isothermal
	—	—	30.1	69.9	1364	Polythermal
			Isotherm for —15°			
			Curve *JM*			
			$NaNO_3 + NaH_2PO_4 \cdot 2H_2O$			
J	84.4	—	—	15.6	767	Polythermal
	69.9	11.3	—	18.8	700	
			$NaH_2PO_4 \cdot 2H_2O + NH_4H_2PO_4 + NaNO_3$			
M	80.5	2.5	17.0	—	588	Polythermal
			Curve *RM*			
			$NaH_2PO_4 \cdot 2H_2O + NH_4H_2PO_4 +$ ice			
R	29.0	22.4	—	48.6	935	Polythermal
			$NaH_2PO_4 \cdot 2H_2O + NH_4H_2PO_4$			
	63.6	—	21.1	15.3	915	Polythermal
			$NaH_2PO_4 \cdot 2H_2O + NH_4H_2PO_4 + NaNO_3$			
M	80.5	2.5	17.0	—	588	Polythermal

TABLE 1 (continued)

Point	Contents in solution (in moles per 100 moles of dry salts)					Method
	$NaNO_3$	NH_4NO_3	$NH_4H_2PO_4$	NaH_2PO_4	H_2O	
			Curve *MN*			
			$NaH_2PO_4 \cdot 2H_2O + NH_4H_2PO_4 + NaNO_3$			
M	80.5	2.5	17.0	—	588	Polythermal
			$NaNO_3 + NH_4H_2PO_4$			
	68.7	25.6	5.7	—	549	Polythermal
	46.4	52.5	1.1	—	361	
			$NH_4H_2PO_4 + NaNO_3 + NH_4NO_3$			
N	45.3	53.4	1.3	—	337	Polythermal
			Curve *ND*			
			$NH_4H_2PO_4 + NaNO_3 + NH_4NO_3$			
N	45.3	53.4	1.3	—	337	Polythermal
			$NH_4H_2PO_4 + NH_4NO_3$			
	29.5	69.4	1.1	—	407	Polythermal
	20.1	78.4	1.5	—	444	
D	—	97.3	2.7	—	524	
			Curve L_1R			
			$NH_4H_2PO_4$ + ice			
L_1	—	95.1	4.9	—	738	Polythermal
	19.1	73.8	7.1	—	804	
	27.7	64.6	7.7	—	839	
	42.1	47.8	11.1	—	925	
	58.2	21.5	20.3	—	993	
	61.9	—	23.3	14.8	991	
			$NaH_2PO_4 \cdot 2H_2O + NH_4H_3PO_4$ + ice			
R	29.0	22.4	—	48.6	935	Polythermal
			Curve L_4R			
			$NaH_2PO_4 \cdot 2H_2O$ + ice			
L_4	58.6	—	—	41.4	1073	Polythermal
	48.5	7.9	—	43.6	975	
			$NaH_2PO_4 \cdot 2H_2O + NH_4H_2PO_4$ + ice			
R	29.0	22.4	—	48.6	935	Polythermal

TABLE 1 (continued)

Point	Contents in solution (in moles per 100 moles of dry salts)					Method
	$NaNO_3$	NH_4NO_3	$NH_4H_2PO_4$	NaH_2PO_4	H_2O	
			Isotherm for −20°			
			Curve L_5Q			
			$NaNO_3$ + ice			
L_5	86.2	13.8	—	—	675	Polythermal
	87.4	—	12.6	—	728	
			$NaH_2PO_4 \cdot 2H_2O + NaNO_3$ + ice			
Q	70.8	10.7	—	18.5	740	Polythermal
			Curve QR			
			$NaH_2PO_4 \cdot 2H_2O + NH_4H_2PO_4$ + ice			
Q	70.8	10.7	—	18.5	740	Polythermal
			$NaH_2PO_4 \cdot 2H_2O + NH_4H_2PO_4$ + ice			
R	63.3	17.7	—	19.0	633	Polythermal
			Curve RM			
			$NaH_2PO_4 \cdot 2H_2O + NH_4H_2PO_4$ + ice			
R	63.3	17.7	—	19.0	633	Polythermal
			$NaH_2PO_4 \cdot 2H_2O + NH_4H_2PO_4 + NaNO_3$			
M	79.3	3.0	17.7	—	650	Polythermal
			Curve QM			
			$NaH_2PO_4 \cdot 2H_2O + NaNO_3$ + ice			
Q	70.8	10.7	—	18.5	740	Polythermal
			$NaH_2PO_4 \cdot 2H_2O + NH_4H_2PO_4 + NaNO_3$			
M	79.3	3.0	17.7	—	650	Polythermal
			Curve MN			
			$NaH_2PO_4 \cdot 2H_2O + NH_4H_2PO_4 + NaNO_3$			
M	79.3	3.0	17.7	—	650	Polythermal
			$NaNO_3 + NH_4H_2PO_4$			
	70.0	24.8	5.2	—	576	Polythermal
	47.9	51.0	1.1	—	376	

TABLE 1 (continued)

Point	Contents in solution (in moles per 100 moles of dry salts)					Method
	$NaNO_3$	NH_4NO_3	$NH_4H_2PO_4$	NaH_2PO_4	H_2O	
			$NH_4H_2PO_4 + NaNO_3 + NH_4NO_3$			
N	47.4	51.5	1.1	—	373	Polythermal
			Curve *BN*			
			$NaNO_3 + NH_4NO_3$			
B	46.0	54.0	—	—	386	Polythermal
			$NH_4H_2PO_4 + NaNO_3 + NH_4NO_3$			
N	47.4	51.5	1.1	—	373	Polythermal
			Curve *NS*			
			$NH_4H_2PO_4 + NaNO_3 + NH_4NO_3$			
N	47.4	51.5	1.1	—	373	Polythermal
			$NH_4H_2PO_4 + NH_4NO_3$			
	30.7	67.7	1.6	—	473	Polythermal
			$NH_4H_2PO_4 + NH_4NO_3 +$ ice			
S	21.1	77.1	1.8	—	488	Polythermal
			Curve L_6S			
			$NH_4NO_3 +$ ice			
L_6	23.2	76.8	—	—	536	Polythermal
			$NH_4H_2PO_4 + NH_4NO_3 +$ ice			
S	21.1	77.1	1.8	—	488	Polythermal
			Curve *RS*			
			$NaH_2PO_4 \cdot 2H_2O + NH_4H_2PO_4 +$ ice			
R	63.3	17.7	—	19.0	633	Polythermal
			$NH_4H_2PO_4 +$ ice			
	67.6	24.1	8.3	—	682	Polythermal
	47.5	50.3	2.2	—	613	
	30.4	66.9	2.7	—	562	
			$NH_4H_2PO_4 + NH_4NO_3 +$ ice			
S	21.1	77.1	1.8	—	488	Polythermal

TABLE 2

Multiple Points in the Reciprocal System $NaNO_3-NH_4H_2PO_4-H_2O$

Point	Contents in solution (in moles per 100 moles of dry salts)					Solid phases	Method
	$NaNO_3$	NH_4NO_3	$NH_4H_2PO_4$	NaH_2PO_4	H_2O		
				Isotherm for —10°			
A . . .	100.0	—	—	—	714	$NaNO_3$	Polythermal
B . . .	41.5	58.5	—	—	322	$NaNO_3 + NH_4NO_3$	
C . . .	—	100.0	—	—	497	NH_4NO_3	
D . . .	—	97.4	2.6	—	497	$NH_4H_2PO_4 + NH_4NO_3$	Isothermal
D * . .	—	97.3	2.7	—	498	The same	Polythermal
L_1 . . .	—	84.8	15.2	—	1243	$NH_4H_2PO_4$ + ice	Isothermal
L_1* . .	—	85.1	14.9	—	1246	$NH_4H_2PO_4$ + ice	Polythermal
L_2 . . .	—	—	30.8	69.2	1325	The same	Isothermal
L_2* . .	—	—	30.1	69.9	1364	The same	Polythermal
F . . .	—	—	23.7	76.3	1141	$NH_4H_2PO_4 + NaH_2PO_4 \cdot 2H_2O$	
H . . .	—	—	—	100.0	1391	$NaH_2PO_4 \cdot 2H_2O$	
J . . .	83.5	—	—	16.5	714	$NaH_2PO_4 \cdot 2H_2O + NaNO_3$	Isothermal
J . . .	83.7	—	—	16.3	721	The same	Polythermal
M . . .	80.3	2.3	17.4	—	579	$NaH_2PO_4 \cdot 2H_2O + NaNO_3 + NH_4H_2PO_4$	Isothermal
N . . .	43.0	55.8	1.2	—	325	$NaNO_3 + NH_4H_2PO_4 + NH_4NO_3$	

* Bergman and Bochkarev's polythermal data [6].

TABLE 2 (continued)

Point	Contents in solution (in moles per 100 moles of dry salts)					Solid phases	Method
	$NaNO_3$	NH_4NO_3	$NH_4H_2PO_4$	NaH_2PO_4	H_2O		
				Isotherm for −15°			
A . . .	100.0	—	—	—	742	$NaNO_3$	Isothermal
B . . .	43.7	56.3	—	—	353	$NaNO_3 + NH_4NO_3$	
C . . .	—	—	—	—	570	NH_4NO_3	
D * . .	—	97.3	2.7	—	524	$NH_4H_2PO_4 + NH_4NO_3$	Polythermal
L_1* . .	—	95.1	4.9	—	738	$NH_4H_2PO_4$ + ice	
L_4 . . .	58.6	—	—	41.4	1073	$NaH_2PO_4 \cdot 2H_2O$ + ice	
J . . .	84.4	—	—	15.6	767	$NaH_2PO_4 \cdot 2H_2O + NaNO_3$	
R . . .	29.0	22.4	—	48.6	935	$NaH_2PO_4 \cdot 2H_2O + NH_4H_2PO_4$ + ice	
M . . .	80.5	2.5	17.0	—	588	$NaH_2PO_4 \cdot 2H_2O + NH_4H_2PO_4 + NaNO_3$	
N . . .	45.3	53.4	1.3	—	337	$NH_4H_2PO_4 + NaNO_3 + NH_4NO_3$	
				Isotherm for −20°			
L_5 . . .	86.2	13.8	—	—	675	$NaNO_3$ + ice	Polythermal
B . . .	46.0	54.0	—	—	386	$NaNO_3 + NH_3NO_3$	
L_6 . . .	23.2	76.8	—	—	536	NH_4NO_3 + ice	
Q . . .	70.8	10.7	—	18.5	740	$NaH_2PO_4 \cdot 2H_2O + NaNO_3$ + ice	
R . . .	63.3	17.7	—	19.0	633	$NaH_2PO_4 \cdot 2H_2O + NH_4H_2PO_4$ + ice	
M . . .	79.3	3.0	17.7	—	650	$NaH_2PO_4 \cdot 2H_2O + NH_4H_2PO_4 + NaNO_3$	
N . . .	47.4	51.5	1.1	—	373	$NH_4H_2PO_4 + NaNO_3 + NH_3NO_3$	
S . . .	21.1	77.1	1.8	—	488	$NH_4H_2PO_4 + NH_4NO_3$ + ice	

TABLE 3

Eutectic Points of the Ternary Systems, ($NaNO_3$–$NH_4H_2PO_4$–H_2O), Diagonals of the Internal Sections, and Univariant Points M and N

System and univariant points	Temperature (°C)	Contents in solution (in moles per 100 moles of dry salts)					Solid phases
		$NaNO_3$	NH_4NO_3	$NH_4H_2PO_4$	NaH_2PO_4	H_2O	
$NaNO_3$—NH_4NO_3—H_2O	—25.7	48.7	51.3	—	—	439	$NaNO_3 + NH_4NO_3 +$ ice
NH_4NO_3—$NH_4H_2PO_4$—H_2O	—16.8	—	96.6	3.4	—	614	$NH_4NO_3 + NH_4H_2PO_4 +$ ice
$NH_4H_2PO_4$—NaH_2PO_4—H_2O	—12.1	—	—	24.0	76.0	1254	$NH_4H_2PO_4 + NaH_2PO_4 \cdot 2H_2O +$ ice
$NaNO_3$—NaH_2PO_4—H_2O	—19.3	85.7	—	—	14.3	816	$NaNO_3 + NaH_2PO_4 \cdot 2H_2O +$ ice
$NaNO_3$—$NH_4H_2PO_4$—H_2O	—20.6	85.0	—	15.0	—	707	$NaNO_3 + NaH_2PO_4 \cdot 2H_2O +$ ice
Section I	—14.0	3.8	21.4	—	74.8	1084	$NH_4H_2PO_4 + NaH_2PO_4 \cdot 2H_2O +$ ice
Section II	—15.8	36.6	21.7	—	41.7	952	The same
Section III	—22.2	65.1	29.9	—	5.0	589	$NH_4H_2PO_4 + NaNO_3 +$ ice
Section IV	—28.2	45.7	63.5	—	0.8	398	The same
Section V	—21.5	29.1	69.4	—	1.5	495	$NH_4H_2PO_4 + NH_4NO_3 +$ ice
Section VI	—20.0	19.6	78.9	—	1.5	488	The same
Section VII	—20.2	70.7	10.7	—	18.5	740	$NaNO_3 + NaH_2PO_4 \cdot 2H_2O +$ ice
	+30.0	26.6	17.8	—	56.7	378	
	+20.0	44.9	18.5	—	36.6	446	
M	0.0	59.4	20.1	—	20.5	553	$NH_4H_2PO_4 + NaNO_3 + NaH_2PO_4 \cdot 2H_2O$
	—10.0	62.9	19.7	—	17.4	479	
	—15.0	63.5	19.5	—	17.0	588	
	—20.5	63.8	19.5	—	16.9	602	
	+30.0	26.7	72.5	—	0.8	147	
	+20.0	29.5	69.7	—	0.8	171	
N	0.0	37.0	62.1	—	0.9	255	$NH_4H_2PO_4 + NaNO_3 + NH_4NO_3$
	—10.0	41.8	57.0	—	1.2	305	
	—15.0	44.8	54.7	—	1.3	337	
	—20.0	46.3	52.6	—	1.1	373	

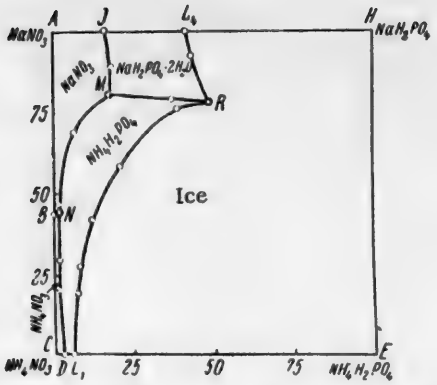

Fig. 2. The isotherm for −15° (polythermal data).

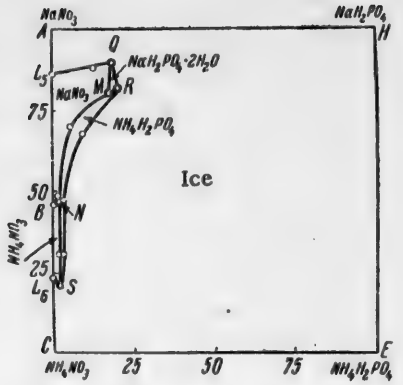

Fig. 3. The isotherm for −20° (polythermal data).

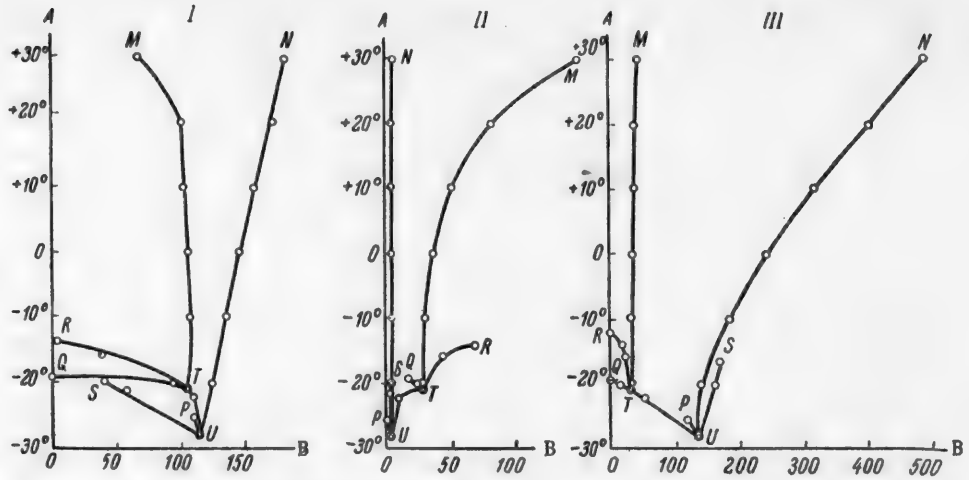

Fig. 4. Invariant points in three projections.
A) Temperature (in °C), B) contents of $NaNO_3$ (I), NaH_2PO_4 (II), and NH_4NO_3 (III) (in moles per 1000 moles H_2O).

Each projection (Fig. 4) contains two invariant points, T and U.

At the point T the solution is in equilibrium with the solid phases $NaNO_3$ + $NaH_2PO_4 \cdot 2H_2O$ + $NH_4H_2PO_4$ + + ice. It corresponds to the composition $NaNO_3$ 27.18%, NH_4NO_3 7.78%, NaH_2PO_4 10.24% and a temperature of −21.0°. At −21.0° the point M disappears; this is directly related to the disappearance of the crystallization field of monosodium phosphate. The explanation for the disappearance of this field is that the ice field of the system grows more rapidly from the directions of the monoammonium phosphate and monosodium phosphate corners, where the total salt contents in the solutions are least. Proof of the fact that four solid phases coexist in equilibrium with the solution at the point T is provided by the intersection of four boundary lines at this point: MT, RT, QT, and UT. a) MT with the solid phases $NaH_2PO_4 \cdot 2H_2O$, $NH_4H_2PO_4$ and $NaNO_3$; b) RT with the solid phases $NH_4H_2PO_4$, $NaH_2PO_4 \cdot 2H_2O$ and ice; c) QT with the solid phases $NaH_2PO_4 \cdot 2H_2O$, $NaNO_3$ and ice; d) UT with the solid phases $NH_4H_2PO_4$, $NaNO_3$ and ice.

The point U is the second invariant point of the system with the solid phases $NaNO_3$ + NH_4NO_3 + $NH_4H_2PO_4$ + + ice.

The coexistence of four solid phases in equilibrium with the solution at the point U is proved by the intersection of four boundary lines at this point: a) NU with the solid phases $NH_4H_2PO_4$, $NaNO_3$ and NH_4NO_3; b) TU with the solid phases $NH_4H_2PO_4$, $NaNO_3$ and ice; c) SU with the solid phases $NH_4H_2PO_4$, NH_4NO_3 and ice; d) PU with the solid phases $NaNO_3$, NH_4NO_3 and ice.

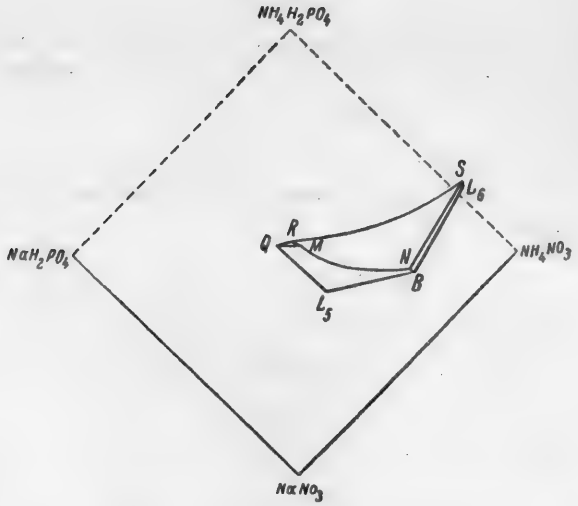

Fig. 5. Space diagram for the −20° isotherm for the system $NaNO_3-NH_4H_2PO_4-H_2O$.

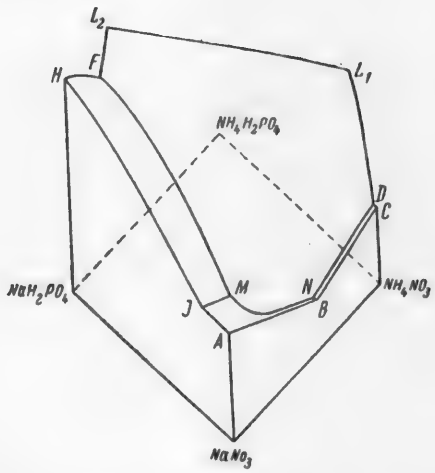

Fig. 6. Space diagram for the −10° isotherm for the system $NaNO_3-NH_4H_2PO_4-H_2O$.

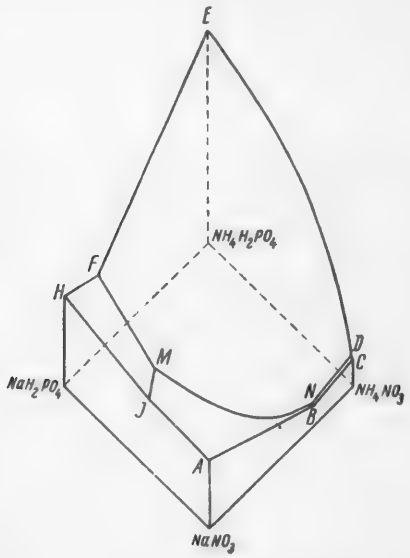

Fig. 7. Space diagram for the +30° isotherm for the system $NaNO_3-NH_4H_2PO_4-H_2O$.

The point U, corresponding to −28.1° and solution composition $NaNO_3$ 25.18%, NH_4NO_3 27.74% and NaH_2PO_4 0.60%, is the final crystallization point of the system.

Space diagrams for the −20° and −10° isotherms for the system $NaNO_3-NH_4H_2PO_4-H_2O$ are given in Figs. 5 and 6. For comparison, the isotherm for +30° [1] is shown in Fig. 7.

The bases of the space diagrams are Jänecke squares, the number of moles of water per 100 moles of salts at the corresponding points being plotted upward. The space diagrams show that in solutions saturated with $NH_4H_2PO_4$ relatively large amounts of water are present, whereas the amounts of water in solutions saturated with NH_4NO_3 are relatively small. The nature of the polythermal variations of the crystallization fields shows that sodium nitrate can be separated out by evaporation, and monoammonium phosphate by cooling of the solution.

SUMMARY

1. Isotherms for −10, −15, and −20° have been derived from polythermal data for the ternary systems, diagonals, and internal sections. The isotherm for −10° was verified by an isothermal method.

Double salts and mixed crystals are not formed in the system.

2. The nature of the polythermal variations of the crystallization fields in the space isotherms for −20°, −10°, and +30°, shows that sodium nitrate can be separated out by evaporation, and monoammonium phosphate by crystallization of the solutions.

LITERATURE CITED

[1] S. Ia. Shpunt, J. Appl. Chem. 30, 7, 985 (1957).*

[2] S. Ia. Shpunt, J. Appl. Chem. 13, 1, 9-18 (1940).

[3] S. Ia. Shpunt, J. Appl. Chem. 13, 1, 19-28 (1940).

[4] S. Ia. Shpunt, J. Appl. Chem. 19, 3, 293 (1946).

[5] S. Ia. Shpunt, J. Appl. Chem. 20, 57, 685 (1947).

[6] A. G. Bergman and N. F. Bochkarev, Bull. Acad. Sci. USSR, Chem. Ser. 1, 248 (1938).

Received October 12, 1955

* Original Russian pagination. See C. B. Translation.

STIRRER SPEEDS IN THE STIRRING OF SUSPENSIONS

I. S. Pavlushenko, N. M. Kostin and S. F. Matveev

The Lensoviet Technological Institute, Leningrad

The stirring of suspensions has been studied by White et al. [1], Shpanov [2], Hixson and Tenney [3], Miller and Mann [4], Mel'nikov [5], and others. The most important problem considered by these authors was the choice of a method for characterization of the quality of mixing and determination of the working rate of the stirrers. This question was examined most fully by Miller and Mann, but their proposed method often leads to an erroneous evaluation of the results of stirring.

It was shown in one of our earlier papers [6] that the operating rate of stirrers can be suitably characterized by the rotation speed at which the distribution of the solid phase in the system becomes almost uniform. This speed, termed the determining speed (n_0) can be found from comparisons of the relative concentrations of the suspended solid phase in the vessel at different levels. The possibility of deriving an expression for calculation of the determining speed from given physicochemical characteristics of the solid and liquid phases of the stirred system was considered in the same paper.

In fact, the sedimentation rate of a solid particle (provided that it is spherical, and with the influence of the walls of the vessel and the influence of simultaneously settling particles neglected) is, as was shown previously [7], given by the following expression:

$$w_s = \varphi\ (\mu, \rho_m, \rho_p, d_p, g),^*$$

while the axial component of the velocity of the liquid moved by a stirrer of a given type (with the distance from the axis of rotation disregarded) has been shown [8] to be represented by the expression

$$w = \varphi'\ (\mu, \rho_m, n, d_M, D).$$

From these two relationships we have

$$n_0 = \varphi''\ (\mu, \rho_m, \rho_p, d_p, d_M, D, g).$$

The concentration of the solid phase is a very important characteristic of a suspension. This can be taken into account by the introduction of the weights of the solid (G_s) and liquid (G_l) phases.** Further, for a complete description of the dimensions of the stirred system the function must also include the height of the layer of suspension (H_0) in the mixer. We then have

---

* The following notation is used throughout this paper: d_M – diameter of the stirrer (in meters), d_p – diameter of the particles (in meters), D – diameter of the vessel (in meters), g – acceleration of free motion (meters/sec.), H_0 – total height of the layer of suspension (in meters), h_v – depth of the vortex reckoned from the stationary liquid level (in meters), n – rotation speed of stirrer (revolutions/sec.), n_0 – determining speed (revolutions/sec.), G_s (G_l) – weight of solid (liquid) phase in the suspension (in kg), v_s (v_l) – volume of solid (liquid) phase in the suspension (in cubic meters), w – linear speed (in meters/sec.), μ – viscosity of the liquid (kg/sec · m^2), ρ_p (ρ_m) – density of solid (liquid) phase (in kg/sec^2 · m^4).

** The amounts of the solid and liquid phases can also be expressed in volume units (v_s and v_l).

$$n_0 = f\ (\mu, \rho_m, \rho_p, d_p, d_M, D, H_0, G_s, G_l, g). \qquad (1)$$

It is desirable to show the whole analysis of this relationship, as the problem in question is a very interesting application of dimensional analysis. The Function (1) can be represented in the form of a mononomial product of powers

$$[n_0] = C \cdot [\mu]^h \cdot [\rho_m]^i \cdot [\rho_p]^k \cdot [d_p]^l \cdot [d_M]^m \cdot [D]^p \cdot [H_0]^q \cdot [G_s]^r \cdot [G_l]^s \cdot [g]^t$$

or in the form of a dimensional equation

$$[1/\text{sec.}] = C \cdot [\text{kg} \cdot \text{sec.}/\text{m}^2]^h \cdot [\text{kg} \cdot \text{sec}^2/\text{m}^4]^i \cdot [\text{kg} \cdot \text{sec.}/\text{m}^4]^k \cdot [\text{m}]^l \cdot [\text{m}]^m \cdot [\text{m}]^p \cdot [\text{m}]^q \times$$

$$\times [\text{kg}]^r \cdot [\text{kg}]^s \cdot [\text{m}/\text{sec}^2]^t.$$

This may be reduced to a system of three equations with ten unknowns

$$\left.\begin{aligned} h + i + k + r + s &= 0 \\ h + 2i + 2k - 2t + 1 &= 0 \\ 2h + 4i + 4k - l - m - p - q - t &= 0 \end{aligned}\right\} \qquad (2)$$

We evidently cannot solve this system of equations for the exponents [2], but it may be transformed by taking any seven quantities as fixed and expressing the other three in terms of these. The total number of combinations which can be taken as fixed is the number of combinations from ten quantities taken seven at a time, i.e., $C_{10}^7 = 120$. This does not mean, however, that all 120 transformations must be performed. This problem, like most others, may be considerably simplified by exclusion of combinations which make the transformations impossible, or give duplicated series of similitude criteria, or give rise to criteria which are not normally used.

Thus, in each of the three Equations (2) the coefficients of i and k are equal, and consequently all combinations which do not contain at least one of these two quantities must be excluded, as they make transformation of the system impossible. The quantities r and s, and also l, m, and p, are respectively found in only one equation in the system, and therefore all combinations which do not contain at least one of the first two, or three of the last four quantities, must be excluded.

Further, it must be taken into account that the system in question contains several quantities which are exponents of physicochemical characteristics of the same dimensions. It is clear that combinations differing, say, only in values of i and k, will give similar criteria, containing either ρ_p or ρ_m. If we take ρ_m as the determining magnitude (as in some instances criteria containing ρ_p have no physical meaning), we find that k must be one of the predetermined quantities. Similarly, if we choose the diameter of the impeller (d_M) as the determining geometrical dimension, we find that the exponents of d_p and D, and H_0, i.e., l, p, and q, must be taken as fixed.

Finally, it must be remembered that the required criterion is composed of physicochemical characteristics the exponents of which appear on transformation of the system of exponent equations, and is not composed of the physicochemical quantities of exponents taken as fixed. As weight does not enter into any of the usual criteria, it is evident that both r and s must be included with the fixed quantities in transformation of the system (2) in order to avoid having an unusual criterion.

Therefore combinations which make transformation of the system (2) possible but which do not give duplicated series of criteria or give rise to a criterion of unusual form must contain the quantities k, l, p, q, r, and s, but must not include i. Evidently there can be only three such combinations: k, l, p, q, r, s, h; k, l, p, q, r, s, m and k, l, p, q, r, s, t. After the necessary steps, we obtain three criterial equations* which are equivalent in principle; the most convenient of these is the one for fixed values of k, l, p, q, r, s, t,

* It may incidentally be noted that Eigenson's conclusions [9] concerning the least number of simplex criteria and the greatest number of complex criteria are not confirmed in practice, as they are apparently not general.

$$\frac{n_0 \cdot \rho_m \cdot d_M^2}{\mu} = C \cdot \left(\frac{d_M^3 \cdot \rho_m^2 \cdot g}{\mu^2}\right)^t \cdot \left(\frac{\rho_p}{\rho_m}\right)^k \cdot \left(\frac{d_p}{d_M}\right)^l \cdot \left(\frac{D}{d_M}\right)^p \times \times \left(\frac{H_0}{d_M}\right)^q \cdot \left(\frac{G_s \cdot \rho_m}{\mu^2}\right)^r \cdot \left(\frac{G_l \cdot \rho_m}{\mu^2}\right)^s. \quad (3)^*$$

This equation may be modified somewhat. It is logical to assume that r = −s.** Then we have

$$\left(\frac{G_s \cdot \rho_m}{\mu^2}\right)^r \cdot \left(\frac{G_l \cdot \rho_m}{\mu^2}\right)^s = \left(\frac{G_s}{G_l}\right)^r,$$

i.e., we have the ordinary expression for weight concentrations (kg/kg).

The final generalized equation for the stirring of suspensions will be of the form:

$$\frac{n_0 \cdot \rho_m \cdot d_M^2}{\mu} = C \cdot \left(\frac{d_M^3 \cdot \rho_m^2 \cdot g}{\mu^2}\right)^t \cdot \left(\frac{\rho_p}{\rho_m}\right)^k \cdot \left(\frac{d_p}{d_M}\right)^l \cdot \left(\frac{D}{d_M}\right)^p \cdot \left(\frac{H_0}{d_M}\right)^q \cdot \left(\frac{G_s}{G_l}\right)^r \quad ***$$

or, in abbreviated notation

$$Re = C \cdot Ga^t \cdot S_\rho^k \cdot \Gamma_{d_p}^l \cdot \Gamma_D^p \cdot \Gamma_{H_0}^q \cdot S_G^r. \quad (4)$$

The purpose of the present investigation was the experimental determination of the exponents of the similitude criteria and the coefficient of Equation (4).

EXPERIMENTAL

The experiments were performed with the aid of special equipment in which the stirrer speed could be varied smoothly between 75 and 750 r.p.m. by means of a direct-current motor and two four-step sheaves [8, 10]. The usual experimental procedure was employed [6]. The apparatus consisted of a glass vessel 300 mm in diameter, with a convex bottom, and three-blade impellers of stainless steel, 75, 100, and 150 mm in diameter with a pitch ratio of 1 [11]. The distance between the stirrer and the bottom of the vessel was kept constant at 30 mm. Samples were taken by means of a special sampling device [6] at 40, 100, 200, and 280 mm from the bottom at points 35 mm from the wall of the vessel.

The solid phases used were carefully sifted narrow fractions of sand (γ = 2630 kg/cubic meter) and iron ore (γ = 4750 kg/cubic meter) with particle sizes 0.95 + 0.7 (d_p = 0.825 mm)–0.5 + 0.28 (d_p = 0.39 mm),–0.25 + 0.105 (d_p = 0.178 mm),–0.105 + 0.8 (d_p = 0.093 mm) and below 0.08 (d_p = 0.39 mm). The liquid phases were water,

* If the amounts of the solid and liquid phases are expressed in volume units, the equivalent equation is of the form

$$\frac{n_0 \cdot \rho_m \cdot d_M^2}{\mu} = C \cdot \left(\frac{d_M^3 \cdot \rho_m^2 \cdot g}{\mu^2}\right)^t \cdot \left(\frac{\rho_p}{\rho_m}\right)^k \cdot \left(\frac{d_p}{d_M}\right)^l \cdot \left(\frac{D}{d_M}\right)^p \cdot \left(\frac{H_0}{d_M}\right)^q \cdot \left(\frac{v_s}{d_M^3}\right)^r \cdot \left(\frac{v_l}{d_M^3}\right)^s.$$

** The validity of this assumption is confirmed below.

*** With the amounts of solid and liquid phases in volume units, the equation is

$$\frac{n_0 \cdot \rho_m \cdot d_M^2}{\mu} = C \cdot \left(\frac{d_M^3 \cdot \rho_m^2 \cdot g}{\mu^2}\right)^t \cdot \left(\frac{\rho_p}{\rho_m}\right)^k \cdot \left(\frac{d_p}{d_M}\right)^l \cdot \left(\frac{D}{d_M}\right)^p \cdot \left(\frac{H_0}{d_M}\right)^q \cdot \left(\frac{v_s}{v_l}\right)^r.$$

carbon tetrachloride (γ = 1630 kg/cubic meter, μ = 1.12 cps*), aqueous solutions of technical glycerin (γ = 1230 kg/cubic meter, μ = 120.6 cps, γ = 1186 kg/cubic meter, μ = 22.97 cps, and γ = 1156 kg/cubic meter, μ = 11.11 cps), and technical sulfuric acid (γ = 1836 kg/cubic meter, μ = 30.1 cps).

The total volume of the liquid and solid phase with the vessel filled to a height of 300 mm was 20 liters in all the experiments.

Thirty-eight series of experiments were performed with 8 different systems, at a constant weight concentration of the solid phase, S/L = 1 : 4 (the volume concentration varied between 0.053 and 0.176 cubic meter/cubic meter). In addition, in order to find the influence of the concentration of the solid phase on the determining speed of rotation, 6 series of experiments were performed in which one fraction of quartz sand (d_p = 0.178 mm) was stirred in water, the weight concentration of the solid phase being varied between S/L = 1 : 20 and S/L = 1 : 2 (the respective volume concentrations were between 0.02 and 0.19 cubic meter/cubic meter).

In each series of experiments the values found for the contents of the solid phase at different points in the vessel (mean values of three determinations) were used to calculate the relative concentrations, i.e., the concentrations of the solid phase as percentages of the concentration which would exist in the system if the solid phase had been distributed uniformly (I), and the variations of the relative concentration of the solid phase at different levels with increase of stirrer speed (n) were plotted;** the determining speeds (n_0) were then found. The experimental data are presented in the Table.

DISCUSSION OF RESULTS

All the graphs for the variations of the relative concentration of the solid phase at different levels of the suspension with increasing speed of the stirrer can be classified into three types.

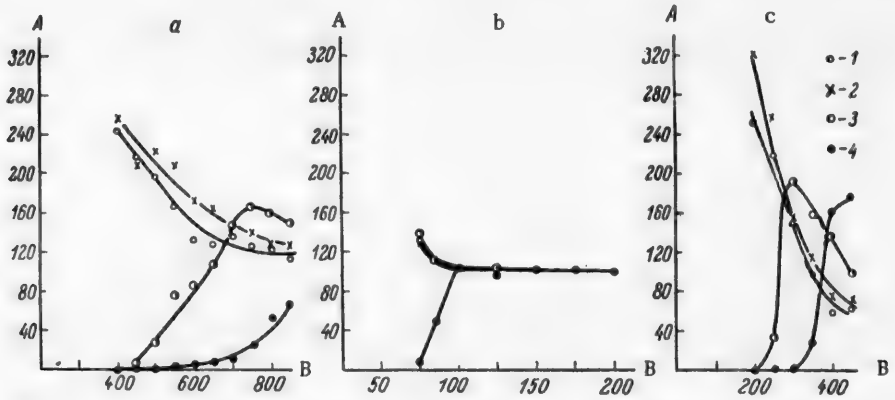

Fig. 1. Variations of the relative concentrations of the solid phase in a suspension at different levels with increasing stirrer speed.
A) Relative concentration J (%), B) stirrer speed, rpm.
Distance from bottom of vessel: 1) 40, 2) 100, 3) 200, 4) 280.
a) System CCl_4 – sand (D = H = 300 mm, d_M = 100 mm); and: d_p = (–0.5 + 0.28) mm, γ_p = 2632 kg/cubic meter; CCl_4: μ = 1.2 cps, γ_m = 1630 kg/cubic meter.
b) System H_2SO_4 – sand (D = H = 300 mm, d_M = 150 mm); sand: d_p = (–0.25 + + 0.105) mm, γ_p = 2632 kg/cubic meter; H_2SO_4: μ = 32.6 cps, γ_m = 1840 kg/cubic meter.
c) System CCl_4 – sand (D = H = 300 mm, d_M = 150 mm); sand: d_p = (–0.95 + 0.7) mm, γ_p = 2632 kg/cubic meter; CCl_4: μ = 1.2 cps, γ_m = 1630 kg/cubic meter.

* All viscosities were determined at 20°; cps = centipoises.
** An average of 31 experimental points are given on each graph.

In the first type of graph (Fig. 1,a) the curve for the variation of the concentration of the solid phase in the upper layer of liquid falls far short of 100% even at the maximum stirrer speed (with the funnel reaching the hub of the stirrer). In such cases the stirring is sluggish and the solid phase is not distributed uniformly throughout the liquid. The stirrer of the design and dimensions chosen is not suitable for stirring the given suspension.

In the second type of graph (Fig. 1,b) all the curves for the variation of the relative concentration of the solid phase beyond a certain speed coalesce into a single line at about 100%; this line remains parallel to the abscissa axis with increase of the stirrer speed. In this case the stirring is intensive, and the distribution of the solid phase is almost uniform throughout the system. The stirrer chosen can be successfully used for stirring the given suspension if operated at the determining speed. It must be emphasized that any further increase of the speed would not influence the uniformity of the distribution of the solid phase.

In the third type of graph (Fig. 1,c) the curve for the variation of the relative concentration of the solid phase in the upper liquid layer not only reaches but considerably exceeds 100%, while the curves for the variations of concentration in the lower layers fall below 100%. Here the stirring is again intensive, but the distribution of the solid phase is less uniform than in the previous case. The selected stirrer is quite suitable for stirring the given suspension if operated at such a speed that the relative concentration of the solid phase in the upper liquid layer is 100%. It must be noted that with further increase of the stirrer speed the distribution of the solid phase will become less uniform, as the solid particles will be preferentially displaced into the upper layers of the liquid. Graphs of this type are characteristic for suspensions containing relatively large particles in liquids of low viscosity. The explanation for the displacement of the solid phase when such suspensions are stirred is that in a liquid of low viscosity the axial velocity component falls steeply from relatively large values at low levels to very small values in the upper layers [8]. Therefore, when the necessary values of the axial component of the velocity vector have been reached at the upper levels, the axial velocities in the lower levels will be excessive and the solid phase will be displaced.

Definition of this effect involves the concept of the determining speed. We define the determining speed as the rotation speed of the stirrer at which the relative concentration of the solid phase in the whole stirred system, or at least in the upper layer of liquid, reaches 100%.

Let us now compare the evaluation of these types of stirring by the methods of Miller and Mann,* and of Mel'nikov [5]. The results of the relevant calculations for the cases illustrated by Fig, 1, a, b, and c, are given below.

Fig. 1	n (rpm)	I_M (%)	τ	n_0 (rpm)
a	850	88.2	5.32	–
b	100	99.15	237	98
c	400	80.3	2.73	375

These calculations show that by Miller and Mann's method (I_M) and by Mel'nikov's method (τ) the stirring is found to be more effective in the first case than in the third, whereas in reality the first case provides a typical example of sluggish stirrer operation, and the third of intensive stirring, with little essential difference from the second. Therefore it follows that the methods for evaluation of the quality of stirring proposed by Miller and Mann, and by Mel'nikov, are formal and do not fully reflect the nature of the effect. It must also be pointed out that the quantities which characterize the degree of uniformity in Mel'nikov's method do not make it possible to estimate the degree of approximation to the optimum conditions.

Further analysis of the data was performed by the usual analytical graphical method.

The results of experiments on the influence of the concentration of the solid phase on the determining rotation speed confirmed the assumption that $r = -s$, i.e., that the exponents of the terms $G_s \cdot \rho_m / \mu^2$ and $G_l \cdot \rho_m / \mu^2$ [Equation (3)] are equal, hence it is legitimate to use the concentration ratio G_s/G_l [Equation (4)]. It was also found that increase of the concentration of the solid phase increases the determining speed only up to S/L = 1 : 5. With further increase of concentration (up to S/L = 1 : 2 in our experiments) the determining rotation speed remains constant (Fig. 2).

* The method of Miller and Mann is described in detail in Kafarov's monograph [12].

Experimental Results

System	Experiment no.	d_p (av. × $\times 10^3$ m)	n_0 (revs./sec.)	Re (experimental values)	Ga	$S_\rho = \frac{\rho_t}{\rho_m}$	$\Gamma_{d_p} = \frac{d_t}{d_M}$	Re (calculated values)	Deviation (%)
$d_M = 0.15$ m; $D = 0.30$ m; $\Gamma_D = \frac{D}{d_M} = 2$									
Water–sand	1	0.035	2.50	$5.64 \cdot 10^4$	$3.32 \cdot 10^{10}$	2.63	$2.33 \cdot 10^{-4}$	$6.16 \cdot 10^4$	− 8.4
	2	0.093	4.25	$9.57 \cdot 10^4$			$6.20 \cdot 10^{-4}$	$9.15 \cdot 10^4$	+ 4.6
	3	0.178	6.25	$1.41 \cdot 10^5$			$1.19 \cdot 10^{-3}$	$1.19 \cdot 10^5$	+18.6
Water–ore	4	0.035	4.67	$1.05 \cdot 10^5$	$3.32 \cdot 10^{10}$	4.74	$2.33 \cdot 10^{-4}$	$9.90 \cdot 10^4$	+ 6.1
	5	0.093	6.50	$1.46 \cdot 10^5$			$6.20 \cdot 10^{-4}$	$1.46 \cdot 10^5$	0.0
Carbon tetrachloride–sand	6	0.035	2.33	$7.60 \cdot 10^4$	$7.00 \cdot 10^{10}$	1.63	$2.33 \cdot 10^{-4}$	$6.55 \cdot 10^4$	+16.1
	7	0.093	2.82	$9.20 \cdot 10^4$			$6.20 \cdot 10^{-4}$	$9.70 \cdot 10^4$	− 5.2
	8	0.178	4.42	$1.44 \cdot 10^5$			$1.19 \cdot 10^{-3}$	$1.26 \cdot 10^5$	+14.3
	9	0.390	5.67	$1.85 \cdot 10^5$			$2.60 \cdot 10^{-3}$	$1.72 \cdot 10^5$	+ 7.6
	10	0.825	6.25	$2.04 \cdot 10^5$			$5.50 \cdot 10^{-3}$	$2.32 \cdot 10^5$	−12.0
Carbon tetrachloride–ore	11	0.178	6.95	$2.77 \cdot 10^5$	$7.00 \cdot 10^{10}$	2.92	$1.19 \cdot 10^{-3}$	$2.02 \cdot 10^5$	+12.4
	12	0.390	11.66	$3.79 \cdot 10^5$			$2.60 \cdot 10^{-3}$	$2.75 \cdot 10^5$	+38.0
Aqueous glycerin (23 cps)–sand	13	0.093	2.17	$2.52 \cdot 10^3$	$8.90 \cdot 10^7$	2.22	$6.20 \cdot 10^{-4}$	$2.26 \cdot 10^3$	+11.5
	14	0.178	2.54	$2.95 \cdot 10^3$			$1.19 \cdot 10^{-3}$	$2.98 \cdot 10^3$	− 1.0
	15	0.390	3.45	$4.00 \cdot 10^3$			$2.60 \cdot 10^{-3}$	$4.05 \cdot 10^3$	− 1.2
	16	0.825	4.45	$5.16 \cdot 10^3$			$5.50 \cdot 10^{-3}$	$5.48 \cdot 10^3$	− 5.8

(continued)

System	Experiment no.	d_p (av. $\times 10^3$ m)	n_0 (revs./sec.)	Re (experimental values)	Ga	$S_\rho = \frac{\rho_p}{\rho_m}$	$\Gamma_{d_p} = \frac{d_i}{d_M}$	Re (calculated values)	Deviation (%)
Aqueous glycerin (11 cps) – sand	17	0.093	2.25	$5.26 \cdot 10^3$	$3.61 \cdot 10^8$	2.28	$6.20 \cdot 10^{-4}$	$5.67 \cdot 10^3$	– 7.1
	18	0.173	2.92	$6.82 \cdot 10^3$			$1.19 \cdot 10^{-3}$	$7.03 \cdot 10^3$	– 3.0
	19	0.390	4.20	$9.81 \cdot 10^3$			$2.60 \cdot 10^{-3}$	$9.60 \cdot 10^3$	+ 2.2
	20	0.825	5.29	$1.23 \cdot 10^4$			$5.50 \cdot 10^{-3}$	$1.29 \cdot 10^4$	– 4.7
Aqueous glycerin (120 cps) – sand	21	0.825	3.17	$7.30 \cdot 10^2$	$3.48 \cdot 10^6$	2.12	$5.50 \cdot 10^{-3}$	$7.50 \cdot 10^2$	– 2.7
Sulfuric acid – sand	22	0.178	1.63	$2.26 \cdot 10^3$	$1.24 \cdot 10^8$	1.43	$1.19 \cdot 10^{-3}$	$2.54 \cdot 10^3$	–11.0
	23	0.390	2.37	$3.25 \cdot 10^3$			$2.60 \cdot 10^{-3}$	$3.47 \cdot 10^3$	– 6.3
	24	0.825	2.97	$4.07 \cdot 10^3$			$5.50 \cdot 10^{-3}$	$4.69 \cdot 10^3$	–13.0
$d_M = 0.1$ m; $D = 0.3$ m; $\Gamma_D = \frac{D}{d_M} = 3$									
Water – sand	25	0.035	6.67	$6.67 \cdot 10^4$	$9.81 \cdot 10^9$	2.68	$3.50 \cdot 10^{-4}$	$6.38 \cdot 10^4$	+6.1
	26	0.093	9.17	$9.17 \cdot 10^4$			$9.30 \cdot 10^{-4}$	$9.45 \cdot 10^4$	–3.0
Carbon tetrachloride – sand	27	0.035	5.00	$7.25 \cdot 10^4$	$2.06 \cdot 10^{10}$	1.63	$3.50 \cdot 10^{-4}$	$6.80 \cdot 10^4$	+6.6
	28	0.093	7.59	$1.02 \cdot 10^5$			$9.30 \cdot 10^{-4}$	$1.01 \cdot 10^5$	+1.0
	29	0.178	9.17	$1.33 \cdot 10^5$			$1.78 \cdot 10^{-3}$	$1.31 \cdot 10^5$	+1.5
Sulfuric acid – sand	30	0.178	4.17	$2.54 \cdot 10^3$	$3.65 \cdot 10^7$	1.43	$1.78 \cdot 10^{-3}$	$2.63 \cdot 10^3$	–3.4
	31	0.390	5.40	$3.29 \cdot 10^3$			$3.90 \cdot 10^{-3}$	$3.58 \cdot 10^3$	–8.1

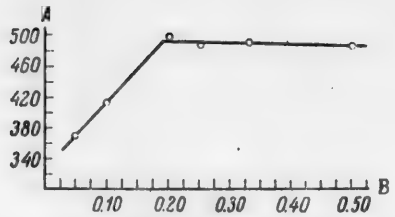

Fig. 2. Determining rotation speed as a function of the concentration of sand in water.
A) Stirrer speed in revolutions per minute, B) S/L weight ratio.

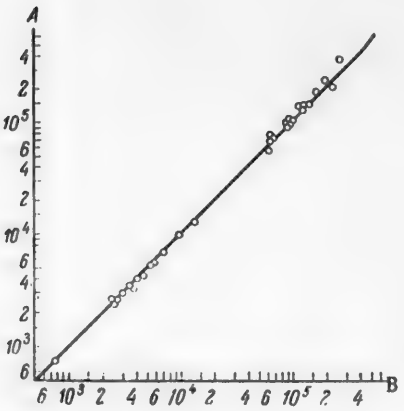

Fig. 3. Correlation graph.
A) Experimental values of Re, B) calculated values Re = 0.105, $Ga^{0.6} \cdot S_\rho^{0.8} \cdot \Gamma_{d_p}^{0.4} \cdot \Gamma_D^{1.9}$.

Thus, in the experiments on the influence of the physicochemical characteristics of the solid and liquid phases on the determining rotation speed the condition $\left(\frac{G_s}{G_l}\right)^{r=0} = 1$ was satisfied, so that the concentration ratio may be eliminated from Equation (4).

Moreover, the condition $H_0 = D = \text{const}$, was satisfied in our experiments. Then evidently $\frac{H_0}{d_M} = \frac{D}{d_M}$, and one of these ratios, $\frac{H_0}{d_M}$, can also be eliminated from Equation (4).

As the result of these simplifications we have the equation

$$Re = C \cdot Ga^i \cdot S_\rho^k \cdot \Gamma_{d_p}^l \cdot \Gamma_D^p \qquad (5)$$

or, in explicit form

$$Re = 0.105 \cdot Ga^{0.6} \cdot S_\rho^{0.8} \cdot \Gamma_{d_p}^{0.4} \cdot \Gamma_D^{1.9}. \qquad (5a)$$

Solving Equation (5a) for the determining rotation speed, we obtain the simple calculation formula

$$n_0 = 0.415 \frac{\rho_p^{0.8} \cdot d_p^{0.4} \cdot D^{1.9}}{\rho_m^{0.6} \cdot \mu^{0.2} \cdot d_M^{2.5}} \text{ 1/revs/sec.} \qquad (6)$$

which clearly reveals the influence of individual factors on the determining rotation speed.

The agreement between the experimental values and the values calculated from Equation (5a) is demonstrated in the correlation graph (Fig. 3).

The applicability of Equation (5a) was confirmed within the following limits:

$$Re = 7.3 \cdot 10^2 - 3.79 \cdot 10^5; \quad Ga = 3.48 \cdot 10^6 - 7 \cdot 10^{10};$$
$$\Gamma_{d_p} = 0.23 \cdot 10^{-3} - 8.25 \cdot 10^{-3}; \quad \Gamma_D = 2 - 3.$$

In the use of Equation (5a) or the calculation Formula (6) it must be remembered that the physical limit of applicability of both equations is the depth of the vortex, which must be less than the depth of immersion of the impeller.

According to our experimental data, the depth of the vortex formed during the stirring of pure liquids by means of impellers of the type described above may be found from the equation:

$$\frac{h_V}{d_M} = 28.4 \cdot \left(\frac{n \cdot \rho_m \cdot d_M^2}{\mu}\right)^{0.05} \cdot \left(\frac{n^2 d_M}{g}\right)^a \cdot \left(\frac{D}{d_M}\right)^b,$$

which may be written in contracted notation as

$$\Gamma_{h_V} = 28.4 \cdot Re^{0.05} \cdot Fr^a \cdot \Gamma_D^b. \qquad (7)$$

When $\Gamma_D < 3$ $a = 1$; $b = -3.8$ $\Gamma_D \geqslant 3$ $a = 2.4$; $b = -2$.

SUMMARY

1. Dimensional analysis was used to derive a criterial equation for calculation of the determining rotation speed, in the general form

$$Re = C \cdot Ga^{i} \cdot S_{\rho}^{k} \cdot \Gamma_{d_p}^{l} \cdot \Gamma_{D}^{p} \cdot \Gamma_{H_0}^{q} \cdot S_{G}^{r}.$$

2. It is shown that the graphs representing the variation of the relative concentration of the solid phase with increasing rotation speed of a blade stirrer can be classified into three types: I) sluggish stirring; II) intensive stirring with the solid phase distributed almost uniformly throughout the system; III) intensive stirring with displacement of the solid phase into the upper liquid layers.

3. In extension of the earlier terminology, it is proposed to define as the determining speed the speed of the stirrer at which the relative concentration of the solid phase in the whole stirred liquid, or at least in the upper layers, reaches 100%.

4. It is shown that the methods proposed by Miller and Mann and by Mel'nikov for evaluation of the quality of stirring are formal and do not fully reflect the nature of the effect.

5. The following formula has been derived for calculation of the determining rotation speed of a blade stirrer in the region in which the concentration of the solid phase does not influence the determining speed:

$$Re = 0.105 \cdot Ga^{0.6} \cdot S_{\rho}^{0.8} \cdot \Gamma_{d_p}^{0.4} \cdot \Gamma_{D}^{1.9}.$$

6. A criterial equation is derived for calculation of the depth of the vortex formed by the action of a blade stirrer, of the form

$$\Gamma_{h_V} = 28.4 \cdot Re^{0.05} \cdot Fr^{a} \cdot \Gamma_{D}^{b}.$$

LITERATURE CITED

[1] A. M. White, S. D. Sumerford, E. Bryant, and B. Lukens, Ind. Eng. Ch. 24, 1160 (1932); A. M. White, S. D. Sumerford, Ind. Eng. Ch. 25, 1025, (1933).

[2] N. V. Shpanov, Bull EKIKhIMASh 1-2 (1934); cited through I. I. Vorontsov, J. Appl. Chem. 18, 19 (1941).

[3] A. W. Hixson and A. H. Tenney, Tr. Am. Inst. Chem. Engrs. 31, 113 (1935).

[4] S. A. Miller, and C. A. Mann, Tr. Am. Inst. Chem. Engrs. 40, 709 (1944).

[5] V. I. Mel'nikov, Coll. Papers, Sci. Res. Inst. Chemical Machinery 16, 88 and 105 (Mashgiz, 1954); Author's Summary of Candidate's Dissertation, MIKhM (Moscow, 1954).

[6] I. S. Pavlushenko, N. M. Kostin and B. N. Iachkula, Trans. Lensoviet Technol. Inst. Leningrad, 41 (Goskhimizdat, 1957).

[7] I. S. Pavlushenko, J. Appl. Chem. 28, 885 (1956).*

[8] N. M. Kostin and I. S. Pavlushenko, Trans. Lensoviet Technol. Inst. Leningrad, 41 (Goskhimizdat, 1957).

[9] L. S. Eigenson, Scale Modeling (Soviet Science Press, 1952).**

[10] P. G. Romankov and I. S. Pavlushenko, J. Chem. Ind. 10, 292 (1947).

[11] Standards for Chemical Equipment Construction, 1 Sci. Res. Inst. Chemical Machinery (Mashgiz, 1950).

[12] V. V. Kafarov, Agitation Processes in Liquid Media (State Chem. Press, 1949).**

Received March 15, 1957

* Original Russian pagination. See C. B. Translation.

** In Russian.

ELECTROLYSIS OF CADMIUM SULFATE SOLUTIONS*

A. M. Ozerov

Research on the electrolysis of aqueous cadmium sulfate solutions has not lost its importance, despite the available publications on the electrodeposition of cadmium [1-8], on the production of corrosion-resistant cadmium alloys [9-12] and cadmium powder [13], on the electrochemical behavior of cadmium under conditions of spontaneous dissolution in aqueous electrolyte solutions [14], etc.

In its properties, cadmium is very close to zinc, and the process for its cathodic deposition is very similar to the corresponding process for zinc. Because of the high hydrogen overvoltage on cadmium, the latter is readily deposited from neutral solutions in spongy form, and from acid solutions of cadmium sulfate in compact and pure form. The only disadvantage is the tendency of its crystals to branch and grow in the direction of the anode. Although the addition of colloids (about 0.3 g of gelatin per liter) improves the situation, it does not completely prevent the formation of growths.

Neutral sulfate electrolytes used for feeding electrolytic cells for cadmium production may contain more electronegative and more electropositive cations than cadmium as impurities. Some of these have an adverse effect on the electrodeposition of cadmium.

The influence of impurities on the electrodeposition of zinc was studied by Stender, Pecherskaia, Turomshina [15-16] and others. These impurities should probably influence the electrodeposition of cadmium similarly.

The present paper reports a study of the electrodeposition of cadmium from pure neutral and acidified solutions of cadmium sulfate without added colloid, up to the "superhigh" current densities which are attracting attention of research workers at the present time.

EXPERIMENTAL

Experimental conditions. The electrolysis was performed in a glass H-shaped vessel, 700 ml in capacity, with circulation of electrolyte (seven complete changes per hour). The flowing feed electrolyte was previously heated in a coil placed in the thermostat containing the electrolytic cell. The cathode consisted of copper foil. The back and sides of the cathode were coated with insulating acid-resistant lacquer. The front working area of the cathode was 5 cm^2; before each experiment the cathode was coated during 10 minutes with a bright, dense, finely crystalline deposit of cadmium at a current density of 5 amps/dm^2 from a solution containing (in g/liter): 200 $CdSO_4 \cdot {}^8/_3H_2O$, 30 $Al_2(SO_4)_3 \cdot 18H_2O$, 80 $Na_2SO_4 \cdot 10H_2O$, 5 $C_{10}H_6(SO_3Na)_2$. The temperature of the solution was 25°. The anode was a lead plate 80 cm^2 in area. The H-shape of the cell and the use of flowing electrolyte prevented the entry of oxygen into the cathode space. The cathode potentials were measured by a direct compensation method with the aid of the PPTV-1 potentiometer. A mercurous oxide half cell was used as the standard electrode (with 2N H_2SO_4). The current efficiency was calculated from the amount of hydrogen liberated per unit time, the volume being reduced to standard conditions with a correction for water vapor pressure. The apparatus is shown schematically in Fig. 1. The reagents were of chemically pure and analytical reagent grades.

DISCUSSION OF RESULTS

Since the electrodeposition of cadmium was studied in pure solutions of cadmium sulfate without added colloids, the cathode surface was very highly developed, even at low current densities, while at high current

* Communication I.

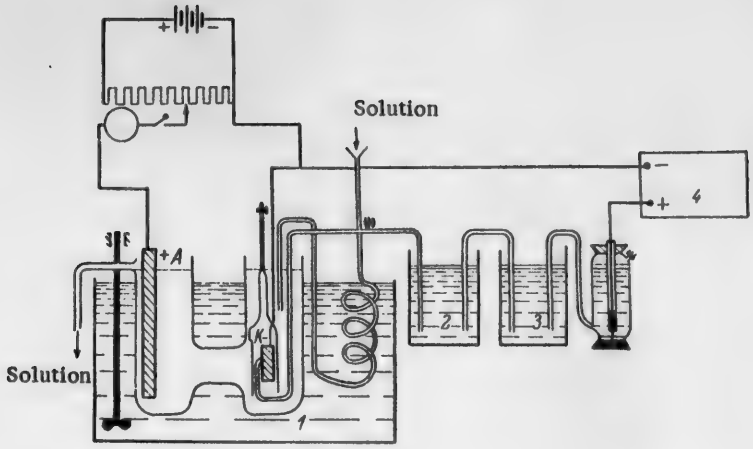

Fig. 1. Diagram of the apparatus.
1) Thermostat, 2) solution under test, 3) 2 N H_2SO_4 solution, 4) potentiometer.

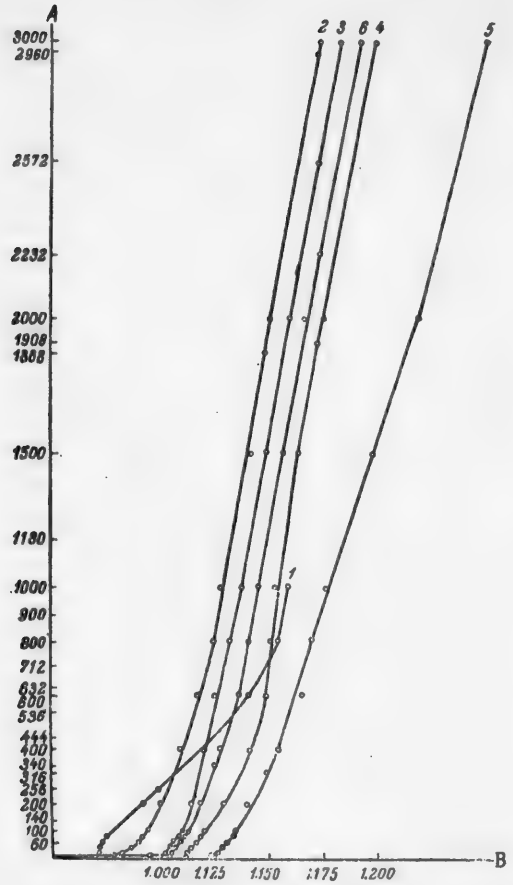

Fig. 2. Variation of potential with current density in electrolysis of solutions. Temperature 30°.
A) Current density D (in amps/m^2), B) potential of cadmium cathode E_V.
Contents of Cd and H_2SO_4 respectively (in g/liter): 1) 60 and 0; 2) 60 and 50; 3) 60 and 100; 4) 60 and 200; 5) 30 and 200; 6) 90 and 200.

densities the cathode deposit was spongy. This led to a sharp change of the true current density. Because of the high hydrogen overvoltage on cadmium, even at very high current densities (10,000 amps/m^2), there was no appreciable evolution of hydrogen at the cathode under these conditions, and therefore the current efficiency with respect to cadmium was close to 100%.

The variations of the cathode potential with the cadmium ion concentration, sulfuric acid concentration, and temperature were studied at various current densities. The results are given in Table 1 and Figs. 2-6.

Earlier investigations by Izgaryshev and Maiorova [3] showed that the cathodic polarization decreases with increasing concentration of cadmium salt in solution (from 0.25 N to 2 N $CdSO_4$), and then increases sharply with further increase of the concentration of cadmium ions, while the anodic polarization remains unchanged. In Izgaryshev's opinion, complex cadmium cations may be formed in cadmium sulfate solutions under certain conditions.

It follows from the data in Table 1 and Fig. 2 that the cathode potential becomes increasingly electropositive with increasing concentration of cadmium ions (at the same acidity, 200 g of H_2SO_4 per liter, and at the same temperature).

Figure 3 is a semilogarithmic plot of E_V as a function of log D in amps/cm^2 (the corresponding values of D in amps/m^2 are marked along the abscissa axis). Table 2 gives the values of the potentials and changes of potential measured in solutions with different concentrations of cadmium ions at equal current densities (at 10, 800, 3000, 6000 amps/m^2 respectively).

It is known that the probability of formation of complex ions such as $[Cd_2SO_4]^{++}$ increases with increasing concentration of cadmium ions in solutions. In very dilute

TABLE 1

Variations of Potential E_V with Current Density D in the Electrodeposition of Cadmium

D (in amps/m²)	Cathode potentials ($-E_V$) in the electrolysis of solutions containing (in g/liter)													
	60 Cd			60 Cd + 50 H_2SO_4			60 Cd + 100 H_2SO_4			60 Cd + 200 H_2SO_4			30 Cd + + 200 H_2SO_4	90 Cd + + 200 H_2SO_4
	Temperature (°C)													
	30°	50°	70°	30°	50°	70°	30°	50°	70°	30°	50°	70°	30°	30°
0	1.067	1.050	1.050	1.077	1.063	1.067	1.094	1.094	1.076	1.111	1.105	1.098	1.119	1.102
10	1.071	1.055	1.050	1.079	1.064	1.064	1.095	1.095	1.079	1.112	1.106	1.0985	1.124	1.104
20	1.0715	1.058	1.051	1.082	1.068	1.065	1.102	1.096	1.080	1.113	1.107	1.099	1.127	1.105
40	1.072	1.061	1.053	1.077	1.073	1.067	1.104	1.097	1.081	1.115	1.109	1.101	1.129	1.107
60	1.073	1.063	1.055	1.090	1.077	1.069	1.106	1.098	1.082	1.117	1.111	1.102	1.132	1.109
70	1.075	1.065	1.057	1.092	1.080	1.071	1.109	1.100	1.083	1.119	1.113	1.103	1.134	1.111
100	1.077	1.067	1.059	1.094	1.083	1.073	1.110	1.101	1.084	1.121	1.114	1.104	1.135	1.113
200	1.092	1.075	1.070	1.100	1.086	1.078	1.115	1.108	1.091	1.130	1.121	1.112	1.140	1.119
400	1.121	1.082	1.075	1.110	1.092	1.086	1.131	1.112	1.098	1.142	1.131	1.121	1.155	1.128
600	1.141	1.093	1.082	1.118	1.100	1.092	1.125	1.119	1.106	1.150	1.139	1.130	1.166	1.137
800	1.155	1.095	1.087	1.125	1.105	1.096	1.133	1.125	1.112	1.152	1.143	1.136	1.170	1.142
1000	1.160	1.100	1.092	1.128	1.115	1.102	1.137	1.133	1.117	1.153	1.146	1.141	1.176	1.146
1500	—	—	—	1.143	1.126	1.114	1.150	1.145	1.132	1.164	1.162	1.154	1.199	1.157
2000	—	—	—	1.153	1.139	1.127	1.161	1.159	1.143	1.176	1.172	1.166	1.222	1.168
3000	—	—	—	1.176	—	1.153	1.185	1.184	1.167	1.201	1.192	1.192	1.352	1.194
6000	—	—	—	—	—	—	—	1.253	1.233	1.272	1.264	—	1.506	1.267
10000	—	—	—	—	—	—	—	1.349	1.325	1.367	—	—	—	—

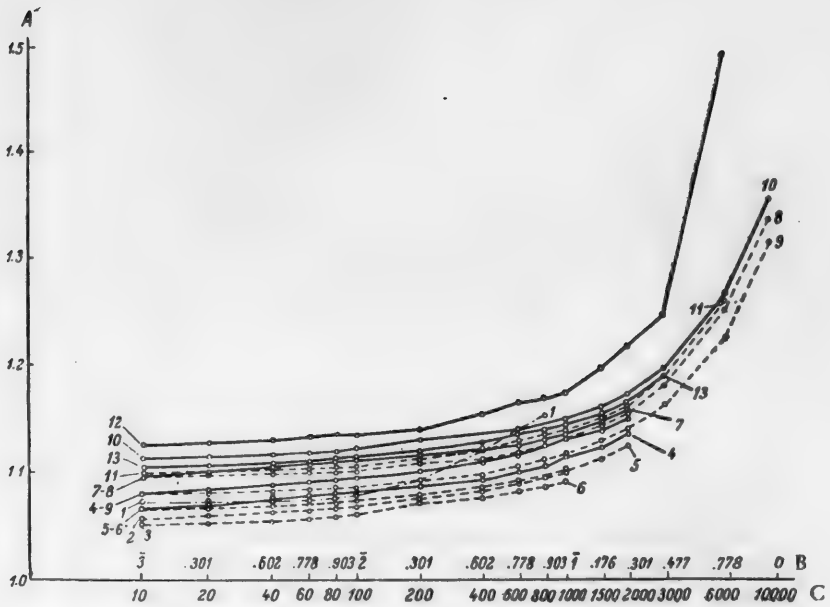

Fig. 3. Potential as a function of the logarithm of the current density in the electrolysis of cadmium sulfate solutions.
A) Potential E_V, B) log D, C) current density D (in amps/m^2).
Contents of Cd and H_2SO_4 respectively (in g/liter): 1, 2, 3) 60 and 0; 4, 5, 6) 60 and 50; 7,8,9) 60 and 100; 10,11) 60 and 200; 12) 30 and 200; 13) 90 and 200.
Temperature (°C): 1, 4, 7, 10, 12, 13) 30; 2, 5, 8) 50; 3, 6, 9, 11) 70.

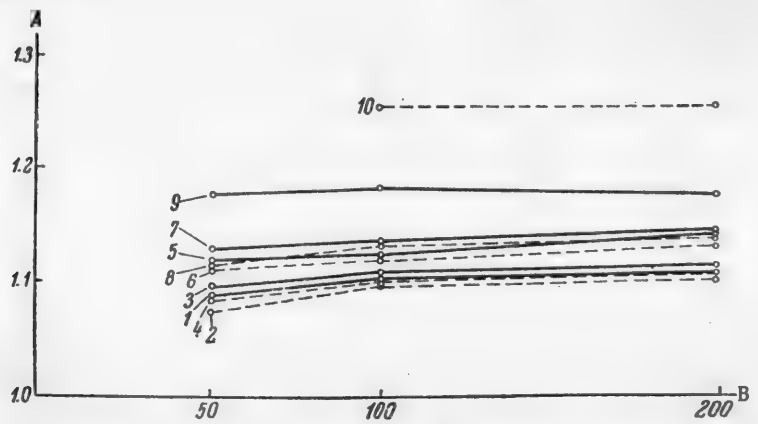

Fig. 4. Variations of potential with sulfuric acid concentration in the electrolysis of solutions containing 60 g Cd per liter.
A) Potential E_V; B) H_2SO_4 concentration (in g/liter).
Current density (in amps/m^2): 1, 2) 40; 3, 4) 100; 5, 6) 600; 7, 8) 1000; 9) 3000; 10) 6000.
Temperature (°C): 1, 3, 5, 7, 9) 30; 2, 4, 6, 8, 10) 50.

solutions of cadmium sulfate the formation of such ions is probably impossible.

It follows from Fig. 3 and Table 2 that Curves 11 and 13 (for 60 and 90 g of cadmium per liter respectively) almost coincide, and the changes of potential ΔE at different current densities are very similar. This suggests that the values of the electrode potentials are determined by the same electrochemical process.

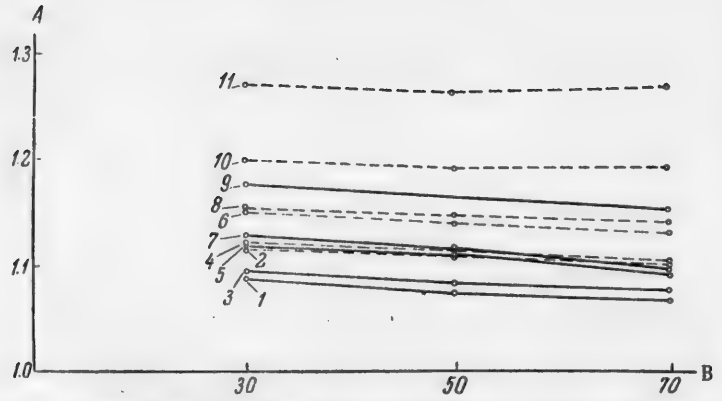

Fig. 5. Variations of potential with temperature in the electrolysis of solutions containing 60 g of Cd per liter and different amounts of H_2SO_4. A) Potential E_V, B) temperature (°C).
H_2SO_4 contents (g/liter) and current densities (amps/m^2) respectively: 1) 50 and 40; 2) 200 and 40; 3) 50 and 100; 4) 200 and 100; 5) 50 and 600; 6) 200 and 600; 7) 50 and 1000; 8) 200 and 1000; 9) 50 and 3000; 10) 200 and 2000; 11) 200 and 6000.

TABLE 2

Variations of Cathode Potential with Cadmium Concentration in Solution

Current density (in amps/m^2)	Values of potential with cadmium contents in solution (in g/liter)		Change of potential (in v) $\Delta E = E_{60} - E_{90}$
	60	90	
10	1.112	1.104	0.008
800	1.152	1.142	0.010
3000	1.201	1.194	0.007
6000	1.272	1.267	0.005

Figure 2 shows that the cathode potential becomes more electronegative with increasing concentration of sulfuric acid (from 50 to 200 g/liter) under the same conditions.

In Fig. 4 the cathode potential is plotted against the sulfuric acid concentration at 30-50° and at various current densities. Analysis of the curves shows that the greatest increases of the cathode potential in the electronegative direction are found at low concentrations of sulfuric acid (from 50 to 100 g/liter), and especially at low current densities (up to 100 amps/m^2). With further increase of the sulfuric acid concentration (from 100 to 200 g/liter) the increase of the cathode potential is slight. It is interesting to note that the increase of potential with increasing acid concentration is less at higher current densities.

The plot of the cathode potential against the temperature for the electrolysis of solutions containing 60 g of cadmium and 50 or 200 g of sulfuric acid per liter at various current densities (Fig. 5) shows that the cathode potential becomes more electropositive with increase of temperature. The cathode potential is almost unchanged over the 50-70° temperature range at high current densities (3000 and 6000 amps/m^2) and high acid contents (200 g/liter).

To follow the changes in the rate of the electrode process with the concentrations of cadmium ions and sulfuric acid in solution, it is necessary to examine the corresponding values of D (amps/m^2) at the same value of the potential. It follows from Fig. 6 that if the rate of the cathode process (at a potential of 1.15 v) in the electrodeposition of cadmium from a solution containing 30 g of cadmium and 200 g of sulfuric acid per liter is taken as unity (Curve 5), the rate is doubled if the concentration of cadmium ions is doubled (60 g/liter , Curve 4), while when the concentration is trebled (90 g/liter) the rate is approximately quadrupled (Curve 6). If, at constant concentration of cadmium ions (60 g/liter), the sulfuric acid concentration is doubled and quadrupled (to 100 and 200 g/liter), the rate of the cathode process decreases by a factor of 1.25 (Curve 3) and 3 (Curve 4) respectively.

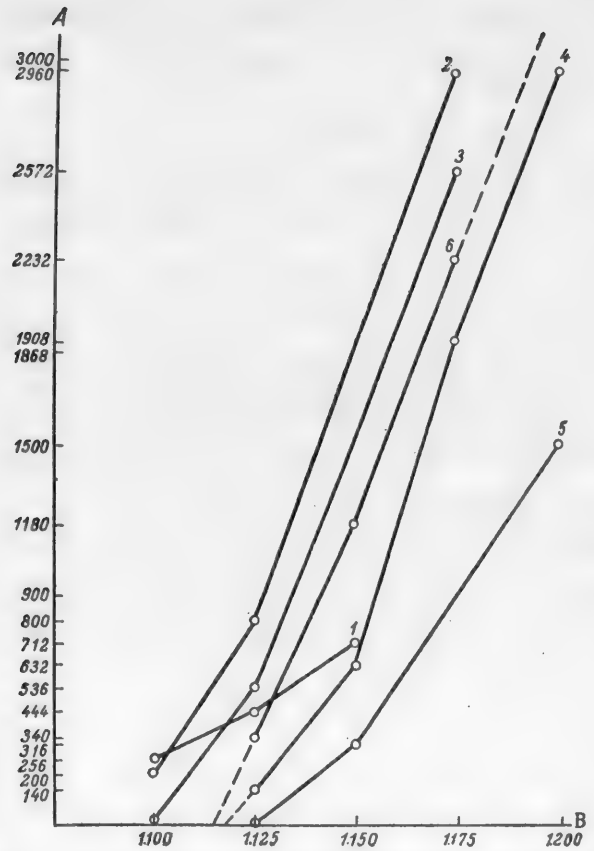

Fig. 6. Variations of the rate of the cathode process with the concentrations of cadmium sulfate and sulfuric acid in the electrolysis of cadmium sulfate solutions. Temperature 30°. A) Rate D (in amps/m^2), B) potential E_V (in v). Contents of Cd and H_2SO_4 respectively (in g/liter): 1) 60 and 0; 2) 60 and 50; 3) 60 and 100; 4) 60 and 200; 5) 30 and 200; 6) 90 and 200.

SUMMARY

1. Since chemical polarization in the electrodeposition of cadmium is slight, in the electrolysis of pure neutral and acidified solutions of cadmium sulfate the cathode surface becomes very highly developed even at low current densities, while at high current density a spongy deposit is formed. This results in a sharp change of the true cathodic current density, and has caused some erroneous conclusions to be drawn in studies of polarization curves. However, if the investigation is carried out in comparable conditions, this fact does not prevent certain correct relative conclusions from being drawn.

2. Analysis of the polarization curves showed that increase of the sulfuric acid content in the solution in the electrodeposition of cadmium is accompanied by an increase of the cathode potential in the electronegative direction, with an improvement in the quality of the cathode deposit; at high concentrations of sulfuric acid (from 100 and 200 g/liter) and at "superhigh" current densities this increase is slight. Increase of the sulfuric acid concentration also decreases the rate of the cathode process. The cathode potential becomes more electropositive with increasing cadmium content and rise of temperature.

LITERATURE CITED

[1] Iu. V. Baimakov, Electrolysis in Metallurgy 1, 356-359 (1933).

[2] N. P. Fedot'ev, Electrolysis in Metallurgy 1, 141-142 (1935).

[3] N. A. Izgaryshev and E. Ia. Maiorova, J. Gen. Chem. 6, 9, 1208 (1936).

[4] E. V. Osipova and N. T. Kudriabtsev, Coll. Roskrepmetiz (1933); in the collection: Struggle Against Corrosion – Struggle for Metal (1935).

[5] Vernik. Trans. Electrochem. Soc. 62 (1932).

[6] V. I. Lainer, S. L. Orlova and P. L. Fal'gel'shtein, Corrosion and its Prevention 4, 2 (1938).

[7] N. A. Izgaryshev and S. I. Orlova, Trans. Inst. Appl. Mineralogy (1931).

[8] V. I. Lainer and N. T. Kudriavtsev, Fundamentals of Electroplating, I, 328-348 (1953).*

[9] V. I. Lainer and N. T. Kudriavtsev, Fundamentals of Electroplating, II, (1946). *

[10] P. P. Beliaev and S. M. Aagababov, Corrosion and Its Prevention, 5, 1-2, 137-143 (1939).

[11] "E.T. S. Silver Jubilee Conference" Metal Industry 76, 24 (1950).

[12] N. T. Kudriavtsev and E. K. Pereturina, J. Appl. Chem. 26, 2, 155 (1953).**

[13] D. N. Gritsan and A. M. Bulgakova, J. Phys. Chem. 2, 258 (1954).

[14] Ia. M. Kolotyrkin and L. A. Medvedeva, J. Phys. Chem. 9, 1344 (1953); 8, 1477 (1955).

[15] A. G. Pecherskaia and V. V. Stender, J. Appl. Chem. 23, 9, 920 (1950). **

[16] U. F. Turomshina and V. V. Stender, J. Appl. Chem. 28, 2, 166 (1955);**28, 4,372 (1955);** 28, 5, 467 (1955).**

Received February 8, 1956

* In Russian.

** Original Russian pagination. See C. B. Translation.

THE IRON ELECTRODE IN THE GALVANIC CELL

N. A. Shurmovskaia and R. Kh. Burshtein

All galvanic cells now being produced by industry contain nonferrous metals. Electrochemists have long been faced with the problem of devising primary sources of current without the use of nonferrous metals [1]. Iron and carbon can be used as electrodes in such cells.

It is known that active carbon can react with atmospheric oxygen, and therefore the anode in such a cell may be an air-depolarized electrode. The use of iron as the cathode in an electric cell involves a number of difficulties. Until recently the only chemical sources of current in which an iron cathode was used was the iron–nickel storage cell. The iron powder used for the iron electrodes of the iron–nickel cell is oxidized in contact with air, the electrode potential being displaced by 0.4-0.8 v in the positive direction; such an electrode is entirely passive with regard to the formation of bivalent iron. To convert the iron electrode into an active state, it is charged. The oxides are reduced during charging and the electrode becomes active. It must also be pointed out that the iron electrodes used in iron–nickel storage cells are greatly subject to self-discharge, so that they cannot be used in primary sources of current.

Electrodes used in galvanic cells must satisfy the following conditions: they must have electrochemical activity without being charged, and they must have good keeping qualities.

Several methods are already known for the preparation of electrochemically active iron electrodes of low self-discharge.

In the work of Burshtein, Kiperman, and Pavlova [2] on iron–carbon cells it was shown that if the iron powder obtained from ferric oxide or magnetite by reduction in hydrogen, nitrogen–hydrogen mixture, or water gas is put into benzene before contact with the air, and then dried in air, electrodes made from this powder have electrochemical activity and have almost no tendency for self-discharge. In another method for the production of iron electrodes suitable for cells, the iron powder made by reduction is put into an aqueous solution of an inhibitor [3] (1% aqueous solutions of water glass, sodium phosphate, or sodium nitrite were used as inhibitors) before contact with air. The powder is then dried in air. The electrodes made from this powder have the same properties as electrodes made from iron powder treated with benzene.

The state of the iron electrode in which it has electrochemical activity and negligible self-discharge we shall term the semipassive state, in contrast to the state of iron used in storage cells, which we shall describe as active.

The semipassive state of the iron electrode may be the consequence either of the fact that the iron is coated with a thin oxide film which prevents spontaneous dissolution of the iron and preserved the electrode in the active state, or of the fact that the electrode has been treated with benzene or with inhibitors used for passivation of iron electrodes, or of the fact that spontaneous dissolution of thermally reduced iron is less than that of electrochemically reduced iron. This paper deals with a study of the mechanism of action of a semipassive iron electrode.

It is known from the work of Burshtein, Shumilova, and Gol'berg that the amount of oxygen sorbed by reduced iron during the rapid stage, which corresponds at room temperature to $2 \cdot 10^{15}$ molecules per cm^2 of actual surface, does not alter the electrochemical activity of a smooth iron electrode, i.e., an electrode coated with such an oxide film has the same potential and the same technological capacity* as it had before the absorption

* We use the term technological capacity to represent the quantity of electricity (in amp-hrs) obtained per 1 g of iron electrode in its discharge to a potential more positive than the hydrogen potential by 280 mv.

of oxygen. If the amount of sorbed oxygen is $4 \cdot 10^{15}$ molecules per 1 cm^2 of actual surface, which corresponds to the slow stage of oxygen sorption, the potential is displaced in the positive direction, and this iron has no technological capacity.

To determine the reasons for the absence of self-discharge in iron electrodes used in the iron–carbon cell, it was desired to study the influence of thin oxide films on powdered iron on cathodic and anodic polarization in alkaline solutions, and the influence of organic solvents on these electrode processes.

EXPERIMENTAL

Method. Iron powders prepared by two methods were used in the experiments. Some of the experiments were performed with powder obtained from iron oxide used for the production of iron storage cells, by reduction with nitrogen–hydrogen mixtures at 500°. The other experiments were carried out with a purer iron powder, prepared by decomposition of iron pentacarbonyl followed by removal of organic impurities.

For the purification, the iron was dissolved in nitric acid, and the ferric nitrate was then decomposed to ferric oxide. This was reduced in hydrogen at 550° [5]. To prevent spontaneous combustion, the powders obtained by thermal reduction were put, before contact with air, into water, or benzene, or sodium silicate solution. The powders were then filtered off and dried at room temperature. The powders were then made into small laminas containing 0.2 g of iron.

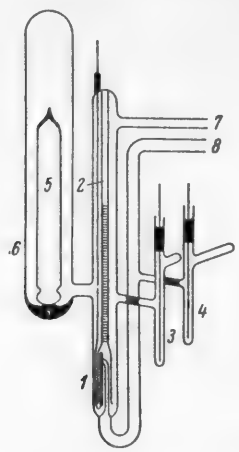

Fig. 1. Apparatus for experiments at low pressure. (Explanation in text).

Two pieces of apparatus (1 and 2) were used for investigation of the electrochemical behavior of iron electrodes with simultaneous determination of gas evolution. One apparatus (1) is described in a paper by Platonova and Levina [6]. It consisted of three communicating cells separated by stopcocks. One contained a gas buret terminating in a cap under which was placed the iron electrode, the second contained a platinum electrode for polarization, and the third contained a mercury–mercurous oxide electrode.

The second apparatus, used for experiments at low pressure, is illustrated in Fig. 1.

The iron electrode was placed in the tube 1 under a cap connected to the gas buret 2. The electrode was connected to a wire sealed into the upper portion of the tube 1. The mercury–mercurous oxide electrodes 3 and 4 were used as the reference electrode and the polarization electrode respectively. A bulb 5 containing the gas-free electrolyte was placed in the tube 6. The tubes 7 and 8 were used for sealing the apparatus to the vacuum installation. The iron electrode was reduced in this apparatus at 500° at 35 mm pressure, with hydrogen circulated at high velocity in the system. The water vapor formed in the reaction was frozen out in traps immersed in liquid nitrogen. When the hydrogen pressure in the system became constant, reduction was taken to be complete. At the end of the reduction the electrode was evacuated under a high vacuum at 500° for 2 hours. The apparatus was then either sealed off from the vacuum installation, or a definite amount of oxygen was absorbed in the electrode before it was sealed off. The bulb with the electrolyte was then broken, the electrolyte was allowed to fill the cell and the auxiliary electrodes, and the determinations were started.

The electrolyte was 4.8 or 0.9 N chemically pure caustic potash in redistilled water. The bulbs containing gas-free electrolyte were prepared in a special apparatus by a method developed earlier [4].

Results and discussion. As was stated earlier, an electrode of smooth iron with $2 \cdot 10^{15}$ molecules per 1 cm^2 adsorbed on its surface retains its electrochemical activity. It was desired to determine how oxygen sorbed by powdered iron influences the potential, technological capacity, and spontaneous dissolution of iron in alkali solutions at various temperatures.

* Laminas are electrodes made from powder pressed in a metallic performated band.

Several electrodes, made from the iron powder used in alkaline storage cells and immersed in water after reduction, were additionally reduced with hydrogen in Apparatus 2. After they had been held under vacuum at the same temperature, they were cooled to room temperature, oxygen was introduced into the apparatus at $2\text{-}5 \cdot 10^{-2}$ mm Hg pressure, and the course of its sorption was determined. The adsorption process was complete when the rate of oxygen absorption fell sharply. This instant corresponded to the end of the rapid adsorption stage. The electrode, covered with a thin oxide film corresponding to $2 \cdot 10^{15}$ molecules of O_2/cm^2, was brought into contact with the air. No evolution of gas* in 9.5 N KOH was observed in the course of 5 days on an electrode with an oxide film made in this way. The potential of the iron electrode was 50-60 mv relative to the hydrogen electrodes, i.e., it corresponded to the potential of an iron electrode in the charged state. The technological capacity of the electrode in discharge by a current of 37.5 ma/g was 41% of the theoretically possible utilization of the iron. Electrodes treated with benzene have the same technological capacity.

It follows from these results that electrodes coated with thin oxide film are similar in properties to electrodes made of iron mass treated with organic solvents. They have the same electrochemical capacity and are equally free from self-discharge. Moreover, the film protects the iron to some extent from further rapid oxidation, as brief action of air at atmospheric pressure did not affect the electrode. However, if an electrode oxidized at low pressure is kept in air for several (3-4) days, it becomes passive. The electrode potential is displaced by 300-400 mv in the positive direction. The loss of activity on prolonged exposure to air is probably caused by thickening of the oxide film in moist air.

Iron treated with organic solvents after reduction also takes up oxygen on contact with air, but the process is slower than on a clean iron powder surface [2]. The oxide film so formed can be easily determined by an electrochemical method. The results of these experiments are given below. Powdered iron treated with benzene remains in the semipassive state for a number of years. The semipassive iron obtained by treatment with organic solvents (benzene, ligroine) is denoted by No. 1, and the iron made by the action of small amounts of oxygen, No. 2.

The difference in the behavior of electrodes made from semipassive iron No. 1 and No. 2 is probably associated with activated adsorption of organic solvents or their oxidation products formed on the iron surface. Recent data on the influence of benzene on photoemission and resistance of a number of metals also indicate that activated adsorption occurs [6]. Activated adsorption of these substances delays the rapid stage of oxygen adsorption and inhibits the slow stage, so that the semipassive state is retained.

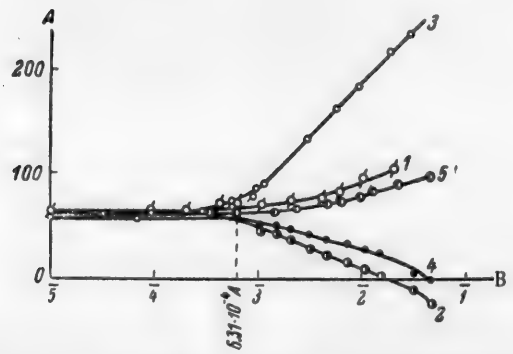

Fig. 2. Polarization curves for iron electrodes before and after removal of oxide film.
A) Electrode potential (in mv), B) logarithm of current density.
(Explanations of the curves are given in the text).

The fact that gas is not evolved at these electrodes indicates that the dissolution of iron is considerably decreased, possibly owing to the presence of oxide film, or that anodic oxidation of the iron takes place. To determine this question, cathodic and anodic polarization curves were plotted for electrodes with the iron powder coated with oxide film, and for electrodes from which the film had been removed by prolonged cathodic polarization.

Figure 2 shows a series of curves for the electrode potentials (relative to a hydrogen electrode in the same solution) against the logarithm of the current densities. In these determinations the potential was measured 3 seconds after a definite current strength had been established. Curves 1 and 2 are cathodic and anodic polarization curves for an electrode made of semipassive iron No. 2, while Curves 3 and 4 were obtained after prolonged polarization of the electrode, which removed the oxide film from its surface. Curve 5 relates to an electrode made from semipassive iron No. 1.

* The rate of liberation of gas from the electrode is almost proportional to the rate of self-discharge.

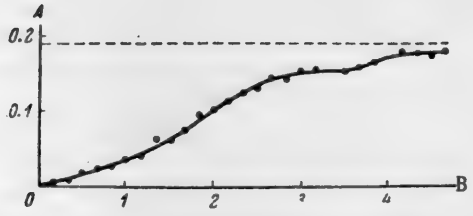

Fig. 3. Rate of gas evolution in the cathodic polarization of an iron electrode with an oxide film. A) Rate of gas evolution (cc/10 minutes), B) time (hours).

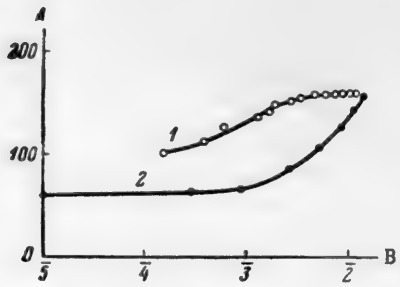

Fig. 4. Electrode potential as a function of the logarithm of the current density. A) Electrode potential (in mv), B) logarithm of current density. (Explanations of the curves are given in the text).

It is seen that the presence of an oxide film on the iron surface does not have any significant influence on the course of the anodic curves. The cathodic polarization curves for the electrode from semipassive iron powders Nos. 1 and 2 are almost identical, and are considerably below the hydrogen overvoltage curve for the electrode from which the oxide film had been removed by prolonged cathodic polarization. Removal of the oxide film leads to gas evolution at a stationary potential. The slope factor of the cathodic curve is 0.1. The spontaneous dissolution current, determined from the overvoltage curve, is $6.3 \cdot 10^{-4}$ amp. These results appear to indicate a decrease of hydrogen overvoltage on iron coated with a thin oxide film, and an increase of the spontaneous dissolution current. However, this contradicts the above experimental data on the absence of hydrogen evolution at a stationary potential at electrodes coated with an oxide film.

Measurement of the gas evolution rate in the cathodic polarization of an electrode made from No. 1 powder, at a current of $2.6 \cdot 10^{-3}$ amp. showed that a considerable proportion of the electricity is consumed in the removal of the oxide film. The results of this experiment are given in Fig. 3.

The dash line represents the rate of gas evolution according to Faraday's law. The curve represents the variation of the gas evolution rate on removal of the oxide film. From the difference between the observed rate of gas evolution at the iron electrode and the rate calculated from Faraday's law it is possible to calculate both the quantity of electricity required to remove the oxide film, and the strength of the polarizing current. The true specific surface of the iron powder was 8 m^2/g. The amount of oxygen per 1 g of the iron electrode, determined from the amount of hydrogen required for its reduction, was 0.47-0.74 cc. Therefore, the amount of oxygen per 1 cm^2 of the true iron surface was $1.6\text{-}2.5 \cdot 10^{15}$ molecules of O_2/cm^2. If the quantity of electricity used for reduction of the oxide film is taken into account, the hydrogen overvoltage on this iron electrode is represented by the curve in Fig. 4.

The reason for the unusual slope of this curve is that different points refer to different amounts of oxygen on the iron surface. It is seen that the lower points lie above the hydrogen evolution curve (Fig. 4, 2) determined immediately after the removal of the oxide film from the iron; this is in agreement with reports in the literature that the hydrogen overvoltage is higher on incompletely reduced iron [7, 8]. Thus, the decreased dissolution of semipassive iron is associated with increase of the hydrogen overvoltage.

In cathodic polarization of semipassive iron its surface apparently retains a certain amount of firmly adsorbed oxygen which is difficult to remove by cathodic polarization. This is demonstrated by the following experiments. When a semipassive iron electrode was subjected to cathodic polarization after discharge, the amount of hydrogen liberated in absence of current was 0.115 cc/hour per 1 g of iron powder. After successive similar cycles the amount of gas liberated became almost constant at 0.375 cc/hour per 1 g of iron. The possible cause of the more complete removal of the oxide film after these cycles is that in the course of electrochemical oxidation fresh iron atoms emerge on the surface, and the $Fe(OH)_2$ formed in this case is reduced more easily than the oxides formed by contact of the iron with gaseous oxygen.

It was of interest to investigate the electrochemical behavior of thermally reduced iron and the influence of thin oxide films on the dissolution of iron. The experiments were carried out in Apparatus 2. The accuracy to which the gas evolution could be measured in this apparatus was 30-40 times as high as in measurements in

Apparatus 1 [6], as in the former case the experiments were performed at the pressure of saturated water vapor. Gas evolution was determined and overvoltage curves plotted for thermally reduced iron electrodes at different temperatures (10, 22, 35, and 42°), and gas evolution was also measured under the same conditions for similar iron electrodes with a thin oxide film on the surface of the iron powder. The experiments were performed with chemically pure iron, purified by the method described above. The electrolyte was 0.9 N caustic potash solution.

The stationary potential of this iron electrode in 0.9 N caustic potash solution is 20-25 mv relative to the hydrogen electrode in the same solution. Our value for the stationary potential differs from the value of 45 mv found in earlier measurements by Platonova and Levina [7]. This is probably because the original iron was prepared under somewhat different conditions. The potential of an iron electrode has been found [9] to depend on the method of preparation. This was attributed to different contents of hydrogen in the electrode.

After reduction of the iron and removal of gas from it, Apparatus 2 was placed in a thermostat maintained at the required temperature. The bulb was then broken and the electrode brought into contact with the electrolyte. It was found in experiments on the dissolution of iron that no gas is evolved at 9-10°. In experiments at 20° and higher the evolution of gas was considerable. The results of experiments on the dissolution of iron at various temperatures are given below.

Temperature (°C)	Dissolution current found by extrapolation from overvoltage curves (in amps).	Dissolution current from gas evolution (in amps).
10	$8.0 \cdot 10^{-5}$	No gas evolution
22	$1.7 \cdot 10^{-4}$	$5.3 \cdot 10^{-5}$
35	$2.4 \cdot 10^{-4}$	$7.2 \cdot 10^{-5}$
42	$3.2 \cdot 10^{-4}$	$1.6 \cdot 10^{-4}$

To compare the results obtained in determinations of gas evolution with those obtained from the overvoltage curves, cathodic polarization curves were determined by the "slow method" at various temperatures. In this case the potential was measured 3 minutes after alteration of the current strength, i.e., when its value became constant at the given current density. The results are plotted in Fig. 5. The temperature coefficient of the hydrogen evolution process is 1.6 mv at a current density of 10^{-3} amp/g in the 10-35° temperature range. The slope factor of the cathodic polarization curves is 0.1-0.11 in the 10-35° range, and 0.07 for the curve at 42°.

The values of the dissolution current calculated from gas evolution data and found from the hydrogen overvoltage curves for the same electrode and under the same temperature conditions are given above.

It is seen that dissolution did not take place at 10°, whereas according to the hydrogen overvoltage curve considerable evolution of gas should occur at this temperature. At 22 and 35° the dissolution current found from gas evolution data is 1/3 of the extrapolated value of the dissolution current found from the hydrogen overvoltage curves. The discrepancy between the dissolution current found from gas evolution and from the overvoltage curves by extrapolation decreases on a further increase of the temperature to 42°. In this case the current determined by by gas evolution is a half of the current found from the cathodic polarization curve.

In one experiment (at 22°), hydrogen overvoltage curves were determined from the current and from gas evolution simultaneously. The data below indicate satisfactory agreement between the results obtained by the two methods.

Cathodic polarization current (in amps)	Amount of gas evolved (reduced to standard conditions)(in cc/hour)	Current strength from gas evolution (amps)	Deviation (%)
$7.9 \cdot 10^{-5}$	0.031	$7.42 \cdot 10^{-5}$	−4.8
$1.36 \cdot 10^{-4}$	0.062	$1.48 \cdot 10^{-4}$	+8.8
$2.94 \cdot 10^{-4}$	0.116	$2.78 \cdot 10^{-4}$	−5.5
$5.8 \cdot 10^{-4}$	0.230	$5.5 \cdot 10^{-3}$	−5.2
$1.24 \cdot 10^{-3}$	0.490	$1.17 \cdot 10^{-3}$	−5.6
$2.64 \cdot 10^{-3}$	1.045	$2.50 \cdot 10^{-3}$	−5.3

The existing differences between the dissolution current at a stationary potential as determined from gas evolution and by extrapolation from the overvoltage curves at 10 and 42° are probably caused by passivation of the iron at a potential close to the stationary value. This agrees with the results of earlier investigations [8].

To determine the influence of the oxide film on the dissolution process, gas evolution was measured in absence of current on iron on which $2 \cdot 10^{15}$ molecules of O_2 per cm^2 of true surface had been adsorbed. The results are compared below with data on gas evolution on iron without an oxide film, obtained under similar conditions. The experiments were performed in the 17-44° range in 0.9 N alkali solution.

Temperature (°C)	Amount of gas evolved (in cc/g·hour)		b/a
	with oxide film (a)	without oxide film (b)	
17	–	0.0086	–
20	0.0012	(0.012)*	10
36	0.0065	0.034	5
42	(0.013)*	0.039	3
44	0.0154	–	

* The data in parentheses were obtained by interpolation from curves for the dissolution of iron as a function of temperature.

In experiments with semipassive iron performed in Apparatus 1 small amounts of liberated gas could not be detected owing to insufficient accuracy of the determinations.

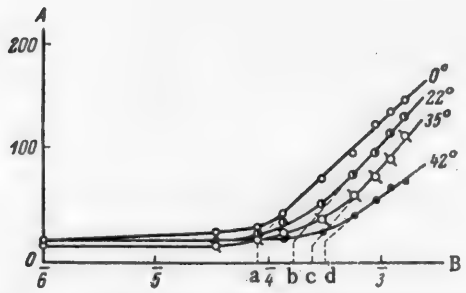

Fig. 5. Curves for the cathodic polarization of an iron electrode at various temperatures.
A) Electrode potential (in mv), B) logarithm of the current density.
Dissolution current (in amps): a) $8.0 \cdot 10^{-5}$, b) $1.7 \cdot 10^{-4}$, c) $2.4 \cdot 10^{-4}$, d) $3.2 \cdot 10^{-4}$.

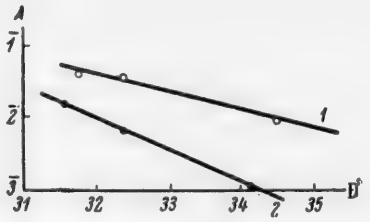

Fig. 6. Variation of the logarithm of the rate of hydrogen evolution on iron with the reciprocal temperature.
A) Logarithm of the dissolution current, B) reciprocal temperature ($1/T \cdot 10^4$). (Explanation of the curves is given in the text).

It follows from these results that a thin oxide film (6 A) on the iron surface, which has no influence on the potential or the technological capacity of the electrode, decreases the rate of spontaneous dissolution of the iron.

Curves for the variation of the logarithm of the rate of hydrogen evolution with the reciprocal of the temperature are given in Fig. 6. Curve 1 refers to gas evolution on iron without an oxide film. Curve 2 refers to an electrode with an oxide film. The apparent energies of activation calculated from these curves are 11,300 and 19,700 calories for reduced iron and iron in the semipassive state respectively.

The decrease of the rate of dissolution of iron in presence of an oxide film on its surface is associated with an increase of the apparent energy of activation. In consequence, the ratio of the rate of gas evolution on electrodes with no oxide film to the rate in presence of such a film decreases with increase of temperature.

Comparison of data on gas evolution for thermally reduced iron with data on gas evolution for iron from which the oxide film had been removed by cathodic polarization confirms the conclusion that not all the oxygen sorbed on contact with gaseous oxygen is removed by cathodic polarization.

Thus, it follows from these results that dissolution of iron electrodes in alkali solutions can be almost entirely prevented by formation of a thin oxide film (6 A $-2 \cdot 10^{15}$ molecules of O_2/cm^2) on the electrode surface as the result of sorption of gaseous oxygen. The iron can be protected against the formation of thicker oxide films by chemisorption of certain atoms or molecules on the surface. It was found that electrodes made of iron treated with benzene do not change their properties when kept in air for several years.

SUMMARY

An investigation of the influence of oxide films on the electrochemical behavior of powdered iron electrodes in alkali solutions showed that the presence of an oxide film ($2 \cdot 10^{15}$ molecules of O_2/cm^2) does not alter the stationary potential or the capacity of the electrode and decreases the spontaneous dissolution of the iron. The dissolution rate of the iron increases with increase of temperature. The apparent energy of activation of the dissolution of iron is 11,300 calories; in the presence of an oxide film the activation energy of this process is 19,700 calories. The dissolution of iron determined from the gas evolution in the temperature range studied does not correspond to the extrapolated value of the dissolution current found from the overvoltage curves, owing to the formation of iron oxides at potentials close to the stationary value.

Passivation of iron by organic substances or sodium silicate solution leads to formation of thin oxide films on its surface, and the presence of these substances on the surface prevents the growth of the oxide films beyond the thickness at which the formation of $Fe(OH)_2$ is impossible.

LITERATURE CITED

[1] V. G. Sochevanov, Galvanic Cells (Gosenergoizdat, 1951) pp. 113-115.*

[2] R. Kh. Burshtein and S. L. Kiperman, Collected Papers on Alkaline Cells with Air Depolarization (1947) p. 93; R. Kh. Burshtein and M. V. Pavlova, Authors' Certif. No. 64304, December 1, 1944, class 436. 4/01.

[3] R. Kh. Burshtein, N. A. Shurmovskaia, and D. L. Kondrashev, Claim No. K-71, Ministry of Electric Power Stations and Electrical Industry, June 9, 1953.

[4] R. Kh. Burshtein, N. A. Shumilova, and K. A. Gol'berg, J. Phys. Chem. 20, 789 (1946).

[5] Iu. V. Kariakin and I. I. Angelov, Pure Chemical Reagents (Goskhimizdat, 1955) pp. 135, 136, 142.*

[6] I. I. Platonova and S. D. Levina, J. Phys. Chem. 21, 331 (1947).

[7] R. Suhrmann, K. Schulz, Z. phys. Chem., N. F. 1, 69 (1954); R. Suhrmann, Z. Metallkunde, 46, 780 (1955).

[8] S. A. Rozentsveig and B. N. Kabanov, J. Phys. Chem. 22, 514 (1948).

[9] W. Patrick and W. Tompsen, J. Am. Chem. Soc. 75, 1184 (1953).

Received August 3, 1955.

* In Russian.

THE MECHANISM OF THE VACUUM-THERMAL DECOMPOSITION OF LIGNIN IN THE LIQUID PHASE AND THE INFLUENCE OF PHYSICAL FACTORS*

V. G. Panasiuk

The F. E. Dzershinskii Institute of Chemical Technology, Dnepropetrovsk

The kinetics of the decomposition of substances formed in thermal decomposition of plant tissues has not yet been studied. There is as yet far from enough experimental data for representation of the decomposition processes of substances formed under different conditions of pyrolysis.

An approximate scheme of the process may be based on certain data obtained by various investigators:

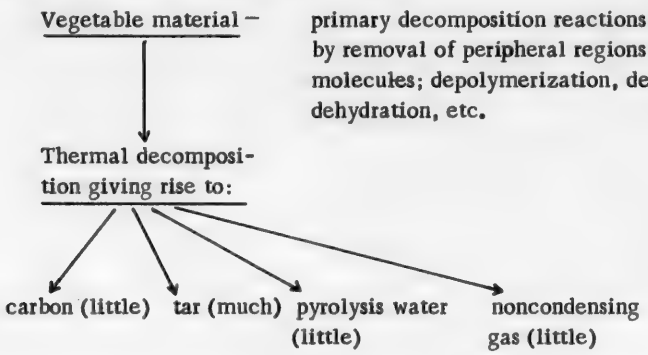

However, the process does not end there. A great variety of causes, such as the influence of the hot walls of the retort, the catalytic action of the heated carbon, the influence of the rapid rise of temperature in the exothermic process, the influence of the increase of the total pressure of the vapor–gas medium, etc., lead to secondary processes which occur at very high rates.

Among the secondary processes is the pyrolysis of the substances formed in the vapor or gas phase; this is accompanied by polymerization and condensation reactions.

As a result of the secondary processes, the above scheme must be extended for tar:

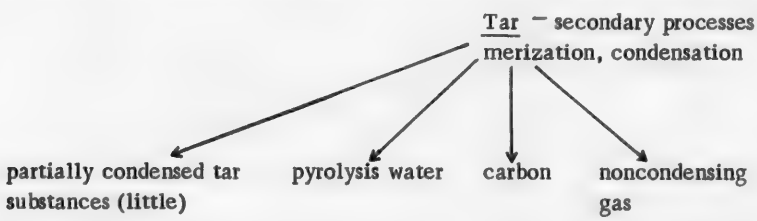

To prevent the occurrence of secondary processes, various workers have used a great variety of factors which made it possible to obtain higher yields of valuable substances from vegetable material. Condensation and

* Communication IV in the series on the thermal processing of hydrolytic lignin.

polymerization processes result in the formation of substances of high molecular weight, so that the yield of valuable low-molecular substances, pyrolysis products, decreases. A study of the kinetics of the thermal processes could provide information on the influence of the conditions of the thermal decomposition process on the rates of polymerization and condensation reactions. This would make it possible to select the most advantageous conditions for the pyrolysis process. It is known that the rates of condensation and polymerization reactions increase with increase of the total pressure of the vapor–gas medium and with temperature. Consequently the secondary processes could be reduced to a minimum by a decrease of the partial pressures of the organic vapors formed in the thermal processes.

To decrease the partial pressures, many workers have suggested that pyrolysis of vegetable materials should be carried out in an inert gas atmosphere [1], or in presence of vapors of substances of low reactivity, such as steam [2], high-boiling hydrocarbons [3], vapor–gas mixtures [1], etc. These measures increased the yield of valuable products of pyrolysis.

To obtain large amounts of valuable chemical substances, we suggest that the thermal process should be carried out in presence of a paste-forming oil under vacuum.

Hydrolytic lignin contains substances of different chemical types, such as lignin itself, cellulose residues, resins, waxy substances, and a certain amount of mineral and nitrogenous substances; i.e., hydrolytic lignin is not a homogeneous substance.

The lignin present in hydrolytic lignin differs from native lignin by a higher degree of condensation of its molecules, and is a substance of high molecular weight. The predominant type of bond between the individual parts of the molecule is the carbon bond. As is known, condensed molecules are split with difficulty, high temperatures being needed.

The conditions for the thermal decomposition of lignin should be as mild as possible in order to reduce secondary processes to a minimum. In addition to the use of tar paste-formers, the use of vacuum is advantageous: the molecules of the valuable chemical substances formed are rapidly removed from the heated space. The existence of a vacuum in the retort is likewise unfavorable for polymerization and condensation reactions, by minimizing the partial pressures of the substances formed.

The comparative yields of substances obtained under different conditions of thermal decomposition of cotton-hull lignin are given in Table 1.

TABLE 1

Comparative Yields of Substances From Hull Lignin Under Different Conditions

Process	Pressure (mm Hg)	Final temperature (°C)	Duration of process (min.)	Yields (% on dry lignin)			
				carbon	tar	pyrolysis water	gas and losses
Dry distillation	Atmospheric	460	180	66.1	6.9	19.3	7.7
The same	40	460	90	48.1	17.3	15.4	19.2
Vacuum-thermal process in anthracene oil	40	460	90	49.2	38.0	4.4	8.4

It is seen that the use of vacuum alone results in a considerable increase of the yield of tar in dry distillation. An even greater increase in the yield of these substances is obtained by means of vacuum-thermal decomposition in anthracene oil. Several experiments were carried out in order to study this method. It was necessary to determine whether the role of the paste former is purely mechanical. Experiments were therefore performed by the vacuum process with oils differing in chemical composition but with similar boiling ranges. The oils used were anthracene oil, solar oil, and "avtol" automobile lubricating oil. If these oils merely prevented secondary processes of thermal decomposition, the yields of tar from lignin would be the same.

The results of these experiments are given in Table 2.

TABLE 2

Yields in the Vacuum-Thermal Decomposition of Lignin in Different Oils (Lignin 1 part, oil 1.5 parts)

Paste former	Yields (% on dry lignin)			
	carbon	tar	pyrolysis water	gas and losses
Anthracene oil	55.2	30.3	7.4	7.1
Solar oil	48.9	12.3	18.4	20.4
Avtol	54.6	4.1	13.2	28.1
Avtol (recycled from Experiment 3)	55.2	15.4	10.5	18.9
Same, from Experiment 4	56.0	28.8	9.8	10.4
Same, from Experiment 5	58.5	1.5	10.8	29.2

TABLE 3

Elementary Composition of Anthracene Oil

Paste former	Contents (as % on the organic matter)	
	C	H
Original anthracene oil	92.88	5.82
Same after 1 cycle	91.02	6.23
Same after 2 cycles	89.90	6.10
Same after 3 cycles	89.84	6.27
Same after 4 cycles	90.12	6.08
Same after 5 cycles	89.73	6.05
Same after 6 cycles	89.08	5.87
Same after 7 cycles	88.54	5.93

The experimental conditions were: final temperature 460°, pressure 40 mm Hg, duration of experiment 90 minutes.

TABLE 4

Hydrogen Balance in the Vacuum-Thermal Decomposition of Lignin

Hydrogen introduced (in g)	Hydrogen removed (in g)
With 100 g of lignin (5.5%) 5.5	With 150 g of heavy tar fractions above 230° (6.1%) 9.15
With 150 g of anthracene oil (5.8%) 8.7	With 55 g of coke (2.1%) 1.15
	With 25 g of oil up to 230° (7.8%) 1.95
	With 10 g of water (11%) 1.10
	With 10 g of gas and losses 0.85
Total hydrogen 14.2	Total hydrogen 14.2

It is seen that high yields of tar are obtained in presence of anthracene oil, whereas in presence of solar oil the yields are almost the same as those obtained by the dry distillation of lignin under vacuum.

A very low yield of tar is obtained in presence of avtol, but when this paste former is recycled it evidently becomes enriched with the decomposition products of lignin and assists the process, especially after the 3rd cycle. After the 4th cycle considerable cracking of the avtol occurs, and the tar yield falls to a minimum.

These results indicate that the vacuum-thermal process cannot be classified as a process of dry distillation, as the paste-forming oils are selective in their action.

To test the hypothesis that the vacuum process is a process of thermal liquefaction, the composition of a repeatedly recycled paste former was investigated.

The thermal liquefaction of various carbonaceous materials in organic solvents is accompanied by redistribution of hydrogen [4]. This process is seen especially clearly in tetralin. Tetralin is a hydrogenating solvent which yields hydrogen to the products of liquefaction and is converted into naphthalene.

This redistribution of hydrogen is not found in the vacuum-thermal decomposition process.

The elementary composition of anthracene oil used as paste former in the vacuum-thermal decomposition of cotton-hull lignin was investigated for the same portion of oil recycled 7 times, i.e., used in 7 consecutive experiments. The portion of the oil which boiled above 230° was recycled each time.

The elementary composition of this oil is given in Table 3.

It is seen that the carbon content decreases by over 4% owing to an increase of the oxygen content of the paste former, but the hydrogen content does not decrease, and even increases somewhat after the first few cycles. After the sixth and seventh cycles the hydrogen content almost reaches its original level.

The hydrogen balance in the vacuum-decomposition process is given in Table 4.

It is seen that the recycled tar paste former even shows an increase, though slight, of hydrogen content.

Thus, there is no transfer of hydrogen from the paste former to the substances formed in the process; they obtain hydrogen from the lignin, as the residual coke has a low hydrogen content. Therefore the vacuum-thermal process cannot be classified as a process of thermal liquefaction.

The remaining alternative is that vacuum-thermal decomposition depends on somewhat different factors.

It follows from Table 2 that anthracene oil favors the formation of high yields of tar from lignin, whereas solar oil and avtol do not. If avtol is recycled two or three times it becomes enriched with the decomposition products of lignin and assists the process considerably.

In the course of observations of the state of lignin in pastes with different organic substances it was noticed that the behavior of lignin in anthracene oil is not the same as in solar oil. A paste of lignin and anthracene oil in 1 :1.5 ratio is a homogeneous dark mixture which is fairly mobile when heated, and does not separate out; the lignin swells somewhat. The paste in solar oil is quite different. It separates out into layers fairly quickly, with oil of unchanged color on top; no swelling of the lignin can be detected.

The effects of swelling of lignin in different media on its vacuum-thermal decomposition were investigated. It is known [5] that swelling increases with increase of temperature; this relationship is represented by the expression $p = RTc$, where c is the concentration of the substance.

TABLE 5

Swelling of Cotton-Hull Lignin in Different Solvents

Medium	Volume increase of the lignin (in %) at temperature (°C)		Notes
	20	100	
Cresol (mixed isomers)	30	60	Some dissolution of lignin
o-Toluidine	30	50	The same
Anthracene oil, 230-300°	25	20	Considerable dissolution
Anthracene oil, 300-360°	–	20	The same
Solar oil	Does not swell	10	No dissolution noted

Swelling of a substance greatly increases with temperature and at a certain temperature, characteristic for a given substance, swelling passes into dissolution. It is evident that as the temperature increases bonds between individual particles are weakened until they are completely broken.

The swelling of lignin in different paste formers may solve the problem of the mechanism of the vacuum process. The swelling of lignin was studied in anthracene oil (230-300° and 300-360° fractions), in solar oil (240-350° fraction), mixed cresol isomers, and o-toluidine. The Fischer method [5] was used for the determinations. The experiments were performed at room temperature and under the action of heat on a boiling water bath for 1 hour. The results are given in Table 5.

A separate experiment on the solubility of lignin in anthracene oil showed that the solubility is 6.4%. The degree of swelling in solar oil is low, and no dissolution was observed. Alkali lignin isolated from hydrolytic lignin swells to the same extent as hydrolytic lignin. Swelling is accompanied by partial dissolution.

It follows that the vacuum-thermal decomposition of hydrolytic lignin can only proceed to a considerable extent in media in which it swells considerably and partially dissolves. The lignin and the paste former form a colloidal system, and the vacuum process takes place with swelling of the lignin, followed by dissolution of the solid in the liquid phase at a certain high temperature.

The results of experiments on the vacuum process with different paste formers are given in Table 6. The duration of each experiment was 90 minutes, under 40 mm Hg pressure. The final temperature was 460°.

TABLE 6

Yields Obtained from Hull Lignin with Different Paste Formers

Paste former	Yields (% on dry lignin)			
	carbon	tar	pyrolysis water	gas and losses
Swelling agents				
Dry-distillation tar, fraction above 230° (1 : 1.5)	50.0	32.6	7.3	10.1
Anthracene oil (1 : 1.5)	55.2	30.3	7.4	7.1
Same (1 : 1.8)	49.2	38.0	4.4	8.4
Naphthalene (1 : 1.5)	60.0	15.7	5.5	18.8
o-Toluidine (1 : 1.5)	55.1	13.3	15.3	16.3
Cresols (1 : 1.5)	48.0	22.0	12.0	18.0
β-Naphthol (1 : 1.5)	48.2	33.3	7.4	11.1
Nonswelling agents				
Solar oil (1 : 1.5)	48.9	12.3	18.4	20.4
Avtol (1 : 1.5)	54.6	4.1	13.2	28.1
Maxut (1 : 1.5)	61.4	8.0	8.9	21.7
Ceresin (process up to 400°)	65.9	12.5	11.4	10.2

TABLE 7

Effect of Amounts of Paste Former on the Yields Obtained from Hull Lignin

Paste former	Lignin–paste former ratio	Yields (% on dry lignin)			
		carbon	tar	pyrolysis water	gas and losses
Dry lignin	0	48.1	17.3	15.4	19.2
Lignin and anthracene oil	1 : 1.3	51.7	22.7	13.1	12.5
The same	1 : 1.5	55.2	30.3	7.4	7.1
The same	1 : 1.8	49.2	38.0	4.4	8.4

TABLE 8

Effect of Degree of Vacuum on the Yields Obtained From Hull Lignin
(1 : 1.8 paste of lignin in anthracene oil)

Operating pressure (mm Hg)	Yields (% on lignin)			
	carbon	tar	pyrolysis water	gas and losses
Atmospheric	57.7	17.1	20.1	5.1
40	49.2	38.0	4.4	8.4
90	49.6	36.9	7.1	6.4
150	51.8	32.6	8.8	6.8

In oils which swell lignin, the yields of tar in the thermal process are fairly high – not less than 30%. In the other three substances which also swell lignin, the tar yields are lower; the yield in presence of toluidine is especially low, only 13.3%. The following explanation may be offered: in the vacuum process the swelling of lignin, which is a favorable factor, must be accompanied by other favorable factors, such as a suitable boiling range of a paste former and the absence of functional groups which may lead to chemical reactions with the products of the thermal decomposition of lignin. For example, naphthalene and cresols boil at fairly low temperatures, and therefore the yields obtained with them are not very high. Toluidine is a base and forms chemical

compounds with the acid products of the thermal decomposition of lignin – acetic and formic acids – and the decomposition of these salts leads to formation of increased amounts of water and gas. The pyrolysis water from this experiment did not have an acid reaction. In cresol mixture the yield of tar is 22%.

It seems hardly likely that a substance of such low boiling point could favor the process, especially under vacuum. The cresol mixture boils in the 190-203° range, while under the vacuum used in the thermal process it should start to boil at 110-115°, far below the temperature at which the thermal decomposition of lignin begins. In reality, however, lignin swells in cresol and forms a colloidal system, and therefore cresol is distilled off under different conditions. For example, up to 200° only 30% was distilled off, and cresol continued to distill up to 300° and over.

The influence of the formation of a colloidal system on the elevation of the boiling temperature of the paste former is clearly illustrated by the following experiment.

A definite quantity of anthracene oil (fraction boiling at 230-340°) was distilled off from the retort under vacuum. An equal weight of oil, but in presence of lignin swollen in it was distilled off under identical conditions. The distillation results are shown in the Figure.

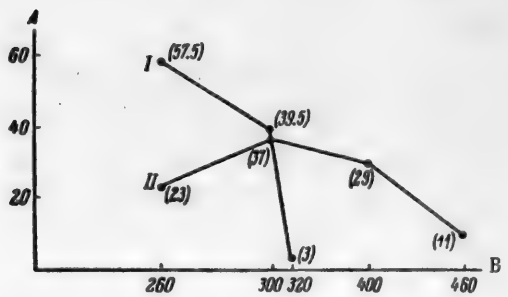

Curves for distillation of oil alone (I) and in presence of lignin (II).
A) Amount of oil distilled off (%), B) temperature (°C).

It is seen that 57% of the anthracene oil boils out up to 260° when distilled alone under vacuum, and the distillation is complete at 300°. However, if the oil forms a colloidal system with lignin the character of the distillation curve changes entirely, and at the temperature of the most intensive thermal decomposition of lignin (280-400°) some oil still remains; this favors high yields of tar from lignin.

The distillation curves for solar oil is almost the same regardless of the presence or absence of lignin. The oil distils off below 300°, and this has little influence on the yields obtained from the lignin.

The amount of oil used for mixing the paste also influences the yields in the vacuum process. To determine the optimum amounts of paste formers in the paste, the experiments detailed in Table 7 were carried out.

The conditions were: final temperature 460°, duration 90 minutes, pressure 40 mm Hg.

A 1 : 1.8 ratio of lignin to oil must be regarded as the limit, as a 1 : 2 paste does not remain homogeneous, and excess oil separates out on top of the paste. A lignin–oil paste in 1 : 1.8 ratio is a homogeneous, well-swollen mixture which does not separate out. The yields obtained with a 1 : 1.3 ratio differ little from the yields obtained by dry distillation under vacuum. In addition to the paste former, vacuum plays an important part in the vacuum process.

The effect of the degree of vacuum is seen in Table 8.

The process conditions were: final temperature 460°, duration 90 minutes. The yield of tar without the use of vacuum was almost the same as in dry distillation of lignin under vacuum. The yield of tar was considerably greater with the use of vacuum. The best yields are obtained at 40 mm Hg; the yields decrease with decrease of the degree of vacuum.

The influence of vacuum on the yields can likewise be explained with the aid of the theory of swelling of substances of high molecular weight. When a substance swells, a pressure is set up in its swollen particles. If the thermal process is carried under pressure (thermal liquefaction), the pressure within the particles is counteracted by the external pressure and, by the Le Chatelier principle, swelling substances should dissolve to alesser extent than nonswelling.

Various investigators who studied the relationship between swelling and degree of liquefaction of various coals in paste formers concluded that swelling coals are liquefied to a lesser extent [6]. For example, Sudzilovskaia [7] reports that solvents which swell coals at low temperatures give a low degree of liquefaction in the conditions used.

The situation in the vacuum-thermal process is quite different. The internal pressure in the swollen lignin particles favors high yields of substances in presence of an external vacuum. It becomes obvious why the yield of tar from lignin is considerably lower at atmospheric pressure but increases with reduction of pressure.

The degree of grinding of the lignin used in the paste has little influence on the yields of valuable chemical products; equal yields of tar are obtained in the vacuum process from lignin with 0.3 mm and 10-12 mm particles.

To summarize the foregoing data on the characteristics of the vacuum-thermal decomposition in the liquid phase, the mechanism of the process can be described as follows. When lignin is mixed into a paste with oil it swells and partially dissolves. A colloidal system is formed. The molecular bonds between the particles in the swollen polymeric lignin are weakened. The resins and waxes present in hydrolytic lignin dissolve in the paste former. The lignin swells, while the cellulose evidently remains unchanged. The chemical bonds between cellulose and lignin are evidently weakened as the result of swelling. As the temperature rises the intermolecular bonds in lignin are progressively weakened until they are entirely broken. The colloidal system has a higher boiling point, which favors the vacuum-thermal process. Heating also causes decomposition of individual macromolecules of lignin, accompanied by decarboxylation, dehydration, and similar processes. The substances of low molecular weight formed in the process are rapidly removed in the vapor state from the heated zone, and are thus protected from secondary processes – polymerization and condensation.

The action of the paste-forming oil may be represented as follows.

First, the paste former is a good heat-transfer medium. It is heated at the walls of the retort, and rapidly transfers heat to the lignin particles which, as is known, have very low heat conductivity. The temperature is equalized uniformly and mild conditions are created for the thermal process. Second, the vapor of the paste former, stable to pyrolysis, lowers the partial pressures of the unstable molecules formed by the thermal decomposition of lignin, thus making the conditions unfavorable for polymerization and condensation. Third, the lignin swells and partially dissolves in the paste-forming oil, and this favors the vacuum-thermal process.

SUMMARY

1. It is shown that the vacuum-thermal process cannot be considered as a process of dry distillation in the liquid phase, as the effects of paste formers are selective; some paste-forming oils favor the process and others do not.

2. The vacuum process cannot be classified as a thermal-liquefaction process either, as a paste former repeatedly recycled in the process does not provide hydrogen for saturation of the liquefaction products.

3. It was shown in a study of the behavior of lignin in pastes with oils which do and do not favor the vacuum-thermal decomposition process that lignin swells and partially dissolves in oils which favor the vacuum process. Lignin does not swell or dissolve in oils which do not favor the vacuum process.

4. The paste-forming oil must have a definite boiling range and must not have a high content of active functional groups which could form saltlike compounds with the products of thermal decomposition of lignin.

5. The best paste former is a mixture of aromatic hydrocarbons containing some phenols, such as anthracene oil and the high-boiling fractions of dry-distillation lignin tar.

6. The yields of valuable chemical products are considerably higher if vacuum is used. The yield of tar from lignin increases with increasing vacuum.

7. The degree of grinding of the lignin does not influence the yield of tar in the vacuum process.

LITERATURE CITED

[1] V. N. Kozlov, The Pyrolysis of Wood (1951).*

[2] P. A. Bobrov, J. Appl. Chem. 6 (1933); Wood Chem. Ind. 3 (1935).

[3] A. K. Slavianskii, Doctorate Dissertation (1946).

[4] M. K. Diakova, Doctorate Dissertation (1951).

* In Russian.

[5] N. I. Nikitin, Chemistry of Wood (Izd. AN SSSR, 1951) p. 125.*

[6] V. Naumov, Colloid Chemistry (1932).*

[7] M. S. Sudzilovskaia, Trans. All-Union Sci. Res. Inst. of Gas and Synthetic Liquid Fuel, 1, 56 (1948).

Received December 12, 1955

* In Russian.

INVESTIGATION OF HYDROXYLATION AND DEHYDRATION OF OLEIC AND STEARIC ACIDS

V. V. Korshak and A. A. Ivanova

Studies of dehydration processes of the esters of natural hydroxy acids [1] and esters of hydroxy acids obtained by artificial hydroxylation [2] are of interest in relation to the synthesis of drying products from nondrying and semidrying oils.

In view of the effectiveness of hydroxylation of saturated and unsaturated compounds by oxidation with atmospheric oxygen [2] it was desired to determine the conditions favoring hydroxylation.

By Bakh's theory [3], oxidation of saturated and unsaturated compounds is now regarded as consisting of the addition of oxygen molecules at bonds between carbon and hydrogen, with formation of peroxides and hydroperoxides [4]. When unsaturated compounds are oxidized with oxygen, the formation of peroxide groups in the β position relative to the double bond has been proved. For example, oxidation of hexene yields the hydroperoxide of hexene-1:

$$CH_2{=}CH{-}\underset{\displaystyle OOH}{\underset{|}{CH}}{-}CH_2{-}CH_2{-}CH_3$$

The conversion of hydroperoxides into hydroxyl-containing compounds is explained by the presence of 1 weakly bonded oxygen atom in the hydroperoxide molecule, so that this oxygen can react with other compounds, and alcohols are formed from hydroperoxides.

The formation of hexyl, heptyl, and other higher alcohols in the oxidation of paraffin wax, reported by Nametkin and Zvorykina [5], can be interpreted in conformity with this oxidation mechanism.

The mechanism of formation of hydroxylic compounds by the action of 1% potassium permanganate solution on unsaturated compounds was interpreted by Vagner [6] as addition of 2 water residues, formed by decomposition of water by the oxygen of the oxidizing agent, to the carbon atoms linked by a double bond.

In the action of atomic oxygen, liberated from benzoyl peroxide, on unsaturated compounds Prilegaeff [7] demonstrated the formation of compounds containing epoxy groups, according to the scheme:

$$C_6H_5\overset{\displaystyle O}{\overset{\|}{C}}OOH + \diagup C{=}C \diagdown \longrightarrow C_6H_5COOH + \diagup \underset{\displaystyle O}{\underset{\diagdown}{C}} - C \diagdown$$

Arbuzov and Mikhailov [8] confirmed that this mechanism applies if peracetic acid is used instead of benzoyl hydroperoxide. Later many investigators showed that the primary products of olefin oxidation are α-oxides, and glycols or their monosubstituted derivatives are formed only as the result of conversion of the latter. For example, Swern et al. [9] represents the reaction between an acid hydroperoxide and an unsaturated compound as follows:

$$R_2{-}CH{=}CH{-}R_3 + R_1CO_3H \longrightarrow$$
$$R_2{-}\underset{\displaystyle O}{\underset{\diagdown\ \diagup}{CH{-}CH}}{-}R_3 + R_1COOH \longrightarrow R_2{-}\underset{\displaystyle OH}{\underset{|}{CH}}{-}\underset{\displaystyle OCOR_1}{\underset{|}{CH}}{-}R_3,$$

thus it is seen that the initial reaction products are compounds with epoxy groups; under the subsequent action of acid the epoxide ring is broken and addition of the acid takes place with formation of a semiesterified glycol.

Miles and Sussman [10] oxidized propylene and other unsaturated compounds with hydrogen peroxide in presence of osmium tetroxide and oxides of other metals in groups IV, V, and VI of the periodic system. Of these oxides, the best hydroxylation results were given by vanadium pentoxide and chromium trioxide, which gave glycol yields from 16.8 to 37.36% from trimethylethylene. Pervanadic and perchromic acids were detected as intermediate products.

On the basis of literature data and the experimental results of the present investigation we concluded that one of the several possible directions of the oxidation of fatty acids radicals in vegetable oil triglycerides, in addition to hydroxylation, is formation of compounds containing epoxy groups which undergo secondary reactions to give rise to compounds with several-fold increase of molecular weight; if the molecular weight reached is high enough, this may lead to formation of solid products or films.

In view of the fact that in the oxidation of unsaturated compounds with atmospheric oxygen at elevated temperatures the formation of oxygen-containing compounds takes place, in the same way as in film formation by drying oils, it seems likely that in the hydroxylation of linoleic and other highly unsaturated acids, also present in semidrying oils, processes will occur which increase rather than decrease their tendency to film formation. It was therefore desirable to study the processes taking place during oxidation of semidrying oils, in their components of low functionality, such as the oleic acid radical, or in saturated acid radicals, which have no functional groups. This accounts for our choice of oleic and stearic acids for investigations of hydroxylation and dehydration processes.

EXPERIMENTAL

Oxidation of oleic acid with peracetic acid and atmospheric oxygen. To elucidate the reactions of fatty acids in oxidation with peracetic acid and atmospheric oxygen, a comparative study of such oxidation was carried out.

The oleic acid used for the oxidation has the following characteristics (at 20°): viscosity in poises 0.2210, specific gravity 0.8928, refractive index 1.4640, color (on the iodometric scale) 1, acid number 197.8, and iodine number (by the Hanus method) 92.

The oxidation with peracetic acid was performed as follows. To 164 g of acetic anhydride of b.p. 136-138°, 36 g of hydrogen peroxide (26-30%) was added dropwise at 40° during 4 hours. To this solution 50 g of oleic acid was added dropwise with stirring at 20° during 3 hours, and the reaction mixture was then poured into 1 liter of cold water. The oxidation product was washed with water and dried in a desiccator over sulfuric acid; the yield was 46 g or 92% on the oleic acid taken. Oxidation of oleic acid with atmospheric oxygen was carried out at 75° in a cylinder equipped with a contact thermometer, the temperature in the cylinder being maintained to an accuracy of ±1°, and with a bubbling device for the air feed. Oxidation of oleic acid with atmospheric oxygen was continued for 60 and for 120 hours. 150 g of oleic acid was taken for each experiment, and the air was fed at a rate of 10 liters/minute. The oxidation gave 140.6 g of oxidation product (yield 93.75%) in Sample 1, and 134.8 g (yield 89.87%) in Sample 2. The experimental results are given in Table I.

Analytical data for oleic acid oxidized with atomic oxygen and molecular oxygen respectively indicate that the nature of the oxidation is similar in the two cases and that the difference, as indicated by the values of the constants, is quantitative only. Thus, hydroxylation occurred in all the experiments, but to different extents. The highest hydroxyl and epoxide numbers were found for the product of oxidation of oleic acid with peracetic acid. The hydroxyl and saponification numbers increase with increased duration of oxidation of oleic acid with atmospheric oxygen, while the epoxide number decreases. This may be the result of interaction of epoxy groups with other groups formed during oxidation. Cleavage of the epoxide ring may give rise to hydroxyl groups. Data on the molecular weight of acid oxidized with molecular oxygen indicate that condensation or polymerization processes occur. As the result of oxidation for 60 hours the molecular weight is increased nearly 5-fold, and after oxidation for 120 hours it is increased nearly 9-fold (Table II). The fact that the acid number (Table I) does not decrease in the course of oxidation indicates that esterification of oleic acid does not take place under these conditions. We must therefore postulate that compounds containing epoxy groups react

with hydroxylic compounds, so that the oxygen content in the polymer formed does not decrease. Elementary analysis data give an indication of the oxygen content in the oxidation products of oleic acid.

TABLE I

Constants of the Products of Oxidation of Oleic Acid with Peracetic Acid and Atmospheric Oxygen

Characteristics	Constants of oxidation products of samples		
	No. 1	No. 2	No. 3
	with peracetic acid	with atmospheric oxygen	
Oxidation time (hours)	3	60	120
Specific gravity at 20°	solid	0.9834	1.0113
Viscosity at 20° (Ostwald, seconds)	–	2189 (11.37 poises)	3 hr. 30 min.
Refractive index at 20°	–	1.4712	1.4752
Color on iodometric scale	1	9	21
Acid number (mg KOH)	188	174	185.3
Hydroxyl number (mg KOH)	160.5	72.5	98
Iodine number (% iodine)	20	38	24.3
Saponification number (mg KOH)	216.5	277	312
Epoxide number (% epoxy groups)*	27	2.61	0
Peroxide number (% of active oxygen)	0.25	0.24	0.14
Carbonyl number (mg KOH)	40	64.2	59

* Epoxide numbers were determined with the use of an acetone solution of KCl.

TABLE II

Molecular Weight and Elementary Composition of Oxidized Oleic Acid

Acid	Molecular weight	C	H	O
		%		
Oleic acid oxidized for 60 hours	1341	69.51	10.71	19.78
	1331	69.38	10.69	19.93
Oleic acid oxidized for 120 hours	2446	67.70	10.30	22.00
	2589	68.04	10.36	21.60
Calculated for oleic acid	282	76.1	12.06	11.34

Hydroxylation and dehydration of oleic acid. Hydroxylation of oleic acid was carried out by the Zaitsev method, described in detail by Zinovyev [11].

Oleic acid with acid number 196 and iodine number 89 was used for oxidation.

In Experiment No. 1, a solution of 29.7 g of potassium permanganate in 2.38 liters of water was added dropwise with stirring to a solution of 100 g of oleic acid and 21.5 g of caustic soda in 2.38 liters of water, cooled to 0°. The resultant liquid was filtered and the filtrate decomposed with sulfuric acid. Acidification yielded 106 g of crude product in 94.64% yield. After recrystallization from hot alcohol the product had m. p. 151° and acid number 164.5. According to literature data [11], the melting point of dihydroxystearic acid is 136.5° and the calculated acid number is 174.

In Experiment No. 2, a solution of potassium permanganate (37.12 g) in 2.975 liters of water was added dropwise with stirring to a solution of 125 g of oleic acid and 26.9 g of caustic soda in 2.95 liters of water, cooled to 0°. Filtration and acidification with sulfuric acid gave dihydroxystearic acid which after crystallization from hot alcohol had m. p. 150° and acid number 165.4. Dehydration of dihydroxystearic acid of acid number 165.4 was carried out in a three-necked flask 50 ml in capacity, fitted with a reflux condenser, thermometer, and mechanical stirrer. The flask contained 10 g of dihydroxystearic acid and 0.2 g of sodium bisulfate (2%).

When the acid was heated with the catalyst to 170°, vigorous frothing occurred, and drops of water appeared in the condenser, indicating the occurrence of dehydration. As the result of heating at 242° for 3.5 hours, the acid yielded 9.18 g of a polymeric product (yield 90%), insoluble in alcohol, benzene, or ether.

The second dehydration experiment was carried out with dihydroxystearic acid of acid number 164.6. 6 of the acid and 0.12 g of sodium bisulfate were taken for the dehydration. As the result of heating at 187-190° for 25 minutes and at 190-200° for 25 minutes, the acid yielded 5.58 g of dehydration product (yield 96.2%). The drops of condensed water gave a characteristic blue color with anhydrous copper sulfate. The dehydration product had the following constants: iodine number 38.8, saponification number 275.8, acid number 54, ester number 221.8, diene number 6. These constants indicate that when dihydroxystearic acid is heated dehydration occurs with formation of double bonds and conjugated double bond systems, but the dehydration process is accompanied by esterification of the acids at the hydroxyl groups of the hydroxy acid, with formation of esters and a decrease of the free acid content.

Further experiments on hydroxylation of oleic acid with atmospheric oxygen, followed by dehydration, showed that the dehydration effect was relatively large in comparison with the esterification effect. Oleic acid distilled at 7 mm and 209-210° was used for the experiments on hydroxylation with atmospheric oxygen. The acid was hydroxylated by oxidation with atmospheric oxygen in a glass round-bottomed cylinder (360 mm high and 50 mm in diameter). The air was fed into the cylinder through a bubbling device at a rate of 10 liters/minute. The oxidation was effected at 155-160°. To determine the influence of catalysts on the course of oxidation, oleic acid was oxidized without catalysts, and in presence of 1% of lead oxide and 0.2% of manganese dioxide. In addition, an experiment was carried out on the oxidation of oleic acid in presence of these catalysts with 7.5% of pentaerythritol, calculated on the weight of the acid. The hydroxylation products were dehydrated at 245-247° in presence of 2% of sodium bisulfite for 4 hours.

The hydroxylation and dehydration times, the yields of the products, and analytical data are given in Tables III and IV.

TABLE III

Preparation Times and Yields of Hydroxylation and Dehydration Products of Oleic Acid

Treatment of Oleic Acid	Amount of acid taken for experiment, in g	Treatment time	Yield of product	
			in g	%
Oxidation without catalyst	90.8	9 hr.	75.46	83.1
Dehydration after oxidation without catalyst	31.62	2 hr.	25.05	79.2
Oxidation with catalyst	103.12	21 hr. 45 min.	82.61	80.1
Dehydration after oxidation with catalyst	29.88	2 hr.	24.38	81.5
Oxidation with catalyst and pentaerythritol	133.66	17 hr. 30 min.	–	–
Dehydration after oxidation with catalyst and pentaerythritol	36.55	2 hr.	33.18	90.7

It follows from these results that hydroxylation and dehydration of oleic acid is not accompanied by any considerable scission of the hydrocarbon chains; this is also shown by the constants of oleic acid before and after hydroxylation and dehydration.

The high acetyl numbers of the oxidized oleic acid samples show that hydroxylation does in fact occur in oxidation with atmospheric oxygen. In addition to hydroxyl groups, keto groups are formed in the oleic acid molecule on oxidation. Apart from addition of hydroxyl groups at the double bonds, hydroxylation also occurs at carbons not linked by double bonds; this is indicated by the considerably greater increases of hydroxyl numbers as compared with the decreases of iodine numbers.

TABLE IV

Constants of Oleic Acid Before and After Hydroxylation and Dehydration

Treatment Conditions	Acid number	Saponification number	Ester number	Acetyl number	Iodine number	Carbonyl number
Oxidation without catalyst	114.52	293.1	178.58	236.9	30.9	32.22
Dehydration after oxidation without catalyst	114.5	285.4	170.9	21.7	40.7	32.9
Oxidation with catalyst	143.7	218.1	74.4	166.3	35.1	36.3
Dehydration after oxidation with catalyst	134.1	260.2	126.1	43.2	45.9	24.2
Oxidation with catalyst and pentaerythritol	91.0	244.3	153.3	175.3	48.7	15.4
Dehydration after oxidation with catalyst and pentaerythritol	67.7	174.2	106.5	55.6	52.2	34.6
Oleic acid before oxidation	175.3	217.5	42.2	27.0	76.4	22.1

TABLE V

Elementary Composition of Oleic Acid Before and After Hydroxylation and Dehydration

Acid	Molecular weight	C	H	O
		%		
Oleic acid (original	285.9	74.7 74.4	10.0 10.0	15.3 15.6
Oleic acid oxidized without catalyst	156.4	65.6 65.7	10.4 10.4	24.0 23.9
Oleic acid oxidized without catalyst and dehydrated	1067.7	76.4 76.3	9.6 9.2	14.0 14.5
Oleic acid oxidized in presence of lead and manganese oxides	507	72.3 72.0	11.7 11.9	16.0 16.1
Oleic acid oxidized in presence of metal oxides and dehydrated	712.5	75.5 75.9	11.1 11.1	13.4 13.0
Oleic acid oxidized in presence of metal oxides and pentaerythritol	985	72.5 72.3	11.4 11.7	16.1 16.0
Oleic acid oxidized in presence of metal oxides and pentaerythritol, and then dehydrated	695.7	76.4 76.7	10.3 10.6	13.3 12.7

The increase of molecular weight as the result of hydroxylation and dehydration of oleic acid confirms the occurrence of polymerization and condensation processes (Table V).

The occurrence of hydroxylation and dehydration processes, and of side reactions in which other oxygen-containing compounds are formed, is also indicated by the elementary analysis data, from which it is clear that the amount of oxygen increases as the result of oxidation and decreases as the result of dehydration. However, it is found in all cases that the loss of hydroxyl groups as the result of dehydration is relatively greater than the decrease of oxygen content, i.e., after almost complete removal of hydroxyl groups a large amount of oxygen remains in the dehydration products (Table V). Therefore, in order to determine what types of oxygen-containing compounds are formed by oxidation of oleic acid, the oxidation products were separated into fractions soluble and insoluble in ligroine.

TABLE VI

Yields of Fractions and Analytical Data

Characteristics of fractions	Oleic acid oxidized in presence of catalyst		Oleic acid oxidized in presence of catalyst and pentaerythritol	
	Solubility of fraction in ligroine			
	Soluble	Insoluble	Soluble	Insoluble
Yield (in g)	8.24	7.8	3.98	6.7
Yield (in %)	47.4 (from 17.4 g)	44.8 (from 17.4 g)	31.0 (from 12.82 g)	52.3 (from 12.82 g)
Acid number	120.7	169.9	172.5	122.85
Saponification number	191.9	247.6	213.4	188.8
Ester number	71.2	77.7	40.9	65.95
Acetyl number	82.7	111.8	66.15	38.65
Iodine number	48.25	37.9	18.37	48.2
Carbonyl number	22.95	75.5	61.0	42.4
Molecular weight (in camphor)	430	1101	902	901
Elementary composition (%) C	74.5 74.1	74.1 74.0	77.4 77.1	73.7 73.2
Elementary composition (%) H	10.7 10.4	10.2 10.2	11.7 11.5	9.1 9.2
Elementary composition (%) O	14.8 15.5	15.7 15.7	10.9 11.4	17.2 17.6

For this, the hydroxylation products were first saponified with 2 N alcoholic solution of caustic soda at 80°. The sodium salts of the acids so obtained were dissolved in 50 ml of hot distilled water and then washed with ether to remove unsaponifiables.

The aqueous salt solution was acidified with hydrochloric acid solution. The liberated acids were separated from the aqueous layer and washed with water to a neutral reaction (to methyl orange). The washed acids were then fractionated in ligroine.

The yields and analytical data of the fractions are given in Table VI.

Analysis of the fractions of oxidized oleic acid confirms that the oxidation products contain hydroxy acids with high hydroxyl numbers, and with higher oxygen contents and molecular weights than the original oleic acid.

Hydroxylation and dehydration of stearic acid. The hydroxylation of stearic acid was effected under the same conditions as the hydroxylation of oleic acid. In each experiment 150 g of chemically pure stearic acid with m. p. 71° was used. The oxidation time was 30 hours. As in the case of oleic acid, 3 experiments were carried out on the oxidation of stearic acid. Experiment No. 1 was carried out without catalyst; Experiment No. 2 was

TABLE VII

Constants and Molecular Weights of Stearic Acid Before and After Hydroxylation and Dehydration

Constants	Stearic Acid						
	Before oxidation	Oxidized without catalyst	Dehydrated after oxidation without catalyst	Oxidized with catalyst	Dehydrated after oxidation with catalyst	Oxidized with catalyst and pentaerythritol	Dehydrated after oxidation with catalyst and pentaerythritol
Yield (%)	–	69.3	64.5	39.2	79.2	64.7	82.09
Acid number	198	157.7	186.3	149.4	108.5	102.1	33.3
Saponification number	194.7	343	305.6	327	298.4	296.4	285.5
Acetyl number	0	23.3	18.1	34.4	27.3	35.7	23.9
Ester number	0	185.3	179.3	177.3	189	194.3	252.2
Iodine number	0	10.6	46.0	2.5	18.4	1.0	12.4
Carbonyl number	0	63.7	30.5	10.6	67	18.9	52.9
Molecular weight	305.5	602.9	632.5	718.7	934.5	557.8	1507.1

TABLE VIII

Elementary Composition of Hydroxylated and Dehydrated Samples of Stearic Acid

Acid	Elementary Composition (%)		
	C	H	O
Stearic acid (original)	76.4	12.5	11.1
	76.77	12.49	10.64
Stearic acid oxidized without catalyst	68.1	8.8	23.1
	68.0	8.0	24.0
Stearic acid oxidized with metal oxides	74.4	10.8	14.8
	74.7	10.0	15.3
Stearic acid oxidized with metal oxides and pentaerythritol	71.2	8.7	20.1
	71.4	8.8	19.8
Stearic acid oxidized in presence of metal oxides and pentaerythritol, then dehydrated.	73.0	9.4	17.6
	73.6	9.5	16.9

performed with 1% of lead oxide and 0.2% of manganese dioxide; Experiment No. 3, with the same catalysts and 7.5% of pentaerythritol, calculated on the weight of the acid.

All the experiments showed that stearic acid is converted into acids containing hydroxyl and keto groups as the result of oxidation. Moreover, oxidation resulted in the formation of additional carboxyl groups, indicating the formation of low-molecular acids.

This probably accounts for the considerably lower yields of oxidation products in presence of catalysts which activate the oxidation process.

However, in the presence of pentaerythritol the course of the process is modified in the direction of oxidation without any great formation of low-molecular acids; this is shown by the high yield of the oxidation product in presence of pentaerythritol. Further evidence for this is provided by the saponification number of this product, which is lower than that of products oxidized without pentaerythritol (Table VII).

The hydroxyl and keto groups formed in stearic acid as the result of oxidation are reactive and therefore interact with other reactive groups to form esters. The formation of esters in indicated by the decrease of the acid number and increase of the saponification number of stearic acid as the result of oxidation.

In the oxidation of stearic acid in presence of catalyst the amount of hydroxyl groups formed is 3 times that of the keto groups. In oxidation without catalyst, more keto groups are formed.

TABLE IX

Characteristics of Fractions Isolated from Oxidized Stearic Acid

Characteristics	Stearic acid oxidized in presence of			
	metal oxides		metal oxides and pentaerythritol	
	solubility of fraction in ligroine			
	soluble	insoluble	soluble	insoluble
Amount of oxidized acid taken for fractionation (in g)	26.47	26.47	13.2	13.2
Amounts of fractions (in g)	10.99	14.05	7.23	4.98
Amounts of fractions (in %)	41.5	53.1	54.7	45.2
Acid number	102.75	175.0	133.0	201.9
Saponification number	184.4	215.0	159.8	306.3
Ester number	81.65	40.0	26.8	104.4
Acetyl number	174.28	120.7	54.6	88.0
Iodine number	71.7	0	3.77	4.98
Carbonyl number	0	29.1	28.8	56.8
Molecular weight	393.35	259.35	269	263
Elementary composition (in %) C	72.7	73.4	72.8	73.2
	72.0	73.5	72.5	73.3
H	11.3	11.4	12.0	11.5
	11.3	11.5	11.7	11.4
O	16.0	15.2	15.2	15.3
	16.7	15.0	15.8	15.4

It follows from these experimental results that oxidation in presence of catalysts and pentaerythritol is more rational than oxidation without catalyst or pentaerythritol, as the former favors milder oxidation without breakdown of the fatty acid molecule, and leads to the formation of a larger amount of hydroxyl groups as compared with the amount of keto groups.

These results show that hydroxy acids are formed as the result of oxidation in all the experiments, while oxidation in presence of pentaerythritol gives a higher yield of these acids, and they have a higher content of hydroxyl groups.

The results of these experiments are in harmony with the results obtained in the oxidation of oleic acid, which was less prone to pyrolysis and other to hydroxylation when oxidized in presence of pentaerythritol.

The results of dehydration of the hydroxylation products of stearic acid are in agreement with the hydroxylation data.

Dehydration of stearic acid oxidized without catalyst or pentaerythritol (at 245-250° in presence of 2% of sodium bisulfate for 4 hours) gives a high yield of volatile products so that the yield of the dehydration product falls to 64.7%, whereas the yield of dehydrated product from acid oxidized in presence of catalysts is 79.8%, and from acid oxidized in presence of catalysts and pentaerythritol it is 82.07% (Table VII).

The decrease of the acetyl numbers and the increase of iodine numbers on dehydration of oxidized stearic acid confirm the validity of the suggested method of hydroxylation and dehydration of semidrying oils in order to increase their degree of unsaturation and film-forming properties [8]. These results also provide additional confirmation of the fact that saturated acids participate together with unsaturated acids in the formation products of the linoxyn type in the preparation of semidrying oils by hydroxylation and dehydration.

Data on the elementary composition of hydroxylated and dehydrated stearic acid samples, given in Table VIII, are in complete agreement with these results.

Investigations of certain fractions, soluble and insoluble in ligroine, obtained from samples of oxidized stearic acid showed, as in the case of fractions of oxidized oleic acid, that they contain hydroxyl and carbonyl groups, indicating the formation of keto hydroxy acids. Only one fraction, soluble in ligroine, obtained from

stearic acid oxidized in presence of metallic oxides, was found not to contain carbonyl groups (Table IX).

Hydroxyl groups are formed during oxidation of stearic acid and are split off during dehydration; this gives rise to double bonds in the same way as in hydroxylation and dehydration of triglycerides. This gives reason to believe that saturated fatty acid radicals are triglycerides in semidrying oils, together with the unsaturated radicals, undergo chemical changes in accordance with the described mechanism of hydroxylation and dehydration of triglycerides, and participate in the formation of film formers of the linoxyn type in chemical treatment of semidrying oils by this method. When stearic acid is oxidized in presence of pentaerythritol, the amounts of low-molecular acids formed are much less than in its absence.

SUMMARY

1. A comparative study of the oxidation of oleic acid with peracetic acid and atmospheric oxygen showed that hydroxyl and epoxy groups are formed at the double bonds in both cases.

2. In the oxidation of oleic acid with atmospheric oxygen, the formation of epoxy groups is accompanied by hydroxylation which does not affect the double bonds; this is attributed to introduction of oxygen between carbon and hydrogen atoms not adjacent to carbon atoms linked together by double bonds.

3. The formation of hydroxyl groups in the oxidation of stearic acid, like the hydroxylation of oleic acid, also occurs by introduction of oxygen between carbon and hydrogen atoms.

4. Dehydration of hydroxylated fatty acids is accompanied by a decrease of the oxygen content and of the number of hydroxyl groups, and by an increase of iodine number.

5. Hydroxylation and dehydration of fatty acids are accompanied by side reactions of condensation and polymerization, whereby the apparent effectiveness of the principal processes is decreased, but because of the high rate of the latter the occurrence of both processes has been confirmed by analytical data, and it has been shown that the dehydration of artificially hydroxylated acids is a process of the same type as the dehydration of natural hydroxy acids and their esters [1].

LITERATURE CITED

[1] V. V. Korshak and A. A. Ivanova, J. Appl. Chem., 27, 5, 523 (1955).*

[2] A. A. Ivanova, J. Appl. Chem., 27, 7, 718 (1955).*

[3] A. Bakh, J. Russ. Phys.-Chem. Soc., 29, 373 (1897); 44, 138 (1912).

[4] K. I. Ivanov, Intermediate Products and Intermediate Reactions of Hydrocarbon Autoxidation (State Tech. Press, 1949), pp. 11-87.**

[5] S. S. Nametkin and V. K. Zvorykina, J. Gen. Chem. 4, 7, 906-914 (1934).

[6] E. Vagner "The Reaction of Oxidation of Unsaturated Carbon Compounds" Dissertation (Warsaw, 1888).***

[7] N. A. Prilegaeff, Ber., 42, 4814 (1909).

[8] A. E. Aruzov, E. M. Mikhailov, J. Prakt. Chem., 127, 1, 92 (1930).

[9] D. Swern, Billen, Findley, Scanlan, J. Am. Chem. Soc., 67, 1786 (1945).

[10] N. A. Milas, S. Sussman, J. Am. Chem. Soc. 59, 2342 (1937).

[11] A. A. Zinovyev, The Chemistry of Fats (1939).**

Received March 26, 1956

* Original Russian pagination. See C. B. Translation.

** In Russian.

*** Russian translation.

PREPARATION AND STUDY OF THE PROPERTIES OF SPACE POLYMERS OF ALKYL ACRYLATES AND ALKYL METHACRYLATES*

A. Ia. Drinberg and A. D. Iakovlev

The Lensoviet Technological Institute, Leningrad

The synthesis of acrylate and methacrylate esters with a three-dimensional structure has attracted the close attention of investigators concerned with increasing the heat stability, mechanical strength, and other properties which are inadequate in these valuable synthetic materials. The reason is that conversion into a three-dimensional state is one of the most reliable ways of improving these properties in polymers. It was believed for a long time that linear polymers of the acrylate and methacrylate series, like many other saturated carbon-chain polymers, cannot be obtained in the three-dimensional state owing to the absence of active functional groups in their molecules. Therefore during the past 10-15 years numerous attempts were made to solve the problem of preparation of space acrylic polymers by the use of copolymers of methacrylate and acrylate esters with polyfunctional agents in the cross-linking reaction, rather than by the use of the individual polymeric esters.

The high reactivity of many polyfunctional monomers, including certain derivatives of methacrylic and acrylic acids (esters of allyl, vinyl, and polyhydric alcohols) [1-5] served as the basis for the synthesis of many space copolymers containing methacrylate and acrylate esters of monohydric aliphatic alcohols [6-12]. Most of these investigations show that if monomers of this type are used in the copolymerization reaction, space polymers are formed even at the earliest polymerization stage.

In contrast to these, copolymerization of small amounts of other diene compounds such as butadiene, isoprene, allyl maleate, allyl lactate–maleate, and others, with acrylates yields soluble copolymers which can be vulcanized [13-15]. These acrylic copolymers, known as "Lactoprenes," have been recommended as a variety of synthetic rubber [14, 16]. The presence of double bonds in "Lactoprenes" makes them vulcanizable by the usual methods with the aid of the common vulcanization agents used for unsaturated rubbers [17].

Various halogen-containing acrylic copolymers ("Lactoprene EV") and polyacrylates, containing nitrile ("Lactoprene BN"), amino, nitro, carboxyl, and other groups which can readily react with vulcanizing agents in their side chains, behave similarly to unsaturated copolymers [18-24]. It is seen that vulcanization of polymers of this type occurs by way of exchange reactions between the functional groups and the cross-linking agents such as amines, glycols, etc.

Much less is known, especially from the theoretical aspect, about the formation of space polymers from individual saturated methacrylate and acrylate polymers. Research carried out in this field by Mast, Rehberg and others [25] has shown that in presence of certain agents (benzoyl peroxide, quinone dioxime) individual polyacrylates can be vulcanized to give products of high tensile strength and of good stability to heat and chemical action. Later, Owen [26], Semegen and Wakelin [27], and others [28] showed in their studies of the vulcanization of polyacrylate rubbers that saturated acrylate esters can be satisfactorily cross linked in presence of alkaline agents. Among such agents, alkaline hydroxides, litharge, amines, lime, and sodium stannate, vanadate, plumbate, and hydrated sodium metasilicate are particularly recommended [26-30].

Methacrylate esters can also be obtained in the cross-linked state.

In a series of investigations by thepresent authors on the cross linking of saturated carbon-chain polymers

* Communication VIII in the series on conversions of saturated carbon-chain polymers.

[31-34] considerable attention was devoted to the cross linking of polybutyl methacrylate, which takes place easily when the polymer is heated in thin films.

Despite the existence of a considerable number of publications on structure formation in saturated alkyl acrylate and methacrylate polymers, the question of the laws governing the process and its chemical basis still remains open; not enough is known about the conditions of formation and the properties of the space polymers. The present investigation is an attempt to fill this gap.

EXPERIMENTAL

The work was performed on polymers of methacrylate and acrylate esters of normal aliphatic alcohols, and in particular on polymers of methyl, ethyl, propyl, butyl, and octyl methacrylates, and methyl, ethyl, butyl, and octyl acrylates. All these polymers were prepared by polymerization of the corresponding monomers. Of these, methyl methacrylate and acrylate and butyl methacrylate were used in the prepared form, and were merely purified to remove inhibitor and distilled under vacuum before polymerization. The other esters were synthesized by methods described in the literature [2, 35-37].

Ethyl and propyl methacrylates were made by direct esterification of methacrylic acid with the alcohols; octyl methacrylate and acrylate and butyl acrylate were prepared by transesterification of methyl esters of the corresponding acids; ethyl acrylate was synthesized from methyl acrylate by acidolysis of the latter with formic acid [38] followed by esterification of the acrylic acid with ethyl alcohol. The properties of the synthesized monomers are given in Table 1.

TABLE 1

Properties of the Synthesized Monomers

Esters	Boiling point		Density	Refractive index	Saponification number (mg KOH/g)
	°C	mm Hg	d_4^{20}	n_D^{20}	
Methacrylates:					
ethyl	116—117	760	0.913	1.4151	488
n-propyl	47—48	13	0.902	1.4192	435
n-octyl	73—74	1	0.881	1.4318	268
Acrylates:					
ethyl	100	762	0.922	—	511
n-butyl	46—47	14	0.901	1.4198	430
n-octyl	85—87	14	0.883	1.4253	296

The monomers were polymerized by the solvent method: in toluene (for monomers with less than 4 C atoms in the alkyl group), and white spirit (for the butyl and octyl esters) at 95-96° for 4 hours. The monomer—solvent ratio was 7 : 3 for most of the esters; a 9 : 1 ratio was used for the octyl esters and butyl acrylate; propyl methacrylate was polymerized in the form of 50° solution in toluene.

The polymerization catalyst was 0.3° of benzoyl peroxide on the weight of the monomer. The polymers were isolated from solution and freed from unpolymerized monomers by precipitation with methanol followed by drying in thin layers on glass at 70-80°.

All the polymers were transparent and colorless; they were soluble in dioxane, benzene, chloroform, acetone, and ethyl acetate; the propyl methacrylate polymer was also soluble in turpentine, while the higher polymeric esters (butyl and octyl) of methacrylic and acrylic acids were soluble in turpentine and white spirit. Some other properties of the polymers are given in Table 2.

Method of investigation. All the polymers were heated in thin films to convert them into space polymers. The conversion was indicated by changes of the following main properties of the polymers: 1) solubility and degree of swelling in the most active solvents; 2) softening temperature; 3) tendency to degradation (in methacrylate polymers); 4) physicomechanical properties of the films. In the case of butyl methacrylate polymer, changes in the elementary composition were investigated.

The tests for conversion into cross-linked polymers were accompanied by indirect determinations of the degree of degradation. The degradation of the polymers was determined from the difference in the weight of the films before and after heat treatment, after the original film had been heated at 80° to constant weight.

TABLE 2

Properties of the Polymers

Polymers	Density d_4^{20}	Softening temperature (°C) [39]	Specific viscosity at 20° *	Properties at room temperature
Methacrylates:				
methyl	1.16	107	0.53	Hard, brittle
ethyl	1.09	78	0.36	Hard, brittle
n-propyl	1.05	62	0.56	Hard, brittle
n-butyl	1.04	41	0.33	Flexible, elastic
n-octyl	0.97	Below 20°	0.30	Soft, plastic
Acrylates:				
methyl	1.18	Below 20°	0.84	Elastic, rubber like
ethyl	1.15	–	1.01	Elastic, viscous
n-butyl	1.12	–	0.45	Viscous, sticky
n-octyl	1.03	–	0.14	Semiliquid, sticky

* 1% solution of the polymer in benzene.

The Influence of Certain Factors on the Conversion of Polymeric Esters Into Space Polymers

Effect of the length of the carbon chain of the alcohol radical in the ester. The influence of the alkyl radical on the tendency to cross linking was studied in parallel experiments in the methacrylate and acrylate series, with polymer specimens in the form of films 80-120 μ thick on glass. The cross-linked polymer contents in the films after the conversion were determined by extraction with benzene in a Soxhlet apparatus. The results are given in Tables 3 and 4.

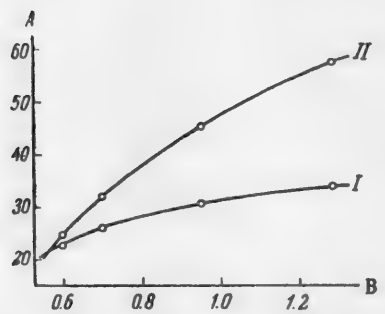

Fig. 1. Influence of intrinsic viscosity on the cross linking of n-butyl methacrylate polymers. Conversion temperature 190°, time 1 hour. A) Conversion (%), B) intrinsic viscosity [η]. I) Degradation, II) conversion into space polymer.

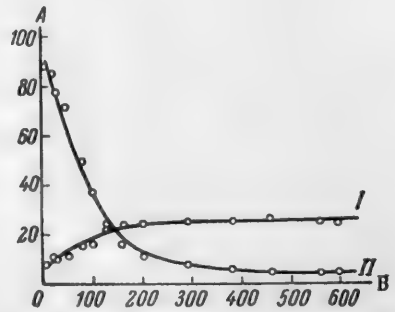

Fig. 2. Influence of film thickness on the rate of cross linking of n-butyl methacrylate polymer. A) Conversion (%), B) film thickness (in μ). I) Degradation, II conversion into space polymer.

It is clear from the data in these tables that acrylate polymers differ in their tendency to cross linking. The tendency depends both on the length of the carbon chain of the alkyl radical and on the substituent in the α-position relative to the carboxyl group.

The experiments show that in the methacrylate series only the polymeric esters containing an alkyl radical with 3 or more C atoms undergo cross linkage.

TABLE 3

Cross Linking of n-Alkyl Methacrylate Polymers
(Duration of conversion 4 hours; extracted with benzene for 2 hours)

Alkyl radical	Conversion temperature (°C)	Weight of polymer taken (g)	Losses by degradation		Amount of insoluble polymer	
			in g	in %	in g	in %
Methyl	160	0.2425	0	0	0	0
	170	0.2234	0.0031	1.4	0	0
	190	0.2659	0.0348	13.1	0	0
Ethyl	160	0.2279	0	0	0	0
	170	0.2234	0.0174	7.1	0	0
	190	0.1586	0.0274	17.2	0	0
Propyl	160	0.2606	0.0022	0.8	0	0
	170	0.1882	0.0066	3.5	0.0710	37.6
	190	0.1948	0.0390	20.0	0.0290	14.9
Butyl	160	0.3124	0.0042	1.3	0	0
	170	0.3316	0.0356	10.7	0.1938	58.5
	190	0.2780	0.1068	38.5	0.1526	55.0
Octyl	160	0.2320	0.0035	1.5	0.1400	60.4
	170	0.2312	0.0284	12.3	0.1676	72.5
	190	0.2088	0.0866	41.5	0.1166	55.8

TABLE 4

Cross Linking of n-Alkyl Acrylate Polymers
(Duration of heating 4 hours; extracted with benzene for 2 hours)

Alkyl radical	Conversion temperature (°C)	Weight of polymer taken (g)	Losses by degradation		Amount of insoluble polymer	
			in g	in %	in g	in %
Methyl	170	0.2278	0.0125	5.6	0	0
	190	0.2656	0.0237	8.9	0	0
Ethyl	170	0.2334	0.0092	4.0	0	0
	190	0.2938	0.0274	9.3	0.0462	15.7
Butyl	170	0.2146	0.0121	5.0	0.1515	70.5
	190	0.2047	0.0376	18.5	0.1581	76.7
Octyl	170	0.2612	0.0204	7.8	0.1861	71.4
	190	0.1965	0.0439	22.3	0.1442	74.0

TABLE 5

Conditions for Polymerization of Butyl Methacrylate

Composition of original mixture (in %)			Polymerization conditions	Polymer viscosity [η]
monomer	solvent	benzoyl peroxide (% on weight of monomer)		
70	30	0.3	Temperature 95-96°, time 4 hours	0.600
80	20	0.3		0.705
90	10	0.3		0.995
100	–	0.3		1.280

In contrast to the methacrylates, acrylate polymers have a greater tendency to form space polymers. Moreover, in the acrylate series the conversion begins with the ethyl acrylate polymer. The rate of conversion of methacrylate and acrylate polymers into the cross-linked state increases with increasing length of the carbon chain in the alkyl group.

Polymers of the lower (methyl and ethyl) methacrylates are not cross linked at 160-190°, or even at higher temperatures (200-250°). Above 250° they undergo considerable degradation and change color, but remain completely soluble in the usual solvents for linear polymers. Similar results were obtained in parallel experiments with factory-made polymers of higher viscosity – block-polymerized (unplasticized) methyl methacrylate polymer, and emulsion-polymerized ethyl methacrylate polymer.

The structure of the monomeric ester also influences the degree of degradation of the polymer. Methacrylates are more prone to degradation than the corresponding acrylates.

The tendency of the polymers to thermal degradation increases with increasing chain length of the alkyl radical.

Effect of intrinsic viscosity. It was reported earlier [31] that the degree of polymerization of butyl methacrylate polymer containing benzoyl peroxide and pentaerythritol tetramethacrylate influences the rate of cross linking of the polymer. The influence of the same factor on the cross linking of butyl methacrylate polymer without any added accelerators was studied in the present investigation.

The monomer concentrations in the original mixtures were varied (Table 5) to give a series of polymers differing in intrinsic viscosity.

The cross linking of these polymers was studied under various temperature conditions. The results showed (Fig. 1) that the rate of cross linking increases with increase of the intrinsic viscosity of the polymer. At a lower temperature (160°) polymers of low viscosity ($[\eta]$ = 0.600 and 0.705) are not converted into space polymers at all, whereas samples of more highly viscous butyl methacrylate polymer ($[\eta]$ = 0.995 and 1.280) undergo cross linking with high yields of insoluble products.

Influence of the thickness of the polymer film. The influence of film thickness as one of the factors in the cross-linking reaction was studied in order to investigate the possibility of bulk cross linking and, if this proved impossible, to establish the optimum conditions of the conversion as determined by the film dimensions.

The conversion in bulk was studied with specimens of butyl and octyl methacrylates and acrylates. It was found that if the polymers are heated at 195° for various times, cross linking occurs only at the surfaces of contact of the polymers with the air, and extends to only a small depth. Additions of benzoyl peroxide, quinone p-dioxime, slaked lime and other substances (in the case of acrylate polymers) in amounts of 3 to 10% make bulk cross linking possible.

In absence of accelerators the polymers are satisfactorily cross linked only in thin films, and the film thickness has a strong influence on the extent and rate of the process (Fig. 2).

The graph shows that the maximum film thickness at which the polymer is converted sufficiently into the insoluble state under the conditions used is 150 μ. In contrast to the cross-linking reaction, degradation of the polymer occurs throughout its bulk and is little affected by the specific surface of the specimen.

Changes in the Properties of Polymeric Esters During Conversion into Space Polymers

The cross linking of methacrylate and acrylate polymers is accompanied by considerable changes in their properties. These changes increase with increasing conversion, determined by the concentration of intermolecular cross links.

The effect of the degree of conversion into space polymers on some of the polymer properties are detailed below.

Change of solubility and degree of swelling in various organic solvents. The solubility of cross-linked butyl acrylate and butyl methacrylate in the following solvents was studied: dioxane, ethyl acetate, acetone, chloroform, benzene, white spirit, and ethyl alcohol (96% = μ). The determinations were continued for 24 hours at room temperature. The results are given in Table 6.

It follows from the data in the table that all these solvents extract a soluble fraction from the polymers, but do not dissolve the polymers completely. A characteristic feature is that the amounts of sol fractions in the cross-linked polymers vary for different solvents. The solubility increases appreciably with polarity of the solvent, and is not directly related to the activity of the solvents toward the linear polymers. This is seen particularly clearly in comparisons of the behavior of butyl methacrylate and butyl acrylate polymers in such solvents as white spirit and ethyl alcohol. These polymers are readily soluble in white spirit and quite insoluble in ethyl alcohol; but in the cross-linked state they are resistant to the former, and swell and partially dissolve in the latter.

The polarity of the solvent influences the swelling even more than the solubility of cross-linked polymers.

TABLE 6

Contents of Sol Fractions in Cross-Linked Butyl Methacrylate (PBMA) and Butyl Acrylate (PBA) Polymers Extracted by Different Solvents
(Conversion conditions: temperature 180°; time 4 hours for PBMA, 2 hours for PBA)

Solvents*	PBMA			PBA		
	weight of polymer taken (g)	content of sol fraction		weight of polymer taken (g)	content of sol fraction	
		in g	in %		in g	in %
Chloroform	0.1185	0.0148	12.6	—	—	—
Acetone	0.1352	0.0304	22.5	—	—	—
Dioxane	0.1285	0.0318	24.8	—	—	—
Ethyl acetate	0.1412	0.0342	24.4	0.2009	0.1768	87.9
Benzene	0.1337	0.0186	10.1	0.1303	0.0705	54.0
White spirit	0.1207	0.0016	1.3	0.1589	0.0088	4.2
Ethyl alcohol (96%)	0.1355	0.0219	16.1	0.0958	0.0472	49.0

* The solvents are in order of decreasing activity toward linear polymers [40].

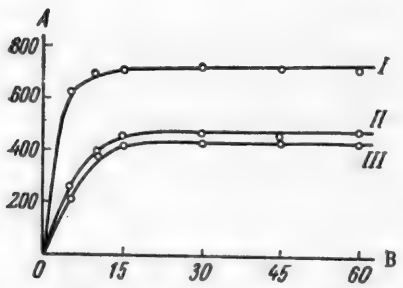

Fig. 3. Kinetics of the swelling of cross-linked butyl methacrylate polymer in various solvents. Conversion temperature 180°, time 6 hours. A) Amount of liquid absorbed (%), B) time of swelling (minutes). Solvents: I) dioxane, II) 96% ethyl alcohol, III) benzene.

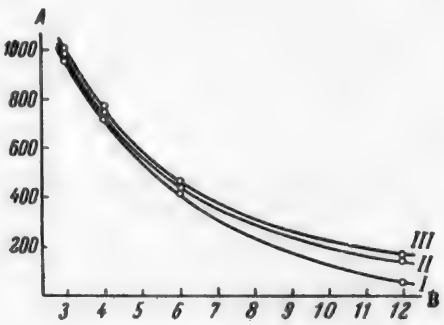

Fig. 4. Effect of degree of conversion of butyl methacrylate polymer into a space polymer on the degree of swelling. Conversion temperature 180°, solvent – benzene. A) Amount of liquid absorbed (in %), B) conversion Time (hours). Duration of swelling (in minutes): I) 15, II) 30, III) 60.

Kinetic curves for the swelling of the gel fraction of cross-linked PBMA in dioxane, ethanol (96%) and benzene are given in Fig. 3. Swelling was determined by the volume method in Dogadkin's apparatus [41].

The relative positions of the swelling curves indicate that the volume of a solvent absorbed directly corresponds to its activity toward cross-linked polymers, are given in Table 6.

The degree of cross linking influences the swelling of the polymeric esters, irrespective of the nature of the solvent. Experiments with PBMA (Fig. 4) showed that the swelling of the polymers in benzene decreases sharply with increase of the heating time.

Changes of softening temperature and thermal stability. Changes of these properties can provide convincing evidence for the existence of a space structure formed in the polymers when they are heated in thin films.

The softening temperatures were determined with the aid of an apparatus designed in the Department of Lacquer and Paint Technology of the Lensoviet Technological Institute, Leningrad [39].

Free films of PBMA of different degrees of cross linking were tested.

The results of the tests, given below, show that the softening temperatures of the polymers are raised considerably by heat treatment. When PBMA has been heated at 180° for 6 hours its softening temperature is more than 2.5 times as high.

Time of heating at 180° (hours)	0	1	2	4	6
Softening temperature (°C)	41	50	57	79	105

The increase of softening temperature as the result of cross linking is seen particularly clearly in polymers of octyl methacrylate and acrylate, and of butyl acrylate. These are viscous or semiliquid substances when in the linear state, but lose their mobility as the result of cross linking and are converted into elastic rubberlike products. The plasticity of the polymers is largely retained in the process.

TABLE 7

Variations of the Physicomechanical Properties of Butyl Methacrylate Polymer Films with the Degree of Cross Linking

Properties	Duration of conversion at 190° (min)				
	0	35	60	120	180
	contents of insoluble fraction (%)				
	0	5.6	58.0	82.0	86.5
Adhesion to St. 3 steel (g/mm)	210	365	480	580	620
Bending strength (mm)	1	1	20	does not withstand 20	
Impact strength (kg/cm)	50	45	15	10	10
Abrasion resistance (rev./mm)	125	8300	17,900	21,600	24,400

The change of the softening temperature is accompanied by alteration of the thermal stability of the polymers. Acrylates, and especially methacrylates, do not have high valence-bond stabilities in the linear state at high temperatures. The former are degraded considerably even at 250°, while the latter are appreciably depolymerized at 200° and over.

Butyl methacrylate polymers of different degrees of cross linking were subjected to comparative tests for thermal stability. Polymer films of known degrees of conversion were placed on their supports (glass) into a glass tube placed horizontally in a thermostat, and heated for 1 hour at 220 and 250°. In order to avoid further cross linking under the action of air, the films were heated in vacuum at a residual pressure of 1-2 mm Hg. The degree of degradation of the polymers, found from the loss in weight of the films, was used as the measure of heat stability.

The investigation showed (Fig. 5) that preliminary cross linking of the polymers at moderately high temperatures (160-200°) considerably increases their stability at higher temperatures. For example, the degradation of cross-linked PBMA (containing about 90% of insoluble fraction) at 220-250° is 1/3 to 1/5 that of the original linear polymer.

If cross-linked PBMA is heated for a long time (48 hours) in air at 180°, almost no degradation occurs. The polymer remains transparent and colorless.

The effect of heat treatment on the adhesion of the polymers to metal surfaces is especially favorable. In contrast to coatings of linear polymers, such converted coatings are not inferior to heat-dried oil or oil-glyptal coatings.

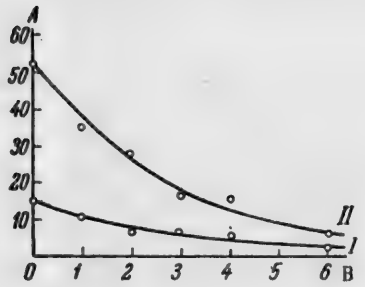

Fig. 5. Effect of the degree of conversion on the resistance of butyl methacrylate polymer to degradation under vacuum.
Conversion temperature 180°, heating time 1 hour. A) Degradation (%), B) duration of conversion (hours). Temperature (°C): I) 220, II) 250.

However, although cross linking eliminates this important defect found in many saturated carbon-chain polymers, it results in some undesirable properties – increased brittleness, decreased elasticity and lower impact strength.

The abrasion resistance, which is directly related to these characteristics, increases sharply as the result of cross linking. The abrasion resistance of a film containing 80-85% of insoluble polymer is nearly 200 times as high as that of the original polymer.

These data on the properties of insoluble alkyl acrylate and methacrylate polymers obtained by heat treatment of linear polymers are entirely consistent with a spatial structure.

SUMMARY

1. It was found in a study of the cross linking of linear n-alkyl acrylate and methacrylate polymers that acrylate (starting with the ethyl ester) and methacrylate (starting with the propyl ester) polymers are converted into insoluble space polymers when heated in the form of thin films in air and in 160-200° range.

2. The relative tendency to cross linking depends on the structure of the monomer: on the length of the carbon chain of the alkyl radical, the nature of the substituent in the α position relative to the alkoxy group, and also on the degree of polymerization of the ester. Increase of the number of C atoms in the alkyl group from 1 to 8 accelerates the conversion of polymerized alkyl acrylates and methacrylates into space polymers and lowers the conversion temperature. Acrylate polymers have a greater tendency than the corresponding methacrylate polymers to form space polymers. The rate of cross linking increases with increasing degree of polymerization.

3. The cross linking of acrylate and methacrylate polymers occurs at the polymer–air interface and is a function of the specific surface of the specimen.

4. Cross linking of the polymers is accompanied by an increase in their polar group content as indicated by increased solubility and swelling in polar solvents; the heat stability and resistance to thermal degradation increases, and some of the physical properties are changed.

LITERATURE CITED

[1] B. N. Rutovskii and K. S. Zabrodina, Org. Chem. Ind. 8, 441 (1940).

[2] M. N. Rutovskii and A. M. Shur, J. Appl. Chem. 24, 8, 851 (1951).*

[3] A. Ia. Drinberg, Sh. N. Golant, and B. M. Fundyler, Investigations in the Field of High Polymers, Paper at the 6th Conference, Acad. Sci. USSR, 172 (1949).

[4] S. M. Zhivukhin, Trans. MKhTI, 17, 181 (1952).

[5] L. Gindin, S. Medvedev, and E. Flisher, J. Gen. Chem. 9, 1694 (1949).*

[6] A. Ia. Drinberg, B. M. Fundyler, and E. P. Podol'naia, J. Appl. Chem. 27, 6, 613 (1954).*

[7] S. Loshack, T. G. Fox, J. Am. Chem. Soc. 75, 3544 (1953).

[8] A. A. Berlin, Progr. Chem. 9, 642 (1940).

[9] W. Norrish, A. Brokman, Proc. Roy. Soc. (London) A, 163, 205 (1937).

[10] B. N. Rutovskii and A. M. Shur, J. Chem. Ind. 7-8, 6 (1946).

[11] A. M. Berlin and I. F. Bogdanov, J. Gen. Chem. 17, 1699 (1947).

* Original Russian pagination. See C. B. Translation.

[12] C. Walling, J. Am. Chem. Soc. 67, 441 (1945).

[13] W. L. Mast, T. J. Dietz et al. India Rubber World, 110, 74 (1944).

[14] W. C. Mast, L. T. Smith, C. H. Fisher, Ind. Eng. Ch. 36, 1027, 1032 (1944).

[15] Off. Gaz. U. S. Pat. Office 616, 1096 (1948); 620, 496 (1949); 622, 535 (1949); 629, 956 (1949).

[16] W. C. Mast and C. H. Fisher, India Rubber World, 119, 596, 727 (1949).

[17] Z. A. Rogovin, in the book: High Polymers, 5, 5 (1946).*

[18] T. J. Dietz, W. C. Mast, R. L. Dean and C. H. Fischer, Ind. Eng. Ch. 38, 960 (1946); 40, 107 (1948); 41, 703 (1949).

[19] W. C. Mast, T. J. Dietz and C. H. Fisher, India Rubber World, 113, 223 (1945); 116, 335 (1947).

[20] T. J. Dietz and J. E. Hansen, Rubber Age, 68, 669 (1951).

[21] W. N. Howerton, T. J. Dietz, A. D. Snyder, G. A. Alder, Rubber Age, 72, 353 (1952).

[22] J. Drogin, India Rubber World, 128, 345, 350 (1953).

[23] E. M. Filachione, Rubber Age, 72, 631 (1953).

[24] G. W. Elanagan, India Rubber World 120, 702 (1949).

[25] W. C. Mast, C. E. Rehberg, T. J. Dietz and C. H. Fisher, Ind. Eng. Ch. 36, 1022 (1944).

[26] H. P. Owen, Rubber Age 66, 544 (1950).

[27] S. T. Semegen and J. H. Wakelin, Rubber Age, 71, 57 (1952).

[28] F. A. Bovey, J. F. Abere, G. B. Rathmann and C. L. Sandberg, J. Polym. Sci. 15, 520, 537 (1955).

[29] G. S. Whitby, Synthetic Rubber,N. Y. 900 (1954).

[30] Off. Gaz. U. S. pat. office, 593, 244 (1946); U. S. Patent 2412475, 2412476; 593, 61 (1946); U. S. Patent 2411899, 2451177.

[31] A. Ia. Drinberg, Sh. N. Golant , and L. I. Gol'farb, J. Appl. Chem. 24, 10, 1078 (1951);** 24, 11, 1181 (1951).**

[32] A. Ia. Drinberg and N. S. Demchenko, J. Appl. Chem. 25, 1, 57 (1952).**

[33] A. Ia. Drinberg andA. D. Iakovlev, J. Appl. Chem. 26, 6, 532 (1953).**

[34] A. Ia. Drinberg and A. M. Bocharova, J. Appl. Chem. 26, 10, 1056 (1953).**

[35] C. Mouerau, M. Murat, L. Tampier, Ann. Chim. 15, 243 (1921).

[36] M. M. Koton and F. S. Florinskii, J. Gen. Chem. 21, 1841 (1951).**

[37] C. E. Rehberg, C. H. Fisher, J. Am. Chem. Soc. 66, 1203, 1723 (1944).

[38] Ratchford, C. E. Rehberg, C. H. Fisher, J. Am. Chem. Soc. 66, 1864 (1944); Monomers (Russian Translation) 2, 5 (IL, 1953).

[39] A. Ia. Drinberg, A. M. Bocharova, and A. D. Iakovlev, Factory Labs. 8, 996 (1956).

[40] G. V. Schulz, Ang. Ch. 64, 12-20, 553 (1952).

[41] B. A. Dogadkin, K. A. Pechkovskaia, and L. Chernikina, Colloid J. 8, 31 (1946).

Received May 17, 1956

* In Russian.

** Original Russian pagination. See C. B. Translation.

AMMONOLYSIS OF p-CHLOROBENZENESULFONAMIDE*

A. M. Grigorovskii and N. N. Dykhanov

The ammonolysis of aryl halides as a method for the synthesis of arylamines was first used in 1870 by the Russian scientists Engel'gardt and Lachinov [1]. The subsequent development of this method was considerably influenced by Soviet work, in which the most prominent position is occupied by the researches of Vorozhtsov and his associates [2-4].

According to the data of Vorozhtsov et al., the reaction of the simplest aryl halide, chlorobenzene, with concentrated aqueous ammonia at 180-220° in presence of cuprous compounds gives aniline (yield 89-90% of theoretical), diphenylamine (yield 1-2% of theoretical), and phenol (yield up to 5% of theoretical). Therefore ammonolysis is accompanied in this process by two side reactions: arylation of the aniline originally formed, and hydrolysis of chlorobenzene [2]. The rates of ammonolysis and the accompanying side reactions are directly proportional to the amount of catalyst, and reach a maximum at 1 : 1 molar ratio of catalyst to aryl chloride. The rates of these reactions are also increased on increase of temperature in this range [3].

Literature data indicate that ammonolysis of chlorobenzene proceeds with greater difficulty than the ammonolysis of its derivatives, i.e., the introduction of a substituent into the chlorobenzene molecule weakens to some extent the bond between the chlorine (or other halogen) atom and the benzene nucleus. The greatest weakening effects on the halogen—carbon bond (activating action on the halogen) are exerted by meta-directing substituents, and of these, by the nitro group. Ammonolysis of o- and p-nitrohalobenzenes can be effected even in absence of catalysts [1], but in these cases the reaction is greatly accelerated in presence of cupric compounds [4]. The presence of a catalyst is an essential condition in all the other examples of ammonolysis of substituted aryl chlorides with a single substituent in the molecule which have been described in the literature.

The activating action of the sulfonamide group on the halogen in the aromatic nucleus has not yet been studied in detail. The only relevant observation was published in 1947 by Grigorovskii and Znaeva [5]. They obtained sulfanilamide (in 38-40 percent of the theoretical yield) by the action of heat on p-chlorobenzenesulfonamide with concentrated aqueous ammonia, together with substances of undetermined structure. The reaction proceeds in presence of cuprous oxide or a mixture of equivalent amounts of copper and copper sulfate at 150° and higher. Quite recently, Tanasescu and Macarovici [6] reported the synthesis of sulfanilamide by the action of heat on p-chlorobenzenesulfonamide with aqueous ammonia in presence of metallic copper at 155-160°. **

Comparison of the ammonolysis conditions for chlorobenzene [2, 3] and p-chlorobenzenesulfonamide [5] shows that the introduction of the sulfonamide group into the alkyl halide molecule, like the introduction of other substituents, weakens the halogen—carbon bond.

---

* Communication III in the series on the synthesis of sulfanilamide and its N-substituted derivatives from chlorobenzene.

** According to our observations, this reaction does not proceed at all below 160° in presence of metallic copper or of the chlorides of zinc, nickel, or cobalt.

Continuing our study of the ammonolysis of p-chlorobenzenesulfonamide, we established that a sulfonamide group occupying the para position relative to the halogen atom in the benzene nucleus alters the direction of the side reactions in ammonolysis. Our investigations showed that when p-chlorobenzenesulfonamide reacts with aqueous ammonia in presence of cuprous compounds under all the conditions tested, ammonolysis is accompanied by a side reaction of arylation which gives N^4-sulfanilylsulfanilamide ("disulfan") (A) and N^1-(p-sulfonamidophenyl)-N^4-sulfanilylsulfanilamide (B), which we term "trisulfan" by analogy with disulfan:

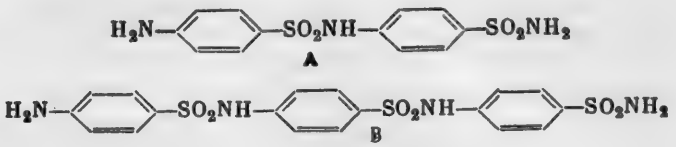

A

B

The structure of disulfan and trisulfan were proved by their hydrolysis products. If either substance is boiled with 60% sulfuric acid, sulfanilic acid and its amide are formed. In agreement with the above formulas, twice as much sulfanilic acid is obtained from trisulfan as from disulfan.

The formation of disulfan and trisulfan in the reaction between p-chlorobenzenesulfonamide and aqueous ammonia is an unusual direction for the arylation which usually accompanies the ammonolysis of aryl halides; it proceeds by arylation of the sulfanilamide originally formed (I), but not at the amino group, as is to be expected by analogy with the formation of diphenylamine in the ammonolysis of chlorobenzene, but at the sulfonamide group:

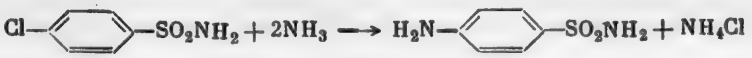

(*I*)

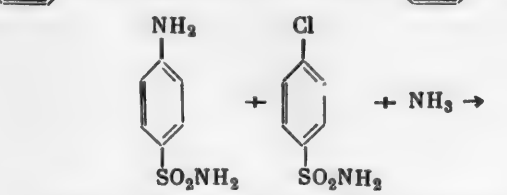

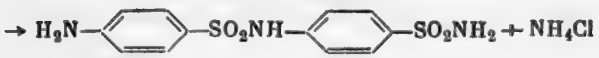

(*II*)

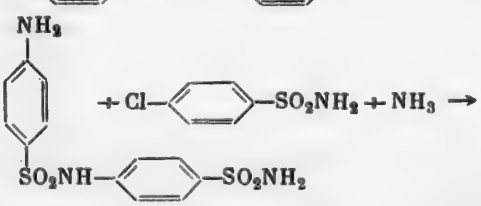

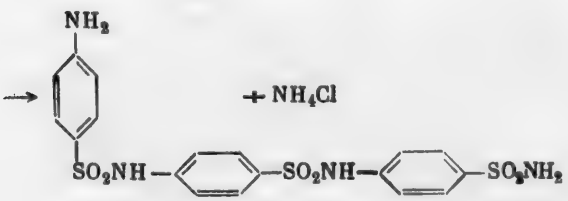

(*III*)

Other examples of the preferential arylation of sulfanilamide in the N^1 position in alkaline media have been reported in the literature [7]. No definite mechanism of the side reaction has yet been conclusively proved.

The scheme given above for the interaction of p-chlorobenzenesulfonamide with aqueous ammonia is confirmed by the absence of any chlorine-containing compounds other than the original p-chlorobenzenesulfonamide in the reaction products before completion of the process, and the absence of N-diethyl-substituted derivatives of disulfan and trisulfan in the products of the reaction of p-chlorobenzenesulfonamide with diethylamine.

In several experiments on the ammonolysis of p-chlorobenzenesulfonamide we attempted to detect p,p'-disulfonamidodiphenylamine and p-hydroxybenzenesulfonamide in the reaction products; the formation of these compounds should be expected according to the scheme proposed for the ammonolysis of chlorobenzene [2]. These substances were not detected.

EXPERIMENTAL

Method used for experiments on the ammonolysis of p-chlorobenzenesulfonamide. The ammonolysis of p-chlorobenzenesulfonamide was effected in an autoclave of Ia1-T steel, 1 liter in capacity, fitted with a stirrer, a thermometer socket, a manometer, and a side tube with a needle valve for entry and outlet of gaseous ammonia. The autoclave was heated to the required temperature in an oil bath.

The autoclave was charged with 1 mole of p-chlorobenzenesulfonamide (191.5 g), of m. p. 146-147° [8], 0.2-1.0 mole of cuprous chloride (19.8-99 g), or, alternatively, a mixture of 0.1-0.5 mole of copper sulfate (25-125 g) and 6.3-31.6 g of metallic copper, precipitated from a solution of the appropriate amount of copper sulfate by addition of iron filings. The necessary volume of 22-25% aqueous ammonia was added to the mixture, and gaseous ammonia was then introduced into the closed autoclave from a cylinder to a pressure of 2 atmospheres at 30°; the concentration of ammonia in the reaction mixture was then 44-45%.

The reaction mixture was heated in the autoclave to 155-160° and stirred at that temperature until the reaction was quite complete, when the pressure ceased to decrease. At the end of the reaction the ammonolyzate was cooled to 70°, and then warmed from 70 to 80° while the ammonia was slowly released to a residual pressure 0.7-1.0 atm. This corresponded to 4.5-5% of ammonia in the ammonolyzate.

The reaction mass was cooled to room temperature, the precipitated sulfanilamide was filtered off, washed on the filter with 1% ammonia solution until the filtrate became colorless, and thoroughly pressed out.

The moist sulfanilamide paste was placed in 1.5 times its own volume of 10% caustic soda solution (on the weight of the paste), the resultant solution was heated to boiling, and air was blown through it until the odor of ammonia could no longer be detected. The precipitated copper oxide was filtered off, and the alkaline solution – the sodium salt of sulfanilamide – was decolorized by boiling with activated charcoal (5% by weight) and addition of sodium hydrosulfite (0.5% by weight). Sulfanilamide was isolated from the clarified filtrate at 60-65° by addition of saturated ammonium chloride solution in 5% excess over the theoretical amount. The precipitated sulfanilamide was filtered off and washed on the filter with 1% ammonia solution until the filtrate was colorless. The usual yield was 74-77 g of sulfanilamide (calculated as the dry substance), of a pale cream color, which was recrystallized with activated charcoal from 8 times its own volume of water, including the moisture in the paste. The yield of pharmaceutical-grade sulfanilamide when the reaction was performed as described above was 68.5-71.5 g, corresponding to 39.5-41.5% of the theoretical.

Investigation of the side products of the ammonolysis of p-chlorobenzenesulfonamide

Separation of the mixture of side products. The weakly ammoniacal mother liquor from the ammonolysis of 1 mole of p-chlorobenzenesulfonamide was neutralized with hydrochloric or sulfuric acid. The side products separated out in the form of a thick dark oil which was converted into a solid amorphous powder after repeated washing with ice-cold water. The powder was filtered off and dried in a desiccator over sulfuric acid. 80-90 g of dry mixed side products was obtained. This mixture was placed in 300 ml of 2 N hydrochloric acid heated to 60-65°; the side products melted and formed a lower oily layer. The liquid was stirred for 15-20 minutes, cooled to room temperature, and the hydrochloric acid extract was decanted off; this treatment with hydrochloric acid was repeated twice more. The portion of the side products insoluble in hydrochloric acid was washed with water until no longer acid to Congo Red; a solid amorphous residue was again formed in the process. This was filtered off and dried in a desiccator. The yield of the dry residue was 50-55 g.

Isolation and identification of N^4-sulfanilylsulfanilamide ("disulfan").* The combined hydrochloric acid extract, obtained as described above, was treated with 15% sodium sulfide solution until the precipitation of black copper sulfide ended, then stirred for 5-10 minutes with 5 g of activated charcoal, and filtered. The filtrate was

* T. A. Veselitskaia took part in this section of the work.

neutralized with 15% ammonia solution. The precipitate was filtered off, washed with water on the filter to a negative reaction for chloride in the filtrate, and dried at 80-90° to constant weight. The yield was 24-25 g of a substance melting at 128-131°, readily soluble in dilute ammonia, alcohol, acetone, and ether, insoluble in aromatic hydrocarbons; after recrystallization from water (1 : 40) the substance was obtained in the form of colorless needles, m. p. 133-134°.

Found %: C 44.78, H 4.23, N 12.60.

The analytical results suggest that the substance can be either p,p'-disulfonamidodiphenylamine [9], or N^4-sulfanilylsulfanilamide [10]. To determine its structure, the substance was hydrolyzed in presence of sulfuric acid. After 5 g of the substance had been boiled for 2 hours with 20 ml of 60% sulfuric acid, the resultant solution was poured into 20 ml of ice-cold water. The precipitate was separated from the acid solution, and washed, first with a little water, and then thoroughly with acetone. When the substance was dried, 2 g of a substance with the properties of sulfanilic acid [11] was obtained. The sulfuric acid solution was neutralized with ammonia; the precipitate formed was filtered off, washed with water, and dried; 1 g of sulfanilamide was obtained.

Isolation and identification of N^1-(p-sulfonamidophenyl)-N^4-sulfanilylsulfanilamide ("trisulfan"). The part of the mixture in the side products from the ammonolysis of p-chlorobenzenesulfonamide (50-55 g) which did not dissolve in 2 N hydrochloric acid was put into 100 ml of methyl alcohol diluted with an equal volume of water. The dark red solution was heated to 50-60° and sodium hydrosulfite was added to it in small portions until precipitation of copper sulfide ceased. The liquid was then heated for 10-15 minutes with 5 g of activated charcoal and filtered.

The colorless filtrate was diluted with water until the formation of a white amorphous precipitate ceased. The precipitate was filtered off and dried in a desiccator. 40-45 g of a dry substance melting at 103-106° was obtained; the substance is readily soluble in dilute solutions of ammonia, caustic alkalies, and alkaline carbonates; it is insoluble in water and aromatic hydrocarbons. When hot saturated solutions of this substance in alcohol, acetone, or pyridine are cooled or diluted, it separates out as a colorless oil which gradually changes into a white amorphous powder which melts at 106-107° after drying.

Found %: C 44.69, H 3.83, N 11.49.

The percentage contents of carbon, hydrogen, and nitrogen suggest that the substance is either p,p',p"-trisulfonamidotriphenylamine, or N^1-(p-sulfonamidophenyl)-N^4-sulfanilylsulfanilamide. To determine the structure of this substance, we studied its hydrolysis products. Hydrolysis of 7.7 g of the substance with 30 ml of 60% sulfuric acid, under the conditions described above for the identification of disulfan, gave 3.5 g of sulfanilic acid and 1.25 g of sulfanilamide.

The only hydrolysis products of the substance were sulfanilic acid and its amide. This led to the provisional conclusion that the substance is N^1-(p-sulfonamidophenyl)-N^4-sulfanilylsulfanilamide; for brevity we named it "trisulfan," by analogy with disulfan. This conclusion was confirmed by the synthesis of trisulfan by another route.

Synthesis of trisulfan. This compound was prepared from disulfan and p-carbomethoxyaminobenzenesulfonyl chloride by the method proposed by Golovchinskaia for the synthesis of disulfan from sulfanilamide [10].

185-186 g of technical trisulfan, m. p. 100-105°, was prepared from 150 g of disulfan and 200 g of technical 90% sulfonyl chloride. After two-fold reprecipitation from methanol by addition of water, the substance had m. p. 105-106°. A mixed sample with trisulfan isolated as a side product from the ammonolysis products of p-chlorobenzenesulfonamide melted without depression. The chemical properties of the trisulfan samples obtained by the two methods were shown to be identical in the benzylation reaction.

10 g of trisulfan, synthesized as described above, was dissolved in 50 ml of pyridine; 8 g of benzoyl chloride was added to the solution, the mixture was heated for 15 minutes, and the gently-boiling solution was then diluted with water. The precipitate was filtered off, dissolved in 25 ml of methanol, and again precipitated by addition of water to the solution; the reprecipitation from alcohol was repeated twice more. This gave 3.6 g of substance with m. p. 244-246°.

The substance is soluble in alcohol, acetone, and pyridine, and insoluble in water.

Found %: N 9.59. $C_{25}H_{22}O_7N_4S_3$. Calculated %: N 9.55.

Synthesis of N^4-diethylsulfanilamide. The autoclave described above was charged with 200 g of p-chlorobenzenesulfonamide (0.5 mole), 99 g of diethylamine (2 moles), 10 g of cuprous chloride (0.1 mole), and 160 ml of water. The mixture was heated for 5 hours at 150-155°. The maximum pressure was 12 atmospheres.

The reaction mixture, cooled to room temperature, was transferred into a flask, 50 ml of 40% caustic soda solution was added, and excess of diethylamine was distilled off by the action of heat. The alkaline solution remaining after removal of diethylamine was boiled for 10 minutes with activated charcoal and filtered. Concentrated hydrochloric acid was added to the filtrate at 20-25° to a weak acid reaction to Congo Red. The fine granular precipitate was filtered off, washed with water until no longer acid, and dried at 80-90° to constant weight. The yield of technical N^4-diethylsulfanilamide, m. p. 130-133°, was 95-97 g, i.e., almost quantitative. After recrystallization from water (1 : 30), 89-91 g of N^4-diethylsulfanilamide with m. p. 133-133.5° was obtained. Its properties agreed with those described in the literature [12]. A mixed sample of the substance with N^4-diethylsulfanilamide prepared as described in the literature melted without depression.

The absence of N-diethyl-substituted derivatives of disulfan and trisulfan in the reaction products of p-chlorobenzenesulfonamide and aqueous diethylamine solution indicates that in the ammonolysis of p-chlorobenzenesulfonamide it is the sulfanilamide formed from the original p-chlorobenzenesulfonamide, and not this compound itself, which undergoes arylation in the side reaction.

SUMMARY

1. In the ammonolysis of p-chlorobenzenesulfonamide, the main reaction is accompanied by a side reaction of arylation of the sulfonamide group with formation of N^4-sulfanilylsulfanilamide and N^1-(p-sulfonamidophenyl)-N^4-sulfanilylsulfanilamide.

2. The formation of N^4-sulfanilylsulfanilamide and N^1-(p-sulfonamidophenyl)-N^4-sulfanilylsulfanilamide in the ammonolysis of p-chlorobenzenesulfonamide is the result of arylation of the sulfanilamide originally formed, and is a peculiar direction of the arylation reaction which usually accompanies the ammonolysis of aryl halides.

LITERATURE CITED

[1] A. N. Engel'gardt and P. A. Lachinov, J. Russ. Phys.-Chem. Soc. 2, 109 (1870).

[2] N. N. Vorozhtsov andV. A. Kobelev, Proc. Acad. Sci. USSR 3, 109 (1934); J. Gen. Chem. 4, 311 (1934); 8, 1106 (1938); 9, 1465 (1939).

[3] N. N. Vorozhtsov and V. A. Kobelev, J. Gen. Chem. 8, 1330 (1938).

[4] N. N. Vorozhtsov and M. N. Krylova, J. Gen. Chem. 4, 324 (1934).

[5] A. M. Grigorovskii and M. N. Krylova, Pharmacy 2, 19 (1947).

[6] J. Tanasescu and M. Macarovici, Bull. stiint. Acad. Romane, Sec. techn. si. Chim. 5, 57 (1953); Referat Zhur. Khim. 12, 169 (1955).

[7] U. S. Patent 2444012, C. A., 42, 6852 (1942).

[8] A. M. Grigorovskii, N. N. Dykhanov, and Z. M. Kimen, J. Gen. Chem. 27, 531 (1957).*

[9] R. Thampi, B. Iyer, and P. Guha, Science and culture, 11, 385 (1946); C. A., 41, 106 (1947).

[10] E. S. Golovchinskaia, J. Appl. Chem. 18, 647 (1945).

[11] C. Laar, Ber., 14, 1934 (1881).

[12] W. Kumler, J. Am. Chem. Soc. 68, 1191 (1946).

Received March 12, 1956

* Original Russian pagination. See C. B. Translation.

USE OF POLYORGANOSILOXANOLS FOR INCREASING THE WATER RESISTANCE OF BUILDING MATERIALS*

M. G. Voronkov, B. N. Dolgov and Z. I. Shabarova

We have previously described two methods for the hydrophobization of building materials by impregnation with solutions of alkyltrichlorosilanes in organic solvents and treatment with aqueous solutions of sodium alkylsiliconates [1-6]. In the present paper we consider a third possible method for increasing the water resistance of building materials, by treatment with solutions of organosilicon polymers – polyorganosiloxanols. These polymers are obtained by hydrolysis, with not less than 10-fold excess of water with ice, of alkyl- or aryltrichlorosilanes $RSiCl_3$ ($R = CH_3$, C_2H_5, C_4H_9, C_6H_5 etc.) and their mixtures with 5-50% of dialkyldichlorosilanes R_2SiCl_2 ($R = CH_3$, C_2H_5 etc.) or, for the higher alkyltrichlorosilanes ($R = C_4H_9$, iso-C_5H_{11}, etc.) with 5-40% of silicon tetrachloride. The hydrolysis may be effected either in a solvent, preferably oxoniogenic (ether), or without solvent. The hydrolysis of alkyltrichlorosilanes first yields alkylsilanetriols $RSi(OH)_3$, which then condense with loss of water to give polyorganosiloxanols $RSiO_n(OH)_{3-2n}$, the molecules of which consist of alternating atoms of oxygen and silicon, the latter being linked to –R hydrocarbon radicals and free –OH groups. Polyorganosiloxanols are solid or semiliquid, white or colorless, odorless substances, soluble in organic solvents. The chemical composition of the hydrolysis products of $RSiCl_3$ predominantly corresponds (for $R = C_2H_5$, C_6H_5) to the empirical formula $RSiO_{1.25}(OH)_{0.5}$ indicative of a cyclic chain structure [7, 8], for example:

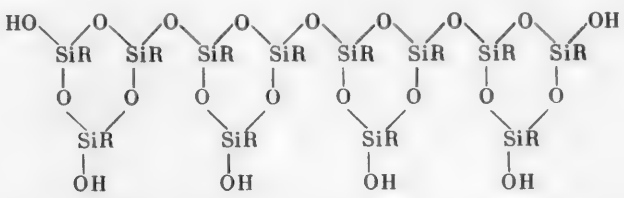

In addition to these hydrolysis products, unstable linear polysiloxanols of the type $H[OSi(OH)R]_nOH$ and cyclic polysiloxanols of the type $[OSi(OH)R]_n$, often soluble in water (especially when $R = CH_3$) are formed. Hydrolysis of mixtures of alkyltrichlorosilanes and dialkyldichlorosilanes or silicon tetrachloride yields compounds of mixed structure, with a lower (in the case of R_2SiCl_2) or higher (in the case of $SiCl_4$) content of OH groups than in the hydrolysis products of pure $RSiCl_3$.

For convenience, we have introduced an abbreviated notation for the polyorganosiloxanes formed by hydrolysis of alkylchlorosilanes of the type R_nSiCl_{4-n} ($n = 0-3$), based on the structure and ratios of the latter. In this notation the first symbol represents the R radical of the original $RSiCl_3$ (M = methyl, E = ethyl, Bu = butyl, Ph = phenyl, etc.), the second and the third represent the R' and R" radicals of the original $R'R"SiCl_2$, etc.; the presence of $SiCl_4$ is indicated by the symbol X, the last in the formula. The first two-digit number following these symbols is the content of the second component in the mixture with $RSiCl_3$, in weight percent; the second such number gives the content of the third component, etc. The symbols are separated by dashes if necessary. For example: M is the hydrolysis product of pure CH_3SiCl_3; MMM –05 is the product of joint hydrolysis of 95% CH_3SiCl_3 and 5% $(CH_3)_2SiCl_2$; EPhM –20 is the product of joint hydrolysis of 80% $C_2H_5SiCl_3$ and 20% $C_6H_5(CH_3)SiCl_2$; BuX –30 is the product of joint hydrolysis of 70% $C_4H_9SiCl_3$ and 30% $SiCl_4$; PrMMX –2020 is the product of

* Communication III in the series on hydrophobization of materials by means of organosilicon compounds.

joint hydrolysis of 60% $C_3H_7SiCl_3$, 20% $(CH_3)_2SiCl_2$ and 20% $SiCl_4$; MMMX-40 is the product of joint hydrolysis of 60% $(CH_3)_3SiCl$ and 40% $SiCl_4$; M-Ph-MMM-4020 is the product of joint hydrolysis of 40% CH_3SiCl_3, 40% $C_6H_5SiCl_3$ and 20% $(CH_3)_3SiCl$, etc.

Preparation of Polyorganosiloxanols

Polymethylsiloxanol (M). 300 g of methyltrichlorosilane of b. p. 65° was added dropwise with vigorous stirring during 4-7 hours to 1.5 liters of cold water and 1.5 kg of ground ice in a thick-walled porcelain or glass beaker 5-8 liters in capacity. After the end of the addition the stirring was continued for 1-2 hours more. The aqueous HCl solution, containing some water-soluble hydrolysis products of low molecular weight (these were generally precipitated in the form of more highly condensed compounds after 1-2 days), was separated from the glutinous or gelatinous deposit of polymethylsiloxanol (yield 130-140 g) on the bottom and walls of the beaker. The deposit was washed thoroughly with water and dissolved in 500-800 ml of acetone (or other suitable solvent). The solution of M in acetone was filtered and stabilized by addition of borax, pyridine, or some other stabilizer. Unstabilized solutions of M in acetone are only stable for 2-3 days, after which they begin to separate out. In presence of a stabilizer an acetone solution of polymethylsiloxanol can be kept for a month. Solutions of M hydrocarbons are less stable and less suitable for waterproofing. Solutions of M prepared by hydrolysis of alcoholic solutions of methyltrichlorosilane, which are considerably more stable on keeping, are likewise less effective. M can also be successfully prepared by the bubbling of air or an inert gas (air, CO_2) saturated with methyltrichlorosilane vapor through a vigorously stirred mixture of water and ice. 1 liter of water and 1 kg of powdered ice was placed in a 4-liter beaker fitted with an efficient mechanical stirrer and a gas inlet tube reaching to the bottom of the vessel. Nitrogen from a cylinder was passed through a Würtz flask containing 150 g of CH_3SiCl_3 (complete evaporation of this amount requires 5-6 hours) to saturate it with methyltrichlorosilane vapor, and then passed through the tube at a rate of 0.5-0.7 liter/minute. The yield of the pastelike deposit of polymethylsiloxanol was 72-75 g. This was then treated and dissolved as described above.

Polymethylsiloxanol is easily soluble in ligroine and in acetone (47-51 g in 100 g of solvent), and less so in toluene (21-23 g) and benzene (17-19 g). When dissolved in aqueous or, preferably, alcoholic alkali (NaOH) it forms sodium methylsiliconate. When kept in the undissolved state, M hardens and is gradually converted into an insoluble substance of high molecular weight. The hardening of polymethylsiloxanol is appreciably accelerated in presence of aqueous ammonia.

The substances MMM-10, MMM-20, and MEE-10 can be prepared exactly in the same way as M, from mixtures of methyltrichlorosilane with 10 and 20% of dimethyldichlorosilane or 10% of diethyldichlorosilane respectively. MMM-10, MMM-20, and MEE-10 are more stable and soluble than M, and their solutions are considerably more stable in storage. However, the water-repellent action of these substances is somewhat less effective.

Polyethylsiloxanol (E) was prepared similarly to M by addition of 327 g of ethyltrichlorosilane with b. p. 129-130° to a vigorously stirred mixture of 1.6 kg of ice and 1.6 liters of water. The properties of E are similar to those of M, but it has better solubility in organic solvents and a lower tendency to condensation.

Polyphenylsiloxanol (Ph) can be prepared most simply and easily by slow addition of 212 g of phenyltrichlorosilane with b.p. 199-201° to 2.5-3 liters of ice-cold water (with stirring). The solid white precipitate of phenylsiloxanol was filtered off an a Buchner funnel, thoroughly washed with water, and dried in a stream of air at room temperature. The yield of moist Ph was 200-210 g (122 g of $C_6H_5SiO_{1.5}$ when dried at 150°). Polyphenylsiloxanol is fairly stable when stored either in the solid form or dissolved in toluene or xylene.

BuX-33 was prepared similarly to M, by slow dropwise addition of a mixture of 192 g of butyltrichlorosilane with b.p. 145-146°* and 88 g of $SiCl_4$ to a mixture of 1.5 liters of water and 1.5 kg of powdered ice.

Hydrophobization of building materials with solutions of polyorganosiloxanols. Dilute (3-15%) solutions of polyorganosiloxanols in organic solvents (toluene, xylene, white spirit, acetone, etc.) are used for increasing the water resistance of building materials. The solution is applied to the surface by spraying, brushing, or dipping; as the solvent evaporates, a very thin water-repellent film of the organosilicon polymer is formed on the walls of the capillaries and pores of the building material. The porous structure of the material is retained, the color and

* Prepared by the reaction of powdered silicon (without Cu) with n-butyl chloride in an autoclave at 300°.

TABLE 1

Water Absorption of Cement Cubes Treated by Surface Applications of Solutions of M

Conc. of M solution (%)	Water absorption (%) after				
	1 day	4 days	7 days	28 days	90 days
0	7.3	7.5	7.7	8.3	8.6
One application					
5	7.0	7.2	7.2	7.8	—
10	1.5	5.4	6.4	7.1	—
15	2.5	5.3	6.1	6.9	—
Two applications					
5	0.5	1.0	1.6	2.9	—
10	0.3	0.7	0.9	1.6	3.4
15	0.2	0.5	0.6	0.9	2.0
Three applications					
5	0.3	0.7	1.4	2.1	3.8
10	0.5	1.0	1.1	1.8	3.4
15	0.2	0.4	0.6	1.1	1.8

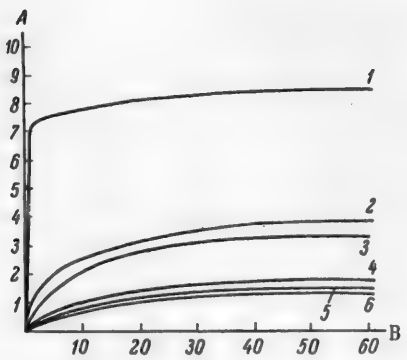

Water absorption of cement cubes.
A) Water absorption (in %), B) time (in days). Cements: 1) untreated, 2) treated with 5% methyltrichlorosilane solution, 3) treated with 10% sodium methylsiliconate solution, 4) treated with 15% solution of Ph, 5) treated with 15% solution of MPh-50, 6) treated with 15% solution of M.

texture of the surface remains unchanged, and the surface does not become glossy. The water-repellent film often combines chemically with the building material by interaction of the metallic hydroxides and oxides in the material with the hydroxyl groups of the polyorganosiloxanol. The solvent assists the fairly deep penetration of the polyorganosiloxanol into the pores of the material (to 2-8 mm or more, according to the porosity), instead of deposition in the form of a film on the outer surface. The water-repellent properties are therefore retained despite weathering or mechanical damage of the surface layer. As the pores are not blocked by the treatment, the rate of transmission of vapors through them ("breathing") remains about the same as in untreated materials.

Water-repellent coatings on building materials, formed from solutions of polyorganosiloxanols, are more resistant in use than water-repellent coatings based on sodium alkylsiliconates and alkylchlorosilanes. Moreover, polyorganosiloxanols differ advantageously from the above two types of organosilicon compounds in being entirely nontoxic and noncorrosive. Polysiloxanols may be applied to most mineral building materials, including brick, sandstone, limestone, concrete, asbestos cement, plaster, cement paints, etc., and, in the form of lacquer coatings, to wood and other organic materials. The consumption of organopolysiloxanol solution per 1 m^2 of treated surface for a single application is 150-500 ml, according to the porosity of the material.

More highly concentrated solutions of polyorganosiloxanols, and mixtures with mineral fillers and pigments (glass, mica, or asbestos dusts, oxides of manganese, titanium , and other metals, Portland cement, etc.) can be

TABLE 2

Water Absorption of Cement Cubes Treated by Surface Application of Solutions of Ph

Concentration of Ph solution (%)	Water absorption (%) after			
	1 day	3 days	7 days	28 days
	One application			
5	6.0	7.6	7.8	8.3
10	2.4	4.5	6.9	7.6
15	1.6	2.5	4.4	4.6
	Two applications			
5	1.7	3.5	6.8	8.2
10	0.6	1.0	2.4	3.4
15	0.3	0.5	0.9	1.5
	Three applications			
5	0.4	0.8	1.4	2.4
10	0.4	0.8	0.9	1.5
15	0.5	0.9	1.2	1.5

TABLE 3

Water Absorption of Cement Cubes Treated by Surface Application of Solutions of E, M, MMM-10, MMM-25, and MPh-50

Preparation	Conc. of solution (%)	Number of applications	Water absorption (%) after		
			1 day	7 days	28 days
E	5	3	2.2	2.9	3.1
E	15	1	2.9	3.1	3.2
MMM - 10	15	2	0.3	0.8	1.7
MMM - 25	15	2	1.7	3.4	5.0
MPh - 50	15	2	0.4	0.7	1.2

TABLE 4

Water Absorption (WA) and Capillary Suction (CS) of Red Clay Bricks Treated by Surface Application of Solutions of M

Conc. of M solution (%)	Water absorption (%) and capillary suction (in cm) after									
	1 hour		3 hours		6 hours		24 hours		48 hours	
	WA	CS	WA	CS	WA	CS	WA	CS	WA	CS
0	8.2	9	13.0	15	19.0	22	22.0	25	22.0	25.0
0.5	0.2	0	0.5	0	2.0	0	7.0	1.5	9.2	2.0
1	0	0	0	0	0	0	0.9	0	1.2	0
2	0	0	0	0	0	0	0	0	0	0
2.5	0	0	0	0	0	0	0	0	0	0

TABLE 5

Salt Resistance of Red Clay Bricks Treated by Surface Application of 2% Solution of M

	Increase in weight (%) after immersion in 5% sodium sulfate solution for				
	1 hour	3 hours	6 hours	24 hours	48 hours
Untreated brick	7.2	11.5	15.8	17.0	20.0
Brick containing 50% (of total saturation capacity) of moisture	1.2	3.3	6.5	7.3	8.2
Air-dry brick	0	0	0	0.1	0.2

TABLE 6

Water Absorption (WA) and Capillary Suction (CS) of Cement–Lime–Sand Plaster Treated by Surface Applications of Solutions of M

Conc. of M solution (%)	Water absorption (%) and capillary suction (in cm) after									
	1 hour		3 hours		6 hours		24 hours		48 hours	
	WA	CS	WA	CS	WA	CS	WA	CS	WA	CS
0	7.5	2	7.9	6	8.0	8	8.5	10	8.5	10
One application										
1	0.4	2	1.5	4	2.4	6	5.3	10	8.0	10
2	0.15	1	1.0	2	1.6	4	3.7	4	5.4	4
3	0.05	0	0.2	0	0.5	0	1.1	0	1.9	0
5	0.1	0	0.4	0	0.7	0	1.5	0	2.6	0
10	0.0	0	0.05	0	0.1	0	0.3	0	0.7	0
Two applications										
5	0.05	0	0.1	0	0.15	0	0.3	0	0.5	0
10	0.0	0	0.05	0	0.1	0	0.2	0	0.4	0
One application on moist plaster										
2	1.5	2	3.9	4	5.2	6	8.1	10	8.6	10
5	0.1	0	0.2	0	0.3	0	0.6	0	1.1	0
10	0.0	0	0.05	0	0.4	0	0.9	0	0.9	0

used for complete sealing of the pores in the surface layer of the building material which gives a reliable surface film impermeable to water and gases, and stable to chemical action, heat, and weather.

In illustration of the use of solutions of polyorganosiloxanols for increasing the water resistance of cement, plaster, and brick, we give below some of the results of our investigations, performed jointly with the Pamfilov Scientific Research Institute of the Academy of Communal Economy, and with certain otherbranch institutes and organizations in Leningrad. These investigations were carried out by N. V. Shorokhov, L. A. Zinin, N. P. Grishanina, and N. I. Firsova, to whom we offer our deep gratitude.

Cement and concrete. The hydrophobization of cement and concrete was studied with 7-cm cubes made from 1 : 3 cement paste (by weight) made from M-2400 Portland cement and river sand. The cubes were kept in air for at least 4 weeks after preparation, and contained 2-3% moisture; they were treated with solutions of the corresponding polyorganosiloxanols applied with a brush (one, two, and three applications at intervals of 1-3 hours).

After two or three days the cubes were weighed and immersed to a depth of 4 cm in water. To determine the water absorption, the cubes were weighed after 1, 4, 7, 28, and 90 days of immersion in water.

Table 1 gives the results on the decrease of the water absorption of cement by treatment with 5, 10, and 15% solutions of methylsiloxanol (M).

These results show that the water absorption of cement can be decreased 25 to 35-fold in one day by 2 or 3 applications of 10-15% solutions of M (2 or 3 applications of 5% solutions are rather less effective). Similar results are obtained after 2 or 3 applications of 10-15% solutions of polyphenylsiloxanol (Table 2).

Table 3 contains some examples of the increase of the water resistance of cement treated with solutions of E, MMM-10, MMM-25, and MPh-50. These results show that hydrophobization with the product of joint hydrolysis of CH_3SiCl_3 and $(CH_3)_2SiCl_2$ is less effective than treatment with the product of joint hydrolysis of CH_3SiCl_3 and $C_6H_5SiCl_3$ (MPh-50), which is more stable than M.

Water-repellent organosilicon coatings based on polyorganosiloxanols are more stable than all other types of organosilicon coatings; this is shown graphically in the Figure.

The salt resistance, weathering resistance, and chemical stability in corrosive media of cement and concrete are also increased by treatment with solutions of polysiloxanols.

Bricks. Ordinary red clay bricks were treated by a single surface application of a solution of polymethylsiloxanol (M) in acetone by means of a brush (one brick absorbs 35 g of solution). Three days after the treatment the bricks were immersed in water to 1/5 of their height and weighed at definite intervals. The decrease of the water absorption and capillary suction of the bricks in relation to the concentration of the M solution is illustrated in Table 4.

These results show that even after a single treatment with 2% solution of polymethylsiloxanol the bricks completely lose their power of absorbing water. They also lose their power of absorbing salt solutions, as is seen in Table 5. Bricks treated with 2% solution of M when in the moist state (50% of complete saturation) can still absorb sodium sulfate solution, but to a much smaller extent than untreated bricks.

Similar increases of the water resistance and salt resistance of bricks are produced by treatment with other polyorganosiloxanols (E, Ph, BuX-33, MMM-10, MPh-50, etc.)

Plaster. Data on the decrease of water absorption and capillary suction of cement–lime–sand (1 : 1 : 4) plaster treated with solutions of M in the dry and moist states (with 1.3 and 7.3% of moisture respectively) are given in Table 6.

The test specimens (blocks 12 × 7 × 2.5 cm) were allowed to harden for a week in a moist atmosphere, then kept for 10 days in air, and treated by one or two applications of M solution (the second application after 20 minutes) by means of a brush. The water absorption and capillary suction were determined 7 days after the treatment. For this, the blocks were immersed in water to 2/5 of their height and weighed at definite intervals.

The results in Table 6 clearly show that even after a single application of 5% M solution both dry and moist plaster almost lose their ability to absorb water by capillary suction. The most effective treatment is a double application of 5-10% solutions, which produces a 17 to 21-fold decrease of water absorption in a 48-hour test. It must be noted that waterproofing of plaster by solutions of polyorganosiloxanols is more effective than treatment with solutions of sodium alkylsiliconates [6].

These convincing examples, the number of which could be increased considerably, show that solutions of polyorganosiloxanols can be used for increasing the water resistance (and thereby the durability) of building materials.

SUMMARY

A method has been developed for the production of polyorganosiloxanols by hydrolysis of alkyltrichlorosilanes and their mixtures with dialkyldichlorosilanes or with $SiCl_4$ in absence of solvents, and the products have been shown to be effective agents for hydrophobization of building materials.

LITERATURE CITED

[1] M. G. Voronkov and B. N. Dolgov, Nature 5, 22 (1954).

[2] B. N. Dolgov and M. G. Voronkov, Inform.-Techn. Pamphlet, Leningrad House Sci. Tech. Propaganda 12 (35) (1954).

[3] S. S. Khrustalev, M. G. Voronkov and B. N. Dolgov, J. Appl. Chem. 28, 916 (1955).*

[4] S. S. Khrustalev and M. G. Voronkov, Inform.-Techn. Pamphlet, Leningrad House Sci.-Tech. Propaganda 7 (30) (1954).

[5] B. N. Dolgov and M. G. Voronkov, J. Leningrad Univ. 5, 185 (1954).

[6] M. G. Voronkov and N. V. Shorokhov, Inform.-Techn. Pamphlet, Leningrad House Sci.-Tech. Propaganda 2 (1956).

[7] A. K. Andrianov, Progr. Chem. 24, 430 (1955).

[8] G. H. Wagner, D. L. Baily, A. N. Pines, M. L. Dunham and D. B. McIntire, Ind. Eng. Chem. 45, 367 (1953).

Received February 29, 1956

* Original Russian pagination. See C. B. Translation

CATALYTIC DECOMPOSITION OF ISOBUTYL ISOBUTYRATE AND ISOAMYL ISOVALERATE*

B. A. Bolotov, B. N. Dolgov and N. P. Usacheva

Among the various mechanisms proposed by different authors for the catalytic reactions of the formation of ketones from primary alcohols, the following are worthy of consideration:

1) Formation of ketones by way of intermediate formation of esters [1, 2].

$$2RCH_2OH \xrightarrow{-H_2} 2RCOH \longrightarrow RCH_2OCOR \xrightarrow[-C_nH_{2n}]{-CO_2} RCOR; \qquad (I)$$

2) formation of ketones through stages of aldol and secondary-alcohol formation [3-5]

$$2RCH_2OH \xrightarrow{-H_2} RCOH \rightarrow RCHOHRCOH \xrightarrow{-CO} RCHOHR \xrightarrow{-H_2} RCOR \qquad (II)$$

Our studies of the conversion of primary alcohols, from n-propyl to n-octyl, in presence of promoted copper catalysts [6-9], have shown that the function of the catalyst changes with the temperature. It seems likely that instead of the ester condensation of aldehydes which occurs at the catalyst surface at low temperatures, reactions of aldol condensation leading to the formation of ketones take place above 300°. It was also shown experimentally that the direction of the conversion reactions of primary alcohols is determined by the pressure in the system in addition to the temperature [10, 11]. Ethyl and n-butyl alcohols at 350-400° and 20-40 atmospheres give rise to saturated hydrocarbons corresponding in composition to ketones formed under atmospheric pressure.

The present paper deals with a study of the reaction conditions and of the composition of the products formed in presence of activated copper catalyst [12] in the catalytic decomposition of esters: isobutyl isobutyrate and isoamyl isovalerate. It was found that at 300-400° these esters decompose with formation of aldehydes and alcohols, whereas at 400-475° they are converted quantitatively into symmetrical ketones: diisopropyl ketone and diisobutyl ketone, the yields reaching 42-50%.

The considerable amounts of carbon monoxide and hydrogen in the gaseous reaction products indicate that the formation of ketones from esters proceeds through an intermediate stage in which the esters are decomposed into aldehydes, followed by aldol condensation. The presence of small amounts of CO_2 and olefins in the gases does not exclude the possible partial formation of ketones by direct decomposition of esters according to Scheme (I).

It was found that the catalytic decomposition of mixtures containing esters in different proportions at 450° gives larger amounts of symmetrical ketones corresponding to the esters present in excess in the original mixtures. If the esters are present in equal proportions, the asymmetrical isopropyl isobutyl ketone is predominantly formed. The total yield of ketones is 40-44%, and does not depend on the ratio of the esters present.

EXPERIMENTAL

The laboratory unit described previously [13] was used for the investigation. The catalyst was precipitated

* Communication III in the series on the catalytic decomposition of resin esters.

TABLE 1

Effect of Temperature on the Catalytic Decomposition of Isobutyl Isobutyrate

Temperature (°C)	Yields of reaction products		Composition of gas (in volume %)				Yield (in wt. % on the original ester)				
	Condensate (in wt. %)	Gas (in liters)*	CO_2	$i\text{-}C_4H_8$	CO	H_2	isobutyraldehyde	isobutyl alcohol	diisobutyl ketone	isobutyl isobutyrate	isobutyric acid
300	92.	1.8	10.0	13.5	39.0	37.5	6.2	8.6	1.7	63.8	1.4
325	85.5	7.4	6.5	19.6	36.2	37.7	8.8	7.0	1.1	55.9	0.9
350	72.0	17.5	3.4	20.8	29.6	46.2	8.8	10.0	3.4	42.2	1.0
375	92.0	6.9	5.0	7.5	33.0	54.5	14.2	8.2	6.0	47.9	1.8
400	88.5	6.4	12.0	0.0	56.0	32.5	10.6	24.5	15.3	31.5	0.9
425	81.0	12.6	10.5	0.0	47.0	42.5	13.9	20.4	23.4	12.2	0.8
450	75.0	22.4	9.2	1.4	38.7	50.7	8.8	17.1	38.2	4.4	0.7
475	68.6	22.7	8.8	2.8	35.6	52.8	1.0	6.4	49.8	0.8	0.5

* Here and in Tables 2 and 3 the yield and composition of the gas were calculated per 100 g of the original ester after subtraction of the hydrogen supplied during the experiment.

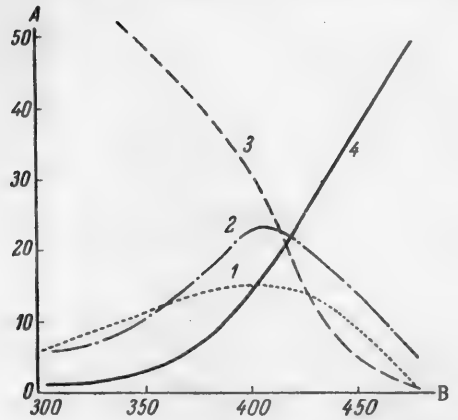

Fig. 1. Effect of temperature on the composition of the conversion products of isobutyl isobutyrate. A) Yield (in wt. % on the original ester), B) temperature (°C).
1) Isobutyraldehyde, 2) isobutyl alcohol, 3) isobutyl isobutyrate, 4) diisopropyl ketone.

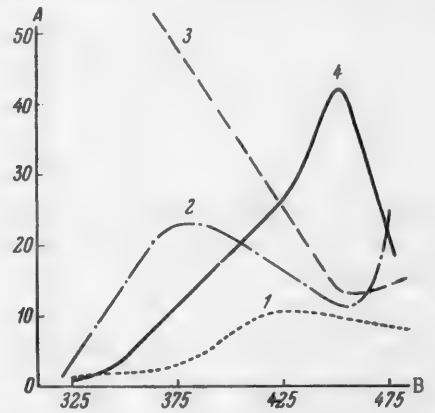

Fig. 2. Effect of temperature on the composition of the conversion products of isoamyl isovalerate. A) Yield (in wt. % on the original ester), B) temperature (°C).
1) Isovaleraldehyde, 2) isoamyl alcohol, 3) isoamyl isovalerate, 4) diisobutyl ketone.

copper catalyst No. 5 [13] promoted with thorium oxide, reduced in hydrogen at 285-300°. The experiments were performed in presence of equimolar amounts of hydrogen relative to the ester. The conversion of the esters was studied in the 300-475° temperature range, at space velocities of 120-150.

The following esters were prepared: isobutyl isobutyrate, b. p. 147-149°, n_D^{20} 1.3995 (literature data [14] – b. p. 148.7°, n_D^{20} 1.3999), and isoamyl isovalerate, b. p. 189-191°, n_D^{20} 1.4132 (literature data [14] – b. p. 190.4°, n_D^{20} 1.4126).

The condensates obtained in the experiments were fractionated and the individual fractions were analyzed for aldehydes, esters, ketones, alcohols, and acids.

Study of the conversion of isobutyl isobutyrate. The variations of the composition of the reaction products in the catalytic decomposition of isobutyl isobutyrate with the temperature are given in Table 1 and plotted in Fig. 1.

Considerable decomposition of the ester occurred even at about 300°, and it was found that the rate of the reaction increases with rise of temperature. At 300-400° the main reaction products were isobutyraldehyde and isobutyl alcohol. Their formation can be attributed to the reactions

$$RC_2HOCOR \rightleftarrows 2RCOH \underset{-H_2}{\overset{+H_2}{\rightleftarrows}} 2RCH_2OH.$$

This is confirmed by the absence of isobutyric acid and the relatively low contents of diisopropyl ketone in the condensates formed at 300-400°. It was found earlier [15] that ketones are formed from primary alcohols of iso structure at temperatures above 400°. Similar behavior was observed in the catalytic conversion of isobutyl isobutyrate. The formation of large amounts of diisopropyl ketone was observed at temperatures above 400°, with corresponding decreases in the alcohol and aldehyde contents of the reaction products. At 475° the ester was completely converted into the ketone, the yield of the latter being 50% calculated on the ester.

It follows from the data on the composition of the gaseous products, given in Table 1, that carbon monoxide and hydrogen predominate over the other gases. Such amounts are only possible if the ketone is formed from an alcohol or aldehyde.

The experimental results suggest that the formation of ketones from esters proceeds through an intermediate stage of aldehyde formation, and the aldehyde is converted into the corresponding ketone through the aldol stage:

$$RCH_2OCOR \rightleftarrows 2RCOH \underset{-H_2}{\overset{+H_2}{\rightleftarrows}} RCH_2OH$$
$$\downarrow\uparrow$$
$$[RCHOHRCOH] \xrightarrow[-H_2]{-CO} RCOR$$

Study of the conversion of isoamyl isovalerate. The study of the catalytic decomposition and of the products formed in the conversion of isoamyl isovalerate was carried out similarly to the experiments with isobutyl isobutyrate.

A careful examination of the results, given in Table 2 and Fig. 2, leads to the conclusion that the conversion of isoamyl isovalerate is almost identical with that of isobutyl isobutyrate. However, there are certain differences in the quantitative composition of the products, namely: the maximum yields of diisobutyl ketone and isoamyl alcohol in the decomposition of isoamyl isovalerate are obtained at lower temperatures than the maximum yields of diisopropyl ketone and isobutyl alcohol obtained from isobutyl isobutyrate. These results are in full agreement with our earlier results obtained in a study of the catalytic conversions of isoamyl and isobutyl alcohols [15].

TABLE 2

Effect of Temperature on the Catalytic Decomposition of Isoamyl Isovalerate

Temperature (°C)	Reaction prod. yields per 100 g ester		Composition of gas (in vol. %)				Yields (in wt. % on the original ester)			
	condensate (%)	gas (liters)	CO_2	i-C_5H_{10}	CO	H_2	isovaleraldehyde	isoamyl alcohol	diisobutyl ketone	isoamyl isovalerate
325	98.6	0.5	28.4	15.1	56.5	0.0	1.1	3.7	0.6	86.3
350	78.2	4.7	16.3	0.2	26.6	55.0	5.2	15.2	3.1	54.5
375	90.3	2.5	15.5	0.0	20.0	64.5	3.0	22.9	12.2	54.7
400	86.3	3.4	31.7	5.0	45.6	17.7	6.5	21.6	18.8	35.7
425	84.0	4.3	12.5	4.5	60.5	22.5	10.3	15.7	24.3	27.3
450	85.0	13.0	16.6	6.0	34.4	43.0	9.2	11.0	41.6	13.4
475	81.0	—	—	—	—	—	8.6	23.9	22.0	14.0

TABLE 3

Yields of Ketones at 450° with Various Ratios of Isobutyl Isobutyrate to Isoamyl Isovalerate

Molecular ratio of esters	Reaction prod. yields per 100 g ester		Composition of gas (in vol. %)				Yields of ketones (in wt. % on original ester mixture)			Total yield of ketones (%)
	condensate (%)	gas (liters)	CO_2	C_nH_{2n}	CO	H_2	diisopropyl ketone	isopropyl isobutyl ketone	diisobutyl ketone	
2 : 1	91.0	21.5	12.7	4.2	41.0	42.0	19.0	15.1	5.0	39.1
1 : 1	80.0	19.2	10.6	5.5	31.0	53.0	15.2	16.6	13.0	44.8
1 : 2	77.0	10.7	19.4	4.6	42.0	34.0	8.9	16.5	19.0	44.4

Catalytic conversion of mixtures of isobutyl isobutyrate and isoamyl isovalerate. The experiments on the conversion of mixtures of esters were performed at the optimum temperature for the formation of ketones from esters (450°) at 2 : 1, 1 : 1, and 1 : 2 ratios of isobutyl isobutyrate to isoamyl isovalerate.

The results of the experiments are given in Table 3. The reaction products always contain three ketones: diisopropyl ketone, isopropyl isobutyl ketone, and diisobutyl ketone. The yield of a given symmetrical ketone increases rapidly with increasing relative content of the corresponding ester. Predominant amounts of the mixed ketone are formed only at 1 : 1 ester ratio.

It was found in the earlier study of the conversion of mixtures of isobutyl and isoamyl alcohols over the same copper catalyst [16] that the maximum yield of the mixed ketone was obtained at 425° and 1 : 1 alcohol ratio. The total yield of ketones was 41-42%, irrespective of the alcohol ratio.

The results obtained with mixtures of esters show that the processes of ketone formation from esters and from primary alcohols are identical.

As in the earlier experiments with alcohols [16], the gases formed in the decomposition of ester mixtures contain large amounts of carbon monoxide. This leads to the conclusion that the reactions of ketone formation from alcohols and from esters have the same mechanism, i.e., they pass through the stage of aldol condensation of aldehydes (Scheme II). However, ketones may also be formed to some extent by direct decomposition of the esters (Scheme I); this is shown by the presence of carbon dioxide and olefins in the gaseous products, and of water in the condensates.

The aldehydes and ketones formed in the catalytic conversions of the esters were isolated in the pure state, their physical constants were determined, and the appropriate derivatives prepared. The results were identical with those published earlier [15, 16], and are therefore not given here.

SUMMARY

1. Isobutyl isobutyrate and isoamyl isovalerate are converted in presence of promoted copper catalyst at 450-475° into diisopropyl ketone and diisobutyl ketone in 42-50% yields, calculated on the esters.

2. The esters decompose at 300-400° to form aldehydes which are then hydrogenated to alcohols. The yields of alcohols are 20-25%.

3. A mixture of two esters gives two symmetrical and one asymmetrical ketone. The yield of the latter depends on the relative proportions of the esters taken, and reaches a maximum at 1 : 1 ratio.

4. The presence of considerable amounts of carbon monoxide in the gases, and of aldehydes and alcohols corresponding to the original esters in the condensates, confirms the earlier hypothesis that esters are decomposed into aldehydes, which are then converted into ketones through aldol condensation.

LITERATURE CITED

[1] M. J. Kagan, I. A. Sobolev and G. D. Lubarsky, Ber. 68, 1140 (1935).

[2] P. Sabatier and Mailhe, Comptes. rend. 152, 669 (1911); Comptes. rend. 154, 175 (1912).

[3] V. I. Ipat'ev and N. A. Kliukvin, Ber. 58, 4 (1925).

[4] V. I. Komarewsky and I. R. Coley, J. Am. Chem. Soc. 63, 3269 (1941).

[5] V. I. Komarewsky and J. G. Smith, J. Am. Chem. Soc. 66, 1116 (1944).

[6] B. A. Bolotov, B. N. Dolgov and P. M. Adrov, J. Appl. Chem. 28, 3, 299 (1955).*

[7] B. A. Bolotov, B. N. Dolgov and K. P. Katkova, J. Appl. Chem. 28, 4, 414 (1955).*

[8] B. A. Bolotov, B. N. Dolgov and L. K. Prokhorova, J. Appl. Chem. 28, 5, 516 (1955).*

[9] B. A. Bolotov, B. N. Dolgov and K. P. Katkova, J. Appl. Chem. 28, 11, 1184 (1955).*

[10] B. A. Bolotov and L. K. Smirnova, J. Gen. Chem. 25, 1987 (1955). *

[11] B. A. Bolotov and L. K. Smirnova, J. Gen. Chem. 26, 5 (1956). *

[12] B. A. Bolotov and B. N. Dolgov, Authors' Claim No. 92622 (1950).

[13] B. N. Dolgov, B. A. Bolotov and L. A. Komissarova, J. Appl. Chem. 28, 1, 71 (1955).*

[14] E. Huntress and E. Mulliken, Identification of Pure Organic Compounds (1946).

[15] B. A. Bolotov, K. P. Katkova and S. B. Izraileva, J. Appl. Chem. 30, 1, 134 (1957). *

[16] B. A. Bolotov and N. A. Rozenberg-Marshova, J. Appl. Chem. 30, 2, 286 (1957). *

Received April 12, 1956

* Original Russian pagination. See C. B. Translation.

BRIEF COMMUNICATIONS

EFFECT OF ADDED SULFIDES ON SOME PROPERTIES OF BORONLESS GROUND-COAT ENAMEL

G. I. Beliaev

Additions of metal sulfides to melts of glasses and enamels confer surface-active properties on these melts [1-6]. The sulfides have limited solubility and can be adsorbed on the melt surfaces, lowering the surface tension [1]. The decrease of surface tension generally improves the wetting of solid phases by the silicate melts. In enameling technology the wetting of metals has an important influence on the formation of the enamel coating which takes place during firing at high temperatures. This firing is accompanied by oxidation of steel and interaction of the silicate melt with the scale and metal, with evolution of large amounts of gases (H_2, CO, CO_2 etc.) which leads to the formation of a porous structure in the enamel coating; the composition of the ground coat changes, it becomes saturated with iron oxides, with consequent crystallization and worsening of the structure, leading to blistering and other faults [2].

Good wetting of the solid phase (oxidized steel) by the silicate melt should favor uniform flow and adhesion of the ground coat to the metal, easier removal of the gas phase from the melt and from the ground coat–steel contact zone [3], and less oxidation of the steel surface [2, 4].

Boronless enamels wet iron oxides much less effectively than borate enamels [5, 6], and oxidize the steel very rapidly during firing [7]. The reason is that boron is present in triple and quadruple coordination in glasses and enamels [8], and is a good glass former, and the [BO_3] triangles with their bonds in a single plane migrate to the surface so that the surface tension of borate enamels and glasses is greatly reduced [1, 6].

For improvement of the wetting of oxidizable melts by boronless enamel melts, Azarov [4, 6, 9] proposed the addition of small amounts of certain sulfides and selenides, and cations with a structure of the noninert gas type (Cd^{2+}, Cu^{2+}, Cu^{+}, Ag^{+} etc.)

The present paper contains the results of experiments on the influence of metal sulfides (antimony glance Sb_2S_3, chalcopyrite $CuFeS_2$, zinc blende ZnS, galena PbS, and iron pyrite FeS_2) on the properties of ground-coat enamels, and in particular on: a) the oxidation of the steel during firing of the ground coat; b) the wetting of the oxidized metal by the melt; c) the flow of the enamel; d) the quality of the ground coat.*

The contact angle θ was determined with the aid of a projection lantern, from a shadow image of a drop of the ground-coat melt formed from an enamel frit [4]. The oxidizability of steel during firing of the ground coats was determined at 880° by our method [7], in which the weight increase of the steel specimen was determined at intervals. The viscosity of the ground-coat melt was estimated from the spreading of a drop and the area occupied by the melt. For determination of the quality of enamel ground coats, a ground-coat slip of the following composition was made in a porcelain ball mill: 100 wt. parts of 35-T frit, 1.0% crystalline borax, 0.5% sulfide, 5% Glukhov clay, 45.0% water. Steel plates 60 × 80 × 0.5 mm in size were coated with the slip by the dipping method. The specimens were dried in a thermostat and fired in a muffle furnace at 820, 860, and 900° for 2, 4, and 6 minutes. The thicknesses of the ground coat was measured by means of an electromagnetic thickness meter [4]. The quality of ground coat after firing was estimated visually and evaluated on a 5-point scale according to

* N. F. Smakota took part in the work.

the presence of holes, bubbles, and blisters. Average results of 3-4 estimations are given in all the tables and figures.

TABLE 1

Oxidation of Steel During Firing of Ground Coats with Added Sulfides

Firing time (min.)	Without additives	Increase in weight of the steel (in mg/dm^2) with additions of				
		Sb_2S_3	ZnS	$CuFeS_2$	PbS	FeS_2
2	47.3	9.7	9.0	3.3	41.7	37.7
4	116.3	22 3	20.7	7.7	93.3	62.3
6	189.0	38.7	37.7	20.7	134.0	92.7
8	253.0	64.0	60.0	41.0	194.0	151.0
10	300.3	95.0	90.7	72.3	241.7	244.3

In the experimental enameling and other investigations, cold-rolled sheet steel from the "Zaporozhstal" works of the following composition (in %): C 0.08, Mn 0.33, S 0.029, P 0.013 and boronless enamel frit No. 35-T from the "Legkolit" works were used. The composition of the frit (in %) was: SiO_2 50.64, Al_2O_3 3.16, Na_2O 21.26, CaF_2 12.90, Na_2SiF_6 3.90, TiO_2 5.05, Co_2O_3 0.46, Ni_2O_3 1.37 and MnO 1.26.

The metal sulfides were ground in a ball mill to pass through a sieve of 10,000 mesh/cm^2, and 0.5% lots by weight were added to the ground-coat frit.

The contact angles of wetting of oxidized steel by the enamel melt containing different sulfides are shown diagrammatically in Fig. 1, and the rates of oxidation of the steel during firing of the ground coat are given in Table 1 and Fig. 2.

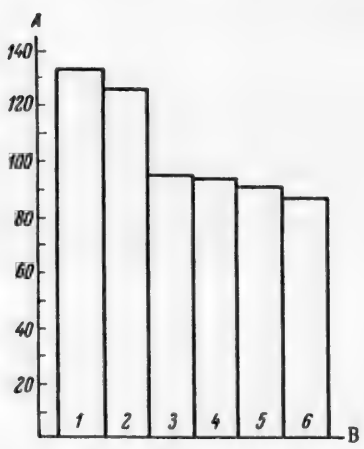

Fig. 1. Contact angle of wetting of an oxidized surface by enamel melts with added sulfides.
A) Contact angle θ (in degrees), B) additives:
1) no additive, 2) PbS, 3) FeS_2, 4) ZnS, 5) $CuFeS_2$, 6) Sb_2S_3.

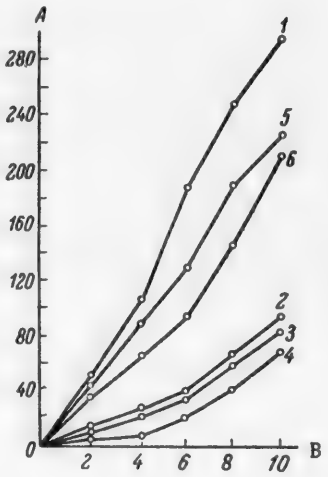

Fig. 2. Effect of added sulfides on the oxidation of steel under the ground coat.
A) Weight increase (in mg/dm^2), B) firing time (minutes).
Additives: 1) no additive, 2) Sb_2S_3, 3) ZnS, 4) $CuFeS_2$, 5) PbS, 6) FeS_2.

The viscosity and the ability of the melt to spread over the oxidized steel surface, estimated from the length of the drop and the area occupied by the melt, are given in Table 2.

It follows from these experiments (Table 2, Figs. 1 and 2) that small additions of sulfides to boronless frits improve wetting considerably and decrease the oxidation of the steel surface during firing of the ground coat.

The most effective additives were chalcopyrite, antimony glance, and iron pyrite. Additions of galena, chalcopyrite, and iron pyrite lower the viscosity and improve the spreading over the steel surface.

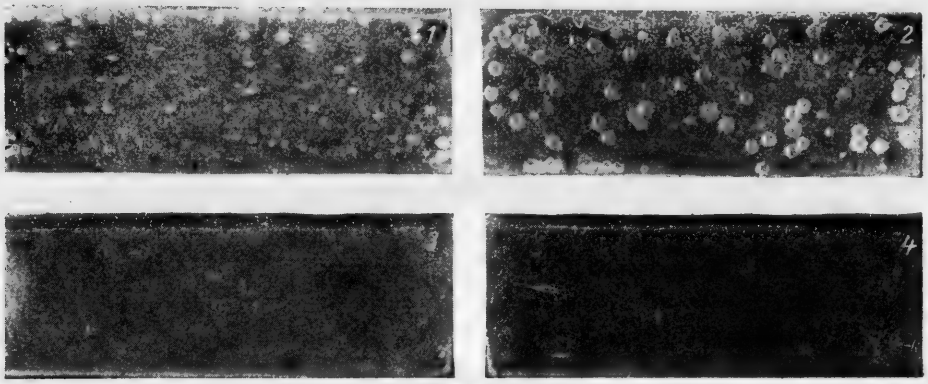

Fig. 3. External appearance of the ground coats after firing.
1) and 2) Without added sulfide, 3 and 4) with addition of 0.5% of chalcopyrite.
Fired at 900° for 4 and 6 minutes.

TABLE 2

Effect of Added Sulfides on the Fluidity of Ground-Coat Enamel

Added sulfide	Length of drop (cm)	Width of drop (cm)	Spreading area (cm^2)
Without additive	6.37	2.03	12.93
Sb_2S_3	6.53	2.03	13.26
ZnS	6.03	2.07	12.48
$CuFeS_2$	6.37	2.27	14.46
PbS	6.30	2.33	14.68
FeS_2	6.20	2.23	13.83

TABLE 3

Evaluation of the Quality of Ground Coats with Different Added Sulfides

Sulfide	Thickness of ground coat after firing (mm)	Mean estimate of coat quality (points)
Without added sulfides	0.19	2.8
Antimony glance	0.19	3.4
Zinc blende	0.21	3.3
Chalcopyrite	0.21	3.4
Galena	0.23	2.6
Iron pyrite	0.21	3.3

Trial enamelings and visual inspection of the specimens showed that metal sulfides (with the exception of galena) improve the spread of the ground coat, decrease the number of blisters and holes, and considerably improve the quality of the enamel coating.

Figure 3 shows photographs of steel specimens covered with ground-coat enamel with and without added chalcopyrite, fired at 900° for 4 and 6 minutes. The enamel coating without sulfide is pitted, while the enamel with 0.5% of chalcopyrite is quite smooth and without pitting.

The average evaluations of the enamel coatings are given in Table 3.

It follows from the data in Table 3 that additions of chalcopyrite, antimony glance, zinc blende, and iron pyrite are the most effective for improving the quality of enamel coats and reducing pitting.

Additions of lead sulfide do not improve but even worsen somewhat the quality of the enamel coats and increase pitting. The probable explanation is that although enamels with added galena are more fluid, their wetting power and ability to inhibit the oxidation of steel during the firing are no better than those of the original enamel without added sulfides.

These experiments with sulfides confirm our earlier conclusions that pitting of ground coats can be diminished by reduction of the rate of oxidation [7] and improvement of the wetting of the steel by the enamel melts [4]. Mazurek [10] also reports a direct relationship between the surface tension of a silicate melt, wetting, and pitting.

SUMMARY

1. Small additions of surface-active substances (metal sulfides) improve the wetting of oxidized steel surfaces by enamel melts and decrease considerably the oxidation rate of the steel during firing of the ground coats. The best results are obtained by additions of chalcopyrite, antimony glance and iron pyrite to boronless ground-coat enamels.

2. It was found that there is a connection between the influence of an additive on the oxidizability and wettability of steel and its effect on the quality of the coat and on pitting: the additives which improve wetting and decrease the oxidation of steel during firing of the ground coat are the most effective in reducing pitting and improving the quality of the ground-coat.

LITERATURE CITED

[1] A. A. Appen and K. A. Shishov, Progr. Chem. 5 (1953).

[2] G. I. Beliaev, in the book: Conference on Production Technology of Enameling (Metallurgy Press, 1956).*

[3] L. D. Kunin, Surface Phenomena in Metals (Metallurgy Press, 1955).*

[4] K. P. Azarov, J. Appl. Chem. 27, 1 (1954).**

[5] L. Stuckert, Die Emailfabrikation, Berlin (1941).

[6] K. P. Azarov, in the book: The Structure of Glass (Izd. AN SSSR, 1955).*

[7] G. I. Beliaev, Trans. Novocherkassk Polytech. Inst. 24 (38) (Industrial Construction Press, 1953).

[8] A. A. Appen, J. Appl. Chem. 27, 6 (1953).**

[9] K. P. Azarov, Proc. Acad. Sci. USSR 76, 4 (1951).

[10] V. V. Mazurek, Boronless Ground-Coat Enamels, Author's Summary of Dissertation, Lensoviet Technological Institute (Leningrad, 1955).

Received September 10, 1956

* In Russian.

** Original Russian pagination. See C. B. Translation.

PRODUCTION OF HIGHLY DISPERSE NONPOROUS SILICA BY COMBUSTION OF ORGANOSILICON COMPOUNDS

A. K. Bonetskaia, E. A. Leont'ev and E. A. Kharlamov

Much work has been done on the development of methods for preparation of silica gel, owing to its great practical importance as the commonest hydrophilic adsorbent, filler in the rubber industry, and support for catalytically active substances. By variations of the conditions of preparation it is possible to obtain silica gels differing greatly in structure, from finely porous samples with effective pore diameters about 20 A to coarsely porous samples with pore diameters up to 200 A. The properties of such silica gels depend to a considerable extent on the specific surface and pore size. Therefore the production of finely divided nonporous silica is of special interest in relation not only to the possible technical applications of such a product, but also to the solution of certain questions in the theory of adsorption when it is necessary to exclude the influence of the pores on the character of a particular adsorption process. We have therefore developed a method and designed a continuous-action laboratory unit for the production of finely divided silica (silica powder) by combustion of ethyl orthosilicate.

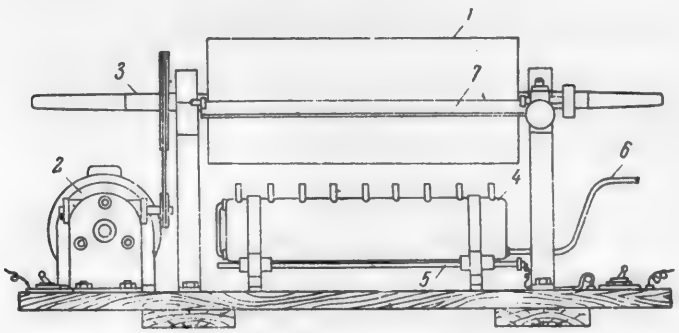

Fig. 1. Apparatus for the production of silica powder. Explanation in text.

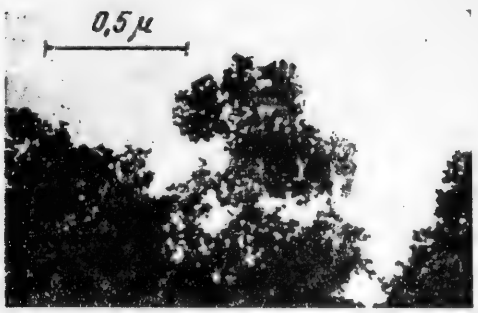

Fig. 2. Electron micrograph of silica powder.

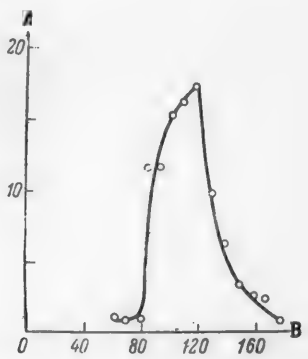

Fig. 3. Particle size distribution curve. A) Number of particles of a given diameter (%), B) particle diameter (in A).

The apparatus (Fig. 1) consists of a hollow metallic drum, the outer surface of which is chromium-plated and polished, and covered with an anticorrosion coating. The drum is rotated by means of a motor 2 about its horizontal axis at 60 rpm. The axis 3 of the drum is a tube with two openings inside the drum for the supply of running water for cooling the surface of the drum.

The water enters through a funnel inserted in a ball bearing (not shown in the diagram) and connected to the hollow axis of the drum by means of a flexible rubber tube. When half the volume of the drum is filled, water flows out through the other end of the tubular axis.

Ethyl orthosilicate is poured into the reservoir 4. It is heated to about 100° by means of the variable heater 5, and compressed air is then forced into the reservoir through the tube 6. The ester vapor escapes through the tubes in the upper part of the reservoir and is burned there.

Under the proper conditions of operation the flame should be small (to avoid excessive loss of the silica powder formed), and it should not be luminous, as this leads to contamination of the silica powder with products of incomplete combustion of the ester. The silica powder formed during the combustion of the ester is deposited on the surface of the rotating drum, which is continuously cooled with running water. The deposited layer of silica is removed by the metal scraper 7 and collected in a receiver.

A very important feature of the method is the possibility of smooth regulation and stability of the supply of compressed air into the reservoir. If not enough air is supplied, the combustion of the ester vapor is incomplete, while with excess air the concentration of the ester vapor decreases and combustion ceases. It must also be taken into account that the usual ethyl orthosilicate as supplied from the factories contains a small amount of silicon tetrachloride, used as the starting material in the production of silicate esters. The combustion products of the ester contain some hydrogen chloride. This may cause appreciable corrosion of the surface of the metal drum and contamination of the silica powder with corrosion products.

The unit described, with a drum 350 mm long and 200 mm in diameter, gave 10 g of silica powder per hour in continuous operation.

The silica powder formed was a very bulky product, with a bulk density about 0.025 g/cc. The specific surface, determined by the low-temperature adsorption of nitrogen, was 240 m^2/g.

In addition, the silica powder was investigated under the electron microscope at 11300 magnification. One of the micrographs is shown in Fig. 2. The sample was placed on the specimen screen and the photograph was taken by transmission without the use of a support, so that the resolving powder of the electron microscope was increased.

The particle sizes were measured directly on the negatives by means of a measuring microscope to an accuracy of 0.01 mm. Particles with well-defined outlines which did not overlap were selected for the measurements.

The results of numerous measurements of particle diameter were used to plot a particle size distribution curve (Fig. 3), which indicates that the silica powder is relatively monodisperse, containing about 90% of particles 80 to 150 A in diameter.

The specific surface, calculated from these results, was 220 m^2/g. The close agreement of the values for the specific surface determined from adsorption data and by statistical analysis of the electron micrographs shows that the silica powder is almost nonporous and highly disperse silica.

The authors express their gratitude to Prof. B. V. Il'in and K. G. Krasil'nikov for their interest and valuable advice, to M. Ia. Ignat'eva for assistance in operation of the unit, and to E. A. Sysoev for determinations of the specific surface.

Received June 21, 1956

THE ACTIVITY OF POTASSIUM IN POTASSIUM – MERCURY AND POTASSIUM – LEAD ALLOYS IN THE LIQUID STATE

A. G. Morachevskii

The M. I. Kalinin Polytechnic Institute, Leningrad

The purpose of the present investigation was determination of the activity of potassium in potassium–lead alloys in the liquid state. The activity of potassium was calculated from the results of measurements of electromotive force (emf) of the cell:

potassium | electrolyte with potassium ions | alloys (1)

As in investigations of sodium alloys [1-3], the electrolyte used was glass, in this instance containing potassium ions. Vierk and Hauffe [4] used glass as electrolyte in studies of the activity of potassium in alloys with mercury. Before the studies of the potassium–lead system, we investigated the activity of potassium in alloys with mercury in order to test the reproducibility of the results and the suitability of different glasses. It was also desired to extend the measurements to the region of alloys with high contents of mercury, which was not studied by Vierk and Hauffe, for more exact calculations of the integral excess free energy.

The activity of potassium was calculated from the emf measurements by means of the equation:

$$\log a_K = -\frac{5040E}{T}$$

The partial molar free energy of potassium can be calculated from the equation:

$$\Delta\bar{F}_K = 4.576T \log a_K.$$

Accordingly, the excess partial molar free energy of potassium $\overline{\Delta F_K^x}$ is:

$$\overline{\Delta F_K^x} = \overline{\Delta F}_K - RT\ln N_K = 4.576T \log \frac{a_K}{N_K} = 4.576T \log \gamma_K.$$

The following form of the Gibbs-Duhem equation was used for calculation of the integral excess free energy:

$$\Delta F^x = (1 - N_K)\int_0^{N_K} \frac{\overline{\Delta F}_K^x}{(1 - N_K)^2} dN_K.$$

Method. The design of the measurement cell was the same as in our investigations of sodium alloys [3]; it was in the main similar to the design used by Hauffe [1, 4]. The experiments were performed in an argon atmosphere. The measurement procedure used for sodium alloys was somewhat modified for studies of potassium alloys. The emf of Alloy I | glass | Alloy II cells was measured; i.e., both electrodes were alloys. Therefore the reference electrode was not pure potassium, but Alloy I, poor in potassium. Measurements of emf of the cell: potassium | glass | Alloy I made it possible to recalculate the data obtained for the first cell. With this method it was possible to use the minimum amounts of pure potassium. Special experiments on alloys of the sodium–lead system, already studied, showed that the accuracy of the modified method remains adequate.

The low-potassium alloys used as the reference electrodes (potassium–mercury and potassium–lead) were prepared in advance in sufficient amounts by fusion of the components under a layer of paraffin wax. Vacuum-distilled potassium was used for studies of the K–Hg and K–Pb systems; "analytical grade" Kahlbaum mercury was used; "granulated pure" grade lead was purified electrochemically with fused salts as electrolyte [5]. To remove oxide, the potassium was introduced into thin-walled glass bulbs through a capillary tube; the bulbs were then sealed. With the potassium in sealed tubes, it was possible to make alloys of any desired composition in an argon atmosphere without subsequent chemical analysis.

Preliminary experiments showed that for investigation of potassium alloys at temperatures up to 500° glass No. 23 (7.4% K_2O) is most suitable, while at temperatures above 500° ZS – 8 glass (3.8% K_2O) should be used. With the use of these glasses we did not find, as Vierk and Hauffe [4] did, that constant values of emf are reached more slowly than they are with sodium alloys.

The temperature was measured by means of a chromel–alumel thermocouple connected to a PP potentiometer; a photoelectric thermoregulator was used to maintain the temperature constant to ±0.5°. The emf of the cell was measured with an accuracy of ±1.0 mv. A PPTV potentiometer and an M-21 mirror galvanometer were used for the emf measurements. Apart from the alteration noted above, the procedure in the experiments with potassium alloys was the same as with sodium alloys [3].

RESULTS AND DISCUSSION

The system potassium–mercury. The emf of the cell K | glass | K + Hg was measured at 200°.* All the alloys were liquid at this temperature. The results of the emf measurements, and the calculated values of activity and partial molar excess free energy of potassium are given below:

N_K	E (mv)	a_K	$\Delta\overline{F}^E_K$
0.761	9.4	0.821	80
0.746	10.6	0.801	80
0.614	19.3	0.667	90
0.521	36	0.470	—115
0.467	59	0.290	—524
0.423	95	0.135	—1250
0.364	168	0.029	—2760
0.358	173	0.027	—2850
0.342	192	0.018	—3240
0.318	239	0.008	—4110
0.308	243	0.006	—4305
0.281	296	0.002	—5440
0.163	542	$1.2 \cdot 10^{-5}$	—10500
0.094	723	$2.6 \cdot 10^{-7}$	—14080

Figure 1 gives the activity isotherms, from our data for 280° and from the data of Vierk and Hauffe for 325°. The corresponding curves for the partial molar excess free energy are given in Fig. 2.

For alloys with less than 50 atomic % of potassium our data are in satisfactory agreement with the data of Vierk and Hauffe. In the potassium-rich region we found small positive deviations from Raoult's law. Roeder and Morawietz [6] who studied the vapor phase over potassium amalgams by different methods, also noted the existence of a region of positive deviations from Raoult's law at 200-275°. According to Roeder and Morawietz, at 300-350° there are only negative deviations from Raoult's law. Pedder and Barrat [7], who determined the activity of potassium by the vapor-pressure method, also reported positive deviations in the potassium-rich region. It must be noted that the positive–negative character of the deviations of the isotherm of potassium activity in the system potassium–mercury, where, according to the phase diagram, the congruently melting compound KHg_2 is the most stable, is in harmony with the general theory developed by Alabyshev and Lantratov [8], according to which there is a connection between the form of the activity isotherm and the composition of the compounds formed in the system. It follows from Fig. 3 that the curve for the integral excess free energy has a sharp maximum at a composition corresponding to the compound KHg_2. This shows that the results of our investigation

* At higher temperature the vapor pressure of mercury over the low-potassium alloys increased appreciably; this could alter the composition of the alloy.

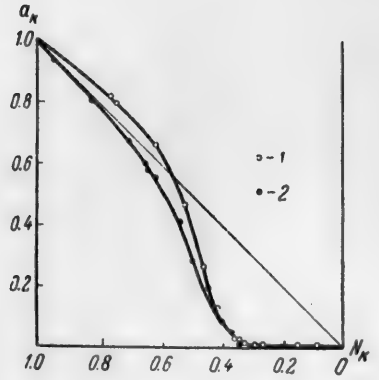

Fig. 1. Activity of potassium in alloys with mercury.
1) The author's data (280°), 2) data of Vierk and Hauffe (325°) [4].

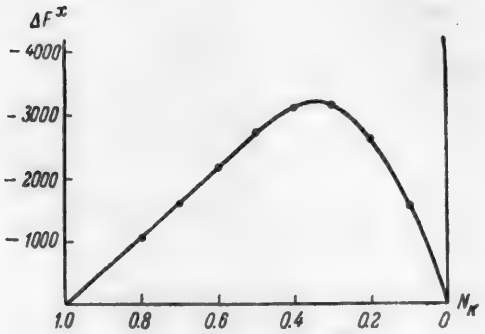

Fig. 3. Integral excess free energy in the system potassium–mercury.

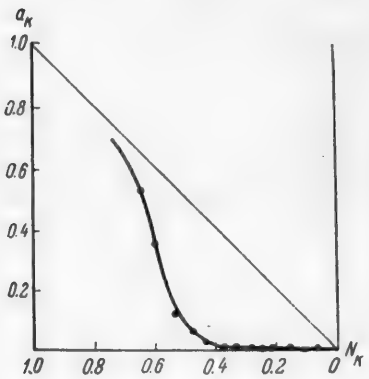

Fig. 4. Activity of potassium in alloys with lead.

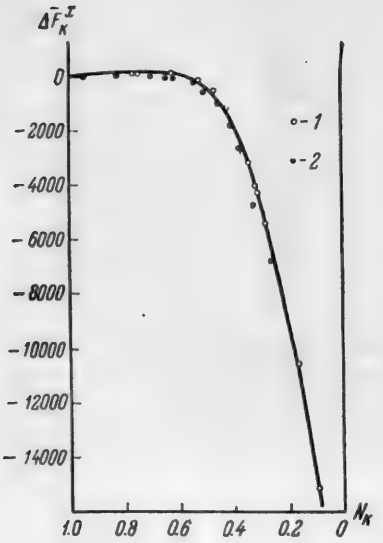

Fig. 2. Excess partial molar free energy of potassium in alloys with mercury.
1) The author's data, 2) data by Vierk and Hauffe [4].

are in full agreement with the phase diagram for the system. The conductivity isotherms of liquid alloys also have maxima corresponding to the compound KHg_2 [9]; the maxima on the viscosity isotherms of liquid potassium–mercury alloys also lie near this composition [10].

The system potassium–lead. The phase diagram for the system potassium–lead has been studied quite inadequately owing to great experimental difficulties, partly caused by the relatively high melting points of the compounds formed. According to Smith [11], the system has a region of phase separation in the liquid state in the range of about 36 to 74 atomic % of potassium. Jänecke [12] considers that a compound of high melting point, probably K_2Pb, is formed in the system. Other compounds– KPb_4, KPb_2 and possibly KPb, melt incongruently. According to Jänecke, the existence of a region of phase separation in the liquid state is very doubtful.

The emf measurements were performed at 575°. At this temperature all the alloys studied were liquid. The results of the emf measurements and the calculated activities and partial molar free energies of potassium are given below:

N_K	E (in mv)	a_K	$\bar{\Delta F}^E_K$
0.643	46	0.533	— 320
0.597	75	0.358	— 860
0.529	151	0.127	—2410
0.477	196	0.068	—3280
0.429	259	0.029	—4560
0.372	296	0.017	—5150
0.329	332	0.011	—5800
0.282	349	0.008	—5910
0.262	408	0.004	—7190
0.220	434	0.003	—7450
0.155	478	0.001	—7880
0.058	608	0.0003	—9200

The activity isotherm for potassium at 575° is given in Fig. 4. The curve for the partial molar excess free energy of potassium is given in Fig. 5. The above experimental data and the curves in Figs. 4 and 5 show that there is no discontinuity of solubility in the system (at least at 575°). If there was such discontinuity, the activity of potassium and therefore the emf of the cell would remain constant over the whole region of phase separation.

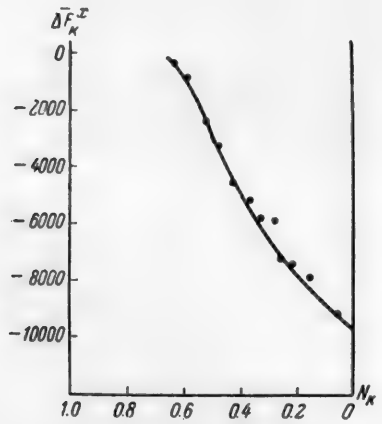

Fig. 5. Excess partial molar free energy of potassium in alloys with lead.

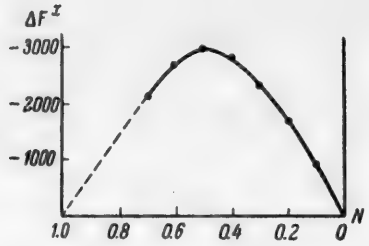

Fig. 6. Integral excess free energy of the system potassium−lead.

The curve for the integral excess free energy is given in Fig. 6. The form of this curve suggests that the compound KPb has the highest melting point in the system potassium−lead. It should be mentioned that the possibility of separation of crystals corresponding to the compound KPb from melts has been reported [13].

In conclusion, I offer my gratitude to Prof. A. F. Alabyshev for his guidance in the work.

SUMMARY

The activity of potassium in alloys with mercury at 280° and in alloys with lead at 575° has been determined. The activity was calculated from results of emf measurements of concentration cells of the amalgam type with glass as the electrolyte. In contradiction to published data, no region of phase separation in the liquid state in the system potassium−lead was found.

LITERATURE CITED

[1] K. Hauffe, Z. Elektroch. 46, 348 (1940).

[2] K. Hauffe, A. L. Vierk, Z. Elektroch. 53, 151 (1949).

[3] A. F. Alabyshev and A. G. Morachevskii, Proc. Acad. Sci. USSR 111, 369 (1956).*

[4] A. L. Vierk, K. Hauffe, Z. Elektroch. 54, 383 (1950).

[5] A. F. Alabyshev and E. M. Gel'man, Nonferrous Metals 2, 37 (1946).**

* Original Russian pagination. See C. B. Translation.
** In Russian.

[6] A. Roeder, W. Morawietz, Z. Elektroch. 60, 431 (1956).

[7] I. Pedder, S. Barrat, J. Chem. Soc. (London), 537 (1933).

[8] A. F. Alabyshev and M. F. Lantratov, J. Appl. Chem. 27, 851 (1954).*

[9] K. Bornemann, P. Müller, Metallurgie, 7, 396 (1910).

[10] I. Degenkolbe, F. Sauerwald, Z. allg. anorg. Ch. 270, 314 (1952).

[11] D. P. Smith, Z. allg. anorg. Ch. 56, 133 (1907).

[12] E. Jänecke, Kurzgefasstes Handbuch aller Legierungen, Heidelberg (1949).

[13] S. C. Pyk, U. S. Patent 2561636 (1951); Ch. A., 47, 8629a (1953); Official Gazette, 648, 1121 (1951).

Received October 13, 1956

* Original Russian pagination. See C. B. Translation.

RELATIONSHIP BETWEEN THE TEMPERATURE AND THE VAPOR PRESSURE OF 20% HYDROCHLORIC ACID

Z. I. Simkhovich*

Kharkov Branch of the All-Union Scientific Research and Design Institute of Chemical Equipment Construction

The data available in reference books and other special literature [1-5] on the temperature–vapor pressure relationships of hydrochloric acid refer to pressures up to 1200 mm Hg.

However, in some branches of industry, such as industrial organic synthesis, reactions are effected in hydrochloric acid media under pressures up to 30 atmospheres. The determination of new data for these relationships at pressures above 1200 mm Hg is therefore of practical importance.

This paper contains experimental data for the vapor pressure–temperature relationships of 20% hydrochloric acid in the pressure range from ~1.5 to ~31 kg/cm^2.

These data were obtained in tests of the acid resistance of experimental enameled autoclaves 5 liters in capacity, intended for organic syntheses in hydrochloric and acetic acid media under pressures up to 30 kg/cm^2 and temperatures up to 250°.

A schematic vertical section of the autoclave used in the tests is shown in Fig. 1. The packing material used was paronit thoroughly rubbed with graphite on both sides. Without graphite, the paronit adhered so firmly to the enamel coating that it split or tore the enamel off the edge of the cover surface on opening. Before the autoclave was filled with acid, the joints were tested by means of carbon dioxide under 40 kg/cm^2 pressure. The autoclave was then charged with 4 liters of chemically pure 20% hydrochloric acid and the inlet was hermetically closed.

Hydrochloric acid of this concentration is generally the most corrosive to enamel [6]. Moreover, 20% hydrochloric acid (more precisely, 20.22-20.3%) at 760 mm Hg is an azeotropic system, making it easier to maintain constant conditions in the corrosion tests. For these two reasons 20% hydrochloric acid is used for tests on enamel and enamel coatings under atmospheric pressure. With increased pressure at least the second factor, if not both, loses it significance. However, 20% hydrochloric acid was used in our tests so that the results of the autoclave tests could be compared with the results of determinations of the acid resistance of enamel coatings under normal pressure.

The acid was heated by means of an electric heater and an oil bath filled with special cylinder oil used in steam engines. The thermometer case was filled with the same oil. The protective tube of the manometer was filled with machine oil, as the high viscosity of the cylinder oil resulted in retardation of the manometer readings.

In the autoclave tests two series of measurements were made; the results are given in Table 1.

The experimental results (Columns 4 and 5 of Table 1) are plotted in Fig. 2 in log P –1/T coordinates, where T is the temperature of the acid (in °K).

It is seen that the points in the upper part of Fig. 2, corresponding to data of Table 1, lie on a curve. However, this curve can be approximately represented by two interesting linear portions (in the region log P > 3.4).

* A. A. Mozhaeva, N. A. Semenova, V. T. Chernova and N. Korobkov took part in the experimental work.

TABLE 1

Temperature and Vapor Pressure of 20% HCl

Manometer readings (in kg/cm²) P_M	Temperature (°C) series I	series II	assumed value t	Absolute vapor pressure (in mm Hg)*	Manometer readings (in kg/cm²) P_M	Temperature (°C) series I	series II	assumed value t	Absolute vapor pressure (in mm Hg)*
2	130	127	128.5	1130	16	180	185	182.5	11270
3	140	—	140.0	1828	18	184	189	186.5	12730
4	146	141	143.5	2554	20	189	194	191.5	14190
5	150	—	150.0	3271	22	193	198	195.5	15640
6	156	152	154.0	3996	24	196	201	198.5	17100
8	160	162	161.0	5446	26	200	204	202.0	18570
10	164	167	165.5	6905	28	203	207	205.0	20030
12	170	174	172.0	8358	30	206	208	207.0	21490
14	174	178	176.0	9817	32	209	—	209.0	22960

* $P = 735 (P_m + 1 - P_{air})$, where $P_{air} = 1 + \frac{t}{273.2}$

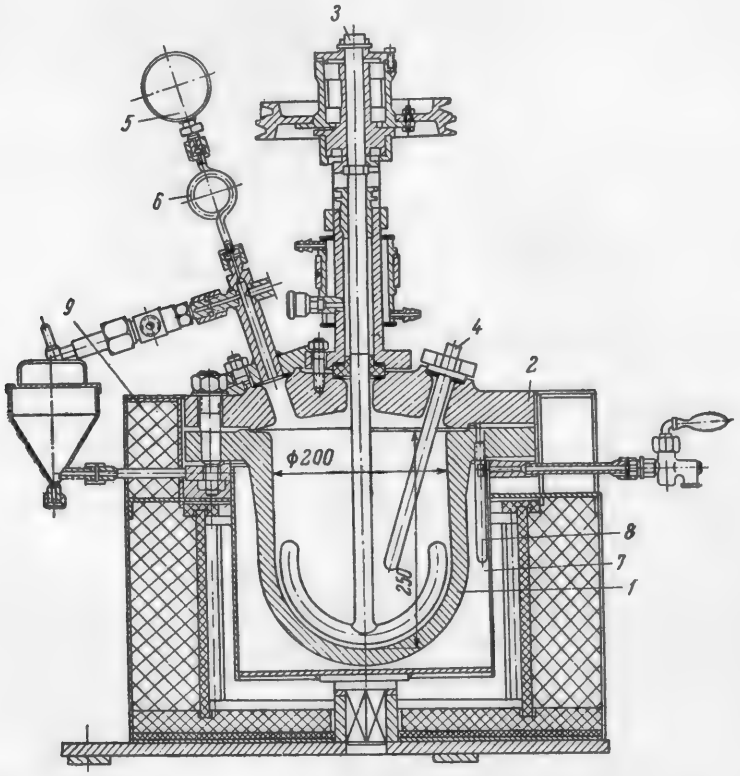

Fig. 1. Schematic vertical section of autoclave.
1) Body, 2) lid, 3) stirrer, 4) thermometer case, 5) manometer, 6) protective tube, 7) oil jacket, 8) thermometer case, 9) electric heater.

The linear portion in the region log P < 2.8 is drawn through points corresponding to published data [3] for the pressure range 2.65-559 mm Hg.

It follows from Fig. 2 that the vapor pressure–temperature relationship for 20% hydrochloric acid in the 2-23,000 mm Hg range (i.e., ~0-31 kg/cm²) may, in the first approximation, be represented by the known [2, 3, 8, 9] empirical formula:

TABLE 2

Values of the Constants A and B for Different Regions

Region No.	Pressure region (in kg/cm²)	Temperature region (°C)	Value of constant A at pressure expressed in		Value of constant B	Deviation limits of calc. from exptl. pressures (%)	Root mean square deviation (%)
			mm Hg	kg/cm²			
1	< 3.5	< 143	9.0900	6.2237	2366	0.0—1.5	0.6
2	3.5—9.5	143—165	12.2923	9.4260	3699	4.8—8.9	7.3
3	9.5—31	165—210	9.4992	6.6329	2484	0.0—3.0	1.3

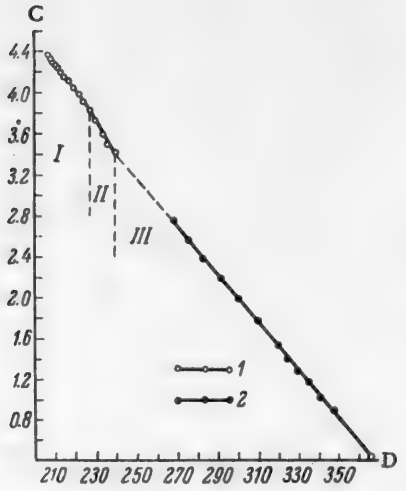

Fig. 2. Temperature—vapor pressure relationship for 20% hydrochloric acid.

C) Log P (P in mm Hg), D) $\frac{1}{T} \cdot 10^3$.

Data: 1) experimental, 2) literature [3]. I) A = 9.4992, B = 2484; II) A = 12.2923, B = 3699; III) A = 9.0900, B = 2366.

$$\log P = A - \frac{B}{T}. \qquad (I)$$

Each pressure region and the corresponding temperature range represented by the linear sections in Fig. 2, has, of course, its own values for the constants A and B.

Table 2 gives these values for all three regions, calculated by the method of least squares [10], and also the deviations of the calculated from the experimentally determined pressures.

The relationship between the values of A for different units of pressure is given by the expression:

$$P = 735\ p, \qquad (II)$$

where P is the pressure (in mm Hg), and p the same pressure in kg/cm².

Hence

$$\log p = A - \log 735 - \frac{B}{T} = A_p - \frac{B}{T} \qquad (III)$$

and

$$A_p = A_P - \log 735 = A_P - 2.8663. \qquad (IV)$$

Table 2 shows good agreement between the calculated and experimental values for the literature data (Region No. 1) and for some of the experimental data (Region No. 3); the respective constants in Equation (I) are also similar for these regions. The agreement between the calculated and experimental data for Region No. 2 is less satisfactory. It is possible that with more accurate measurements in Regions Nos. 2 and 3 the temperature—vapor pressure relationship for 20% hydrochloric acid could be represented by Equation (I) with constant values of A and B over the whole pressure range from 2 to 23,000 mm Hg.

Vapor pressures of 20% hydrochloric acid at temperatures above 100°, calculated by means of Equation (I) with the three values of the constants given in Table 2 are given below.

	Vapor pressure of 20% hydrochloric acid										
Temperature (°C)	110	120	130	140	150	160	170	180	190	200	210
Pressure (kg/cm²)	1.1	1.6	2.3	3.2	4.8	7.7	10.7	14.2	18.7	24.2	31.0

LITERATURE CITED

[1] Landolt-Börnstein, Physikalisch-chemische Tabellen, 2, 2, Berlin, 1345-1346 (1931).

[2] Technical Encyclopedia, Handbook of Physical, Chemical and Technological Data, V, 465-466 (Moscow, 1930).*

[3] Chemist's Reference Book, III, 239, 241-242, 279 (State Chem. Press, 1952).*

[4] Iu. V. Kariakin, Pure Chemical Reagents, 281 (Moscow-Leningrad, 1947).*

[5] M. S. Vrevsky, Papers on the Theory of Solutions, 175-176 (Moscow-Leningrad, 1953).*

[6] A. M. Trakhtenberg, Chem. Machinery Constr. 7 (1940).

[7] L. H. Horsley, Analytical Chemistry, 19, 8, 508-600 (1947).

[8] M. Kh. Karapetiants, Chemical Thermodynamics, 174-177 (Moscow-Leningrad, 1949).*

[9] B. F. Dodge, Chemical Engineering Thermodynamics (Russian translation) 302-306 (Moscow, 1950).

[10] G. M. Fikhtengolts, Mathematics for Engineers, 2 (Moscow, 1937).*

Received July 11, 1956

* In Russian.

MAGNITUDE OF THE LOSSES OF BASKUNCHAK COMMON SALT WHEN STORED IN HEAPS

E. I. Akhumov

As is known, enormous amounts of common salt are stored in the open in heaps (in the form of truncated rectangular pyramids) on specially prepared platforms (covered with concrete, asphalt, or wood), the platforms being sloping and surrounded by drainage trenches.

The question of the most probable natural loss standards for Baskunchak salt stored in heaps is discussed in this paper.

Salt stored in heaps undergoes a number of physicochemical processes induced both by the action of various meterological factors such as atmospheric precipitation, air humidity, wind, temperature variations, etc., and a number of other causes: the kind of salt and its form of granulation, height of the heap, etc.

It must be pointed out that meterological factors vary both daily and over longer intervals, and therefore their influence on a soluble substance such as common salt is very complex.

The combined action of all these factors leads to a caking of the salt [1]. The caked salt, especially after prolonged storage in heaps, turns into a monolithic mass which is so strong that the heap can only be broken up with the aid of explosives.

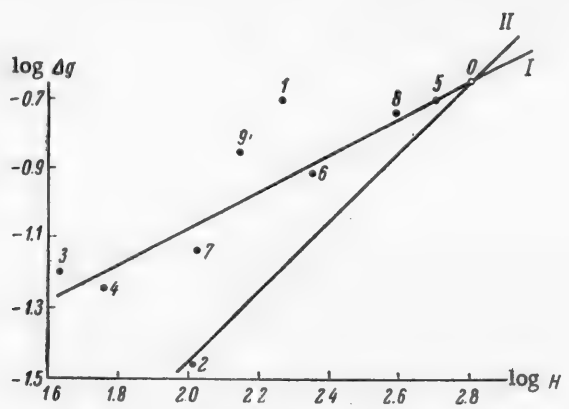

Loss Δg (in tons/m^2) of Baskunchak salt in heaps, as a function of the atmospheric precipitation H (in mm).
I) Experimental heaps, II) theoretical loss by solution.

The bulk density of caked salt depends on its kind, granulation, height of the heap, and especially the storage time. Thus, the bulk density of Baskunchak salt varies between 1.1 and 1.4 tons/m^3, the actual density being 2.15 tons/m^3 [2]. It follows that the volume of the spaces in the heap varies between 35.1 to 48.8% of the whole heap.

It might seem that this porous structure of the salt should favor disintegration of the heap under theaction of atmospheric precipitation, with rapid solution of the salt, as the conditions for the percolation of the solution

TABLE 1

Data on the Storage of Baskunchak Salt in Experimental Heaps [3]

Site of heap	Dates: heap laid	Dates: heap broken up	Storage time t (months)	Wt. of dry salt in heap (tons): when laid G_1	Wt. of dry salt in heap (tons): when broken up G_2	Wt. of dry salt in heap (tons): loss during storage per period G_1-G_2	Area of heap base S (in m^2)	Weight of dry salt in heap: $\frac{G_1}{S}=g_1$	Weight of dry salt in heap: $\frac{G_2}{S}=g_2$	Weight of dry salt in heap: $\frac{G_1-G_2}{S}=\Delta g$	Precipitation H (in mm) during storage period	log H	$-\log \Delta g$
Baskunchak	12-9-38	12-9-39	12	204.4	181.4	23.0	117.0	1.747	1.550	0.197	182.5	2.2613	0.7055
	6-4-39	12-17-39	6.4	159.1	155.6	3.5	100.3	1.586	1.551	0.035	102.7	2.0115	1.4559
	12-17-39	4-15-40	4	155.6	149.3	6.3	100.0	1.556	1.493	0.063	42.8	1.6314	1.2007
Aral'sk	11-5-47	6-15-48	7.3	134.2	128.8	5.4	96.0	1.398	1.342	0.056	57.2	1.7574	1.2518
Leningrad	11-25-38	11-23-39	12	225.5	197.8	27.7	140.0	1.611	1.413	0.198	495.1	2.6947	0.7033
	12-12-47	6-12-48	6	178.0	164.8	13.2	108.0	1.648	1.526	0.122	221.9	2.3461	0.9136
	10-8-38	1-27-39	3.5	232.8	222.6	10.2	140.0	1.663	1.590	0.073	104.9	2.0207	1.1367
Iaroslavl'	7-23-48	5-20-49	10	160.5	142.9	17.6	96.0	1.672	1.489	0.183	383.5	2.5838	0.7375
	11-16-48	5-14-49	6	154.3	140.2	14.1	100.8	1.531	1.391	0.140	137.9	2.1396	0.8539

TABLE 2

Losses of Baskunchak Salt Stored in Heaps, Calculated from Equation (11) (as % of the initial amounts of dry salt)

Precipitation H (in mm)	Salt losses at heap packing density (in tons/m^2): 1	2	3	4	5	6	7	8	9	10
100	8.49	4.24	2.83	2.12	1.70	1.41	1.21	1.06	0.94	0.85
200	12.22	6.11	4.07	3.05	2.44	2.04	1.75	1.53	1.36	1.22
300	15.14	7.57	5.05	3.78	3.03	2.52	2.16	1.89	1.68	1.51
400	17.62	8.81	5.87	4.40	3.52	2.94	2.52	2.02	1.96	1.76
500	19.82	9.91	6.61	4.95	3.96	3.30	2.83	2.48	2.20	1.98
600	21.78	10.89	7.26	5.44	4.36	3.63	3.11	2.72	2.42	2.18
700	23.60	11.80	7.87	5.90	4.72	3.93	3.37	2.95	2.62	2.36
800	25.35	12.67	8.45	6.34	5.07	4.22	3.62	3.17	2.82	2.53
900	26.98	13.49	8.99	6.74	5.40	4.50	3.85	3.37	3.00	2.70
1000	28.51	14.25	9.50	7.13	5.70	4.75	4.07	3.56	3.17	2.85

through the heap appear to be entirely favorable, However, this is far from being the case. The author inspected, in 1949, heaps of salt which had stood at least 30 years on the shore of lake Bol'shoi Kalkaman, and were in good condition.

The reason for this stability of salt heaps is that in course of time a dense layer is formed on the surface of the heap, with a higher content of insoluble substances than in the salt within the deep zones of the heap. This layer contains, both the impurities in the salt (insoluble residues, calcium sulfate, etc.) and various solid particles carried by the wind (sand, dust, etc).

This layer greatly decreases erosion of the heap and therefore decreases considerably the losses of salt during storage in the heap.

These and other considerations lead to the conclusion that the specific loss Δg of salt stored in a heap, determined by a number of factors A, B, C, ...

$$\Delta g = f(A, B, C, \dots) \tag{1}$$

can, in the first approximation, be represented by a power function of the type

$$\Delta g = K \cdot A^a \cdot B^b \cdot C^c \dots, \tag{2}$$

where a, b, c, ... are constants, and K is a coefficient.

For a period of a year, Equation (2) is written:

$$\Delta g_1 = K \cdot A_1^a \cdot B_1^b \cdot C_1^c \dots \tag{3}$$

Then from Equations (2) and (3) we have:

$$\frac{\Delta g}{\Delta g_1} = \left(\frac{A}{A_1}\right)^a \cdot \left(\frac{B}{B_1}\right)^b \cdot \left(\frac{C}{C_1}\right)^c \dots \tag{4}$$

or

$$\Delta g_0 = A_0^a \cdot B_0^b \cdot C_0^c \dots \tag{5}$$

Equation (5), written in dimensionless or critical form, reflects the annual periodicity of the processes in common salt stored in heaps in the open.

With this approach it is possible to apply the theory of similitude to study the losses of common salt in heaps, with theoretically based experiments on models and in laboratory conditions.

Let us consider the case when only the most important factor is taken into account, namely the atmospheric precipitation H during the storage period, which mainly determines the loss of salt from the heap. Equation (4) then assumes the form:

$$\frac{\Delta g}{\Delta g_1} = \left(\frac{H}{H_1}\right)^a \tag{6}$$

or, after transformation:

$$\log \Delta g = \alpha + \beta \log H, \tag{7}$$

where α and β are constants.

To determine the natural losses of salt stored in heaps in different salt undertakings and storage bases of the USSR, several experimental heaps of the same type were laid in 1938-1948 in regions differing in average annual precipitation: Aral'sk (50 mm), Baskunchak (150 mm), Leningrad (567 mm), Iaroslavl' (600 mm). Although the heaps were not large (130-230 tons) and the storage periods short (3.5-12 months), the results [3] are of great practical interest.

These data (given in Table 1) were used to plot points corresponding to the experimental heaps in log H – –log Δg coordinates (see Figure). The graph shows that Equation (7) is generally applicable (Line I). Points 1 and 2, the reliability of which, according to the tabulated data (Table 1) is dubious, do not fit on this straight line.

The equation for the most probable Line I (see Figure) with the numerical values of α and β found by the usual method, is:

$$\log \Delta g = -2.123 + 0.526 \log H, \quad (8)$$

where H is in mm and Δg in tons/m^2.

If the loss of salt from the heap was caused only by solution in atmospheric precipitates and complete drainage of the saturated solution from the heap, the following relationship should hold in theory:

$$\log \Delta g = -3.446 + \log H, \quad (9)$$

derived on the assumption that the solubility of sodium chloride in water is almost constant in the 0-25° range, and is 358 g/1000 g H_2O.

Line II (see Figure), which is a plot of Equation (9), shows that for H < 618 mm (the coordinates of the Point 0 are found by simultaneous solution of Equations (8) and (9) the actual losses are greater than losses by solution, while for H > 618 mm they are less. This shows that about 600 mm must be precipitated on the heap before a dense surface layer capable of weakening considerably the influence of meterological factors in the heap is formed on it.

Therefore Equation (9) is unsuitable for practical calculations of salt losses in heaps, as it gives erroneous results: too low for small precipitations and too high for large.

From the practical standpoint, the relative loss of salt x (in %) during storage in a heap is of most interest:

$$x = 100 \frac{\Delta g}{g}, \quad (10)$$

where g is the packing density of the heap, i.e., the quantity of salt per unit area of the heap base.

Equations (9) and (10) give the empirical expression:

$$x = 10^{-0.121} \cdot H^{0.526} \cdot g^{-1}, \quad (11)$$

which represents the most probable relative losses of Baskunchak salt stored in heaps. Equation (11) was used to compile a table of the relative losses of Baskunchak salt in heaps in relation to the atmospheric precipitation during storage and of the packing density of the heap (Table 2).

The data in Table 2, based on actual results for experimental heaps, may be used for calculations of the losses of Baskunchak salt when stored in heaps.

A detailed examination of the general state of the problem, and especially of the USSR standards for losses of salt in heaps, adopted in industry and in commerce respectively (these differ considerably), indicates that the problem has not been adequately studied, and that it is necessary to carry out reliable experimental studies both on experimental heaps, with exact consideration of the meterological conditions, and on models of heaps under laboratory conditions, with extensive use of the theory of similitude.

LITERATURE CITED

[1] N. E. Pestov, Physicochemical Properties of Granular and Powdered Chemical Products (Izd. AN SSSR, 1947).*

[2] E. S. Telentiuk, Bull. Central Scientific Research Salt Laboratory, Leningrad 9, 78 (1939).

[3] B. F. Vinunov, Trans. VSNII, Food Industry Press, 1 (9), 72 (1954).

Received May 28, 1956

* In Russian.

EFFECT OF BIVALENT MANGANESE ON THE ELECTRODEPOSITION OF ZINC

Iu. B. Kletenik

The V. M. Molotov State University, Rostov

In the nature and degree of its influence on the electrodeposition of zinc from sulfate electrolytes, manganese occupies an intermediate position between metal cations more active and less active than zinc. The question of this influence has been under consideration for a relatively long time, mainly in relation to the influence of quadrivalent and septivalent manganese [1-2].

In the literature available to us we found only one paper on the influence of bivalent manganese [3]. However, even in that investigation the manganese was introduced into an electrolyte which was not divided into anode and cathode compartments by a diaphragm. The bivalent manganese was oxidized at a lead anode, and in fact the influence of its highly oxidized forms was investigated, the influence of the bivalent ions, known to be small, being masked. The question of the influence of the latter is of definite interest, especially in relation to the possible adoption of the diaphragm process for the industrial electrodeposition of zinc.

The present paper deals with a study of the influence of bivalent manganese on the deposition of zinc from neutral and acid solutions. Since the question of the deposition of zinc from an acid solution is related to the hydrogen overvoltage andthe dissolution of zinc, the effects of manganese on these were also studied.

All the experiments were performed at 25 ± 0.2° (the dissolution of zinc, at 22-23°). A sulfate electrode was used as the reference electrode. The potential difference was measured by the compensation method with the PPTV-1 potentiometer. The electrolyte was stirred mechanically in all the determinations of the polarization curves. Manganese was introduced into the electrolyte in the form of manganese sulfate which also contained all the components of the electrolyte. The anode was a platinum plate. The anode and cathode spaces were separated by a glass diaphragm. After the addition of manganese the anolyte became pink while the cathode compartment remained colorless.

All the reagents were of chemically pure grade, and the electrodes were cast from spectroscopically pure zinc.

The first series of experiments was carried out at current densities between 10^{-5} and 10^{-2} amp./cm^2, when chemical polarization is not yet masked by concentration polarization.

The first experiments were with solutions containing 110 and 35 g of zinc per liter. It was found that addition of manganese (15 g of anhydrous manganese sulfate per liter) to a solution containing 110 g of zinc per liter causes a small decrease of potential on closed circuit (2-3 mv). Addition of the same amount of manganese to a solution containing 35 g of zinc per liter produces the opposite effect: the potential increases somewhat on closed circuit, but the electrode potential on open circuit also increases. Evidently the effect of dehydration of the zinc ions predominates in the first solution, and the influence of manganese on the ionic strength of the solution predominates in the second. Additions of manganese have no effect on the quality of the electrolytic deposit of zinc.

For investigation of the influence of bivalent manganese ions on the hydrogen overvoltage on zinc, zinc electrodes were used; these were mechanically cleaned, etched, and coated with a layer of electrolytic zinc in an acidified solution of zinc sulfate at current density $2 \cdot 10^{-3}$ amp./cm^2.

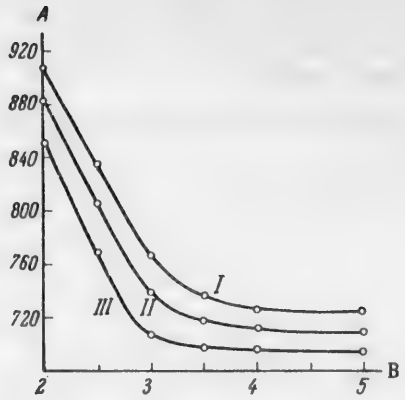

Fig. 1. Hydrogen overvoltage on zinc.
A) Overvoltage (in mv), B) $-\log D$ (D in amp./cm^2).
Solutions: I) 0.1 N H_2SO_4, II) 0.1 N H_2SO_4 + + 3 g $MnSO_4$ per liter, III) 0.1 N H_2SO_4 + + 15 g $MnSO_4$ per liter.

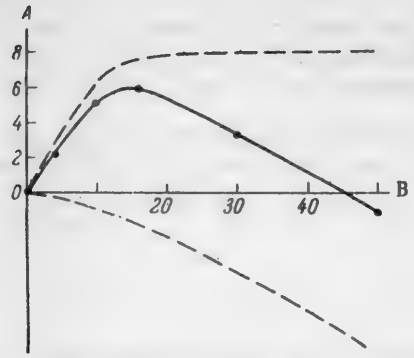

Fig. 2. Rate of solution of zinc in a solution of 0.1 N H_2SO_4 + $MnSO_4$.
A) Change of solution rate ΔV (%), B) $MnSO_4$ concentration (g/liter).
The curves are explained in the text.

The polarization curve, for electrodes prepared by this method, in 0.1 N H_2SO_4 is given in Fig. 1 (Curve 1). The curves obtained after addition of 3 and 15 g of manganese sulfate per liter are shown in the same diagram. Further additions of manganese do not produce any appreciable change of potential.

The depolarizing action of manganese can be attributed to its catalytic action as an electron carrier.

The influence of bivalent manganese ions on the rate of solution of zinc in acid was studied with specimens of cast zinc in 0.1 N H_2SO_4. The solution rate was found from the amounts of hydrogen liberated. The reproducibility of the results obtained for specimens of equal dimensions after the same preliminary treatment was inadequate for the detection of relatively small changes in the rate of solution. Therefore the zinc specimens were kept for five minutes in 0.1 N H_2SO_4, washed quickly, and immersed in 0.1 N H_2SO_4 with added manganese for 5 minutes. The validity of this method is proved, first by the fact that there is no question of oxide passivation of zinc in an acid medium, or of differences of such passivation inthese two solutions, and second, by the fact that when the specimen was returned to the first solution its rate of solution was the same as before. The results of these experiments are plotted in Fig. 2 (continuous curve). Each point was determined three times (for three different specimens) and the average values were taken.

It is interesting to note that the limiting concentration of added manganese, beyond which further additions have a negligible effect on the hydrogen overvoltage, is close to the manganese concentration corresponding to the maximum on the curve for the solution of zinc. It is possible that the influence of manganese reduces to its depolarizing action. The curve for the solution rate can be regarded as representing the net result of two influences of manganese – its specific influence (upper broken curve tentatively plotted from data on the depolarizing action of manganese), and its influence on the ionic strength of thesolution, lowering the activity of sulfuric acid (lower broken curve, found from the difference between the first two curves). It has also been suggested that manganese and zinc form an electrolytic alloy which gives rise to microcouples with regions of pure zinc, so that the rate of solution of zinc increases. However, attempts to detect manganese in electrodeposited layers of zinc obtained at very different current densities and concentrations of manganese in the electrolyte were unsuccessful, although a qualitative test for manganese (with $NaBiO_3$) indicated the presence of several micrograms of Mn per 1 cm^2 of the deposited layer.

Addition of 15 g of manganese sulfate to solutions containing zinc sulfate and 0.1 N H_2SO_4 does not produce any significant changes of potential and does not affect the character of the deposited layer.

Since manganese decreases the hydrogen overvoltage without any appreciable influence on deposition of zinc itself, it should have a more pronounced effect on the electrodeposition of zinc in very acid solutions, when considerable amounts of hydrogen are liberated together with zinc.

The current efficiency for zinc deposition was determined in electrolysis of a solution containing 60 g of zinc and 100 g of sulfuric acid per liter, under approximately "standard" conditions. At current density $5 \cdot 10^{-2}$ amp./cm^2 (500 amps./m^2) the current efficiency of hydrogen evolution was about 1.3%. Addition of 30 g of manganese sulfate per liter increased the current efficiency of hydrogen evolution by 20% of the original value, corresponding to a decrease of 0.26% in the current efficiency for zinc deposition.

The effect of manganese sulfate on the conductivity of "standard" electrolyte (60 g of zinc and 100 g of sulfuric acid per liter) was determined at 25°. The results are given below.

$MnSO_4$ (g/liter)	λ ($\Omega^{-1} \cdot cm^{-1}$)
0	0.4543
3	0.4483
9	0.4426
15	0.4302
25	0.4207
35	0.4075
50	0.3901

It is seen that increase of the concentration of manganese lowers the conductivity of the "standard" electrolyte.

SUMMARY

1. It is shown that in neutral solutions of zinc sulfate, bivalent manganese has a small effect on the potential of zinc deposition, differing in direction for solutions of different concentrations.

2. In 0.1 N H_2SO_4 solution, manganese has a depolarizing effect on the evolution of hydrogen on zinc, and increases the solution rate of zinc.

3. Manganese has no appreciable influence on the quality of electrodeposited zinc.

4. In the deposition of zinc from a "standard" electrolyte, bivalent manganese somewhat lowers the current efficiency.

5. Accumulation of considerable amounts of manganese sulfate in the electrolyte lowers its conductivity appreciably.

In conclusion, the author offers his gratitude to Assistant Professor O. A. Osipov for much help in the course of the work.

LITERATURE CITED

[1] A. I. Gaev and O. A. Esin, Electrolysis of Zinc (1937).*

[2] A. G. Pecherskaia and V. V. Stender, J. Appl. Chem. 23, 9, 920 (1950).**

[3] V. Iu. Zaidler, V. D. Ponomareva, and V. V. Stender, J. Appl. Chem. 17, 4-5, 282 (1944).

Received December 15, 1955

* In Russian.

** Original Russian pagination. See C. B. Translation.

THE OVERVOLTAGE OF HYDROGEN EVOLUTION

P. V. Sergeev

The concept of hydrogen overvoltage is one of the most important concepts in the theory and practice of the electrolytic production of metals from acid electrolytes. An extensive literature is devoted to explanations of this effect. However, this complex question is still not fully understood and is attracting the attention of numerous investigators.

In studies of hydrogen overvoltage an important part has been played by the Tafel equation, which was derived first experimentally and then theoretically [1, 2].

$$\eta_H = a + b \cdot \log D,$$

where D is the current density and a and b are constants.

The constant b in the Tafel equation is about 0.12 for all metals at room temperature, and increases by approximately 0.0004 for each degree rise in temperature. The value of a greatly depends on the nature of the cathode metal [2-5].

In this paper we present a relationship which can be used for very simple determinations of constants a and b in the Tafel equation. This relationship was confirmed experimentally.

In accordance with the established views [5], hydrogen evolution from acid in aqueous solutions at a hydrogen cathode with an insoluble anode begins when the voltage equal to the decomposition voltage of the electrolyte is reached at the electrodes of the cell. If the anode is made from an inert material such as lead, but the hydrogen cathode is replaced by zinc or some other material, the voltage at the cell electrodes corresponding to the start of evolution of hydrogen at the cathode increases considerably. The difference between the voltages of hydrogen evolution at the cathode in the two cases is numerically constant, i.e., it is a component of the hydrogen overvoltage for the given instance, independent of the current. Therefore the concept of hydrogen overvoltage itself can be used for finding the constant a in the Tafel equation from the expression

$$a = U_1 - U_{decomp.} \qquad (1)$$

where a is the constant in the Tafel equation, U_1 is the voltage at the cell electrodes at current density 1 amp./m^2, the anode being lead formed by prolonged electrolysis, or platinized platinum, and the cathode being the metal under investigation. At current density 1 amp./m^2 the second term in the Tafel equation is zero; $U_{decomp.}$ is the decomposition voltage of aqueous sulfuric acid.

The most likely explanation for the commencement of hydrogen evolution at a nonhydrogen cathode at voltages exceeding by the value a the decomposition potential of the acid is that a counter emf arises in the cathode region of the cell, numerically equal to a, owing to electrochemical interaction between the cathode material and the solution.

It is clear from Equation (1) that for determination of the constant a in the Tafel equation it is merely necessary to determine the voltage in this cell at current density 1 amp./m^2, the decomposition voltage of sulfuric acid being well known.

The possibility of determining the constant a by this method was verified experimentally for zinc, cadmium, cobalt, iron, aluminum, and copper cathodes.

The following values of a were found for these cathodes (Table 1).

TABLE 1

Values of the Constant a

Cathode material	Zn	Cd	Co	Fe	Al	Cu
Value of a (in v)	0.68	0.36	0.25	0.21	0.47	0.34

The experiments were performed with the use of a laboratory cell, at electrolyte temperature ~20°, H_2SO_4 concentration ~100 g/liter, and ~24 mm between the electrodes. Single-sided electrodes with equal effective surfaces were used. The anode was smooth lead formed by prolonged electrolysis; the cathodes consisted of the pure metals, thoroughly cleaned and polished until bright, as in the experiments of Pecherskaia and Stender [6]. The cell voltage was recorded only after it had reached a steady or maximum value. Electrical instruments of 0.5 class were used for the experiments, and the internal resistance of the voltmeter was over 100,000 ohms. The decomposition voltage of aqueous sulfuric acid solution was taken as 1.67 v [7] in the calculations.

It was observed during the experiments that, first, the cell voltages at current density 1 amp./m^2 for Zn, Cd, and Co cathodes almost exactly coincide with thedecomposition voltages of $ZnSO_4$, $CdSO_4$, and $CoSO_4$ – the salts formed in the electrolyte by solution of the anode – and second, that steady cell voltages in the case of aluminum and copper take a long time to become established.

To verify that the values in Table 1, determined experimentally from Equation (1), are in fact the constants a in the Tafel equation, Pecherskaia and Stender's experimental data on hydrogen overvoltage [6] were compared with data calculated from the Tafel equation in which the current density was taken in amp./m^2 and the values of a given in Table 1 were used. Stender's experimental data and the calculated values are compared in Table 2.

The good agreement between the experimental and calculated values confirms that Equation (1) is quite suitable for determination of the constant a in the Tafel equation for use in calculations of hydrogen overvoltage.

The observed small differences (not over 5%) between the experimental and calculated values are within the limits of experimental error and can to some extent be attributed to the fact, for example, that in calculations based on Equation (1) the tabular value of the decomposition voltage of sulfuric acid, 1.67 v was used rather than the decomposition voltage for the actual solution. However, the decomposition voltage of a real solution can be determined quite simply in a cell with inert electrodes, such as platinized platinum, at current density 1 amp./m^2. It follows from Equation (1) that the cell voltage will then be equal to the decomposition voltage, as the value of a in this case is zero.

Therefore Equation (1) is also of practical value, as it makes it possible to determine, by a very simple experiment, the value of the constant a in the Tafel equation, i.e., to find the hydrogen overvoltage at current density 1 amp./m^2, and also to find the decomposition voltages of solutions. An experiment similar to the determination of a can also be used for determination of the constant b in the Tafel equation; it is merely necessary to measure the voltage at the electrodes of the given cell at some current density other than 1 amp./m^2, if the oxygen overvoltage on a standard lead anode at this current density and the potential drop in the electrolyte are known. The constant b is easily found from these data.

This method for determination of the constants a and b in the Tafel equation is incomparably simpler than the method generally used, and it will therefore greatly reduce the expenditure of materials and time in studies of effects associated with hydrogen overvoltage.

In conclusion, we must draw attention to an inaccuracy which has crept into the practical application of the Tafel equation.

It is known that originally the Tafel equation was an empirical formula, but recently it has been shown that it can be derived on fairly strict theoretical grounds. Therefore, if the Tafel equation, considered as a theoretical

TABLE 2

Comparison of Experimental and Calculated Values for Hydrogen Overvoltage

Current density (in amps/m²)	Hydrogen overvoltage (in v) at cathodes made of											
	zinc		cadmium		cobalt		iron		aluminum		copper	
	exptl.	calc.*	exptl.	calc.*	exptl.	calc.*	exptl.	calc.*	exptl.	calc.*	exptl.	calc.*
1	—	0.68	—	0.36	—	0.25	—	0.21	—	0.47	—	0.34
10	0.83	0.85	0.51	0.57	0.32	0.35	0.36	0.33	0.58	0.56	0.48	0.47
100	1.01	1.02	0.71	0.78	0.42	0.45	0.47	0.45	0.67	0.65	0.60	0.6
1000	1.17	1.19	0.93	0.99	0.52	0.55	0.60	0.57	0.76	0.74	0.74	0.73

* The constant b in the calculations was based on Stender's data [6].

equation, is used, all the quantities in it must be expressed in the same system of units. However, this fundamental rule is not obeyed in the use of the Tafel equation. Current and voltage are measured in amperes and volts, i.e., units of the practical system, and the electrode areas are measured in cm^2, i.e., units of the absolute system, without the use of conversion factors between the two systems of units [1, 2, 3, 5]. It is easy to show that for a given experimental value of ηH the constant a in the equation is increased by 4 v owing to the incorrect use of the systems of units. With such use of the equation it is difficult to interpret the physical nature of the constant a. To eliminate this error, if the voltage and current are expressed in volts and amperes, the electrode areas must also be expressed in practical units, i.e., in m^2, and the current densities must be given in amps./m^2. Determination of the constant a in the Tafel equation at the very high current density 1 amp./cm^2 or 10,000 amps./m^2 makes it difficult to reveal the physical nature of this quantity and, in particular, explains why our values for this constant, given in Table 1, are lower than those given in the literature [3, 5]. Our values of a have a quite definite physical meaning, and represent the actual voltage which must be applied, above the decomposition voltage, to cause evolution of hydrogen in a given cell. The values of a determined at current density 10,000 amps./m^2 evidently have no physical meaning.

SUMMARY

1. Equation (1) can be used for determination of the constants a in the Tafel equation for hydrogen overvoltage on a very wide range of metals.

2. In the Tafel equation, the current density must be stated in amps./m^2 and not in amps./cm^2.

3. Equation (1) can be used for experimental determination of the constant a in the Tafel equation. A slightly modified experimental procedure can be used for determination of the constant b in the Tafel equation; hydrogen overvoltages can therefore be determined over a very wide range of current densities.

LITERATURE CITED

[1] N. A. Izgaryshev and S. V.. Gorbachev, Course of Theoretical Electrochemistry (Goskhimizdat, 1954).*

[2] A. I. Brodskii, Physical Chemistry, II (Goskhimizdat, 1946).*

[3] A. K. Lorents, J. Phys. Chem. 24, 7, 853 (1950).

[4] N. E. Khomutov, Proceedings of Conference on Electrochemistry (Izd. AN SSSR, 1953).

[5] A. N. Frumkin, V. S. Bagotskii, Z. A. Iofa, and B. N. Kabanov, Kinetics of Electrode Processes (Izd. MGU, 1952).*

[6] A. G. Pecherskaia and V. V. Stender, J. Phys. Chem. 24, 7 (1950).

[7] V. I. Perel'man, Chemist's Concise Handbood (GONTI, 1954).*

Received August 9, 1955

* In Russian.

EFFECT OF STIRRING OF THE ELECTROLYTE ON THE ELECTROLYTIC DEPOSITION OF POWDERED COPPER

A. V. Pomosov and V. A. Branshtein

Electrochemistry Laboratory, The S. M. Kirov Polytechnic Institute of the Urals

It is known that the transition from compact to loose deposits of copper occurs at the limiting current density. It is therefore reasonable to suppose that factors in electrolysis which favor a decrease of the limiting current density should not only favor the formation of disperse cathodic deposits, but should also have a dispersing action on the powderlike copper deposits formed. Conversely, conditions which favor an increase of the limiting current density should lead to the formation of coarsely disperse or compact deposits.

From the equation for concentration polarization, the limiting current can be expressed as

$$i_{lim} = \frac{zF\Delta}{(1 - n_{Cu^{\cdot\cdot}})\,\delta} C_0,$$

where Δ is the coefficient of diffusion, $(1 - n_{Cu^{\cdot\cdot}})$ is the sum of the transference numbers of all the ions except the copper ($Cu^{\cdot\cdot}$) ion in the diffusion layer.

It follows that the magnitude of the limiting current, and hence the structure of the particles of the disperse metal deposit, can be influenced by variations of the thickness of the diffusion layer (δ) in addition to variations of the concentration of the discharging ions (c_0), temperature (by its influence on Δ), and direct variations of the current density (i_c).

Indeed, as the intensity of stirring of the electrolyte increases, and as the thickness of the diffusion layer (δ) decreases correspondingly, the conditions in the cathode region will progressively favor the deposition of powders of low dispersity and high bulk density. The easier access of the discharging ions should lead to the formation of less dendritic (arborescent) particles in the powder.

Whereas the effects of the concentration of copper ions, cathodic current density, and temperature have been studied repeatedly [1-3], the effects of stirring of the electrolyte on the thickness of the diffusion layer (δ) have not been sufficiently studied. Nevertheless, it has been reported by Borok, Bal'shin, and Gavrilov [4] that stirring of the electrolyte has a strong influence on the bulk density and is a very important technological factor in the production of copper powder.

We therefore carried out a special investigation of the effects of stirring of the electrolyte on the electrodeposition of copper in powder form.

EXPERIMENTAL

Copper powder was obtained by electrolysis of acid solutions of copper sulfate, of the following composition (in g/liter): $CuSO_4 \cdot 5H_2O$ 80, H_2SO_4 120. The electrolyte was made with distilled water, twice-recrystallized first-quality copper sulfate, and sulfuric acid sp. gr. 1.83, analytical reagent grade. The cathode current density was 16 amps./dm^2, and the temperature of the electrolyte was 50 ± 1°. The cylindrical anodes were made from M-1 electrolytic copper. The cathode was a copper rod 11 mm in diameter. With electrodes of this shape the distribution of the current over the cathode was more uniform and therefore uniform deposits of copper powder

were obtained over the whole cathode surface. The electrolysis was performed in a cylindrical ebonite vessel 5 liters in capacity. The solution was stirred by means of a stirrer situated in the interelectrode space below the cathode. The stirrer speed was regulated by means of a rheostat, and the number of revolutions in unit time was measured with the aid of a transmission mechanism. The powder was removed manually from the cathode every 30 minutes, and the duration of each experiment was 4.5-5 hours.

The electrolyte composition was kept constant by circulation of the solution. The powder was washed free of electrolyte, stabilized with soda soap [1], and dried in a vacuum oven. The granulometric composition was determined by analysis on standard sieves during 10 minutes.

The powders were examined under the microscope at 100-fold magnification in order to study the influence of stirring of the solution on the structure of the particles in copper powder. To determine the dendrite ratio of the loose cathodic deposit, 5-6 counts of arborescent particles visible in the microscope field were made, and their ratio to the total number of visible particles was calculated.

RESULTS AND DISCUSSION

It follows from the data in the Table that stirring of the electrolyte has a pronounced influence on the granulometric composition and the bulk density of the powderlike deposit. The content of the coarse fraction (particles from 160 to 450 μ) increases considerably with increasing rate of stirring and reaches 43-46%, while the content of the fine fraction, with particles of 80 μ and smaller, decreases.

Granulometric Composition and Bulk Density of Copper Powder in Relation to the Stirring Speed

Stirrer speed (rpm)	% contents of fractions with particle size (in μ)				Bulk density (g/cc) of fractions with particle size (in μ)		
	160–450	112–160	80–112	< 80	160–450	80–112	80
300	9.7	12.2	35.6	40.5	Not found	1.19	1.03
600	21.6	16.2	27.4	41.5	2.28	1.54	1.18
900	23.3	18.8	31.5	24.5	2.63	1.79	1.26
1500	46.6	15.2	14.5	16.6	2.81	2.26	Not found
2200	43.0	18.9	20.6	14.8	3.0	Not found	

The bulk densities of all the fractions increase with increasing stirring speed.

Thus, stirring decreases the dispersity of the powder, the metal particles become more compact, and the powder becomes heavier. The experiments show that it is possible to obtain copper powder of a predetermined granulometric composition and bulk density by regulation of the stirring rate. The fluctuations of temperature and copper concentration in the electrolyte, highly probable in technological practice, and certain other factors, will have less influence on the dispersity of the cathodic deposit, as the electrolysis conditions are more stable than in cells without stirrers.

However, the dendrite ratio of the copper powder decreases with increasing speed of stirring of the electrolyte (Fig. 1). This effect is the consequence of easier access of the discharging ions to the cathode, which favors the formation of more compact particles. A decrease of the dendrite ratio of the copper powder is undesirable, as it leads to worse pressability of the powdered metal.

This probably accounts for the fact that electrolysis with stirring of the electrolyte solution is very rarely used for the production of quite homogeneous and standard disperse copper. However, this difficulty is easily avoided. To increase the dendrite ratio of the metal powder we utilized the known influence of chloride ions on the structure of the particles in loose copper deposits [3, 5]. Chloride ions were introduced in the form of hydrochloric acid, and the rate of stirring was 1500 rpm.

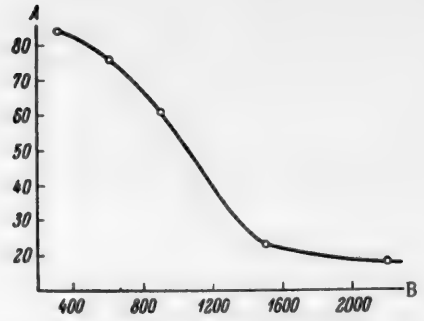

Fig. 1. Dendrite ratio as a function of the stirring rate.
A) Dendrite ratio (%), B) stirring rate (rpm).

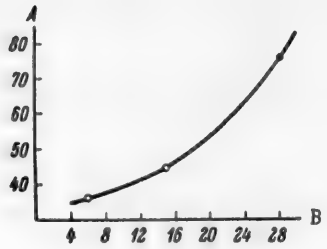

Fig. 2. Dendrite ratio as a function of the concentration of chloride ions.
A) Dendrite ratio (%), B) Cl' ion content (in mg/liter).

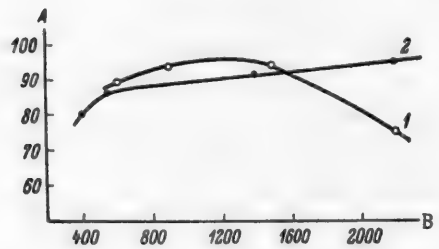

Fig. 3. Current efficiency (η) as a function of the stirring rate.
A) Current efficiency (%), B) stirring rate (rpm).
Electrolyte composition, g/liter of $CuSO_4 \cdot 5H_2O$ and H_2SO_4 respectively: 1) 80 and 120, 2) 40 and 120.

It is seen in Fig. 2 that in these conditions, with vigorous stirring, chloride ions had a pronounced influence on the structure of the deposit, favoring the formation of powders containing particles of a well-developed dendritic structure.

In addition to its influence on the structure of disperse cathodic deposits, stirring of the electrolyte during electrolysis has an appreciable effect on the current efficiency with respect to copper powder, and on the cell voltage. The current efficiency increases with stirring rate, reaching its maximum value of 93.5-94% at 1000-1500 rpm, and then falls to 75% at 2200 rpm (Fig. 3, Curve 1). The maximum on the current efficiency–stirring rate curve is due to partial deposition of compact metal at high stirrer speeds. If a more dilute solution is used for electrolysis (Fig. 3, Curve 2), when deposition of compact copper becomes impossible even at very vigorous stirring of the solution, the current efficiency increases steadily with stirrer speed. The explanation for this is that the proportion of discharging copper ions increases owing to their easier access to the cathode and to decreased concentration polarization in their discharge.

Naturally, the decrease of concentration polarization also led to a considerable fall of the voltage at the cell terminals, down to 0.7-0.8 v, from 1.2-1.3 v in absence of stirring.

SUMMARY

1. It was found that the dispersity and dendrite ratio of copper powder decrease, and the bulk density increases with increasing rate of stirring of the electrolyte.

2. It is shown that electrolytic copper powders of standard physical properties can be obtained by regulation of the rate of stirring of the solution.

3. It is shown that copper powder with a high dendrite ratio can be obtained in vigorously stirred electrolytes, by addition of chloride ions to the electrolytes.

LITERATURE CITED

[1] A. I. Levin and A. V. Pomosov, Trans. Urals Polytech. Inst. 43, 145-147 (Mashgiz, 1953).

[2] O. K. Kudra and E. B. Gitman, Electrolytic Production of Metal Powders (Acad. Sci. Ukrainian SSR Press, 1952) p. 65.*

[3] O. A. Esin and L. G. Levian, Trans. Urals Industrial Inst. 25, 28 (Metallurgy Press, 1947).

[4] B. A. Borok, M. Iu. Bal'shin and N. A. Gavrilov, Sci. Res. Inst. Machine Building 3, 27 (1935).

[5] A. V. Pomosov, Dissertation, The Urals Polytechnic Institute, Sverdlovsk (1952).

Received January 16, 1956

* In Russian.

THE POSSIBILITY OF USING COVERING LIQUIDS TO PREVENT VOLATILIZATION OF AMMONIA FROM AMMONIACAL ELECTROLYTES

M. L. Pertsovskii and V. K. Kamkin

The Kurgan Agricultural Institute

The attention of research workers is being increasingly drawn to ammoniacal electrolytes for galvanic coatings.

The ammoniacal electrolyte developed by Levin for zinc plating, which has been tested under production conditions, has good throwing power and gives bright microcrystalline coatings with good adhesion to the basis metal, with current efficiency about 100% [1]. The ammoniacal electrolyte for nickel plating, proposed by Morozov, gives bright deposits of nickel up to 30 μ thick at current densities up to 6 amps/dm^2 [2]. Frantsevich-Zabludovskaia and Zaiats have described ammoniacal electrolytes for deposition of alloys of tungsten and molybdenum with metals of the iron group [3]. Ammoniacal electrolytes can also be used for removing copper coatings [4].

The chief obstacle to the industrial utilization of such electrolytes is the volatilization of ammonia. It is therefore desirable to develop a method for protecting the electrolyte surface from the air by a layer impermeable to ammonia.

At one time a layer of kerosene was used to prevent spattering of chromium electrolyte [5]. Although such covering liquids have not gained acceptance in electroplating technology, they may be suitable for use with ammoniacal electrolytes. The present paper reports a study of this question.

EXPERIMENTAL

In view of the requirements to which a covering liquid must conform (density less than unity, inertness toward the electrolyte), we tested kerosene, transformer oil, and vaseline oil as covering liquids.

As the spreading coefficient of hydrocarbons on water is low [6], continuous stable layers of these liquids are only formed at considerable thicknesses: 1 mm for kerosene, 1.4 mm for transformer oil, and 5 mm for vaseline oil.

Volatilization Rate of Ammonia (in g/m^2·hour) from Aqueous Solution with Covering Layers (Initial ammonia concentration 12 g/liter, t = 24-28°)

Without covering layer	Kerosene, 1.4 mm thick	Kerosene, 8.3 mm thick	Transformer oil, 1.4 mm thick	Vaseline oil, 5.5 mm thick
40	1.08	0.15	0.03	0.01

The experiments on the influence of the layers of covering liquids on the volatilization rate of ammonia were performed as follows. 100 ml of an aqueous solution of ammonia or ammoniacal electrolyte was put into a crystallizing dish 100 mm in diameter, with the required amount of the covering liquid. At definite time intervals 1 ml portions of the electrolyte were removed by means of a micropipet, diluted with 10 ml of water, and titrated with 0.1 N HCl in presence of methyl orange to determine the ammonia concentration.

Even the preliminary experiments with aqueous ammonia solutions showed that covering layers of these oils greatly diminish the volatilization rate of ammonia; this is illustrated by the data below.

The subsequent experiments were carried out with an ammoniacal zinc-plating electrolyte of the following composition (in g/liter): $ZnSO_4 \cdot 7H_2O$ 30, $(NH_4)_2SO_4$ 40, NH_3 50, H_3BO_3 20, joiner's glue 2.

The results of these experiments are given in Tables 1 and 2.

TABLE 1

Rate of Evaporation of Ammonia from Zinc-Plating Electrolyte Without Covering Liquid (t = 24-28°)

Evaporation time from start of experiment (hours)	Concentration of ammonia in electrolyte (g/liter)	Average concentration of ammonia between two determinations (g/liter)	Average evaporation rate of ammonia (in $g/m^2 \cdot \cdot hour$)
0	51.5	–	–
0.75	39.2	45.3	226
1.5	33.4	36.5	90
2.3	27.9	30.6	84
4.0	21.4	24.6	62
6.2	17.4	19.4	35

TABLE 2

Rate of Evaporation of Ammonia from Zinc-Plating Electrolyte Protected by a Layer of Covering Liquid (t = = 24-28°)

Covering liquid	Duration of experiment (hours)	Concentration of ammonia in electrolyte (g/liter)		Average evaporation rate of ammonia (in $g/m^2 \cdot \cdot hour$)
		initial	final	
Transformer oil, layer 1.5 mm thick	628	51.3	41.5	0.22
Same, 3 mm thick	628	51.3	45.2	0.13
Same, 6 mm thick	628	51.3	43.3	0.18
Vaseline oil, layer 3 mm thick*	120	44.7	44.3	0.05
Same, layer 5 mm thick	120	45.0	44.4	0.07
Same, layer 10 mm thick	120	45.0	44.8	0.06

* A layer of vaseline oil 3 mm thick is unstable.

It follows from these results that covering layers of transformer oil, and especially of vaseline oil, decrease the volatilization rate of ammonia from the electrolyte to negligible amounts. Kerosene proved less suitable for the purpose.

It was further necessary to find whether it is possible to immerse a metal specimen in the electrolyte through the layer of covering liquid without contamination of the specimen surface with oil, as thorough degreasing is an essential condition for the production of good coatings.

It was found that this is possible if the specimen is previously degreased thoroughly and moistened with water (which is always the case in the usual procedure for the preparation of metal surfaces for electrocoating). It was found in repeated experiments with steel, copper, and zinc plates that thoroughly degreased and moistened plates remain clean and uniformly wetted by the electrolyte when immersed through layers of transformer or vaseline oil. When individual drops of oil were occasionally drawn in during immersion of the plate into the electrolyte, they were detached from the plate by light shaking and rose to the surface, where they merged with the covering layer. When the plates were removed from the electrolytes, a little oil came out with them, but it did not wet the metal, being separated from it by a film of water. When the plates were washed in water the oil was completely removed, and the surfaces were uniformly wetted by water.

In the tests of the covering liquids, smaller amounts of vaseline oil than of other oils adhered to the plates, both in immersion and during withdrawal.

It was desirable to compare the probabilities of contamination of metal surfaces, wetted with water, by these covering liquids.

In these experiments a drop of the liquid was allowed to fall from a height of 5 cm onto a polished steel plate, degreased and wet with water. The plate was washed in running water and its wetting by water was tested. It was found that after a drop of kerosene had been applied by this method, it immediately spread over the surface of the plate, and after the plate had been washed the place where the drop had fallen was not wetted by water – the metal surface was contaminated. A drop of transformer oil spread less; the water was displaced from the metal surface around the drop, and this annular zone became covered with a thin film of oil. The drop of oil adhered to the metal. After the plate had been washed, water did not wet this region.

Quite different results were obtained in similar tests of vaseline oil. The drop assumed the shape of a small lens which floated freely on the water film covering the plate, and moved easily under its own weight when the plate was slightly tilted. The oil could not be made to adhere to the plate even after it had been rubbed on the surface with a glass rod. Washing in water removed the drop of vaseline oil, and the whole plate was quite uniformly wetted by water.

A further group of experiments was performed with vaseline and transformer oils. A small drop of oil was placed on a dry, polished iron plate, and the plate was immersed in the ammoniacal zinc electrolyte. The oil, which had previously spread somewhat over the metal, collected into a drop, and its area of contact with the metal contracted considerably. Observations with the aid of a lens showed that the contact angle (within the drop) was acute, about 40-45°, in transformer oil, and obtuse (about 100-110°) in vaseline oil.

These experiments show that when vaseline oil is used as a covering liquid the risk of contamination of a wet metal surface with the oil is almost eliminated.

To test the practical suitability of vaseline oil as a covering liquid, several experiments on zinc plating in the electrolyte of the composition given above were carried out. The volume of electrolyte was 500 ml, the thickness of the layer of vaseline oil was 6 mm, the cathode current density was maintained at 0.8-1 amp./dm^2, and the temperature of the electrolyte was 26-28°. Iron plates 100 × 25 × 1 mm in size, M-12 nuts, and M-8 bolts were plated. The objects were degreased, pickled, and washed before the plating. After the plating they were washed in running water and dried in a drying oven.

The zinc coatings were bright, dense, and uniform, and the threads on the bolts and nuts were well coated with zinc. In external appearance the articles did not differ in any respect from articles plated in the same electrolyte without covering liquid. Bend tests on the coated plates showed good adherence of the zinc to the basis metal.

SUMMARY

1. If the surface of an ammoniacal zinc-plating electrolyte is covered with a layer of vaseline or transformer oil a few mm thick, the volatilization rate of ammonia is diminished to 1/1000 or less of its former value.

2. Of the liquids tested, vaseline oil is the most suitable for formation of covering layers. The evaporation rate of ammonia is lowest in presence of a layer of vaseline oil. It does not wet metals previously wetted with water. Vaseline oil is not volatile under normal conditions [6] and it presents no fire risks (its flash point in a closed cup is not below 185°) [7].

3. The articles to be plated are not contaminated by the oil either when immersed or when withdrawn from the electrolyte. The quality of the coatings does not differ in any respect from that of coatings formed in the same electrolyte without covering liquid. This also applies to objects of complex outline, including threaded articles.

4. The use of covering layers of vaseline oil on ammoniacal electrolytes eliminates the principal disadvantage of the latter – volatilization of ammonia – and the possibilities of their practical utilization are therefore much improved.

5. The possible use of covering liquids for protection of electrolyte surfaces from the air merits further study in relation to other aqueous electrolytes; these investigations are being continued.

LITERATURE CITED

[1] A. I. Levin, Trans. Urals Industrial Inst. 27, 119 (1947).

[2] E. V. Morozov, Dissertation (Mendeleev MKhTI, 1954).

[3] T. F. Frantsevich-Zabludovskaia and A. I. Zaiats, Summaries of Papers at the 4th Conference on Electrochemistry (Izd. AN SSSR, 1956).

[4] V. I. Lainer and N. T. Kudriavtsev, Fundamentals of Electroplating (Metallurgy Press, 1953) p. 386.*

[5] B. A. Kuznetsov, Electrolytic Chrome Plating of Metals (State Sci.-Tech. Press, 1932).*

[6] N. K. Adam, The Physics and Chemistry of Surfaces (Russian translation) (State Tech. Press, 1947) p. 277.

[7] GOST 3164-52; Chemical Products, edited by I. G. Molotkov (Goskhimizdat, 1954) p. 912.*

Received May 11, 1956

* In Russian.

THE DEGRADATION PRODUCTS OF SUGARS AND THEIR INFLUENCE ON THE PROPERTIES OF CARAMEL

A. L. Sokolovskii and V. N. Nikiforova

Our spectrophotometric investigations in the ultraviolet region [1-3] showed that the degradation products of sugars formed during the production of caramel may contain varying amounts of the following compounds: sugar anhydrides, reversion products, hydroxymethylfurfural, acid products (formic and levulinic acids) and coloring substances – humins.

However, separation and identification of the degradation products of sugars, and especially of the degradation products formed in the initial stages of heating, by spectrometric and chemical methods is very difficult because of the similar properties of these substances.

Characteristics of Caramel

Additions to sucrose (%)	External appearance of caramel	Contents of reducing substances (%)	Keeping qualities of caramel when stored under cover
0.37 of hydroxymethylfurfural	Pale yellow, transparent, sticky	–	Completely crystallized on second day
0.73 of hydroxymethylfurfural	Yellow, transparent, sticky	–	Completely crystallized after 2 days
0.25 of humins (in acetone solution)	Dark, sticky	0.56	Crystallized on cooling
0.1 of humins (after dialysis)	Dark, sticky	–	Crystallized on second day
1.3 (as dry substance) of fermented solution after purification with charcoal	Pale, transparent	0.6	Crystals in individual pieces on 6th day of storage
10 (as dry substance) of fermented solution purified with charcoal	Pale, transparent	5.0	Kept 20 months without crystallization
10 (as dry substance) of fermented solution after ion-exchange purification	Yellow, transparent	2.8	Kept 8 months without crystallization

In the present investigation, paper chromatography was used for separation of the degradation products of sugars formed on heating. In most of the experiments the solvent was a mixture of butanol, ethanol, and water in 4 : 1 : 5 ratio, while in some experiments a mixture of isopropyl alcohol (90 ml of 75%) and glacial acetic acid (10 ml) was used. The chromatograms were developed by solutions of resorcinol or diphenylamine. Sugar solutions of various concentrations (10, 30, and 70%) heated under reflux, and sugars heated at various temperatures without added water (melts) were investigated.

The chromatographic results showed that hydroxymethylfurfural is readily formed in solutions of sugar of low concentrations by the action of heat, whereas only very small amounts are formed, and only after prolonged heating, in concentrated solutions. The condensation (reversion) products, which lie above the original sugars on the chromatogram, are, on the contrary, formed in large amounts by the action of heat on concentrated solutions and especially on melts, the amounts increasing and the composition becoming more complex with increasing time and temperature. It must be pointed out that when sucrose is decomposed by fusion, even at very high temperatures (185-190° for 10 minutes) no water-insoluble humus substances are formed such as those formed by the action of heat on 10-30% solutions. Therefore water present in the solutions favors irreversible changes in sugars; i.e., changes in the direction of considerable dehydration, with formation of hydroxymethylfurfural and humus substances. A decrease in the proportion of free water in the decomposition reaction leads to the appearance of considerable amounts of reversion products.

Fructose shows a great tendency to condensation reactions. It was noticed that the compounds formed when fructose solutions are heated are very hygroscopic; they lie below fructose on the chromatograms.

Since the production of caramel involves the action of high temperatures on concentrated sugar solutions (70-85%), it is quite evident that anhydrides and reversion products form the main bulk of the degradation products of sugars formed during the production of caramel.

To determine the influence of individual decomposition products of sugars on the properties of caramel, the following compounds were obtained in more or less pure form: hydroxymethylfurfural, the primary degradation products of sugars (mixture of anhydrides and reversion products), and coloring substances – humins.

Hydroxymethylfurfural was obtained by extraction with ethyl acetate from sucrose solutions heated under reflux for 20 hours. After removal of ethyl acetate under reduced pressure, theresidue was dissolved in water and the solution was decolorized by means of charcoal. The purity of the hydroxymethylfurfural was checked spectrophotometrically (by its absorption curve). On the assumption that the molar extinction coefficient of hydroxymethylfurfural at 283 mμ = 16,900, the amount present in solution can be calculated.

Two kinds of humus substances were obtained: 1) in the form of a brown-black powder, sparingly soluble in water, and 2) as a colored solution which remained in a Cellophane bag after dialysis, in water, of a sucrose solution after heating.

The primary degradation products of sugars were obtained by fermentation of the unchanged sugar (7-8% solutions of sucrose melts). Thoroughly washed baker's yeast in 1.5 : 1 ratio (relative to the solids content of the solution) was used for the fermentation. The turbid fermented liquid was centrifuged, filtered, yeast was removed by addition of zinc sulfate to the filtrate, and the filtrate was further purified by means of activated charcoal or ion-exchange resins ("Aspatit").

The isolated decomposition products of sugars were used in experiments on the preparation of caramel from sucrose (see Table); the amounts of hydroxymethylfurfural and humins added were considerably greater than the amounts usually present in caramel (0.01-0.001%).

It is clear from the data in the Table that all the caramel samples to which hydroxymethylfurfural or humins had been added crystallized very rapidly, while caramel to which primary degradation products of sugars had been added was stable for a considerable period. The primary degradation products isolated by us could, of course, have contained hygroscopic compounds. There is no doubt that further identification of these hygroscopic products of the decomposition of sugars is necessary for the production of caramel which is quite stable on keeping.

SUMMARY

1. The principal constituents of the degradation products of sugars formed during preparation of caramel are anhydrides and reversion products. Caramel also contains small amounts of products of more extensive decomposition of sugars: hydroxymethylfurfural, coloring matter, and humins.

2. The degradation products of sugars influence the properties of caramel. Condensation (reversion) products help to keep the caramel in the amorphous state. Hydroxymethylfurfural and humins have only an adverse effect by increasing the color and hygroscopicity of the caramel.

3. The presence of fructose in the raw material is undesirable, as fructose readily gives rise to hygroscopic products under the action of heat.

LITERATURE CITED

[1] B. V. Evstigneev and V. N. Nikiforova, Biochemistry 15, 94 (1950).

[2] B. N. Evstigneev and V. N. Nikiforova, Biochemistry, 16, 3, 250 (1951); Proc. Acad. Sci. USSR 73, 3, 523 (1950).

[3] V. B. Evstigneev, V. N. Nikiforova, and A. L. Sokolovskii, Trans. VKNII VIII, 91-119 (1952).

Received February 6, 1956

ON THE SUBJECT OF THE PAPER BY M. V. GOFTMAN AND A. I. GOLUB: "CATALYTIC OXIDATION OF THE PRINCIPAL POLYCYCLIC COMPOUNDS OF COAL TAR AND ITS FRACTIONS"

B. M. Pats

During the past two years M. V. Goftman and A. I. Golub have published several communications in the technical journals on the subject of vapor-phase catalytic oxidation of coal-tar products [1, 2, 3].

Their main task was a search for what are in their opinion the optimum conditions of oxidation: catalyst temperature, concentration of the vapor-air mixture, and contact time.

It may be admitted that M. V. Goftman and A. I. Golub have presented some more accurate data on the subject. For example, as is shown in the Table, they obtained somewhat different results than those given by others for the yields of phthalic anhydride by the oxidation of various compounds.

The yields of phthalic anhydride in the oxidation of various raw materials, according to the data of Goftman and Golub [3] and of Kinney and Pinkus [4]* are given in the Table.

Materials	Goftman and Golub		Kinney and Pinkus	
	yield (wt. %)	nominal consumpt. of raw material per 1 ton of phthalic anhydride	yield (wt. %)	nominal consumption of raw material per 1 ton of phthalic anhydride
Naphthalene	81.6	1.2	90.8	1.1
Phenanthrene	49.6	2.0	35.2	2.8
Anthracene	22.2	4.5	51.3	1.9
Fluorene	52.2	1.9	—	—
Chrysene	47.6	2.1	—	—
Phenanthrene fraction	32.3	3.1	—	—
1st anthracene fraction	22.7	4.4	—	—
2nd anthracene fraction	13.8	7.3	—	—
Naphthalene fraction	73.1	1.4	—	—
Light middle oil	25.1	4.0	—	—
1-Methylnaphthalene	—	—	34.1	2.9
2-Dimethylnaphthalene	—	—	38.5	2.7
2,3-Dimethylnaphthalene	—	—	40.7	2.4
200-235° fraction	—	—	75.0	1.3
235-270° fraction	—	—	28.2	3.6
Crude anthracene	—	—	24.1	4.2

It is seen that Goftman and Golub obtained a higher yield of phthalic anhydride from phenanthrene, whereas the American authors had a higher yield of phthalic anhydride from naphthalene and anthracene. It is difficult to attribute these results to anything but differences in the oxidation conditions used in the respective investigations.

* The maximum yields are given in both cases.

Extension of the production of phthalic anhydride from individual compounds other than naphthalene as raw material is not a promising proposition. The economics of the process is the decisive factor here. It follows from the Table that the consumption of raw materials in the production of phthalic anhydride from pure phenanthrene, fluorene, or anthracene is considerably higher than in the production of phthalic anhydride from naphthalene. If the production cost of phthalic anhydride is not to increase, the cost of the original anthracene, phenanthrene, or fluorene must be a fraction of the cost of naphthalene, which is unlikely.

The data in the Table show that only the naphthalene fraction gives a relatively acceptable consumption of raw material per ton of phthalic anhydride. As regards the other oils, including light middle oil, the yield of phthalic anhydride obtained by their oxidation is so low that their use for the production of phthalic anhydride is uneconomic. If it is also taken into account that in the oxidation of these substances a large proportion is burned to CO_2, the proposition is seen to be quite unacceptable. If the oils are to be burned, this should be done in boiler furnaces and not over vanadium catalysts, so that at least the heat of combustion is utilized; moreover, these oils have better uses in the national economy.

Thus, of the group of oils and fractions in question, only the naphthalene fraction is of interest. Incidentally, Goftman and Golub draw attention to the high yields of phthalic anhydride in the oxidation of the naphthalene fraction, and quote values in excess of 100%. Their calculations are conditional and artificial, as they are based on the assumption that naphthalene is the sole source of formation of phthalic anhydride and the other constituents of the fraction, which also form phthalic anhydride, are ignored. The utilization of the naphthalene fraction instead of technical naphthalene for the production of phthalic anhydride is mainly a problem of technical economics.

The suitability of this process is determined by the relationship between the cost of production of technical naphthalene from the naphthalene fraction and the advantages gained by its direct oxidation. It must be remembered, however, that the conversion of the naphthalene fraction to phthalic anhydride should be effected at the coal-tar chemical works, that its evaporation requires modification of the existing evaporator design, and that the oils isolated from it have independent uses.

Without disputing the fact that phthalic anhydride can be made from different materials, we must point out that naphthalene, and to some extent o-xylene, are likely to remain the principal materials for a long time.

Objective consideration of the question leads to the conclusion that until such a raw material as naphthalene has become fully exhausted it is hardly feasible to introduce another.

The potentialities in this field are considerable. The production of naphthalene can be more than doubled by a decrease of the losses in its isolation from tar, which at present reach 40-50%, by utilization of technical naphthalene, and by increasing the naphthalene content of tar by acceptable modifications in coking processes. Finally, an indirect reserve is an increase of the yield of phthalic anhydride in the oxidation of naphthalene from 60-70% to 80-90%, which is a very real and quite feasible task. Incidentally we may note that as the result of work carried out by the Ukrainian Institute of Coal Chemistry jointly with the Rubezhnoe Chemical Combine and the local branch of the Scientific Research Institute of Organic Intermediates and Dyes, successful trials have been made of the industrial use of technical naphthalene for production of phthalic anhydride.

It follows from the above that the method proposed by M. V. Goftman and A. I. Golub for the vapor-phase oxidation of coal-tar products other than naphthalene is not justified.

The efforts of research workers must be primarily directed toward increasing the yields of phthalic anhydride in the oxidation of naphthalene.

This does not exclude research on the production of phthalic anhydride from other raw materials, but here the task of research workers lies not in repetition of earlier work in this field but in a search for original ways for increasing the yields of phthalic anhydride and thereby making the process more economical.

LITERATURE CITED

[1] M. V. Goftman and A. I. Golub, J. Appl. Chem. 28, 5, 507 (1955).*

[2] M. V. Goftman and A. I. Golub, J. Appl. Chem. 29, 8, 1256 (1956).*

[3] M. V. Goftman and A. I. Golub, Coke and Chemistry 2, 51 (1956).

[4] Kinney and Pinkus, Ind. Eng. Ch. 43, 2880 (1951).

Received October 16, 1956

* Original Russian pagination. See C. B. Translation.

PRODUCTION OF RAW MATERIALS FOR ORGANIC SYNTHESIS FROM COAL-TAR FRACTIONS*

M. V. Goftman and A. I. Golub

In his comments, B. M. Pats touches on a number of questions which differ in their significance.

B. M. Pats's principal objection is that, in his opinion, the production of phthalic anhydride should be based on increasing naphthalene production, and not on direct oxidation of tar fractions. We agree that everything possible must be done to increase the production of naphthalene.

However, one should look further than B. M. Pats does in this question. Increase of the output of naphthalene, even on the technical product, will not save the situation; this is shown by the experience in the United States, where it is considered that the demand for raw materials for phthalic anhydride production exceeds not only the actual output of naphthalene, but even its potential resources in tar.

Some figures in support of this may be quoted. After the war the production of naphthalene in the U.S.A. began to grow rapidly owing to the increased demand for phthalic anhydride, and now exceeds 150,000 tons. There is not enough domestic naphthalene in the U.S.A. and 45,000 tons is imported annually. It is considered in the U.S.A. that the production of naphthalene must be raised to 250,000 tons in the next few years, but even then the deficiency will be 75,000 tons.

We therefore considered it appropriate to carry out research which would lead to a large increase in the available sources of materials for the production of phthalic anhydride.

It is interesting to note that B. M. Pats, who compares our work with that of Kinney and Pinkus, which, despite a number of faults, maintains the correct outlook on the general direction of the utilization of tar, does not explain why the Americans are looking for new sources of raw materials for phthalic anhydride production and do not intend to restrict themselves to naphthalene and o-xylene.

The problem is concerned not only with sources of naphthalene, but also with the grade of naphthalene which must be produced for the manufacture of phthalic anhydride. Our phthalic anhydride industry continues to use costly crystalline naphthalene, the extraction of which from coal tar involves heavy production losses. This, of course, introduces a further difficulty in covering the demand for naphthalene.

At the same time, literally the whole world has long been utilizing technical naphthalene (pressed and even centrifuged) and in some cases naphthalene fractions. We went even further and investigated the possibility of using other tar fractions, i.e., we went in the direction of evident technical progress. This not only increases considerably the possible utilization of the raw material, but lowers the cost significantly (three to four-fold).

Incidentally, we did not recommend the use of pure products such as fluorene, phenanthrene, etc. for oxidation (precisely on economic grounds), but studied the oxidation of these hydrocarbons in order to develop the optimum conditions for their oxidation in mixtures, i.e., in fractions.

Let us now consider B. M. Pats's comment that our calculations of the yield of phthalic anhydride from the naphthalene fraction were incorrect. Our object was not so much to determine more precisely the yield of phthalic anhydride, as to cast doubt on the totally unjustified opinion of some specialists who considered (and

* Reply to the paper by B. M. Pats: "On the Subject of the Paper by M. V. Goftman and A. I. Golub: "Catalytic Oxidation of the Principal Polycyclic Compounds of Coal Tar and Its Fractions" (see p. 1336 of this issue).

some still consider) that under our conditions the faulty practice of oxidation of pure naphthalene should be continued.

Our work on the oxidation of washed naphthalene fractions indeed confirmed that it is possible to use the available naphthalene in these fractions more efficiently than by the extraction of pure naphthalene, even in 100% yield. This is because the losses of naphthalene during its isolation are avoided, and because accompanying substances such as methylnaphthalenes are also oxidized to phthalic anhydride. The criticism made by B. M. Pats, that we allegedly do not take into account the oxidation of the accompanying substances and calculate the yield of phthalic anhydride on naphthalene only, is more than strange. Any unprejudiced reader of our papers can see that in addition to the nominal yields calculated on the naphthalene in the fraction, which demonstrate the existence of additional sources of raw materials for phthalic anhydride production, we also give the weight yield for the whole fraction; incidentally, this is a little less than the yield from pure naphthalene.

As regards the comment by B. M. Pats that the yield of phthalic anhydride can be increased (evidently by the use of a different catalyst), this applies not only to naphthalene, but equally to the naphthalene fraction. On the basis of our and other work, the Eastern Scientific Research Institute for Coal Chemistry (VUKhIN) is conducting trials on the oxidation of naphthalene fractions over a potassium–vanadium–sulfate–silica gel catalyst, which gives higher yields of phthalic anhydride from naphthalene than vanadium pentoxide does. Even now successful results have been obtained by oxidation of naphthalene fractions, and production trials are to be carried out.

Thus, instead of making concrete comparisons between the oxidation of naphthalene and the naphthalene fractions, B. M. Pats passed to general considerations. He argues that the naphthalene fractions should be oxidized at the coal-tar chemical works. He must surely know that this was proposed as long ago as 1955 by one of the coal-tar chemical works jointly with VUKhIN, and also by the State Institute for the Planning of Industrial Coke By-Product Establishments. For some reason B. M. Pats proves to us that other evaporators must be used. As the results of experiments on exhaustive evaporation, with the residues in the evaporators taken into account, we ourselves refer in our papers to the necessity of using evaporators from which the residues can be discharged. Incidentally, such evaporators, which can moreover be cleaned out without interruption, are already available in the new phthalic anhydride units, and our proposed industrial trials of the oxidation of naphthalene fractions will be carried out in a unit equipped with such evaporators.

It is quite impossible to agree with B. M. Pats that oxidation of the higher tar fractions is inappropriate. He concentrates his attention on the oxidation of light middle oil, which gave poor results (and we therefore do not recommend its oxidation), and refers only incidentally to oxidation of the phenanthrene–anthracene fraction whereby it is possible to obtain, together with phthalic anhydride, considerable amounts of anthraquinone, which is at present made by a costly synthetic process. Moreover, considerable amounts of maleic anhydride, the consumption of which has risen sharply in recent years, are produced in the oxidation of this fraction. As regards the partial combustion of this fraction, the heat evolved can easily be utilized. Even now the heat of reaction is used in the new phthalic anhydride units for supplying all the power required and for heating the building.

In our opinion, it follows from the foregoing that both the main arguments and the particular comments made by B. M. Pats are unfounded.

Received December 19, 1956

COMPOSITION OF THE BUTYLENES OBTAINED IN THE S. V. LEBEDEV PROCESS

V. V. Pigulevskii and V. V. Leont'eva

The question of the composition of butylenes formed as by-products in the synthesis of divinyl from alcohol by the Lebedev process is of both practical and theoretical interest.

Lebedev showed [1] that mainly β-butylene is present in these products, but he also admitted the possible presence of α-butylene. Petrov [2] was the first to detect a small amount of isoprene in the amylene–piperylene fraction. Gorin [3] showed the theoretical possibility of the formation of isoprene by reactions of the condensation type in the Lebedev process. The presence of isobutylene has not been previously reported.

The purpose of the present investigation was to study the composition of the butylenes formed in the Lebedev process.

These hydrocarbons are concentrated in the butylene fraction of the rubber-synthesis gases – technical pseudobutylene. This fraction was the main object studied in this investigation.

EXPERIMENTAL

Determination of the composition of technical pseudobutylene. The investigation involved low-temperature rectification of the gas in a column of our design, followed by chemical analysis of the fractions.

The rectification column consisted of a glass tube of 5 mm internal diameter and 120 cm long. The packing was a twist of three spirals (internal diameter 1.2 mm) made from Nichrome wire (0.2 mm in diameter) and wound on a Constantan wire rod 1.5 mm in diameter (Fig. 1). The column was contained in a silvered evacuated tube. The top of the column was cooled by means of a mixture of solid carbon dioxide and alcohol. The temperature was measured by means of a four-point copper–Constantan thermocouple, with a potentiometer of the PP type, to an accuracy of 0.2°. The separating power of the column was verified by fractionation of synthetic mixtures of isobutylene and n-butane. The separating power of the column under the operating conditions, calculated by the Obolentsev and Frost formula [4], was equivalent to 19.5 theoretical plates. 30-40 ml of the liquefied gas (7-10 liters in the gaseous form) was taken for the rectification. The gaseous fractions were collected at 15-20 ml/minute, and this rate was changed to 2-4 ml/minute during transition from one fraction to the next.

Total unsaturation of the gaseous fractions was determined by absorption in 1% bromine solution. Complete gas analysis was carried out in the Orsat apparatus [5].

Isobutylene was determined by the Deniges–Isakova method, by formation of complex compounds with mercury salts [6, 7]. Divinyl in the gas was determined by the bromination method [8]. Technical pseudobutylene was obtained from one of the synthetic-rubber factories, where it had been separated by rectification from the main bulk of the divinyl and the remaining divinyl was removed by absorption in copper salt solutions.

In the distillation of technical pseudobutylene there was a considerable plateau at −6.5°, corresponding to the α-butylene fraction, with a fairly sharp transition from the α-butylene to the β-butylene fraction (Fig. 2). The β-butylene fraction itself had a plateau at +1° and at +3.6°; this is explained by the presence of both the trans isomer (b. p. +0.9°) and the cis isomer (b.p. +3.6°) in the fraction.

As a result of the fractionation and analysis of the fraction, the technical pseudobutylene was found to have the following composition:

Contents	in ml	in vol. %
Hydrogen	~2	traces
Carbon dioxide	~1	traces
Methane, ethane, propane	21	0.3
Ethylene	~1	traces
Propylene	41	0.5
Isobutylene	304	3.7
α-Butylene	1671	20.6
β-Butylene	5681	70.2
Divinyl	136	1.7
n-Butane	169	2.1
Residue (C_5)	69	0.8

It was therefore found that technical pseudobutylene from synthetic rubber production contains about 20% α-butylene in addition to β-butylene, the ratio being β-C_4H_8 : α-C_4H_8 = 3.4 : 1. In addition, it contained up to 3.7% of isobutylene, and n-butane. During fractionation the isobutylene was concentrated in the α-butylene fraction, which contained 12.0% of it.

The next step in the work was an attempt to determine at which stages of the process the isobutylene is present.

Determination of isobutylene at various stages of the process. Qualitative tests were carried out for isobutylene directly in the contact gas formed in the Lebedev process.

The contact gas from an experimental unit was liquefied in solid carbon dioxide, and the divinyl–butylene condensate was then treated with maleic anhydride in sealed tubes at 60° to remove divinyl. The unreacted part of the condensate was evaporated off and treated with mercuric nitrate solution with warming. In all cases a characteristic yellow precipitate of the complex compound of butylene was formed [6, 7].

Next, isobutylene was determined in the exit gas from the rodless polymerization of divinyl, containing a considerable amount (70-80%) of this olefin. The exit gas from rodless polymerization was definitely found to contain isobutylene; it is seen in the data below that up to 0.6% is present.

Composition of gas (vol. %)		
Divinyl	Isobutylene	
76.2	0.48	0.47
75.0	0.58	0.56
77.2	0.58	0.60

In addition, isobutylene was extracted from this gaseous mixture by treatment of the liquefied gas (10 ml) with 45% sulfuric acid for 11 hours. In these conditions isobutylene was extracted completely, forming isobutylsulfuric acid. This was saponified with water, and aqueous trimethyl carbinol was distilled off; this was dehydrated in presence of sulfuric acid [9]. The gaseous mixture of air and the reaction product after dehydration contained 1.1% of isobutylene, corresponding to 0.1% in the original mixture with divinyl. Thus, the loss of isobutylene in this multistage treatment was 0.4% (absolute).

DISCUSSION OF RESULTS

It was found that technical pseudobutylene contains β-butylene (~70%), α-butylene (~20%), and isobutylene (~3%), in the ratio β-C_4H_8 : α-C_4H_8 : iso-C_4H_8 = 3.4 : 1 : 0.18. The 3.4 : 1 ratio of β- to α-butylene corresponds to the equilibrium ratio at about 400° [10, 11]. Therefore α- and β-butylene formed in the Lebedev process are present in the equilibrium ratio.

The presence of isobutylene at other stages of the process shows that this hydrocarbon is formed during the catalytic reaction of the alcohol; it must originate from α- and β-butylene, which are partially isomerized to isobutylene in presence of the Lebedev catalyst. The presence of n-butane (~2%) in the gas must be attributed to partial hydrogenation of n-butylene over the same catalyst.

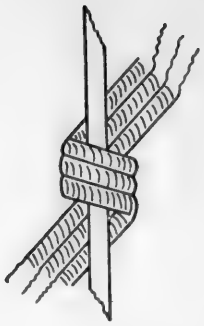

Fig. 1. Packing of rectification column.

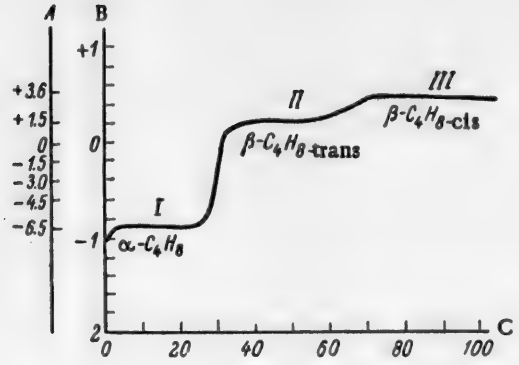

Fig. 2. Fractionation of technical pseudobutylene. A) Temperature (°C), B) potentiometer readings (mv), C) composition (vol. %).

SUMMARY

1. It was found that in a study of the butylenes formed in the Lebedev process that α- and β-butylene are present in the equilibrium ratio.

2. Isobutylene was found in the gaseous products formed during synthetic rubber production. It is suggested that isobutylene is formed by isomerization of α- and β-butylene.

3. The gaseous products were found to contain n-butane.

LITERATURE CITED

[1] S. V. Lebedev, J. Gen. Chem. 3, 698 (1933).

[2] A. A. Petrov and A. F. Sapozhnikova, J. Gen. Chem. 18, 4, 640 (1948).

[3] Iu. A. Gorin, Trans. All-Union Sci. Res. Inst. Synthetic Rubber 3, 17 (1951).

[4] R. D. Obolentsev and A. V. Frost, Petroleum Economy 8, 35 (1947).

[5] M. I. Dement'eva, Analysis of Hydrocarbon Gases (State Fuel Tech. Press, 1951) p. 106.*

[6] G. Deniges, Comptes rend. 129, 1, 1043, 1145 (1898).

[7] N. A. Isakova and A. M. Rakhmanina, Trans. All-Union Sci. Res. Inst. Synthetic Rubber, 3, 137 (1951).

[8] A. I. Guliaeva, V. F. Polikarpova and Z. K. Remiz, Analysis of the Products Formed in the Production of Divinyl from Ethyl Alcohol by the Lebedev Process (Goskhimizdat, Moscow-Leningrad, 1950).

[9] V. V. Pigulevskii and M. G. Averina, J. Appl. Chem. 30, 3, 426 (1957).**

[10] H. H. Voge and N. C. May, J. Am. Chem. Soc. 68, 4, 550 (1946).

[11] A. V. Frost, J. Gen. Chem. 9, 1813 (1939).

Received October 28, 1956

* In Russian.

** Original Russian pagination. See C. B. Translation.

CALCULATION METHODS IN THE LACQUER AND PAINT INDUSTRY

I. R. Morozov

If a functional relationship exists between two physicochemical variables Y and X between the limits a and b, in some instances this relationship can be represented by the following equation:

$$Y_n = Y_a : (A \cdot Y_b \cdot X_n + 1)^B, \quad (1)$$

Such functions include the following curves: 1) viscosity of water as a function of temperature; 2) specific viscosity of collodion mixtures as a function of the contents of the components; 3) viscosity of solutions of chlorinated polyvinyl chloride resin as a function of solvent composition; 4) acidity of glyptal (alkyd) resins as a function of the esterification time; 5) esterification time as a function of the temperature in the production of these resins; 6) condensation time of film formers for lacquers and paints as a function of the original formulation.

In illustration, Tables 1-7 give calculated viscosities, acidities, and times, compared with experimental data from the literature and obtained by direct experiments. Each table contains the values of the constants A and B found by solution of a system of two equations based on the above Equation (1) with known values of Y and X for two points on the curve, and expressions for the independent variable X.

The acid numbers and esterification times were studied under laboratory conditions in the preparation of alkyd resin modified with vegetable oil (FPV-2 resin).

The procedure was as follows: cottonseed oil alcoholized with glycerol and phthalic anhydride were heated to a definite temperature, the oil was added in a slow stream to the anhydride with brisk stirring, and the mixture was heated for various times. It was found that the acid number (AN) immediately after the mixing could be represented by the expression

$$AN = 237 - (0.53 \cdot T + 0.001 \cdot T^2). \quad (2)$$

where 237 is the acid number of the mixture of the original components before the esterification reaction, and T is the esterification temperature in °C.

Subsequent variations of the acid number with the esterification time were represented by Equation (1).

The condensation times of the film formers of different formulations were determined for the following compositions (in %):

Components	Compositions	
Tung oil	50	25
Cottonseed oil	16	41
Calcium resinate	34	34

Compositions I and II were mixed in various proportions and heated at 250° until 50% condensation, as tested by the "air bubble" method, was reached.

It is clear from the data in Tables 1-7 that there is satisfactory agreement between the experimental and calculated values. It is useful in the lacquer and paint industry to be able to calculate the compositions of collodion mixtures and polyvinyl chloride solutions for given viscosities, esterification times and temperatures

TABLE 1

Viscosity of Water

[A = 17, B = 1.4; $X = (T_n - T_0) : (140 - T_0)$]

Temperature (°C)	Absolute viscosity of water y = f (X)		Temperature (°C)	Absolute viscosity of water y = f (X)	
	calculated	literature data [1]		calculated	literature data [1]
0	1.60	1.60	80	0.35	0.35
10	1.18	1.20	90	0.32	0.32
20	0.93	0.95	100	0.28	0.28
30	0.74	0.80	110	0.26	0.26
40	0.62	0.62	120	0.24	0.24
50	0.53	0.53	130	0.22	0.22
60	0.46	0.46	140	0.20	0.20
70	0.40	0.40			

TABLE 2

Viscosity of Collodion Mixtures

[A = 1, B = 1.13 and 0.88 (respectively); $X = n_{II} : 10$]

Contents of collodions in mixture (n) (in g)		Engler viscosity of mixtures			
I	II	observed	calculated	observed	calculated
0	10	0.99	0.99	0.99	0.99
1	9	1.04	1.04	1.026	1.035
2	8	1.10	1.10	1.078	1.08
3	7	1.17	1.18	1.13	1.14
4	6	1.23	1.26	1.18	1.20
5	5	1.31	1.36	1.25	1.27
6	4	1.41	1.47	1.33	1.35
7	3	1.58	1.60	1.43	1.44
8	2	1.74	1.76	1.54	1.54
9	1	1.92	1.91	1.66	1.64
10	0	2.15	2.15	1.81	1.81

Note. The adequate accuracy of these calculations is confirmed by experimental data obtained by different workers (reports from works laboratories).

TABLE 3

Viscosity of Chlorinated Polyvinyl Chloride Solutions

[A = 1, B = 0.5, 0.158, 0.735 and 0.73 (respectively); $X = n_{II} : 10$]

Contents of solvents (n) in solvent mixture (in g)		Viscosity of resin solutions at 15% concentration							
		I butyl acetate II acetone		I solvent II butyl acetate		I solvent II acetone		I solvent II acetone	
I	II	observed	calculated	observed	calculated	observed	calculated	observed	calculated
10	0	24	24	40	40	40	40	140	140
8	2	15	14.9	30	30	20	19.8	47	45
6	4	12	11.7	27	27.5	14	13.9	41	32
4	6	10	10	26	25.9	11	11	25	24
2	8	9	8.8	24.5	24.5	9	9.2	20	20
0	10	8	8	24	24	8	8	17	17

Note. The observed viscosities in Table 3 were determined by means of the FE-36-2 viscosimeter.

TABLE 4

Initial Acid Numbers of the Mixtures. Equation (2)

Temperature (T)	Initial acid number of mixture of alcoholized oil and phthalic anhydride			Temperature (T)	Initial acid number of mixture of alcoholized oil and phthalic anhydride		
	calculated	observed	literature data [2]		calculated	observed	literature data [2]
160	127	127	127	230	62	61	—
180	109	105	—	260	33	33	33
200	91	90	88				

TABLE 5

Data on Acid Numbers of Resins

[A = 1; B = 1.67, 3.18 and 2.42 (respectively); X = D : 24]

Esterification time (hours)	Acid number of resin at temperature (°C)								
	160			200			260		
	calculated	observed	literature data [2]	calculated	observed	literature data [2]	calculated	observed	literature data [2]
0	127	127	127	91	90	88	33	33	33
2	—	—	—	56	55	54	28	28	28
3	88	90	93	44.6	45	43	19.6	20	19
4	78	80	82	36.6	36	36	15.6	16	16
5	71.5	72	72	30	30	30	14.6	15	15
6	65	66	67	25	25	25	12.7	12.5	12.5
7	59	60	60	21	21	20	11.4	11	10.5
8	54	55	55	18	18	18	10	10	9.5
9	49.5	50	51	15.4	15	15	8.9	9	85
10	46	46	47	13.4	13	13	8	8	8
11	42.5	43	44	11.4	11	11	—	—	—
12	40	41	41	10	10	10	—	—	—
13	38	38	39	—	—	—	—	—	—
14	35	35	36	—	—	—	—	—	—
15	33	33	34	—	—	—	—	—	—
16	31	32	32	—	—	—	—	—	—
17	29.4	29	30	—	—	—	—	—	—
18	27.5	28	28	—	—	—	—	—	—
19	26.1	26	—	—	—	—	—	—	—
20	24.8	25	—	—	—	—	—	—	—
21	23.6	24	—	—	—	—	—	—	—
22	22.2	22	—	—	—	—	—	—	—
23	21.2	21	—	—	—	—	—	—	—
24	20	20	20	—	—	—	—	—	—

required for production of alkyd resins of given acid numbers, and formulations of film formers of given degrees of condensation.

It is shown in Table 3 that the chlorinated polyvinyl chloride resin taken for the investigation had relative specific viscosities of 8 and 17 seconds in acetone solution at 15% concentration.

TABLE 6

Esterification Time [X = (T −160):(260 −160)]

Temperature (°C)	Esterification time (hours)			Acid number (in mg KOH)
	calculated	observed	literature data [2]	
160	17	17	17	30
180	—	9	—	
200	5	5	5	
230	2.13	2.1	—	
260	1	1	1	
	$A = 0.33$; $B = 10$			
160	20	20	—	25
180	9.2	9	—	
200	6	6	6	
230	2.86	3	—	
260	1.5	1.5	1.5	
	$A = 0.466$; $B = 4.9$			
160	24	24	—	20
180	11.2	11	—	
200	7	7	7	
230	4.25	4.5	—	20
260	3	3	3	
	$A = 1.33$; $B = 1.29$			
160	28	28	—	15
180	13.2	13.5	—	
200	9	9	9	
230	5.5	5.5	—	
260	5	5	5	
	$A = 1.6$; $B = 0.79$			
160	33			10
180	15.7	16	—	
200	12	12	12	
230	9.2	9.5	—	
260	8	8	8	
	$A = 2.26$; $B = 0.484$			

TABLE 7

Condensation Time
(A = 1; B = 0.77; $X = n_{II}:10$)

Content (n) of composition II in mixture (in g)		Condensation time of lacquer film former (hrs)	
I	II	observed	calculated
0	10	27	27
2	8	15	14.7
4	6	10.5	10.5
6	4	8.5	8.3
8	2	7	6.9
10	0	6	6

SUMMARY

It is shown that Equation (1) may be used for calculations of the functional relationships between temperature and viscosity of water, formulation and viscosity of collodion and chlorinated polyvinyl chloride solutions, esterification time and acid value of alkyl resins, temperature and esterification time of the same resins, and formulation and esterification time of film formers for lacquers and paints.

LITERATURE CITED

[1] T. J. Rhodes, Industrial Instruments for Measurement and Control (Russian translation)(1947) p. 195.

[2] A. M. Lubman and L. N. Liskina, Bull. Exchange of Experience in the Lacquer and Paint Industry 5, 21 (1953).

Received September 7, 1955

COMPOSITION OF THE TURPENTINE FROM THE RESIN OF PICEA AJANENSIS FISCH.

N. I. Uvarova, O. V. Morozova and R. P. Ivanova

Chemical Division of the Far Eastern Branch, Academy of Sciences USSR

The demands of industry for turpentine and rosin increase year by year, and it is therefore quite natural to seek fresh sources of these materials.

Conifers such as cedar [1, 2, 3] and spruce [4, 5, 6] are tapped for sap. Turpentine obtained fromthe oleoresin of Picea ajanensis was studied in the present work. The tapping was performed in the Primor'e region, on the Shkotova Plateau, in No. 35 Forestry Unit, on 24 trees of average diameter 26.2 cm, by the method of Tolkachev and Sineliubov [7]. The bark was stripped June 12, and the oleoresin gathered September 16. The average yield of oleoresin per tree was 116 g, the turpentine content being 7.1%.

The turpentine was studied by Bardyshev's method [8]; it was found to contain the following components: L-α-pinene 30.5%, L-β-pinene 24%, L-camphene 1.5%, D-Δ^3-carene 15%, L-limonene and dipentene 1.5%, terpene alcohols 3.5%, and high-boiling components 17%.

EXPERIMENTAL

The turpentine was distilled in steam from the oleoresin of Picea ajanensis, and dried over Na_2SO_4. It had the following characteristics : d_4^{20} 0.8707, n_D^{20} 1.4745, $[\alpha]_D^{20}$ −18.6°, acid number 0.23, ester number 7.4.

180.2 g of the turpentine was distilled over a rectification column of 25 theoretical plates, at reflux ratio 50. The distillation results are given in the Table and the Figure.

L-α-pinene. Fractions 2-10 were distilled over metallic sodium; b. p. 154-154.5° at 750.7 mm Hg, d_4^{20} 0.8580, n_D^{20} 1.4653, $[\alpha]_D^{20}$ −34.4°.

5 g of L-α-pinene was converted into the nitrosochloride (2.5 g) by the usual method [9]; when dissolved in chloroform and then precipitated by methanol this had m. p. 101-102°; after a second reprecipitation, 101-103°; the melting point did not rise after further purification.

L-β-pinene. Fractions 23-26 after distillation over metallic sodium had b. p. 163-164° at 751.5 mm Hg, d_4^{20} 0.8702, n_D^{20} 1.4782, $[\alpha]_D^{20}$ −23.90°.

10 g of the L-β-pinene fraction was oxidized with $KMnO_4$ to give 1.1 g of crude nopinic acid; this melted at 122° after recrystallization from benzene, and 126-127° after a second recrystallization; the melting point remained unchanged after further recrystallizations.

L-camphene. Camphene was determined in Fractions 11-16. Isoborneol acetate was prepared by the method of Bertram and Walbaum [10], and the camphene content was found by the Bardyshev method [11]. This fraction contained up to 25% camphene; this is equivalent to 1.5% reckoned on the total turpentine.

D-Δ^3-carene. Distillation of Fractions 33-35 over metallic sodium yielded the D-Δ^3-carene fraction; b. p. 169.5-171° at 750 mm Hg, d_4^{20} 0.8621, n_D^{20} 1.4742, $[\alpha]_D^{20}$ +7.20°.

D-Δ^3-carene nitrostate, prepared by the usual method [9] had m. p. 140° after recrystallization from benzene; the m. p. did not alter after further purification.

Fraction No.	Boiling point (°C) at 20 mm	% distilled off	d_D^{20}	n_D^{20}	$[\alpha]_D^{20}$	Principal component of fraction
1	52.6	2.0	0.8564	1.4655	—32.69	L-α-pinene
2	52.6	3.7	0.8583	1.4655	—33.20	
3	52.6	5.7	0.8582	1.4653	—34.02	
4	52.6	7.7	0.8583	1.4653	—34.48	
5	52.6	9.8	0.8584	1.4653	—34.48	
6	52.6	11.5	0.8582	1.4653	—34.48	
7	52.6	13.0	0.8582	1.4653	—34.48	
8	52.6	14.5	0.8585	1.4653	—34.40	
9	52.6	16.3	0.8582	1.4653	—34.45	
10	52.6	18.9	0.8585	1.4653	—34.40	
11	52.6	19.7	0.8584	1.4654	—34.48	
12	52.6	21.3	0.8587	1.4656	—34.94	
13	52.6	23.2	0.8587	1.4656	—34.47	
14	52.6	25.0	0.8591	1.4657	—34.45	
15	53.6	26.7	0.8593	1.4663	—34.44	
16	54.1	28.5	0.8600	1.4672	—33.50	
17	54.1	30.3	0.8620	1.4695	—32.25	
18	55.6	32.2	0.8687	1.4718	—30.10	
19	58.6	34.1	0.8662	1.4739	—28.20	L-β-pinene
20	59.1	35.9	0.8679	1.4758	—25.81	
21	59.4	37.9	0.8689	1.4770	—24.40	
22	59.6	39.6	0.8696	1.4773	—24.38	
23	59.6	44.4	0.8702	1.4730	—24.36	
24	59.9	47.7	0.8702	1.4782	—22.98	
25	60.3	49.6	0.8705	1.4783	—22.50	
26	60.6	51.4	0.8705	1.4780	—22.05	
27	60.6	53.3	0.8704	1.4780	—20.90	
28	61.7	54.8	0.8694	1.4778	—18.17	
29	63.6	56.5	0.8684	1.4769	—17.27	
30	63.6	58.2	0.8672	1.4760	— 9.22	D-Δ^3-carene
31	64.6	60.2	0.8666	1.4756	— 4.15	
32	66.1	61.9	0.8658	1.4748	0	
33	66.6	63.4	0.8648	1.4740	+ 5.78	
34	67.6	65.4	0.8640	1.4745	+ 8.50	
35	68.4	67.3	0.8635	1.4755	+ 5.76	
36	68.6	69.2	0.8616	1.4760	+ 5.57	
37	69.6	70.9	0.8598	1.4768	+ 3.25	
38	71.6	72.6	0.8567	1.4790	— 3.96	L-limonene with dipentene
39	72.6	74.5	0.8833	1.4848	— 4.98	
Residue		92.9	0.9355	1.4855	— 4.01	
Losses		7.1				

L-limonene with dipentene. From fraction 38 a substance was obtained with b.p. 172-173° at 748 mm Hg, d_4^{20} 0.8548, n_D^{20} 1.4780, $[\alpha]_D^{20}$ −4.0°.

2.9 g of this substance was dissolved in a mixture of anhydrous ether and ethanol (11.2 g), cooled to −5°, and 5 g of bromine was added; the mixture was then put into a refrigerator. Crystals (0.2 g) deposited on standing. After a first recrystallization from ethyl acetate the m. p. was 119°; after a second, 125°. A mixed sample of the tetrabromide with known pure dipentene tetrabromide gave no melting-point depression.

The high-boiling fraction contained 50.85% of terpene alcohols; reckoned as $C_{10}H_{17}OH$, this is 3.5% of the original turpentine.

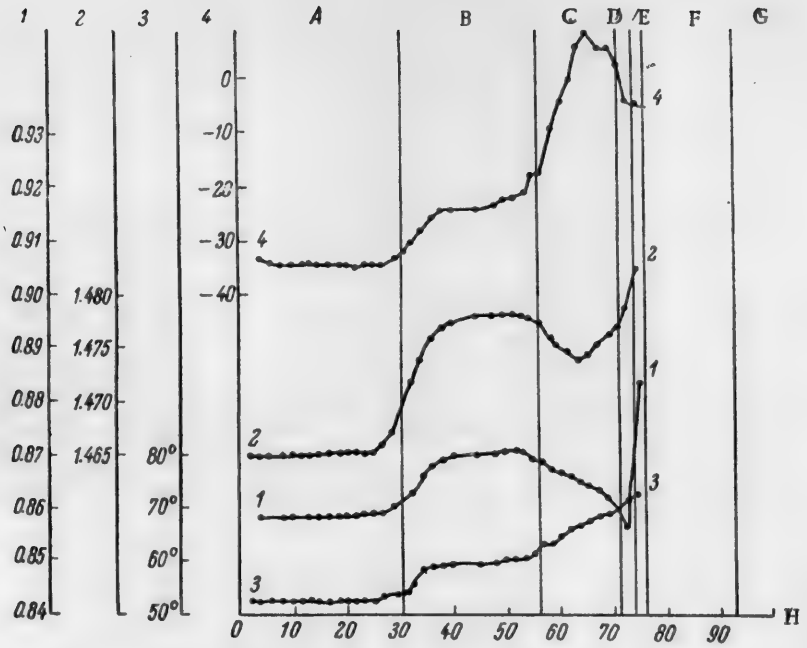

Distillation results for Picea ajanensis turpentine.
1) d_4^{20}, 2) n_D^{20}, 3) b. p. at 20 mm Hg, 4) $[\alpha]_D^{20}$.
Zones: A) L-α-pinene, B) L-β-pinene, C) D-Δ^3-carene, D) L-limonene with dipentene, E) terpene alcohols, F) high-boiling components and residue, G) losses.

SUMMARY

A sample of turpentine isolated from the oleoresin of Picea ajanensis was found to contain the following components: 30.5% L-α-pinene, 1.5% L-camphene, 24% L-β-pinene, 15% D-Δ^3-carene, 1.5% of L-limonene with dipentene, and 17% high-boiling components.

LITERATURE CITED

[1] E. I. Liubarskii, Trans. Far Eastern Regional Sci. Res. Inst. 1, 5 (1929).

[2] G. V. Pigulevskii and S. V. Netupskaia, J. Appl. Chem. 23, 724 (1950).*

[3] S. V. Netupskaia, Oleoresin of the Siberian Cedar (Western Siberian Branch Acad. Sci. USSR Press, 1947).**

[4] I. A. Arbuzova, J. Appl. Chem. 8, 884 (1935).

[5] I. I. Bardyshev, A. L. Piriatinskii, K. V. Bardysheva and O. I. Cherniaeva, J. Appl. Chem. 23, 847 (1950).*

[6] K. N. Korotkov and Kh. A. Cherkes, Bull. Acad. Sci. Belorussian SSR 4, 91 (1953).

[7] A. K. Tolkachev and M. A. Sinelobov, Wood Processing and Wood Chem. Ind. 12, 12 (1954).

[8] I. I. Bardyshev, Trans. Central Sci. Res. Inst. Wood Chem. 10, 129 (1951).

[9] N. Ia. Dem'ianov, V. I. Nilov, and V. V. Vil'iams, Essential Oils, Their Composition and Analysis (State Press, Moscow-Leningrad, 1930).**

[10] J. Bertram and H. Walbaum, J. pr. Ch. 2/49 (1894).

[11] I. I. Bardyshev, J. Appl. Chem. 26, 1299 (1953).*

Received March 8, 1956

* Original Russian pagination. See C. B. Translation
** In Russian.

THE DIRECT SYNTHESIS OF ETHYLCHLOROSILANES

K. A. Andrianov, S. A. Golubtsov, I. V. Trofimova and A. S. Denisova

The reaction between halogenated derivatives and elementary silicon in presence of a catalyst (copper) is of interest as one of the most convenient methods for the preparation of alkyl and aryl chlorosilanes and polymers based on them. Nevertheless, the only example of this reaction to have been described in detail is the interaction of silicon with methyl chloride; no systematic investigations of the direct synthesis of ethylchlorosilanes have been published in the literature.

Rochow [1] obtained a mixture of products containing 26% of diethyldichlorosilane by the reaction of ethyl chloride with silicon–copper alloy (20% copper), but the main product of the reaction (37%) was silicon tetrachloride. Mamedaliev et al. [2] reacted silicon–copper alloy with ethyl chloride, and with a mixture of ethylene and hydrogen chloride, and likewise obtained mainly silicon tetrachloride. Of patent data [3], the following are the most interesting and complete. When ethyl chloride was passed over silicon–copper alloy with added cobalt activated with chlorides of copper, a mixture containing 40% diethyldichlorosilane, 30% ethyltrichlorosilane, and 30% low-boiling products and diethylchlorosilane was formed; about 70% of the silicon was utilized, but neither the yield calculated on ethyl chloride nor the reaction conditions are given in the patent.

It was shown in our previous communication [1] that copper had a dual role as a catalyst in the reaction between ethyl chloride and silicon. On the one hand, its presence favors the formation of the most valuable product – diethyldichlorosilane – according to the equation:

$$Si + 2C_2H_5Cl \rightarrow (C_2H_5)_2SiCl_2,$$

and on the other, copper may catalyze the decomposition of ethyl chloride to ethylene and hydrogen chloride; the latter then immediately reacts with silicon in presence of ethyl chloride, and as a result the reaction products contain ethyltrichlorosilane, ethyldichlorosilane, and diethylchlorosilane. It was shown that the predominant direction of the reaction depends on the composition and the activity of the catalyst.

In the present investigation, which was carried out in 1952-1953, it was found that the apparatus used for the reaction, which determines the optimum reaction conditions, is not less important as a factor which influences the course of the reaction between gaseous ethyl chloride and solid silicon–copper catalyst.

Effective contact between the gas and the surface of the silicon–copper mass is necessary for successful synthesis (satisfactory yields, productivity, and composition of the reaction products). Moreover, good heat transfer and uniform temperature throughout the reaction zone are very important. It should be taken into account that the reaction of ethyl chloride with silicon is an exothermic process (the heat of reaction calculated from the above equation is 52 kcal./mole), and therefore there is a risk of considerable local overheating at individual points in the reaction mass. This can accelerate undesirable side reactions leading to the formation of gaseous decomposition products of ethyl chloride (ethylene, hydrogen, etc.) and can eventually change the direction of the reaction entirely.

To study the influence of conditions on the course of the reaction between ethyl chloride and silicon–copper alloy, we carried out the process in different types of synthesis apparatus. The results show that if the conditions are suitable for fairly effective contact between the reactants, and if the temperature is maintained uniform (with good agitation of the mass), the reaction can be directed toward the formation of the most valuable products (diethyldichlorosilane, ethyltrichlorosilane) in satisfactory yields and with a good output rate.

It is known that reaction between solids and gases, especially if heat has to be removed, can most conveniently be carried out in "fluidized" beds (with agitation of the solid particles by the stream of gas). By using this method, we raised the productivity of the process approximately 100-fold (as compared with the process without agitation), the yield on ethyl chloride was increased 3-fold, and on silicon 7-fold, and the composition of the reaction products was also improved.

EXPERIMENTAL

The starting material in all the experiments was an alloy of M-1 copper and Kr-1 silicon; its content by analysis was 70.2% Si, 21.2% Cu, 1.8% Fe with traces of aluminum and chromium.

The apparatus used for synthesis of ethylchlorosilanes is shown schematically in the Figure. Ethyl chloride from the cylinder 1, immersed in a water thermostat 2, passed through the reducing valve 3 and rheometer 4 into the reactor 5, which contained powdered silicon–copper alloy previously dried thoroughly in a stream of nitrogen. The synthesis temperature varied between 270 and 330° in different experiments. The reaction products passed through the water condenser 6 into the receiver 7. The unreacted ethyl chloride was condensed in the trap 8, cooled in a mixture of solid carbon dioxide and acetone. The flow of ethyl chloride through the reactor was continued until the rate of collection of ethylchlorosilanes in the receiver 7 began to decrease appreciably.

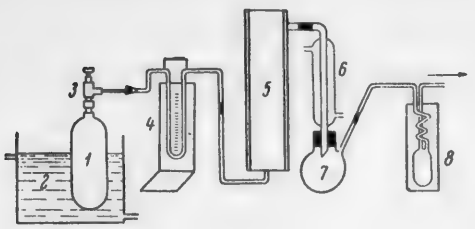

Apparatus for synthesis of ethylchlorosilanes.

The liquid reaction products collected in the receiver during the entire experiment were analyzed by fractionation of the mixture through a column with an efficiency of 20 theoretical plates. The composition of the mixture of ethylchlorosilanes was calculated by the method used by us earlier [4] (the weight of the unchanged ethyl chloride was subtracted from the total weight of the reaction products in calculations of the composition and productivity).

In view of the fact that the reaction of ethyl chloride with silicon always produces a complex mixture of ethylchlorosilanes and therefore the reaction cannot be represented by any one equation, the following data were used for evaluation of the results: a) yield of ethylchlorosilane mixture (nominally calculated as diethyldichlorosilane in accordance with the equation given above) as a percentage of the theoretical on diethyl chloride and silicon; b) % content of the most valuable product – diethyldichlorosilane – in the mixture of chlorides; c) yield of the mixture of ethylchlorosilanes per hour per 1 kg of the contact mass (productivity of the contact mass).

The results of some of the most typical experiments are given in the Table; the results obtained in any given experiment are characteristic of a particular procedure used for the synthesis of ethylchlorosilanes.

Direct Synthesis of Ethylchlorosilanes

Expt. No.	Wt. of alloy taken (g)	Time (hours)	Ethyl chloride consumption (g)	Yield of mixture of chlorides (g)	Productivity (g of mixture per 1 kg of mass per hour)	Yield, % of theoretical		Composition of reaction products (wt. %)			
						on ethyl chloride	on silicon	ethyldichlorosilane	ethyltrichlorosilane*	diethyldichlorosilane	residue in still
1	817	97	1069	235	3	18	7.5	8	38	5	49
2	600	19 (9)	233	102	19	35	10	29	32	9	30
		(10)	275	130	22	39		21	35	20**	19
3	600	24	2520	642	44	21	27	37	14	13**	31
4	612	5	1976	1203	395	52	52	34	30	30	6
5	3100	8	9300	6260	250	55	52	14	25	43	18

* Contained some diethylchlorosilane.

** 5% of fractions boiling above 132° was also obtained.

In Experiment No. 1, the reaction between the silicon–copper alloy and ethyl chloride was effected without agitation. The finely divided alloy (alternating with ceramic rings) was loaded into a vertical steel tube provided with an electric heater. The productivity in this method was extremely low, and the experimental cycle was therefore very long, with low utilization of the silicon; this was probably due to unsatisfactory contact between ethyl chloride and the surface of the alloy. The yield reckoned on ethyl chloride, and the composition of the reaction products, were also quite unsatisfactory; the amount of diethyldichlorosilane was very low, and the reaction products contained large amounts of the least valuable, high-boiling compounds. It seems likely than in absence of agitation the course of the reaction is not determined by the mean temperature, which was about 270-300°, but by the existence of considerable local overheating at individual, most active points of the contact mass; at these points ethyl chloride is rapidly decomposed with formation of gaseous products together with some carbon.

In Experiment No. 2 the reaction with the finely divided alloy was effected in a vertical apparatus heated in a saltpeter bath and fitted with a band-type stirrer rotating at 40-60 rpm. The use of a stirrer resulted in an increase of productivity, a corresponding decrease of the time required for the synthesis (owing to better contact between the alloy and ethyl chloride), and some improvement in the composition of the reaction products.

Increase of the stirrer speed in Experiment 3 to 150 rpm produced a further increase of productivity and resulted in better utilization of the silicon.

In Experiments 4 and 5 the process was carried out in a "fluidized bed;" the results are qualitatively different from the others with regard to the yields, productivity, and composition of the reaction products.

The results of Experiment 5 show that reproducible results are obtained if the amount of alloy in the reaction vessel is increased.

SUMMARY

1. It is shown that the course of the reaction between ethyl chloride and silicon–copper alloy depends not only on the catalytic activity and composition of the alloy, but also, to a considerable extent, on the effectiveness of the contact between the gas and the surface of the solid phase and on the uniformity of the temperature distribution in the reaction zone.

2. A method is proposed for the production of ethylchlorosilanes from ethyl chloride and silicon in a "fluidized" bed; by this method the productivity can be raised to 200-300 g of mixed ethylchlorosilanes per 1 kg of contact mass per hour, the yields on ethyl chloride and silicon to 50-55%, and the content of diethyldichlorosilane in the reaction products to 40%.

LITERATURE CITED

[1] E. G. Rochow, J. Am. Chem. Soc. 67, 963 (1945).

[2] Iu. G. Mamedaliev et al., Proc. Acad. Sci. Azerbaidhzan SSR, 6, 365 (1950); 8, 153 (1952).

[3] British Patent No. 681387 (1952); Ch. A. 47, 4129 (1953).

[4] K. A. Andrianov, S. A. Golubtsov, I. V. Trofimova, A. S. Denisova and R. A. Turetskaia, Proc. Acad. Sci. USSR 108, 3, 465 (1956).*

Received August 23, 1956

* Original Russian pagination. See C. B. Translation.

SYNTHESIS OF DERIVATIVES OF β-DIKETONES

V. V. Perekalin and K. S. Parfenova

In our studies in the field of chemistry of unsaturated nitro compounds, one of us jointly with Sopova investigated reactions of certain β-diketones (acetylacetone, benzoylacetone) with nitro olefins [1].

The continuation of this work consisted of a study of the reactions of cyclic β-diketones with unsaturated nitro compounds, in order to develop a new method for the preparation of derivatives of β-diketones and to carry out pharmacological studies of the reaction products.

Derivatives of aromatic β-diketones are used as active blood anticoagulants (2-phenylindandione) and antispasmotics (amino derivatives of phenylindandione).

We therefore studied the reactions of a number of cyclic β-diketones (dimedon, indandione, and phenylindandione) with various aliphatic and aromatic nitro olefins (nitroisohexylene, nitrostyrene, p-dimethylamino--ω-nitrostyrene, etc.)

The reactions were effected with good yields at room temperature in presence of basic catalysts (sodium methoxide, triethylamine).

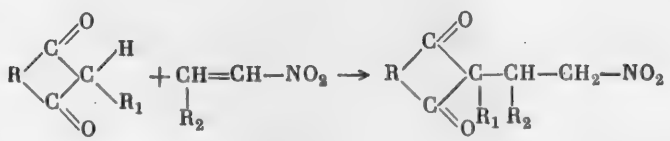

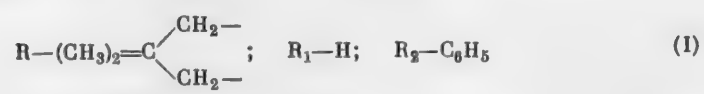

(I)

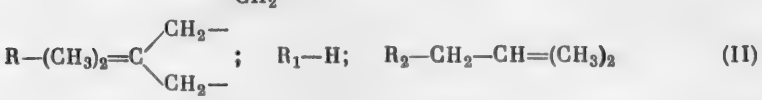

(II)

(III)

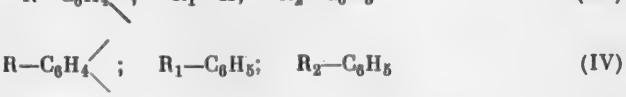

(IV)

This is apparently a general reaction, which can be used for the synthesis of a great variety of nitro alkyl, nitro aryl, and nitro heterocyclic derivatives of β-diketones. The importance of this reaction is enhanced by the possibility of conversion of the nitro derivatives into the corresponding amines and carboxylic acids.

EXPERIMENTAL

Condensation of dimedon with nitrostyrene. A mixture of 0.140 g (0.001 mole) of dimedon and 0.149 g (0.001 mole) of nitrostyrene in 5 ml of absolute methanol containing a trace of sodium methoxide was kept 6-8 hours at room temperature. As the solvent evaporated, a white crystalline condensation product (I) was precipitated. M.p. 135° from methanol (with decomposition). Yield 0.197 g (65% of theoretical).

Condensation of dimedon with nitroisohexylene. A mixture of 0.5 g (0.0038 mole) of nitroisohexylene and 0.54 g (0.0038 mole) of dimedon in 10 ml of absolute methanol containing a trace of sodium methoxide was kept for a week at room temperature. A crystalline condensation product (II) was deposited. M. p. 152-153° from methanol (with decomposition).

Condensation of indandione with nitrostyrene. A mixture of 0.146 g (0.001 mole) of indandione and 0.149 g (0.001 mole) of nitrostyrene in 5 ml of benzene containing 1 drop of triethylamine was kept for 1 hour at room temperature. After evaporation of the solvent a condensation product (III) remained in the form of an oil, which crystallized when rubbed with a few drops of methanol. M. p. 195° (from methanol–benzene mixture). Yield 0.118 g (40% of theoretical).

Condensation of phenylindandione with nitrostyrene. To a mixture of 0.444 g (0.002 mole) of phenylindandione and 0.288 g (0.002 mole) of nitrostyrene in 5 ml of benzene 1 drop of triethylamine was added. The reaction mixture was left 1 hour at room temperature. After evaporation of the solvent an oil remained, which crystallized when rubbed with a few drops of acetone.

The condensation product (IV) was filtered off and washed with a small amount of acetone. M. p. 164-165° (from acetone). Yield 0.42 g (53% of theoretical).

LITERATURE CITED

[1] V. V. Perekalin and A. S. Sopova, J. Gen. Chem. 24, 513 (1954).*

Received March 12, 1956

* Original Russian pagination. See C. B. Translation.

JOURNAL OF APPLIED CHEMISTRY OF THE USSR IN ENGLISH TRANSLATION

August, 1957

TABLE OF CONTENTS

TABLE OF CONTENTS (continued)